

1986

Analytical application of laser excited Shpol'skii spectroscopy: direct identification and quantitation of polynuclear aromatic compounds

Abdelmonaim Elbaz Elsaid
Iowa State University

Follow this and additional works at: <https://lib.dr.iastate.edu/rtd>

 Part of the [Analytical Chemistry Commons](#)

Recommended Citation

Elsaid, Abdelmonaim Elbaz, "Analytical application of laser excited Shpol'skii spectroscopy: direct identification and quantitation of polynuclear aromatic compounds" (1986). *Retrospective Theses and Dissertations*. 7998.
<https://lib.dr.iastate.edu/rtd/7998>

This Dissertation is brought to you for free and open access by the Iowa State University Capstones, Theses and Dissertations at Iowa State University Digital Repository. It has been accepted for inclusion in Retrospective Theses and Dissertations by an authorized administrator of Iowa State University Digital Repository. For more information, please contact digirep@iastate.edu.

INFORMATION TO USERS

This reproduction was made from a copy of a manuscript sent to us for publication and microfilming. While the most advanced technology has been used to photograph and reproduce this manuscript, the quality of the reproduction is heavily dependent upon the quality of the material submitted. Pages in any manuscript may have indistinct print. In all cases the best available copy has been filmed.

The following explanation of techniques is provided to help clarify notations which may appear on this reproduction.

1. Manuscripts may not always be complete. When it is not possible to obtain missing pages, a note appears to indicate this.
2. When copyrighted materials are removed from the manuscript, a note appears to indicate this.
3. Oversize materials (maps, drawings, and charts) are photographed by sectioning the original, beginning at the upper left hand corner and continuing from left to right in equal sections with small overlaps. Each oversize page is also filmed as one exposure and is available, for an additional charge, as a standard 35mm slide or in black and white paper format.*
4. Most photographs reproduce acceptably on positive microfilm or microfiche but lack clarity on xerographic copies made from the microfilm. For an additional charge, all photographs are available in black and white standard 35mm slide format.*

***For more information about black and white slides or enlarged paper reproductions, please contact the Dissertations Customer Services Department.**

UMI University
Microfilms
International

8615045

Elsaid, Abdelmonaim Elbaz

**ANALYTICAL APPLICATION OF LASER EXCITED SHPOL'SKII
SPECTROSCOPY: DIRECT IDENTIFICATION AND QUANTITATION OF
POLYNUCLEAR AROMATIC COMPOUNDS**

Iowa State University

PH.D. 1986

**University
Microfilms
International** 300 N. Zeeb Road, Ann Arbor, MI 48106

Analytical application of laser excited Shpol'skii spectroscopy:
Direct identification and quantitation of polynuclear aromatic compounds

by

Abdelmonaim Elbaz Elsaid

A Dissertation Submitted to the
Graduate Faculty in Partial Fulfillment of the
Requirements for the Degree of
DOCTOR OF PHILOSOPHY

Department: Chemistry
Major: Analytical Chemistry

Approved:

Signature was redacted for privacy.
In Charge of Major Work

Signature was redacted for privacy.
~~For the Major/Department~~

Signature was redacted for privacy.
For the Graduate College

Iowa State University
Ames, Iowa

1986

TABLE OF CONTENTS

	Page
CHAPTER 1. INTRODUCTION	1
Biological Activity of Polycyclic Aromatic Hydrocarbon (PAHs)	1
Occurrence of PAHs in the Environmental Systems	2
Analytical Overview	3
Chromatographic Hyphenated Techniques	4
Optical Spectroscopic Techniques	5
Low Temperature Luminescence Spectroscopy	6
CHAPTER 2. LASER EXCITED SHPOL'SKII SPECTROSCOPY	9
Shpol'skii Effect	9
General characteristic features of Shpol'skii effect	9
Quasilinear spectra	9
Multiplet site structure	11
Weak phonon wing	12
Temperature effect	13
Solvent effect	14
Concentration effect	16
Cooling rate effect	17
Presence of other impurities	19
Tunable dye laser excitation of Shpol'skii systems	19
Scope of application	20
Laser Technology	24
Excimer laser	25
Dye lasers	28
Frequency doubler	30
Object of the Present Work	32
CHAPTER 3. APPARATUS, MATERIALS AND PROCEDURES	33
Apparatus	33

	Page
Fluorescence excitation source	33
Excimer laser	33
Dye laser	33
Frequency doubler	36
Optical system	36
Sample holder, vacuum sample chamber and refrigeration unit	40
Detectors and data processing	43
Materials	44
PNAs, solvents and solution preparation	44
Laser dyes, solvents and solution preparation	44
Excimer laser gases	44
Environmental samples	50
Procedures	50
Wavelength calibration	50
Dye laser tuning procedure	51
Sample loading and cooling procedures	54
Excitation and emission spectra	54
Analysis of real samples	55
Qualitative analysis	55
Quantitative analysis	55
CHAPTER 4. RESULTS AND DISCUSSION	57
Illustration of the LESS Technique	57
The LESS of PNAs: Typical Spectra, Problems and Their Solutions	64
Benzo(a)pyrene	65
Deuterated analogs as internal reference compounds	65

	Page
Phosphorescence spectra	67
Detrimental effects of frost film formation	69
Inhomogeneous solid solution formation	71
Spectrum of 7-methylbenzo(a)pyrene; an example of line overlap	72
7,10-Dimethylbenzo(a)pyrene	83
Benzo(e)pyrene; an example of the analytical utility of phosphorescence emission	85
Perylene and Perylene-d ₁₂ ; an example of strong self-absorption	89
Indeno(1,2,3-cd)pyrene, anthanthrene, benzo(k)fluoranthene, and benzo(b)fluoranthene; examples of relatively large shifts in the multi-site spectra	95
Coronene; an example of impurity effect on the spectrum of a given compound	108
Observed Luminescence Spectra of PNAs	110
CHAPTER 5. ANALYTICAL APPLICATIONS	154
Samples Analyzed	154
Urban air particulate sample (SRM 1649)	154
Diesel particulate (SRM 1650)	154
SRC-II	154
Carbon blacks	155
Sample Extraction Procedures	155
Particulate samples	155
SRC-II sample	156
Identification of PNAs in SRC-II and Carbon Black	157

	Page
Quantitative Determination of PAHs in Urban Air and Diesel Particulate Samples	160
Internal reference method	160
Standard addition method	161
Internal reference-standard addition combination	161
REFERENCES	170
ACKNOWLEDGEMENTS	182

CHAPTER 1. INTRODUCTION

Biological Activity of Polycyclic Aromatic Hydrocarbon (PAHs)

PAHs are of interest in many fields of chemical and biological sciences (1). From an environmental point of view, PAHs represent a class of undesirable compounds, because they are now recognized as major environmental pollutants (2,3). It has been estimated that some 70 to 90% of human and animal cancers are caused by environmental factors (4,5). Among the environmental chemicals concerned, PAHs comprise the largest group of carcinogens (6). Extensive research studies have shown that many PAHs are potential carcinogens (7-9), cocarcinogens (6,10), mutagens (11), teratogens (12), and many others promote chronic respiratory and/or metabolic diseases (13).

Most PAHs, however, are biologically inert and require metabolic activation to exert their mutagenic and carcinogenic effects (14). Animal studies indicate that PAHs are metabolized to epoxides, dihydrodiols, phenols, and quinones and exert their biological and toxic effects only after metabolism (15). Although efforts to relate molecular structure to biological activity have been only moderately successful, certain correlations have emerged. The most active molecules have from four to six fused aromatic rings and possess an unsubstituted, carbon-carbon bond flanked by two aromatic rings. This portion of the molecules is often called the K-region and is distinguished by its relatively high electron density and olefin-like character (16). It is, therefore, expected that the carcinogenic activity of a particular compound is dependent on various structural features of the molecules such

as shape, size, and steric factors (17-19). Hence, isomeric parent PAHs may differ markedly in their activities. Benzo(a)pyrene and benzo(e)-pyrene are typical examples; the former is a well-known carcinogen whereas the latter is a relatively innocuous compound (20).

Alkyl substitution at various positions on the parent PAH can dramatically enhance or diminish activity, depending on the position of substitutions (21). Within the series of methylated benzo(a)anthracene (B(a)A), for example, the isomers have very different biological activities (22). B(a)A itself has only very weak activity (23). In the monomethylated derivatives of B(a)A, 7-methyl B(a)A has the highest carcinogenic activity among the B(a)A derivatives (22). Although the 8-methyl and the 12-methyl isomers are only weakly carcinogenic, the 7,12-dimethyl B(a)A and the 7,8,12-trimethyl B(a)A compounds are among the most potent carcinogenic PAHs and has been found to be considerable more active than the 7-methyl derivative (23-25). Moreover, the carcinogenicity of certain heterocyclic analogs of PAH may be greater than that of 3-methylbenz(j)aceanthrylene, a very potent carcinogen (26). Recent studies indicate that aromatic amines and the nitrogen heterocyclics, for example, contribute to a greater extent than the PAHs to the mutagenicity of some liquid fuels (27-29).

Occurrence of PAHs in the Environmental Systems

Polycyclic hydrocarbons are widely dispersed in the atmosphere (30,31), soil (32), and waters of the earth (33) and can be formed from natural sources as well as anthropogenic (induced or altered by presence and activity of man) sources (34,35). An interesting natural source of

these compounds is their long-term formation from biological material (34). For example, fossil fuels (petroleum, shale oil, etc.) contain extremely complex mixtures of these compounds (35-37). Natural sources may also include natural combustion, volcanoes, and biosynthesis (32). Anthropogenic sources are by far the major contributors of PAH primarily as a result of incomplete combustion of organic matter. It is believed (38) that two distinct reaction steps are involved, namely, pyrolysis and pyrosynthesis. At high temperatures, organic compounds are partially cracked to smaller, unstable molecules (pyrolysis). These fragments, mostly radicals, recombine to yield larger, relatively stable aromatic hydrocarbons (pyrosynthesis). Petroleum refining, shale oil recovery operation, coal combustion, coke production, automobile exhaust, residential furnaces, and tobacco smoke are a few examples of anthropogenic sources responsible for accidental, or purposeful, release of PAH into the aquatic, terrestrial, ambient air, or work place environment.

PAHs can be taken into the body by different routes (inhalation, skin contact, and ingestion), and because of their prevalence in the environment, exposure to them is virtually unavoidable. As a consequence, the analytical characterization, both qualitative and quantitative, has attracted much attention in recent years.

Analytical Overview

Although many analytical approaches have been devised (38,39), no one analytical technique has been found sufficient to solve all of the analytical problems. It is, therefore, not surprising that various

multi-technique approaches have been required (38). There are several problems involved in the analysis of PAHs. Firstly, adequate clean-up procedures are needed since the PAHs must be separated from other organic substances in the complex mixtures which are often encountered in environmental samples. Secondly, high separation efficiency is necessary if structural isomers are to be separated. Furthermore, high detection sensitivity is required for detecting the low concentrations of PAHs and other biologically significant compounds found in environmental samples. Finally, photochemical transformation during sample separation and processing is particularly relevant to possible losses during analysis (40,41).

Chromatographic Hyphenated Techniques

The classical techniques of column adsorption (42), paper (43), and thin-layer chromatography (43) have been widely used in the separation of complex PAH mixtures into simpler fractions prior to further separation by higher resolution techniques and/or identification of mixture constituents (42). More sophisticated techniques, such as capillary column gas chromatography (43) together with mass spectrometry (44), high performance liquid chromatography in combination with ultraviolet or fluorescence spectroscopic detection (45,46), microcapillary liquid chromatography (47), gas-liquid chromatography using nematic liquid crystal column (48), and supercritical fluid chromatography (49,50) are now generally used for the analytical separation and identification of PAHs.

Optical Spectroscopic Techniques

Various optical spectrometric techniques have been extensively employed for PAHs analysis, including absorption spectroscopy (conventional ultraviolet-visible absorption (51) as well as photoacoustic (52)), luminescence spectroscopy (conventional fluorescence (53,54) and phosphorescence (55), synchronous fluorescence (56,57), room temperature phosphorescence (56-58), derivative and wavelength modulation (59), time-resolved fluorescence (60), two-photon induced fluorescence (61), total luminescence (62), and low temperature techniques), vibrational spectroscopy (infrared (63), Fourier transform infrared (64) and Raman (65)), and nuclear magnetic resonance (66). All of these methods vary in respect to speed, reproducibility and sensitivity and have been used with varying degrees of success.

For any optical spectroscopic technique to be useful in characterizing a very complex sample, it must have adequate sensitivity so that trace constituents can be determined. Further, it should exhibit adequate selectivity so that fractionation and separation steps prior to the actual analysis can be held to a minimum. To achieve high analytical selectivity, an analytical spectroscopic technique should produce highly structured and specific spectra useful for "fingerprinting" purposes, and should minimize the extent of overlap of spectral bands due to different constituents of complex samples. This is why ambient temperature luminescence spectrometry, in spite of its high sensitivity has been utilized to a limited extent for the qualitative and quantitative determinations of PAHs in complex mixtures (67-72). The limitation

arises from the fact that molecular absorption and emission spectra from room temperature solutions are generally broad and featureless, because the molecules in fluid media can easily be affected by their immediate environments that shift their electronic levels. This broad feature causes severe spectral overlap, making the identification of the constituents of a complex mixture difficult.

Low Temperature Luminescence Spectroscopy

It has been known for a long time that molecular luminescence spectra can be sharpened by use of low temperature matrices. More recently, it has become evident that the use of low temperature techniques can offer important advantages for the measurement of fluorescence in complex environmental samples (73). Narrowing of lines at low temperature improves spectral resolution and enhances selectivity and the fluorescence spectra usually are sufficiently characteristic to serve as "finger prints" for individual PAHs. The "rigidity" of a cryogenic solid minimizes or completely eliminates fluorescence quenching, provided that aggregation of solute molecules in the low-temperature sample can be avoided (74). The highly-structured absorption and emission spectra obtained in these techniques reduce the severity of inner-filter effects (absorption of fluorescence emitted by one compound, either by other molecules of that same compound or by those of another sample constituent) by reducing the overlap between a fluorescence spectra and the corresponding absorption (excitation) spectrum (75,76). Since quenching and inner-filter effects ultimately are the factors limiting the accuracy of quantitative fluorometric analysis in complex samples, the

elimination of these effects should greatly enhance the ability of fluorescence to deal with real samples without lengthy preliminary sample clean-up steps (73).

High-resolution spectrofluorimetric detection methods ($T \ll 77\text{K}$) have been developed. These are based on the Shpol'skii effect, matrix isolation, fluorescence line narrowing in organic glasses, and supersonic jet fluorescence spectroscopy. For Shpol'skii spectroscopy (the technique used in the present work), polynuclear aromatic compounds are dissolved in appropriate n-alkane solvents as hosts and the resulting solutions are frozen to cryogenic temperature. The obtained luminescent spectra are quasilinear (line-like) with bandwidths under tunable dye laser excitation on the order $1\text{-}10\text{ cm}^{-1}$ (77,78). In matrix isolation spectroscopy, a liquid or solid is vaporized under vacuum and mixed with a large excess of a diluent inert gas. This gaseous mixture is then deposited on a cold surface for spectroscopic analysis. The deposited solid is usually at a temperature of 15K or less. Typical bandwidths of PAH absorption or luminescence under matrix isolation conditions are of the order $50\text{-}200\text{ cm}^{-1}$ (79-81). In fluorescence line-narrowing spectroscopy, tunable laser excitation is used to selectively excite a narrow portion of a judiciously chosen, inhomogeneously broadened absorption band of fluorescent species imbedded in glasses at liquid helium temperature (82-84). In supersonic jet fluorescence spectroscopy, supersonic expansion of an inert carrier gas through an orifice into a vacuum is used to cool the gas to very low translational temperature (less than 1K). At these temperatures, supersonic jet spec-

tra can be obtained. A typical carrier gas-to-solute mole ratios is on the order of 10^4 - 10^6 for large molecules (85-87). All of these techniques have been utilized for the analysis of mixtures of PAH.

CHAPTER 2. LASER EXCITED SHPOL'SKII SPECTROSCOPY

Shpol'skii Effect

Many methods have been developed for the investigation of spectra of complex compounds in mixed crystals. When the molecules under investigation are introduced into a crystal lattice of another substance and the study is carried out at a sufficiently low temperature, a condition is achieved in which, first of all, the interaction between the emitting molecules and surrounding medium is at a minimum and, secondly, the amount of vibrational energy of each molecule is small. With a suitable selection of the crystalline structure into which the molecule is introduced, it is possible to obtain very sharp spectra of quite complex compounds (88-92). Shpol'skii and co-workers made wide use of such a method of mixed crystal for the study of luminescence spectra of aromatic hydrocarbons. They used a comparatively simple procedures. Highly dilute solution of the aromatic compound (10^{-4} - 10^{-5} M) in an appropriate normal alkane solvent was frozen to temperature ≤ 77 K to form a crystalline mass. The obtained luminescence spectra were quasilinear and the observed bandwidths were of the order 1 - 10 cm^{-1} (93-97). This type of line narrowing phenomenon is now called the "Shpol'skii effect". Since those early observations in 1952, this phenomenon has received extensive study in terms of both its fundamental chemical physics and its application to chemical analysis.

General characteristic features of Shpol'skii effect

Quasilinear spectra Typical observed bandwidth of the quasilinear Shpol'skii spectra (absorption and fluorescence) are of the order

$1-10\text{ cm}^{-1}$ (98). There is now general agreement that there are two very necessary conditions that must be met for observing these sharp line spectra. These conditions are: (a) observation at cryogenic temperature and (b) occurrence of the solute species in a strictly oriented manner, at very low concentrations in a solid crystalline host (99-102).

It might seem that lowering the temperature should automatically result in quasilinear spectra; however, in fact, temperature is only one parameter among several other interrelated parameters (e.g., type of the solute, type of the solvent, solute concentration, cooling rate, presence of certain impurities and their concentration) that play a major role in achieving quasilinear spectra. In a given Shpol'skii matrix, the width of a particular band in the spectrum of an analyte can be thought of consisting of two contributions (103): homogeneous and heterogeneous broadening. Homogeneous broadening originates from the fact that any spectral transition has a certain inherent energy uncertainty, ultimately related in the limiting case to the excited-state lifetime through constraints imposed by the Heisenberg uncertainty principle. This "inherent" contribution to the observed spectral bandwidth depends in rather a complex way upon the energy level structure and excited-state decay properties of the matrix in which the analyte is situated (104,105) and defines the limit of spectral resolution that can be achieved in any fluorescence measurement, assuming that each molecule of the analyte experience the same local environment on the fluorescence time scale. Heterogeneous broadening is produced by environmental heterogeneity at the molecular level. In general, different molecules of

an analyte, experiencing slightly (or perhaps drastically) different local microenvironments within the sample, will exhibit different energies of interaction with the matrix material. Consequently, the electronic transition energies for different molecules of the same compound will be somewhat different, and the resulting spectrum of the sample (which can be thought of as a weighed average of the individual spectra of the molecule comprising the sample) will be broad. The extent of heterogeneous spectral broadening is huge compared with that of homogeneous broadening. The extent of heterogeneous broadening can be reduced by three obvious general approaches: (a) using an inert matrix material with which the analyte is unlikely to exhibit highly energetic interactions, (b) decreasing the extent of microenvironmental heterogeneity by making the matrix behave in as similar a manner as possible to a perfect crystal, and (c) employing an excitation source having a linewidth which is substantially smaller than the width of the heterogeneously broadened absorption spectral band. In reality, combination of tunable dye laser as an excitation source with Shpol'skii system (as employed in the present work) realizes these three approaches for minimizing the extent of the heterogeneous broadening and provides an excellent way to obtain quasilinear luminescence spectra.

Multiplet site structure A remarkable characteristic feature of Shpol'skii quasilinear spectra is the frequently observed multiplet structure of the vibronic bands, i.e., the spectrum consists of the superposition of several identical molecular subspectra, displaced relative to one another. The composite spectrum of multiplets is often a

unique signature of a given solute-solvent system. There have been many theories on the interpretation of the nature of multiple structure (106-111). There is now general agreement that these multiplets arise from several different orientations (sites) of the solute molecules in the solidified matrix (108-115). These different orientations lead to non-equivalent crystal field effects and, hence, multiple site spectra. For a given solute, the number of sites, their degree of resolution, their wavelengths, and their relative intensities depend on the choice of solvent (116), cooling rate (117,118), matrix temperature (119), excitation wavelength (120), and concentration of the solute (121).

Weak phonon wing In a typical Shpol'skii fluorescence spectrum, the vibronic bands are usually accompanied on the long-wavelength side of the spectrum by a series of additional features, usually superimposed on a broad, rather diffuse, band. The origin of the diffuse bands is now rather well-understood. The quasilinear portions of a Shpol'skii fluorescence spectrum correspond to purely electronic transitions of the solute and no changes in the vibrational state of the crystalline matrix accompanies the emission process. Hence, the quasilinear portion of a Shpol'skii fluorescence spectrum is referred to as the phonon-free or zero-phonon region (quanta of lattice vibrational energy are commonly termed phonons). On the long wavelength side of a zero-phonon fluorescence band and on the short-wavelength side in case of absorption, there occurs a much broader band called a phonon wing or a phonon sideband. In the latter, the electronic transition in the solute is accompanied by changes in the vibrational state of the lattice. This broad phonon band

arises from the simultaneous creation (in fluorescence) or annihilation (in absorption) of matrix phonons during the electronic transition of the solute. The term "electron-phonon coupling" is often used to describe this process (122-126). It is desired that the degree of such coupling be weak (126), otherwise the zero-phonon lines will be weak and difficult or impossible to detect. The intensity ratio of the zero-phonon line to that of the phonon sideband commonly is known as the "Debye-Waller factor" (124). This quantity is known to be both temperature and solvent dependent (126-128) and it can be increased by the judicious choice of matrix material and by lowering the matrix temperature. Fortunately, in a Shpol'skii system the phonon wings are weak due to the weak interactions between the guest molecules and host matrix lattice (126); thus, an intense zero-phonon line usually is obtained at 77 K although lower temperature may be required for certain solutes.

Temperature effect The sharpness of Shpol'skii effect spectra depends on the final temperature of the matrix. For example, at 77 K, the spectrum of pyrene in n-hexane contains about 60 lines, whereas at 4 K, the same solution shows more than 220 lines (129). At low temperatures, molecular rotation is restricted and the nonradiative processes are suppressed, leading to the intensification of the luminescence emission of the solute; furthermore, the matrix vibrational states are minimized and the interaction between the emitting molecules and surroundings is at a minimum. Also, as the temperature is decreased, electron-phonon coupling is reduced and enhancements of the zero-phonon bands are achieved. In some cases, it is sufficient to decrease the temperature

to 77 K, e.g., for n-alkane solutions of a large number of aromatic hydrocarbons (130,131) while in other cases, it is necessary to cool the solution tested to 20 K or 4 K (e.g., porphyrins (132), chlorophyll (133), diphenylpolyene (134), and benzophenone solutes (135)).

Solvent effect The identity of the solvent is rather critical in producing truly "quasilinear" fluorescence spectra (136). The crystallinity of the solvent matrix is a prerequisite (126). Furthermore, the solvent has to be inert toward the analyte molecule (89) and there must be a geometric/dimensional match between solute-solvent combination (95,136). Normal saturated hydrocarbons (n-alkanes) were the originally chosen solvents and are still the most widely used. A feature of Shpol'skii systems is that only a few n-alkane solvents may be an appropriate host for an extended list of classes of compounds. As previously mentioned, the crystallinity and the inertness of the n-alkane solvents will alleviate and limit both the heterogeneous broadening and the phonon sideband effects, resulting, therefore, in narrow intense zero-phonon bands. Historically, the physical interpretation of the Shpol'skii effect has invariably been based on some dimensional and geometrical correlations between the aromatic solute molecules and the n-alkane hosts. These correlations are readily visualized for catacondensed (linearly fused benzene ring) aromatic molecules, as shown in the top half of Fig. 1A. A match in the linear dimensions, geometric fit, and bond angles for these solute-solvent is clearly apparent (78). For pericondensed (nonlinearly fused benzene ring) molecules, these similarities are not as obvious as can be seen in the lower half of Fig. 1A.

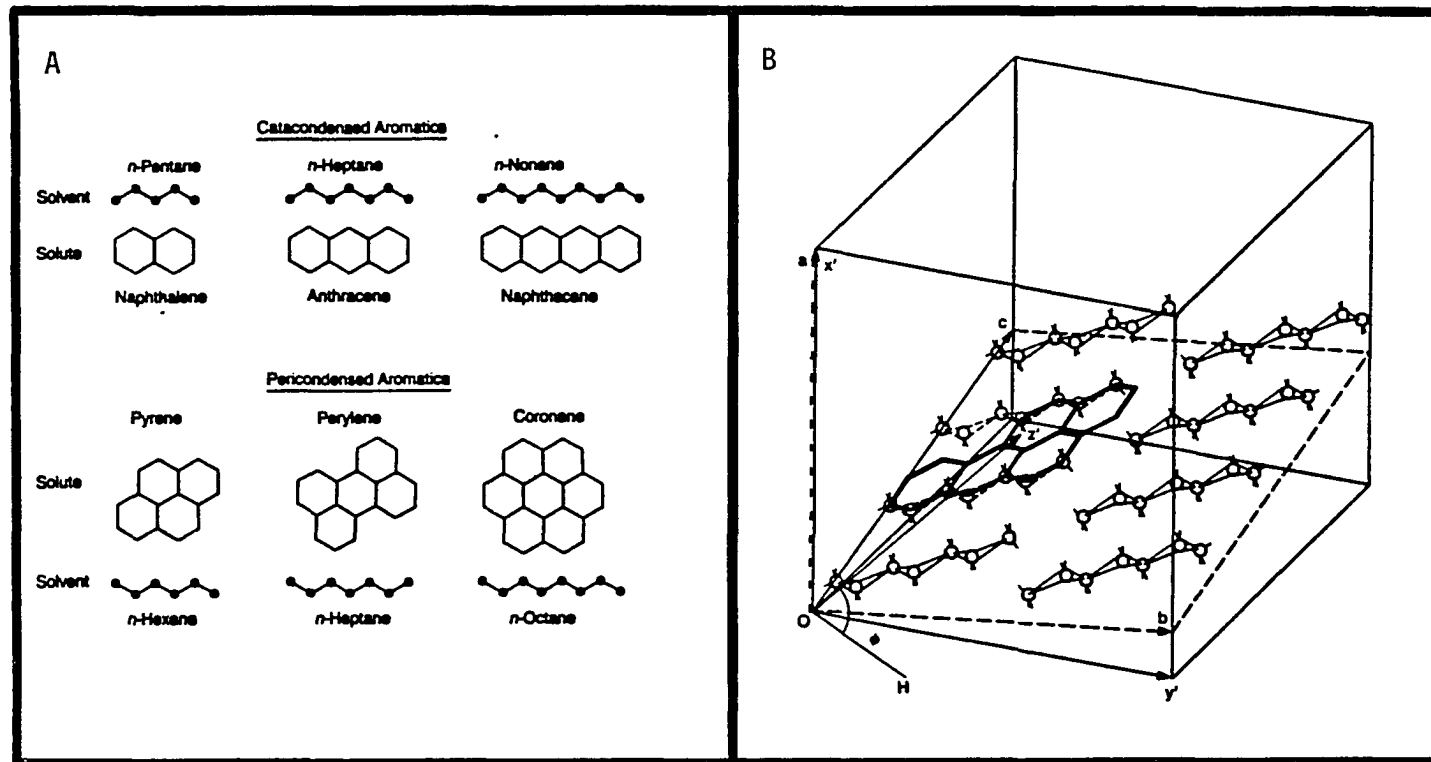


Figure 1. Geometric relationships of *n*-alkane and PAH molecules, which attempt to rationalize the Shpol'skii "key and hole" rule (A) and schematic representation of the orientation of paraffin chains in an *n*-heptane single crystal and substitution of benzo(a)pyrene for *n*-heptane molecules in a lamellar plane; the planar *n*-heptane molecules occur as parallel zig-zag chains, with the chain axis making a 71° angle with the crystal growth axis, a

The solvents indicated are those that have been experimentally determined to give quasilinear spectra (78). Because of the strong correlation of development of the Shpol'skii effect with dimensional and geometric similarities between the solvent host and solute molecules, the explanations of the Shpol'skii effect generally have been based on the Shpol'skii "key and hole" rule, i.e., the n-alkane carbon skeleton chain lengths are equal to the longest dimension of the carbon skeleton of the guest aromatic molecules (95,136). This rule, however, is not as restrictive as may be implied, although serious mismatches of the n-alkane chain length with solute molecular dimension may lead to severe line broadening (137). It is generally believed that planar aromatic compounds are oriented in the alkane lattice with their aromatic planes parallel to the carbon skeleton chains of the alkane molecules (138-140). An example of one such situation, benzo(a)pyrene in crystalline n-heptane, is shown in Fig. 1B. Benzo(a)pyrene is believed to occupy a site created by the displacement of two heptane molecules (shown as dashed lines) in an n-heptane single crystal. The orientation of all the impurity molecules in the solid solution will not be identical. In fact, substitution in a limited number of crystallographically different sites is observed. The important consideration is that all of the PAH molecules that occupy specific types of crystallographic sites are in strictly oriented positions, experience identical molecular fields, and behave as isolated molecules (78).

Concentration effect The dependency of Shpol'skii effect spectra on concentrations has been of great concern. Depending on the na-

ture of the solvent and the cooling rate, two totally different concentration behaviors of quasilinear spectra are often observed. In the first kind, quasilinear emissions are observed at low concentration and as the concentration increases, diffuse bands are superimposed on the quasilinear spectrum. This behavior has been interpreted as follows. The solute molecules are of comparable sizes, and the quasilinear emissions at low concentrations are due to the matrix-isolated solute molecules, whereas the broad emissions observed at high concentrations are due to the formation of aggregates of the solute molecules, or even precipitation of microcrystals of these molecules. In the second kind, the spectra consist of diffuse bands at low concentrations and as the concentration of solute increases, the spectra become quasilinear but are still accompanied by diffuse bands. The diffuse bands at low concentrations have been attributed to severe site heterogeneous broadening, presumably due to a mismatch of molecular dimension. The appearance of quasilines at higher concentrations is associated with the alignment effect of the solvent crystal lattice near the solute molecules. As the solute concentration increases further, the extent of orderliness of the solute molecules relative to the solvent is also increased, leading to a decrease of site heterogeneity (141-143).

Cooling rate effect The rate of cooling of sample solutions plays an important role in determining the width and intensity of the quasilinear luminescence emission spectra observed from aromatic hydrocarbons in Shpol'skii matrices (144,145). Two different observations have been described depending on the type of aromatic solutes. First,

quasilinear spectra were obtained independently of the cooling rate provided that the solute concentration was lower than the threshold concentration, at which crystallites appeared (146-149). In this case, the dimension of solute molecules allowed substitution of two or more n-alkane molecules and exhibited spectroscopic properties with all the characteristic features of isolated molecules. For the second type of observations, quasilinear spectra were obtained only if a fast cooling rate and suitable concentration conditions were fulfilled (149-153). Because of the low solubility of polynuclear aromatic hydrocarbons in n-alkane, the occurrence of the quasilinear spectra were attributed in this case to the formation of highly supersaturated solid solutions. In the presence of a dissolved materials, the crystal structure of a solid solution depends on the crystallization conditions. With a slow cooling rate, the precipitation of the solute is expected as soon as the experimental conditions allow molecular movement and migration. Therefore, phase separation due to the formation of aggregates or crystallites of solute will occur. These aggregates and/or crystallites have different spectroscopic properties from that of isolated molecules, e.g., different absorbitivity, smaller quantum yield, occurrence of solute-solute interaction, etc. (146), hence, broad spectra are obtained. Furthermore, when quasilinear spectra are observed, particularly when accompanied by broad bands from aggregates and/or crystallites, the distribution of molecules among different sites changes, depending upon the cooling rate and solute concentration. Therefore, fast reproducible

cooling rates with appropriate solute concentration are needed to minimize these undesirable effects.

Presence of other impurities An impurity, other than the analyte in question, can substantially affect the structure of a crystalline solution. For example, the impurity may stabilize a crystalline modification of the host that would be unstable under the prevailing conditions if there were no impurity, e.g., the fluorescence and absorption spectra of perylene in n-pentane at concentration $<10^{-4}$ M consist of diffuse bands; these spectra become quasilinear in the presence of pyrene at concentration $>10^{-3}$ M. Other impurities may deform the crystal lattice causing restructuring of the matrix through formation of local or dispersed aggregates. As a result, the analyte molecules may become incorporated in more than one media and their behavior as isolated molecules will be destroyed. Finally, impurities other than the analyte may alter the external appearance of the growing crystals; the extent of this effect depends on the concentration and solubility of the impurity and the conditions of crystallization (154-156).

Tunable dye laser excitation of Shpol'skii systems

Although Shpol'skii spectra are quasilinear, a complex mixture of several PAHs or their derivatives, occupying several types of crystalline sites in the Shpol'skii matrix may still present the analyst with hopeless spectral overlap. An additional refinement must, therefore, be added by selectively exciting only those molecules of a specific compound occupying the same crystallographic site in the matrix. Since the absorption spectra of PAHs in Shpol'skii matrix are also quasilinear,

these narrow absorption bandwidths allow the selective excitation of a given PAH species present in a complex mixture. Thus, site-specific excitation of a given PAH species can be obtained through the utilization of narrow-bandwidth, tunable dye-laser excitation. The capability of exciting these site-specific spectra not only enhanced specificity but also provides added flexibility in the event that spectral interferences by other sample constituents invalidate the use of one site-specific line. Should such interferences occur, other interference-free, site-specific lines may usually be selected. Because the number of photons emitted by a sample increases linearly (up to the point of saturation) as the number of excitation photons, the best signal levels are obtained with high power laser excitation. Moreover, because of the narrow absorptive feature exhibited by PAHs in a frozen Shpol'skii matrix, narrow band lasers can provide more effective excitation of PAH luminescence and, consequently, an enhanced detection sensitivity. In fact, coupling the laser with its powerful advantages (monochromaticity, high intensity, phase coherence, high degree of collimation, short pulse duration, polarized radiation, and low stray light) makes the Laser Excited Shpol'skii Spectroscopy (LESS) a technique of tremendous potential for high resolution spectroscopy.

Scope of application

The discovery that quasilinear spectra can be obtained from polyatomic molecules stimulated a large number of studies in the field of the electronic spectroscopy of complex organic compounds. The quasilinear spectra are very characteristic and exhibit absolute individual-

ity as well as selectivity. Further, they can be exceedingly useful for "fingerprinting" PAHs in complex samples, even when these compounds have similar chemical properties. Moreover, the quasilinear spectra can also be used to make accurate observations of molecular properties, such as electronic and vibrational transitions (157,158).

The wide array of organic compounds that exhibit quasilinear spectra in Shpol'skii hosts are documented in an excellent review (159). Typical aromatic structures that should provide quasilinear spectra in appropriate n-alkane solvents are shown in Fig. 2. Analytical applications of conventional Shpol'skii spectroscopy and of LESS for the analysis of PAH mixtures have been documented (160-174). A summary of recent observations on the Shpol'skii effect spectra is given in a recent article (78).

In spite of the large number of applications published to date, there have been repeated assertions in the literature that Shpol'skii effect spectroscopy is potentially burdened with a number of shortcomings that may limit the ultimate analytical utility of the technique. These limitations have been identified as: (a) nonreproducibility in relative site populations, hence, nonreproducibility in the relative fluorescence intensity of site-specific lines (175,176); (b) the bandwidths may be dependent on freezing rate (177,178), final temperature (145) and solute concentration (99); (c) restricted linear working range because of aggregate formation; (d) excessive scattering of the excitation radiation by the polycrystalline solid (175); (e) difficulties of achieving a proper match of molecular dimensions between the solvent and



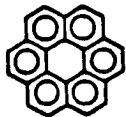
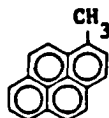
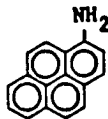
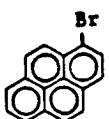
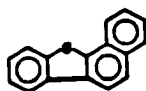
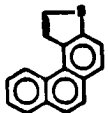
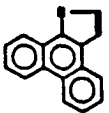

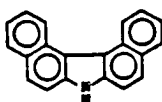
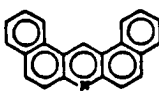

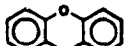
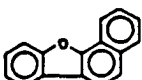
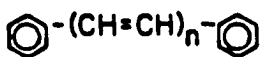
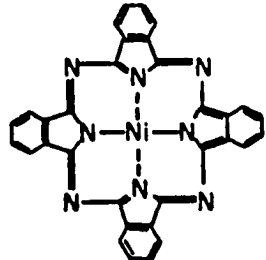
Normal PAHs	 Anthracene	 Benzo(a)pyrene	 Coronene
PAHs Derivatives	 1-Methylpyrene	 1-Aminopyrene	 1-Bromopyrene
S-Heterocyclic	 Benzo(b)naphtho- (2,1-d)thiophene	 Phenanthro- (3,4-b)thiophene	 Phenanthro- (9,10-b)thiophene
N-Heterocyclic	 Carbazole	 7H-Dibenzo- (c,g)carbazole	 Dibenzo(a,j)- acridine
O-Heterocyclic	 Dibenzofuran	 Xanathene	 Benzo(b)naphtho- (2,1-d)furan
Diphenylpolyenes	 $\text{C}_6\text{H}_5-(\text{CH}=\text{CH})_n-\text{C}_6\text{H}_5$ $n = 1 - 7$		
Organometallic	 Nickel phthalocyanine		

Figure 2. Typical aromatic structures that can provide quasilines in appropriate n-alkane solvents

solute molecules (84,179); (f) low solubility of PAHs in n-alkane solvents (180); (g) limitation of solutes to those soluble in n-alkane; (h) inner filter and enhancement effects (181); (i) intermolecular interactions that may effect site structure and population (182); and (j) the high spectral resolution achieved in Shpol'skii matrices is beyond the capabilities of most commercial fluorescence spectrometry (176).

The recent work by Yang et al. and others (169-174) has demonstrated that these limitations can either be eliminated or significantly reduced by introducing a number of refinements. A major innovation recently introduced into the technique was the use of unbleached dye laser excitation of the luminescence. This innovation plus refinements in procedures and experimental conditions have made it possible to either eliminate or reduce the limitations discussed above to tolerable proportions, as exemplified by the following:

- 1) The laser monochromaticity allows: (a) site specific excitation of a given PAH occurring in a complex mixture; (b) produces sharper line luminescent spectra; and (c) causes lower level of exciting light scatter to the analyte luminescent signal.
- 2) Higher analyte signal levels are obtained because of the higher radiant fluxes in the monochromatic exciting radiation leading to improvement in power of detection.
- 3) The higher powers of detection provided by (2) makes it possible to work at much lower solute concentration levels, typically down to 10^{-6} M. At these concentrations and when fast reproducible cooling regimes are followed, the spectra of the molecules at various sites

have reproducible bandwidths and intensity ratios which resulted from: (a) reduction of inner filter effect; (b) elimination of aggregates and microcrystallites formation; and (c) minimization of solute-solute interaction. Further, the linear dynamic range is extended to more than 3.5 decades showing better conditions for quantitative analysis.

- 4) Further improvement in limits of detection achieved through the reduction in stray light contribution to the analyte signal by the use of holographic gratings (to reduce far scatter), filters, and good optical engineering.
- 5) The high degree of collimation of laser beams permits the use of much smaller sample volumes for which more rapid and reproducible cooling regimes can be implemented.
- 6) The use of mixed solvents (159,182) and solvents such as cyclohexane and tetrahydrofuran (182) to expand the scope of application to a broad range of compounds.
- 7) The use of internal reference and standard addition techniques to internally compensate for residue inner filter and enhancement effects (182,184).

Laser Technology

The word laser is an acronym for light amplification by stimulated emission of radiation. A stimulated emission occurs when a photon strikes an already excited atom, thereby causing that atom to emit its stored photon, with the condition that the energy of the impinging photon is exactly equal to the energy of the stored photon. Another re-

quirement for the stimulated emission is that the lasing medium contains more excited atoms than unexcited ones. Laser operation occurs inside a resonant optical cavity, in which the amplification process builds up or strengthens until a very intense beam is formed. The optical cavity may be filled with a gas, a semiconductor, or a dye solution.

The use of lasers has had a dramatic impact in analytical spectroscopy. New spectral information, difficult or impossible to gather by classical spectroscopy, extremely high resolution spectroscopy, and selective excitation and detection of single and molecular quantum states are examples of the role played by lasers in analytical chemistry (185-187).

In the present study, a dye laser pumped by an excimer laser was used to excite the Shpol'skii effect luminescence emission. When excitation wavelengths lower than 340 nm were needed, the output beam of the dye laser was frequency doubled using a doubling crystal.

Excimer laser

Excimers are molecules that exist only in the electronically excited state. The basic principles of an excimer laser are illustrated in the schematic energy level diagram of Fig. 3A. An excited diatomic molecule is formed either via an association reaction involving an excited atom x^* and another atom y or by the recombination of a positive ion x^+ and a negative ion y^- . In such a reaction, the reactants spiral in towards one another from an initially large value of internuclear separation towards values close to 0.1 nm at which the energy curve corresponding to the excited bound molecular level $(xy)^*$ has its mini-

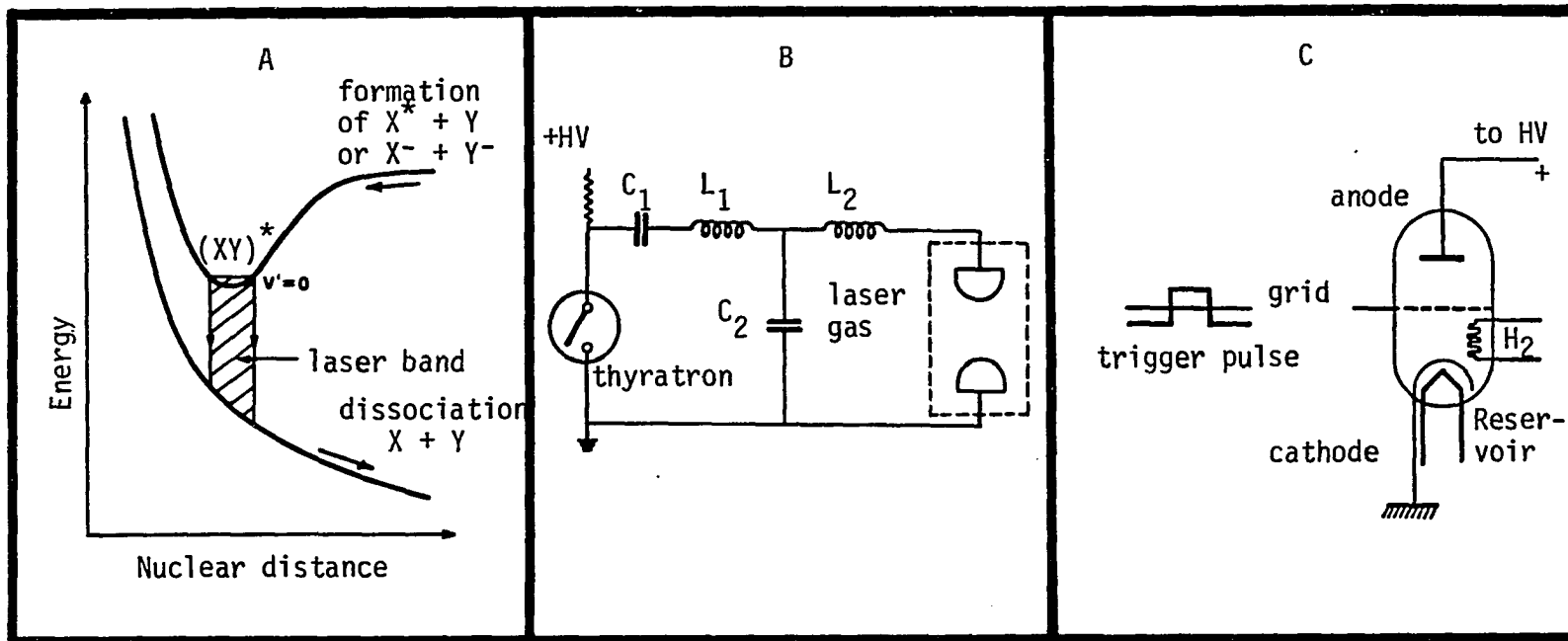


Figure 3. Energy levels of an excimer laser (A), typical excimer laser discharge circuit (B), and typical layout of a standard thyatron (C)

mum. The formation reaction usually involves a third collisional partner z , which could be another atom of type x or y or of a different species, or it could initially be part of a molecular combination xz or yz . The departure of z following the collision allows $(xy)^*$ to stabilize in a low vibrational level.

The upper laser level is usually pumped by a pulsed electron beam, thus, making an excimer laser a pulsed source. This upper level is populated not by excitation from the ground state, but via the reactions mentioned above. Another feature shared by all excimer systems is that the lower laser level (the molecular ground state) is either fully repulsive or has at most only a very shallow potential well. This means that the lower level is totally unstable and this is very advantageous from the point of view of obtaining a population inversion (188-191).

When a large number of excimers has been created in a given volume, laser action can be produced on the transition between the upper (bound) state and the lower (unbound) level. A simplified diagram of the principal components of a typical excimer laser, pulse-generating circuit is shown in Fig. 3B. When the thyatron switch (Fig. 3C) is closed, the energy stored on the primary capacitor C_1 is transferred to the peaking capacitor C_2 and, subsequently, discharged into the excimer gas load. The repetition rate of the pulses is controlled by the thyatron.

One important example of excimer laser is the xenon chloride laser (192). In its lowest excited state configuration, xenon displays properties similar to those of the corresponding alkali metal atom, cesium. In this state, xenon can then react with halogen-containing molecules to

produce diatomic noble gas-halide molecules in strongly bound ionic states. Unlike the alkali-halide state, however, these are excited states which radiate energy upon decaying to lower electronic states.

The high optical power densities achievable from laser sources make them ideal candidates for optically pumping organic dyes.

Dye lasers

The active substance for a dye laser is a highly fluorescent organic dye dissolved in a suitable organic solvent. The energy level diagram for a typical dye molecule is given in Fig. 4A. Each electronic state is actually made up of a set of vibrational levels (the heavier lines in the figure) and rotational levels (the lighter lines). The rotational lines are not normally resolved and, therefore, give rise to a continuum of levels between the vibrational levels. Intense radiation originating from the pump excimer laser that has a wavelength within the absorption band of the dye can excite a relatively large number of molecules into the excited S_1 manifold level, from which electronic transitions to some higher lying vibrational levels of S_0 may be stimulated by the laser action. Although the laser emission has a much narrower bandwidth than the normal fluorescence (see Fig. 4B), it can hardly be called "monochromatic" radiation. As a result of the closely spaced vibrational-rotational levels in the ground electronic state of the dye molecules, many transitions are allowed. As a consequence, broad-band emission with bandwidths ranging from 5 to 10 nm occurs depending on the compound used. However, when a fine-tuning device, e.g., a wavelength-selecting grating or prism, is inserted into the cavity, the output of

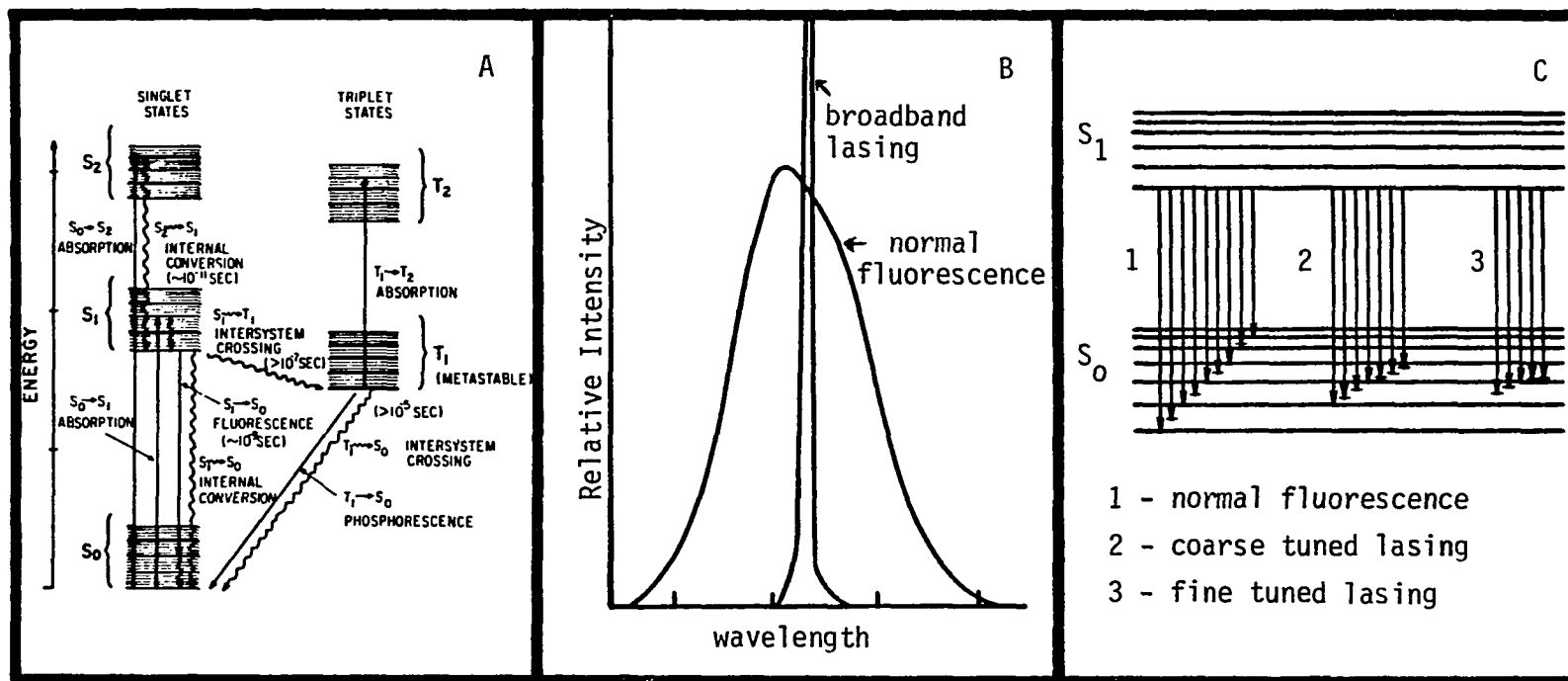


Figure 4. Energy level diagram of an organic laser dye molecule (A), a comparison of the emission bandwidth for normal fluorescence and broadband lasing of a typical laser dye (B), and an idealized energy diagram comparing normal fluorescence emission with coarse tuned and fine tuned lasing (C)

the laser can be narrowed to as little as 0.01 nm, as shown in Fig. 4C. (Dye laser fine-tuning procedures will be described in detail in Chapter 3). Because of the broad fluorescing spectral range of a dye, the emitted radiation can be fine tuned over a range of perhaps 40 nm. With a series of different dyes, dye tuning can be accomplished across a large spectral range from the UV to the near IR (193-195).

There are two distinctly different methods of pumping, namely, longitudinal (196) and transverse pumping (197,198). In longitudinal pumping, the pump beam (from a ruby laser) enters the dye laser cavity at a small angle to the cavity axis ($\sim 3^\circ$). In transverse pumping (the type used in the present study), the pump-laser radiation impinges on the dye cuvette in a direction normal to the axis of the dye laser emission. In the simplest case, a cylindrical lens focuses the pump-laser beam into a simple rectangular cuvette so that the line image lies directly behind and parallel to the entrance window and coincides with the optical axis of the dye laser.

Frequency doubler

The frequency doubler is a second harmonic generation (SHG) system used to obtain tunable laser output in the 217-365 region through the use of nonlinear optics. Basically, the frequency doubler takes the fundamental beam output of the dye laser and generates its second harmonic in the following manner. If an electrical field is applied across a material, a polarization will be induced. At low fields, this polarization will be linearly proportional to the electric field. However, there is a limit to the size of the electric field that can be applied

and the relation between the material polarization and the applied field remains linear. This is because the electron bonding energies decrease with the increasing electric field and, at sufficiently high electric field, the polarization fields induced in the material eventually become comparable to these electron bonding energies. Finally, the electron will be pulled off and dielectric breakdown occurs. Electromagnetic waves propagating through a material behave similarly (due to their oscillating electric field). When a laser beam with a given frequency interacts with a material far from any of its absorption lines and under the very high field strength encountered in the focused laser beam, the electric fields are comparable to electron bonding energies, thereby, inducing dielectric breakdown. The material will, therefore, distort any laser beam passing through it. This distortion is found to be the result of the addition of one or more harmonics to the original laser beam. Thus, the changes in the optical characteristics of crystals can be used to produce laser beams on new frequencies.

To obtain efficient conversion of the primary laser beam, the beam must be of high intensity and must be directed into the crystal at one specific angle - the angle at which phase matching of the input ground wave and the produced doubling frequency wave occurs. This angle can be reached by tilting the crystal with respect to the optical axis. It has been shown that the original and second harmonic beams propagate through the crystal at slightly different velocities, and that the second harmonic beam produced deep within the crystal has a different phase to that second harmonic beam produced near the surface of the crystal.

This timing difference produced at different points in the crystal reduces the power of the second harmonic beam. However, usually the second harmonic generated at the crystal surface is negligible compared to the intensity of the one generated in the bulk of the crystal. The most successful technique for phase matching uses birefringence (double refraction) to cancel out the effects of dispersion (199-201).

Object of the Present Work

To date, the LESS approach has been successfully utilized for the direct selective detection and quantitative determination of a variety of PAHs in various matrices. For this technique to gain wider acceptance, a far broader application base needs to be developed. In addition, potential problems that may emerge need to be identified and solutions need to be provided. Finally, an atlas of reference spectra useful for the selective identification of individual PAHs needs to be completed. The work reported in this thesis addresses all of these needs.

CHAPTER 3. APPARATUS, MATERIALS AND PROCEDURES

Apparatus

A block diagram of the LESS system is shown in Fig. 5. The components of the system are summarized in Table 1. A more detailed description for these components is given below.

Fluorescence excitation source

The excitation source was a tunable dye laser pumped by an XeCl excimer laser. To reach excitation wavelength from 217-360 nm, the output beam of the dye laser (for some suitable dyes) was frequency doubled using a frequency doubler.

Excimer laser The Model EMG101 excimer laser utilized a gas mixture composed of 60 mbar xenon, 80 mbars of 5% hydrogen chloride in helium and 800 mbar argon. The emitted XeCl laser beam had a rectangular shape (dimensions $\sim 10 \times 25$ mm), a peak output wavelength of 308 nm, a pulse energy of 120-140 mJ per pulse at a pulse duration of ~ 10 ns, a pulse repetition rate of 30 Hz, and the capacity to pump all dye lasers from 320 nm to about 970 nm.

Dye laser The Model FL500 Lambda Physik dye laser followed the design of Hansch (198). It incorporated an oscillator-amplifier setup. A holographic grating, beam expanding telescope, dye cell, and coupling mirror were utilized in the oscillator stage. The grating, in connection with a conventional sine bar mechanism, could be either set at a specific wavelength or scanned linearly in wavelength by a wavelength scan controller Model LF500. The dye laser output had a beam width of

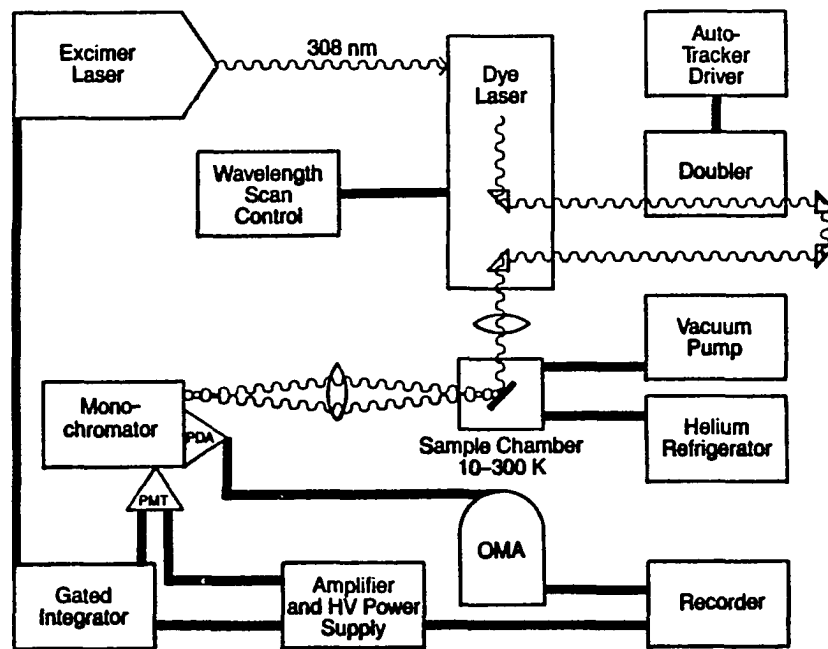


Figure 5. Schematic diagram of the experimental apparatus utilized for the observation of laser-excited Shpol'skii spectroscopy

Table 1. Experimental apparatus of laser-excited Shpol'skii spectroscopy system

No.	Component	Model No.	Manufacturer
1	Excimer multigas laser	EMG101	Lambda Physik, West Germany
2	Dye laser	FL2000	Lambda Physik, West Germany
3	Dye laser scan controller	FL500	Lambda Physik, West Germany
4	Frequency doubler	512SHG	Interactive Radiation Inc., Northvale, NJ
5	Monochromator (0.64 m)	HR-640	Instruments SA, Inc., Metuchen, NJ
6	Microprocessor scan controller	980022-23	Instruments SA, Inc., Metuchen, NJ
7	Silicon photodiode array	1412	EG&G Princeton Applied Research, Princeton, NJ
8	Detector controller	1218	EG&G Princeton Applied Research, Princeton, NJ
9	System processor	1215	EG&G Princeton Applied Research, Princeton, NJ
10	Photomultiplier	R955	Hamamatsu Co., Middlesex, NJ
11	HV power supply	110	Pacific Photometric Instrument, Emeryville, CA
12	Omingraphic x-y recorder	2200	Houston Instrument, Austin, TX
13	Cryogenic refrigerator	CSW-202	Air Products and Chemicals, Inc., Allentown, PA
14	Temperature indicator/controller	3700-APL-E	Air Products and Chemicals, Inc., Allentown, PA
15	Diffusion vacuum pump	1397	Welch Scientific Co., Skokie, IL
16	Turbo vacuum pump	TCP040	Pfeiffer, West Germany
17	Thermocouple and emission regulated ion gauge	710	NRC Equipment Co., Newton, MA

~0.02 nm FWHM (full width at half maximum). Further details about the dye laser components, laser dyes experimental conditions, and dye laser tuning will be described later in this chapter.

Frequency doubler The Inrad Model 512SHG Autotracking system employed in the present work consisted of a doubler (crystal assembly) and an electronic autotracker. The autotracker sensed the UV output of an angle-tuned, second-harmonic generation crystal (potassium dihydrogen phosphate, KDP, crystal) and adjusted the phase match angle so as to achieve maximum conversion from the visible into the ultraviolet. The active feedback design of the system accommodated crystal temperature changes produced either by ambient or laser-induced heating. After passage through the crystal, the beams were guided by quartz prisms into the sample cell, Fig. 6.

Optical system

A schematic diagram of the optical system is shown in Fig. 6. Initial optical alignment (aligning the dye laser components, positioning the excimer laser and centering the pump beam on the dye cell to match the optical axis of the cavity) was performed using a continuous wave He-Ne laser with emission at 632.8 nm (C. W. Radiation, Inc., Mountain View, CA).

In the oscillator stage of the dye laser, the grating and the output coupler were the boundaries of the optical cavity. A holographic diffraction grating with 2440 1/mm (used in the first order) was the wavelength selecting element of the dye laser. The grating reflected only one wavelength depending on the input angle and the plane front of

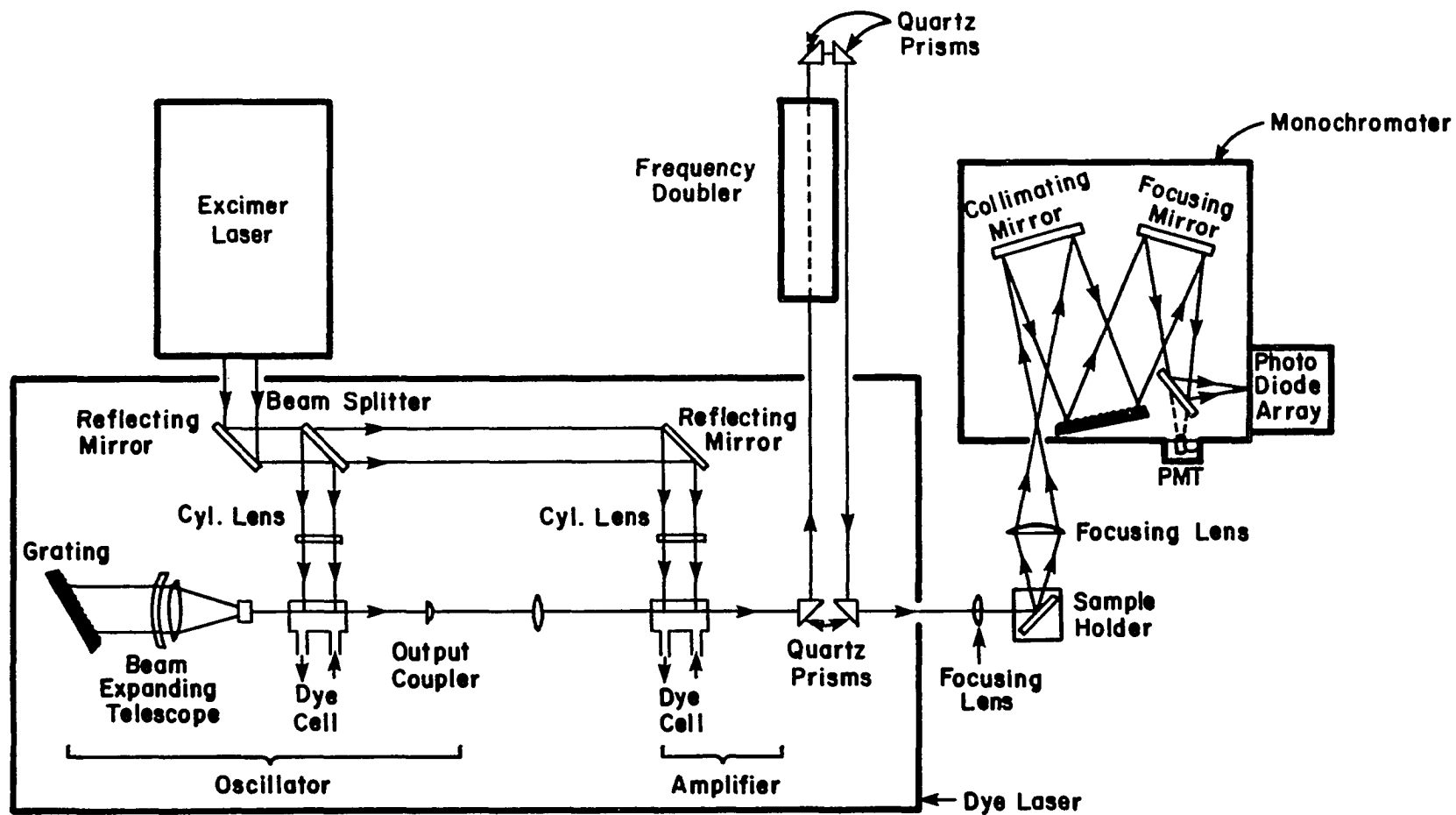


Figure 6. Optical schematic diagram of the LESS system

the outcoupling lens. The output coupler (the other end of the resonator) was a $f = -50$ mm plane-concave lens. The plane surface faced the dye cell and served as a 4% feedback mirror and the concave side faced a $f = 150$ mm convex lens. The latter was used to focus the oscillator beam into the amplifier cuvette. A beam expanding telescope (25x), consisting of diverging and converging lenses, was inserted between the grating and oscillator cell for better beam quality, smaller beam bandwidth, and exact wavelength selection. The reduction in bandwidth corresponds to the expanding factor as the divergence was lowered and more lines of the grating were illuminated. The optical axis of the dye laser was fixed by the entrance aperture (0.6 mm) of that telescope. The possibility of continuous tuning was maintained as wavelength changes were caused by rotation of the grating only.

With the aid of the two reflecting mirrors ($R \approx 98\%$) and by means of the quartz beam splitter, the pump beam was split into two beams of intensities about 10% and 90% of the original beam. The former was focused into the oscillator (responsible for the spectrally pure laser emission) and the latter into the amplifier (employed for the high peak power) cuvettes by two cylindrical focusing lenses ($F = 118$ mm of quartz glass). With controlling knobs of the cylindrical lens, the focused pumping beam was centered into the dye cell to match the optical axis of the dye laser. Due to this focusing, a thin line of fluorescence appeared across the front of the cell. The excitation laser pulses were so intense that an almost total population inversion occurred (for a given dye concentration in a given solvent). Spontaneous emitted pho-

tons of different frequencies then irradiated the grating and out-coupling mirror. Because of wavelength selection by the grating, only photons of certain wavelength were amplified and the emission was then stimulated for only part of the fluorescent spectrum, namely, the wavelength reflected by the grating back into the optical axis. The sideways position of the output coupler could be changed to steer the oscillator beam into the amplifier cell. The position of the two reflecting mirrors (Fig. 5) assured a 1-1.5 ns optical delay line (the time of the pump beam to reach the amplifier cuvette) such that the amplifier was only pumped when the oscillator emitted the small bandwidth beam instead of the superradiance at the beginning of the pulse.

When the frequency doubling system was required, the dye laser output was diverted to pass through the doubler by a system of quartz prisms. The two quartz prisms positioned inside the dye laser were mounted on a stage that could be reproducibly moved in and out of the optical path of the dye laser output. The dye laser or the second harmonic generation output beam was focused onto the sample (contained in a multiple sample holder) by another $f = 150$ mm plano-convex lens (the laser beam could be steered horizontally or vertically as needed by the lens control knobs). The luminescence generated in the sample was focused by a fused-silica, 100 mm focal length, and 76.2 mm diameter plane convex lens onto the entrance slit of a scanning monochromator. The distance between the focusing lens and the sample holder or the entrance slit was twice the focal length of the lens. The emission axis was perpendicular to the exciting laser beam. The sample holder was

positioned so that the angle between the sample face and the incident laser beam in the horizontal plane was about 55° in order to avoid collecting the laser radiation reflected off the sample holder optical window surface.

A 0.64 meter Czerny-Turner monochromator was used to disperse the luminescence emission. This f/5.7 monochromator was equipped with a 110 x 110 mm plane holographic grating having 1200 l/mm and a reciprocal linear dispersion of 1 nm/mm. Scanning of the monochromator was accomplished by a microprocessor scan controller. The monochromator was fitted with two interchangeable detectors, a photomultiplier tube (PMT), and a photodiode array detector (PDA). The selection of either detector was achieved by a simple change in position of a beam directing mirror. All of the optical components shown in Fig. 4 were mounted on an optical table (Newport Research Corp., Fountain Valley, CA).

Sample holder, vacuum sample chamber and refrigeration unit

A schematic diagram of the multiple cell holder is shown in Fig. 7A. The holder was designed to contain four cells and made of oxygen-free, high-conductivity copper of approximately 20 μ l capacity. The dimensions of the holder were 3.8 cm x 1.6 cm x 1.0 cm. A fused quartz plate (sealed to the main body of the holder via four O-rings, indium gaskets, and a copper retaining diaphragm) was used as the optical window. Sample solutions were injected into cell ports with a syringe, after which the parts were sealed with stainless steel set screws. The entire sample was then cooled to liquid N_2 temperature by emersion be-

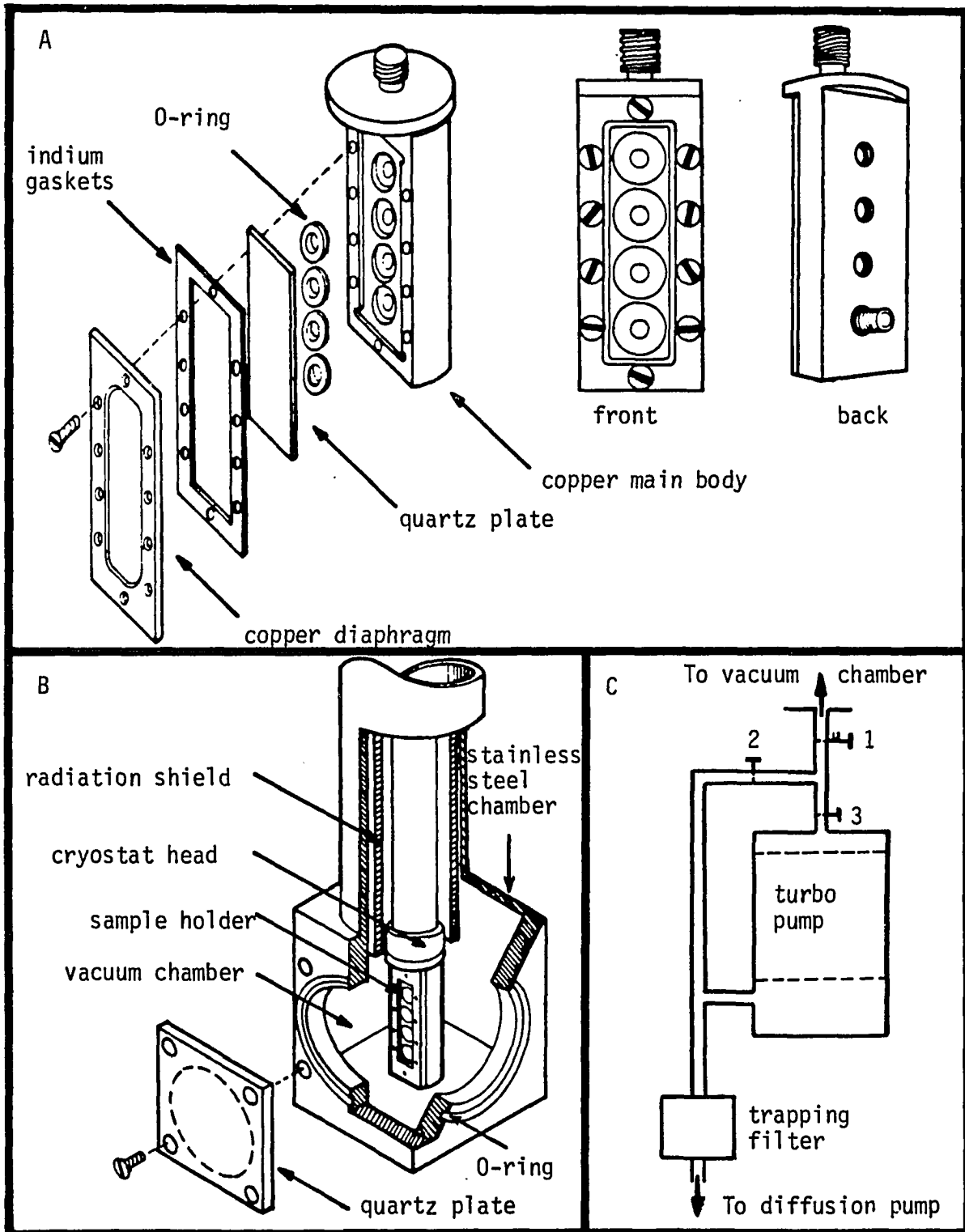


Figure 7. Exploded and assembled views of multiple sample holder (A), vacuum sample chamber (B), and part of the vacuum system (C) (sketches are not to scale)

fore mounting the holder in thermal contact with the cryostat head through an indium washer, Fig. 7B.

The cryogenic refrigeration system was a water-cooled, closed helium refrigerator that cooled the sample holder down to 15°K. The cryostat head along with the sample holder was inserted into a stainless steel chamber. The chamber had two 3.5 cm diameter viewing ports at 90° with respect to each other and was sealed with an O-ring and a square quartz plate. Inside the vacuum housing, a radiation shield was inserted between the cryostat head and the chamber walls to minimize radiation leakage to the cryostat cold surface.

In addition to thermal isolation of the sample, evacuation of the sample chamber was necessary to prevent ambient water vapor from condensation on the cold sample holder. Part of the vacuum system used in the present work is shown in Fig. 7C. A mechanical pump in series with a 2 in. diameter diffusion pump provided the first stage of vacuum. A turbo pump, backed by the diffusion pump and a trapping filter, reduced the pressure to $\sim 10^{-5}$ mbar. The vacuum system was designed in such a way that it prevented oil molecules (from the trapping filter) from diffusing to and condensing upon the cold sample holder when the pressure inside the vacuum chamber became very low. At the beginning of a run, while the three valves were closed, 1 to 3, the three pumps would be turned on, then valve 2 would be opened. When the pressure inside the vacuum chamber became about 100 mbar, valve 2 would be closed and valve 3 would be opened. To release the vacuum inside the chamber, valve 3 would be closed and valve 1 would be opened, and to establish the vac-

uum, valve 1 would be closed and valve 2 would be opened. Finally, the design allowed the refrigerator-vacuum assembly to be reproducibly raised or lowered to position anyone of the four cell parts in the optical path of the dye laser beam.

Detectors and data processing

Two detectors were used in the present work, namely, a photodiode array detector (PDA) and a photomultiplier tube (PMT). In the Model 1412, the PDA is a series of light-sensitive elements (1024 photodiode) etched onto a silicon chip. The elements work in parallel to simultaneously monitor a range of wavelength (through a 30 nm window) spread across the face of the chip by the holographic diffraction grating of the monochromator. Incident photons generate a charge that is stored on individual diodes. The accumulated charges are then switched sequentially by shift registers to form the detector output after being amplified. The Model 1218 Solid State Detector Controller stored the information that specified the detector scanning and provided for the setting of exposure times. The Model 1215 OMA-2 console, which was used as the data processing system, incorporated all the control functions required for the Model 1218 operation.

A side-on Hamamatsu photomultiplier tube, Model R955, operated at 1100 V was also employed as a detector. The power supply used for this tube was a Model 110 HV.

The spectra obtained from both detectors were recorded on a Model 2200 Omigraphic x-y recorder.

Materials

PNA's, solvents and solution preparation

The normal and heterocyclic polynuclear aromatic hydrocarbon compounds (collectively called PNAs in this thesis) are listed in Table 2. The n-alkane solvents (pentane, hexane, heptane, octane, nonane, decane, undecane and dodecane) were all 99% purity or more and were obtained from Aldrich.

Standard gravimetric and volumetric procedures were used in preparing the PNAs reference solutions. An ultrasonic bath was used to facilitate dissolution of some of the compounds. Freshly prepared PNA solutions were generally used. Stock solutions were prepared with a concentration level of at least 100 ppm and were stored in dark location when not in use; these precautions were followed to minimize absorption losses and photochemical decomposition of the PNAs.

Laser dyes, solvents and solution preparation

A variety of laser dyes were utilized in order to generate tunable radiation in specific spectral regions. These dyes (supplied by Lambda Physik, Gottingen, W. Germany or Exciton Chemical Co., Inc., Dayton, OH) and the relevant experimental parameters attended to these used in the laser systems are given in Table 3. The dye solvents were of spectroscopic grade and were obtained from Aldrich.

Excimer laser gases

The excimer laser gases, namely, xenon (Spectra Gases, Inc.), 5% hydrogen chloride in helium (Cryogenics Rare Gas Laboratory, Inc.) and

Table 2. Polynuclear aromatic compounds involved in the study

No.	Compound	Formula	MW	No. of Rings	Purity %	Source No. ^a
<u>Normal PAH</u>						
1	Anthracene	C ₁₄ H ₁₀	178	3	99.9	1
2	Anthracene-d ₁₀	C ₁₄ D ₁₀	188	3	98 ^b	1
3	Benzo[a]anthracene	C ₁₈ H ₁₂	228	4	99	2
4	Benzo[a]anthracene-d ₁₂	C ₁₈ D ₁₂	240	4	98 ^b	3
5	Chrysene	C ₁₈ H ₁₂	230	4	99	2
6	Chrysene-d ₁₂	C ₁₈ D ₁₂	242	4	98 ^b	3
7	Fluoranthene	C ₁₆ H ₁₀	202	4	99	2
8	Pyrene	C ₁₆ H ₁₀	202	4	99	2
9	Pyrene-d ₁₀	C ₁₆ D ₁₀	212	4	98 ^b	3
10	Benzo[b]chrysene	C ₂₂ H ₁₄	278	5	N ^c	4
11	Benzo[b]fluoranthene	C ₂₀ H ₁₂	252	5	N ^c	4
12	Benzo[k]fluoranthene	C ₂₀ H ₁₂	252	5	99.5	4
13	Benzo[a]pyrene	C ₂₀ H ₁₂	252	5	99+	1
14	Benzo[a]pyrene-d ₁₂	C ₂₀ D ₁₂	264	5	97 ^b	3
15	Benzo[e]pyrene	C ₂₀ D ₁₂	252	5	99	2

^aSources are: 1 - Aldrich Chemical Company, Inc., Milwaukee, WI.
 2 - Analabs, Inc., North Haven, CT.
 3 - Merck & Co., Inc./Isotopes, St. Louis, MO.
 4 - Commission of the European Communities, Community Bureau of Reference BCR.
 5 - Sigma Chemical Company, St. Louis, MO.
 6 - ICN Pharmaceuticals, Inc., Life Sciences Group, Plainview, NY
 7 - Alfred Bader Library of Rare Chemicals, Inc., Milwaukee, WI.
 8 - Professor M. L. Lee of Brigham Young University, Provo, UT.

^bAtom %D.

^cNot indicated.

Table 2. Continued


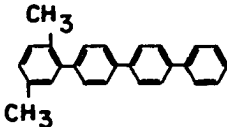
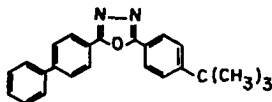
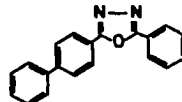
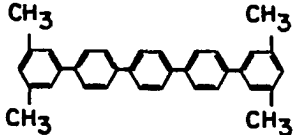
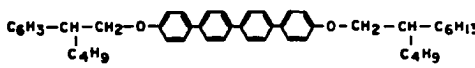
No.	Compound	Formula	MW	No. of Rings	Purity %	Source No. ^a
16	Dibenzo[a,h]anthracene	C ₂₂ H ₁₄	278	5	97	1
17	Perylene	C ₂₀ H ₁₂	252	5	99	2
18	Perylene-d ₁₂	C ₂₀ D ₁₂	264	5	97 ^b	3
19	Anthanthrene	C ₂₂ H ₁₂	276	6	99	2
20	Benzo[ghi]perylene	C ₂₂ H ₁₂	276	6	99	2
21	Dibenzo[a,i]pyrene	C ₂₄ H ₁₄	302	6	P ^g ^d	5
22	Indeno[1,2,3-cd]pyrene	C ₂₂ H ₁₂	276	6	N ^c	4
23	Coronene	C ₂₄ H ₁₂	300	7	98	1 & 2
<u>PAHs Derivatives</u>						
24	1-Aminoanthracene	C ₁₄ H ₁₁ N	193	3	N ^c	1 & 6
25	1-Aminopyrene	C ₁₆ H ₁₁ N	217	4	N ^c	1
26	2-Aminopyrene	C ₁₆ H ₁₁ N	217	4	N ^c	7
27	4-Aminopyrene	C ₁₆ H ₁₁ N	217	4	N ^c	7
28	7-Methylbenzo[a]pyrene	C ₂₁ H ₁₄	266	5	N ^c	7
29	7,10-Dimethylbenzo[a]pyrene	C ₂₂ H ₁₆	280	5	N ^c	7
<u>Heterocyclic PAHs</u>						
30	Dibenzofuran	C ₁₂ H ₈ O	168	3	99+	1
31	Dibenzofuran-d ₈	C ₁₂ D ₈ O	176	3	98 ^b	3
32	Benzo[b]naphtho[1,2-d]thiophene	C ₁₆ H ₁₀ S	234	4	N ^c	8
33	Benzo[b]naphtho[2,1-d]thiophene	C ₁₆ H ₁₀ S	234	4	N ^c	8
34	Benzo[b]naphtho[2,3-d]thiophene	C ₁₆ H ₁₀ S	234	4	N ^c	8
35	Benzo[2,3]phenanthro[4,5-bcd]thiophene	C ₁₈ H ₁₀ S	258	5	N ^c	8
36	Chryseno[4,5-bcd]thiophene	C ₁₈ H ₁₀ S	258	5	N ^c	8

^dPractical grade.

Table 2. Continued

No.	Compound	Formula	MW	No. of Rings	Purity %	Source No. ^a
37	Dibenzo[a,j]acridine	C ₂₁ H ₁₃ N	279	5	Pg ^d	5
38	13H-dibenzo[a,i]carbazole	C ₂₀ H ₁₃ N	267	5	98	1
39	7H-dibenzo[c,g]carbazole	C ₂₀ H ₁₃ N	267	5	95	2

Table 3. Laser dyes used and their experimental conditions

No.	Dye Name	MW	Structure (202)	Solvent	Oscillator ^a Concen. (g/l)	Lasing Wave- length (nm)	
						Peak	Range
1	P-terphenyl	230		cyclohexane	0.70	339	323-362
2	DMQ	334		cyclohexane	0.17	359	341-368
3	BPBD	354		dioxane	0.30	363	356-385
4	PBD	298		dioxane	0.20	378	353-381
5	QUI	606		dioxane	0.20	390	368-402
6	BBQ	675		ethanol:toluene (1:1)	0.35	385	366-400

^aThe concentration inside the amplifier was 1/3 of the concentration in the oscillator.

Table 3. Continued

No.	Dye Name	MW	Structure (202)	Solvent	Oscillator ^a Concen. (g/l)	Lasing Wave- length (nm)	
						Peak	Range
7	PBBO	347		dioxane	0.40	396	386-420
8	DPS	332		dioxane	0.25	406	399-415
9	Stilben 3	562		methanol	0.65	425	412-443
10	Coumarin 120	175		methanol	0.82	441	423-462
11	Rhodamine 590	479		metahnol	1.2	581	569-608

argon (Matheson Gas Products, Inc.) were all of ultra-high purity (>99.99%).

Environmental samples

The environmental samples involved in the present work were urban air particulate (National Bureau of Standards Reference Material, SRM-1649), diesel particulate (SRM-1650), carbon black, and solvent-refined coal liquid (SRC-II). Carbon black was donated by Professor Milton L. Lee (Department of Chemistry, Brigham Young University, Provo, UT). Other samples were provided by the National Bureau of Standards (NBS). The nature of these samples and their preparations for analysis will be described in Chapter 5. Diphenylmethane (used in sample preparations) was obtained from Aldrich.

All chemicals involved in the present study were used as received without further purification, except diphenylmethane which was purified by distillation under vacuum.

Procedures

Wavelength calibration

Accurate wavelength adjustment of the monochromator is essential if corrected spectra are to be obtained and for qualitative and quantitative application studies sensitivity and selectivity may be sacrificed if the monochromators are not set at the optimum wavelengths. Since monochromators may go out of adjustment relatively frequently (and especially in the present system when the position of the beam directing mirror is changed while selecting in the process of choosing one of the

two detectors). Thus, a quick and convenient method for wavelength calibration is highly desirable. In the present work, wavelength calibration was performed before recording the luminescence spectra. For this purpose, a procedure based on using a sharp spectral lines from an auxiliary light source, recommended by American Society for Testing and Materials (ASTM) and others (203-205) was used to calibrate the emission monochromator which was then used to calibrate the mechanical counter of the dye laser. To calibrate the emission monochromator, a low pressure mercury pen lamp (Model 4987-003, Hamamatsu Corp., Middlesex, NJ) was inserted between the sample holder and the focusing lens in the front of the monochromator (Fig. 6). With suitable bandwidth and suitable instrument amplification (to avoid saturation of the detector, the sharp atomic emission lines of mercury (204) in the region where the spectrum would be recorded were used to calibrate the monochromator. This method allowed the emission monochromator to be calibrated over a wide wavelength range. After the initial calibration of the emission monochromator, a sharp dye laser line at a peak wavelength (to be used for exciting the fluorescence and obtaining the excitation spectrum for a given compound) was used to calibrate the mechanical counter of the dye laser.

Dye laser tuning procedure

In this work, the optical multichannel analyzer (OMA) was employed for the fine tuning of the dye laser using the scattered laser radiation. As can be seen from Fig. 6, the dye laser was initially set up in front of the excimer laser so that the pumping beam could be focused into both the oscillator and amplifier cuvettes. The following proce-

dure was then used in tuning the dye laser with the sample holder (e.g., containing frozen n-octane) in its usual position and the mechanical counter of the dye laser positioned at the peak wavelength of the dye in the dye laser cells.

1. The amplifier cuvette was removed.
2. A piece of white cardboard (or a fluorescing card in case of UV dyes) was placed adjacent to the grating to observe the zero order reflected by the grating.
3. The output coupler was blocked by a piece of paper inserted between it and the oscillator cuvette.
4. The pump beam was aligned in the oscillator cell to coincide with the optical axis of the dye laser. This alignment could be achieved by fine adjustment of the height and the tilt control knobs of cylindrical focusing lens. The adjustment was somewhat critical as the entrance aperture of the telescope (which fixes the dye laser axis) was only 0.6 mm. Alignment was concluded when the brightest circular image appeared on the cardboard.
5. The output coupler block was removed and the output coupler lens (in a swivel mount) was adjusted until a distinct diffraction pattern consisting of bright and dark vertical strips appeared on the cardboard. This is a necessary condition for laser action to occur.
6. At this stage, the laser spot can be easily seen on a reflecting white cardboard placed in front of the output coupler. As a further check, the output coupler was blocked by a piece of paper

inserted between dye cuvette and the output coupler to determine whether the diffraction pattern vanished. A check was also made to assure that the laser spot disappeared when a piece of paper was inserted between the telescope and the grating.

7. Once the laser spot was visualized, further tuning was accomplished via the OMA system. The oscillator beam was allowed to reach the sample holder where the scattered laser beam could be seen on the microprocessor screen of the OMA system. The scattered laser beam bandwidth and intensity could then be further "tweaked up" (could also be performed visually or by an energy meter) by trying different oscillator controls (height and tilt of the cylindrical lens as well as of the output coupler). The adjustment of the oscillator was conducted when the scattered laser beam had the smallest possible bandwidth and the highest intensity (at the dye peak).
8. The amplifier pump beam was then blocked and the amplifier cell was inserted in its position.
9. The lens between the output coupler and the amplifier was adjusted in the horizontal and vertical planes to steer the laser beam through the amplifier cuvette so that the laser beam appeared almost unobscured.
10. The amplifier pump beam block was then removed, and the axis of the amplifier pump beam adjusted by the height and the tilt of the cylindrical lens until it coincided with the oscillator beam transversing the amplifier cuvette. At this point, the output laser beam had the lowest bandwidth and highest intensity.

Sample loading and cooling procedures

To assure reproducible freezing-cooling cycles, the following procedures were followed. The multiple sample holder (designed to accommodate four samples) was first laid down horizontally with the optical window facing downwards. The sample solutions were then injected into the sample holder ports with syringes. The ports were sealed (one at a time to avoid changes in the sample concentration by solvent evaporation especially when n-pentane or n-hexane was used as solvent) with stainless steel screws such that no air remained in the ports. While still in a horizontal orientation, the sample holder was immersed in liquid nitrogen to solidify the sample. After a few minutes in liquid nitrogen, the sample holder (held in a liquid nitrogen soaked piece of cloth) was rapidly attached to the cold finger of the He cryostat precooled to 77°K. The cold finger was then quickly inserted in the vacuum housing, which was slightly pressurized with helium gas to prevent ambient air from entering. Thereafter, the cryostat pump evacuated the vacuum chamber. Cool down from ~77°K to 15°K required ~10 min. The reproducibility of the cooling rate was confirmed by the reproducibility of the relative intensities in the multiple site spectra of PAHs such as benzo(b)fluoranthene and indene(1,2,3-cd)pyrene.

Excitation and emission spectra

The excitation spectra and the proper, selectively-excited emission spectra (details will be given in Chapter 4) for a given compound were usually obtained by the following three steps: (a) a dilute solution of a particular PAH in the Shpol'skii host was irradiated by a short wave-

length, ~300 nm, to determine the nonselectively excited emission fluorescence spectra, (b) the excitation spectrum of the analyte was then determined by setting the spectrometer on the most intense emission peak exhibited by the spectrum obtained in the previous step, and (c) selective determination of the emission spectrum by setting the tunable dye laser on one of the most intense peaks in the excitation spectrum determined in step (b). If the nonselectively excited fluorescence spectrum showed several sites, the excitation and the emission spectra for each site could be determined by repeating steps (b) and (c) for each site.

In this work, no attempt was made to correct the observed spectra for the wavelength-dependent efficiency of the dye laser, the day-to-day variation in the laser energy, the spectral variations introduced by the monochromator-detectors combination and the spectrometer throughput.

Analysis of real samples

The procedures associated with the qualitative characterization and quantitative analysis of multicomponent mixtures in environmental samples by LESS are summarized here and will be described in more detail in Chapter 5.

Qualitative analysis The following were employed in the course of identification of various PNAs.

- 1) Specificity of the emission and excitation spectra.
- 2) The standard addition technique.

Quantitative analysis The following methods were used in quantitation of different PAHs.

- 1) Internal standard method.

- 2) Standard addition method.
- 3) Internal standard-standard addition combination technique.

CHAPTER 4. RESULTS AND DISCUSSION

Illustration of the LESS Technique

The Shpol'skii effect can be illustrated by the behavior of a very dilute solution (of ~ 1 ppm) of benzo(a)pyrene (B(a)P) in n-octane. When this solution is rapidly frozen to a temperature of 15 K and the fluorescence emission recorded, a sharp quasilinear spectrum is obtained as shown in the top spectrum of Fig. 8. This spectrum is very characteristic for B(a)P and very reproducible under certain experimental conditions. One of these conditions is the final temperature of the matrix. To demonstrate the temperature effect on the sharpness of the spectrum, different spectra were recorded while the temperature was gradually increased. The warming up procedure was chosen to study the temperature effect rather than the cooling down procedure to avoid the side effects that may arise from the slow cooling. The recorded spectra are shown in Fig. 8. It is seen that at room temperature, the fluorescence spectrum is broad. In fact, at room temperature, the specific vibrational structure that contains most of the characteristic information on a particular PAH is lost. Obviously, the temperature decrease from 300 to 15 K effects an enormous increase in spectral resolution. However, it must be emphasized that such enormous enhancements in resolution occur, for any PAH, only in certain very specific solvents. For example, as shown in Fig. 9, n-octane is an appropriate Shpol'skii solvent, whereas ethanol is not. In case of the ethanol solvent, severe heterogeneous band broadening apparently occurs, even at 15 K.

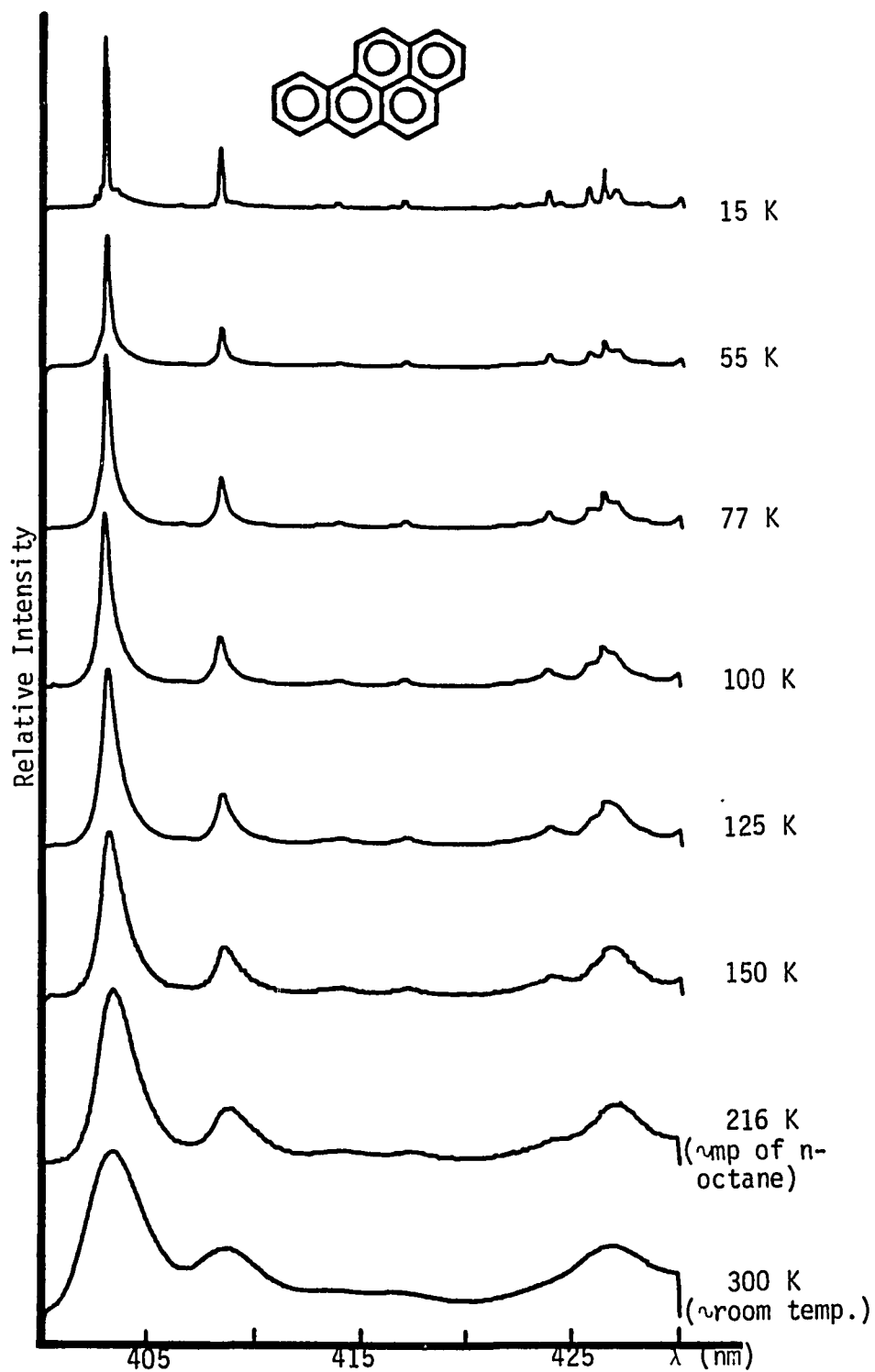


Figure 8. Effect of temperature on the sharpness of the fluorescence spectrum of benzo(a)pyrene in n-octane; $\lambda_{\text{ex}} = 339 \text{ nm}$

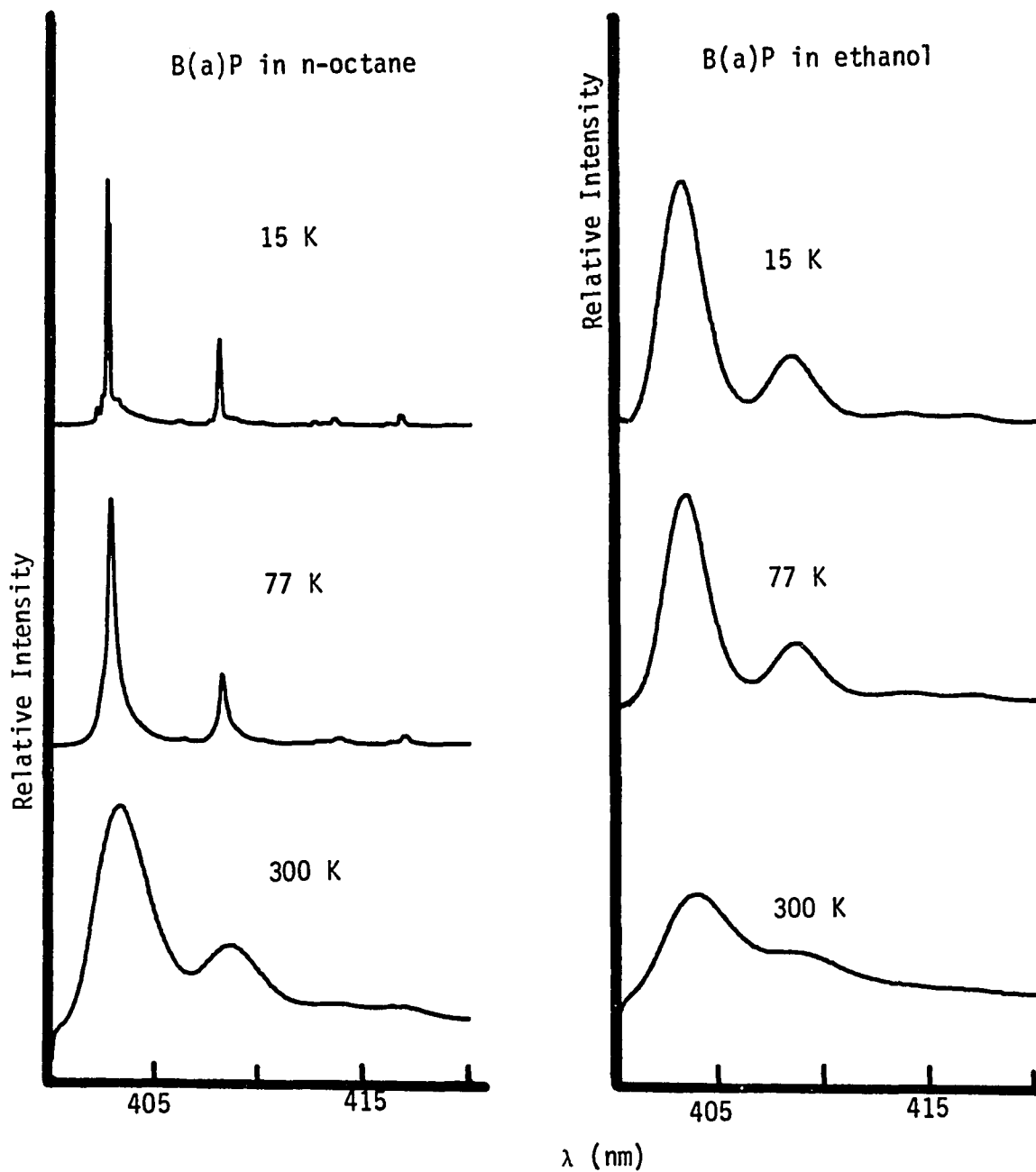
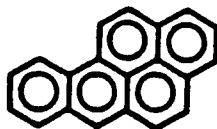


Figure 9. Fluorescence spectra of benzo(a)pyrene in n-octane and ethanol at different temperatures ($\lambda_{\text{ex}} = 339 \text{ nm}$)

Most successful observations of the Shpol'skii effect for PAH compounds have been made when *n*-alkane solvents were used. It has generally been accepted that matrices formed from the straight-chain hydrocarbon solvents of suitable molecular dimensions are required to obtain quasilinear emission spectra. A striking demonstration of the need to select the correct *n*-alkane solvent can be made by comparing the fluorescence spectra obtained for B(a)P in eight *n*-alkane solvents, ranging from *n*-pentane to *n*-dodecane, at $\lambda_{\text{ex}} = 339$ nm. As shown in Fig. 10, nonselective excitation at 339 nm into the congested region of the upper vibrational manifold of the excited singlet state leads to the emission of spectra of B(a)P molecules occupying different number of sites depending on the *n*-alkane solvent, e.g., 4 in *n*-heptane, 4 in *n*-octane, and 9 in *n*-nonane. As indicated earlier, these multiplets arise from a distribution of occupancy of different lattice sites by the solute molecules, resulting in different solute-host interactions. From Fig. 10, one can observe that *n*-octane is superior to other solvents for B(a)P and this is in a direct agreement with the "key and hole" rule mentioned before. The spectrum of B(a)P observed in *n*-dodecane is in agreement with previous observations that the use of *n*-paraffins with large molecules as solvents leads to diffuse spectra (88).

The occurrence of only a single sharp line in the 0-0 region of B(a)P in *n*-octane is not characteristic of all PAHs. As a consequence of the multiplet structures, the Shpol'skii effect spectra are generally quite complex and, hence, spectral interference has been a problem, particularly for the analysis of PAH mixture spectra when broadband

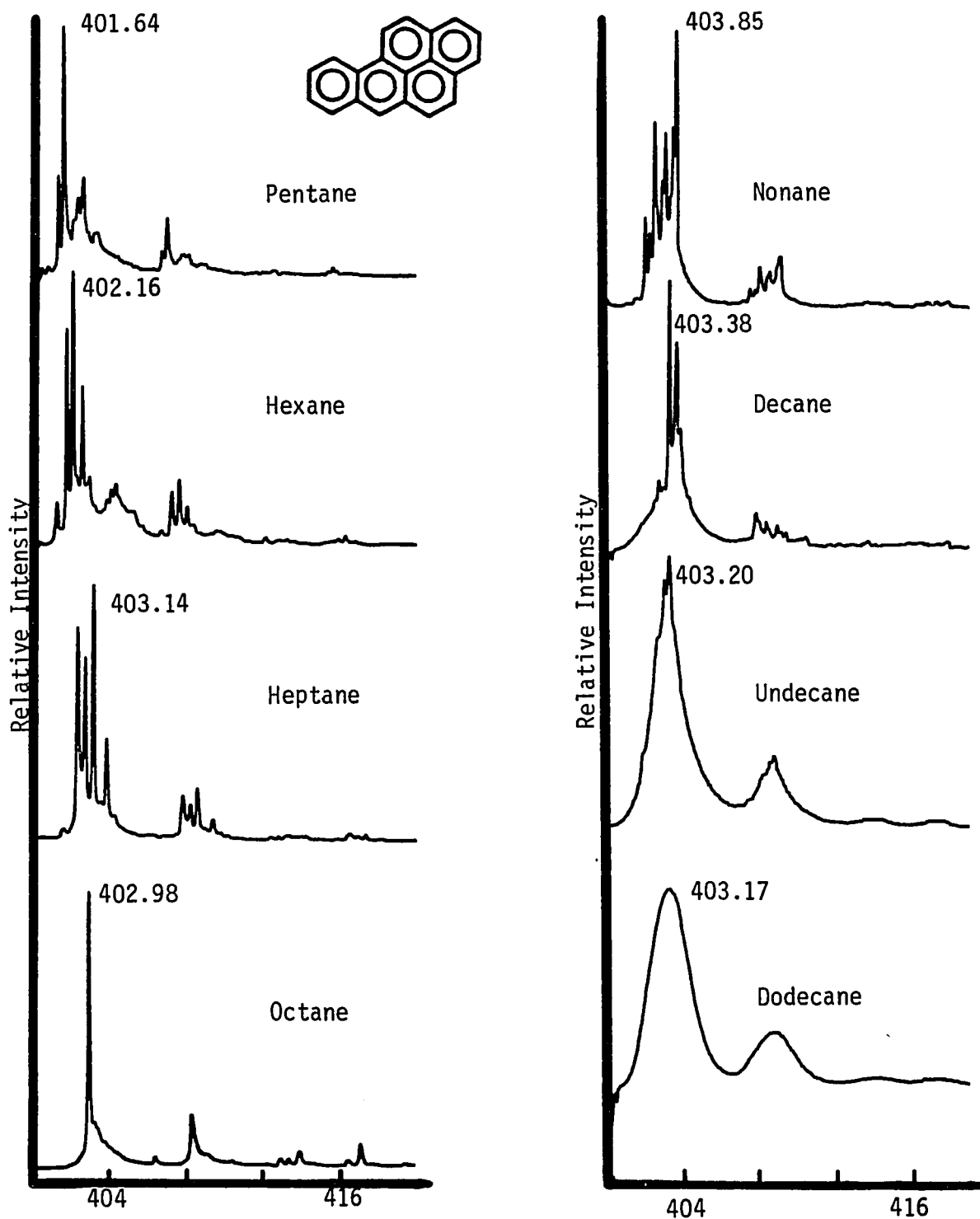


Figure 10. Solvent effect observed in the fluorescence spectra of 1 ppm benzo(a)pyrene in different n-alkane solvents at nonselective excitation wavelength of 339 nm

excitation sources have been utilized. However, due to the narrow absorption bandwidths ($\text{FWHM} < 10 \text{ cm}^{-1}$) of PAHs in n-alkane hosts, the complication of multiple sites common to Shpol'skii matrices has been largely eliminated by narrow-band, dye laser excitation.

The site selection technique of LESS involves several experimental steps. To illustrate these steps, the behavior of B(a)P in n-heptane (see Fig. 11) is chosen as an example. Initially, nonselective excitation at 339 nm into the congested upper vibrational manifold of the excited state leads to emission spectra of molecules occupying different lattice sites, as shown by spectrum A of Fig. 11. In the 0-0 region of this spectrum, it is easy to distinguish at least four sharp lines, which result from molecules occupying at least four different crystallographic sites. The wavelengths of these 0-0 transitions are at 402.36, 402.71, 403.14 and 403.88 nm and are indicated in the figure as site 1, 2, 3 and 4, respectively. If the spectrometer is now set to monitor the emission of 402.36 nm while the tunable dye laser output is scanned through the wavelength intervals shown for spectrum B, the excitation spectrum of molecules occupying site 1 may be obtained. The resulting excitation spectrum (Fig. 11B) clearly shows that the best wavelength to excite the fluorescence emission of B(a)P molecules occupying site 1 is 393.28 nm. If the laser radiation is now tuned to 393.28 nm, the fluorescence spectrum of site 1 molecules, as shown in Fig. 11B', may be recorded. In an analogous fashion, the best laser wavelengths for exciting analyte molecules that occupy crystallographic sites 2, 3 and 4 were determined to be 393.61, 394.00 and 394.72 nm,

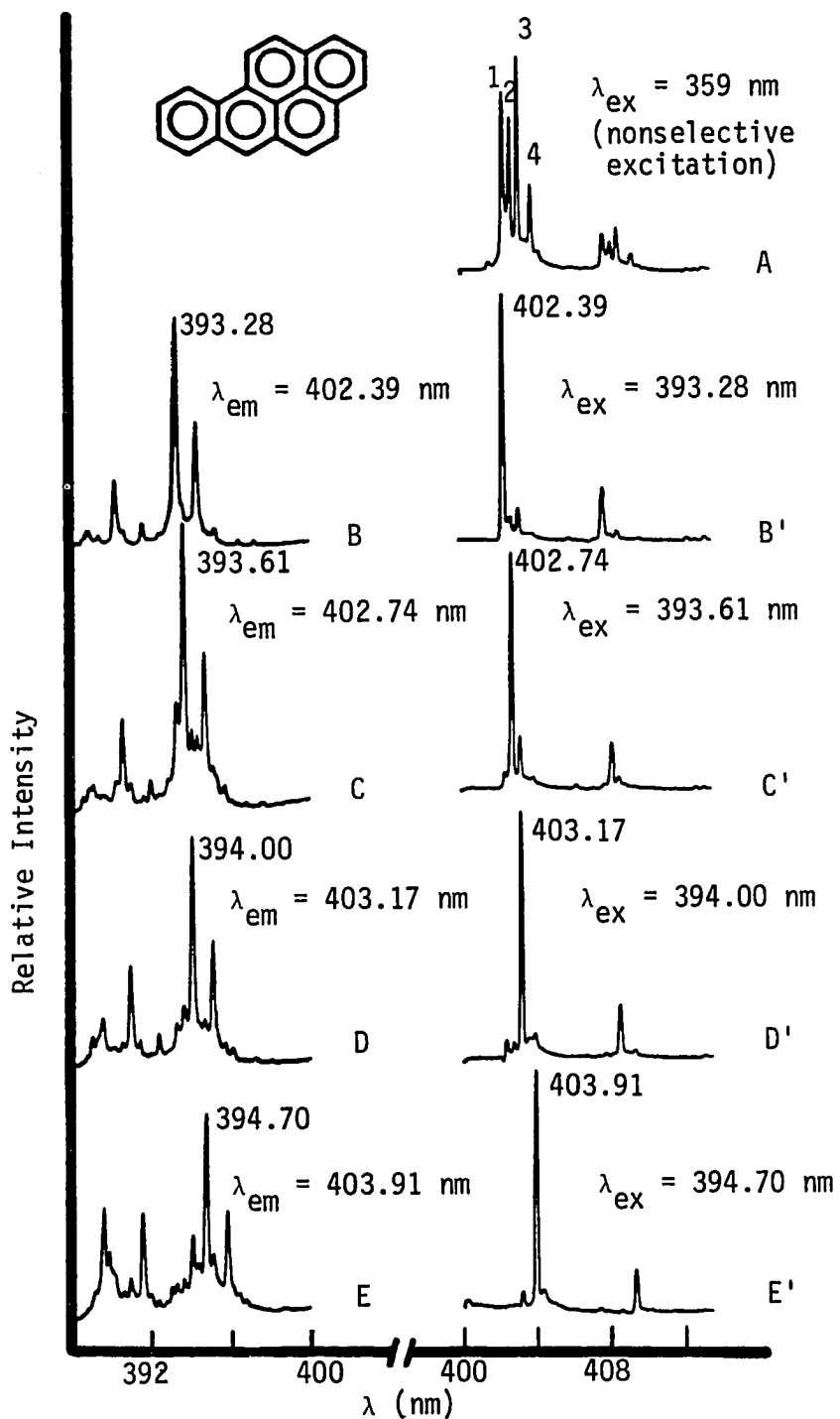


Figure 11. Fluorescence excitation and emission spectra of benzo(a)-pyrene at a concentration of 0.5 ppm in n-heptane

respectively. The resulting fluorescence spectra from these excitation wavelengths can be seen in spectra C', D' and E' in Fig. 11. It should be noted that the relative intensities of the 0-0 multiplets shown in Fig. 11A do not indicate the relative site concentrations, unless the molecules in all the sites are evenly excited with a broadband light source. Selective excitation of spectrum A in Fig. 11 clearly shows the site-specific, fine structure luminescence spectra that are so informative. Further, the capability of exciting only site specific spectra (B', C', E' and F) not only enhances specificity but also provides added flexibility in the event that spectral interferences by other sample constituents invalidates the use of one site-specific line. Should interferences occur, other interference-free, site-specific lines may then be selected as will be seen shortly.

The LESS of PNAs: Typical Spectra, Problems and Their Solutions

A necessary prerequisite to the routine use of LESS as an analytical technique is a knowledge of the excitation and emission wavelengths best suited to selectively identify one compound in the presence of others. In the remainder of this chapter, the characteristics of the spectra of some PNAs (including normal PAHs, PAH derivatives, sulfur-heterocyclic, nitrogen-heterocyclic, and oxygen-heterocyclic compounds) will be presented along with enumeration of problems encountered in applying the observed spectra to the identification and quantitation of selected PNAs.

Benzo(a)pyrene

Because of its biological activity and its importance as an environmental pollutant, B(a)P was selected as a "marker" compound for some preliminary studies. The nonselectively excited fluorescence emission spectrum of B(a)P in *n*-octane is shown in Fig. 10D. The excitation as well as the selectively excited fluorescence emission are given in Fig. 12A and B, respectively. The simplicity of this emission spectrum can be attributed to occupancy of basically only one site by the analyte molecules. Under these conditions, nonselective and selective excitation fluorescence spectra are approximately identical as shown by comparing Fig. 12B with Fig. 10D. This observation was found to be generally true for other PAHs. In these cases, only the selective emission spectra will be presented. In fact, the presence of a single, sharp and intense 0-0 transition of B(a)P provides an excellent opportunity for the determination of low concentrations of B(a)P in environmental samples.

Deuterated analogs as internal reference compounds

Deuterated analogs have the potential of being ideal internal reference compounds. When used in this way, the internal reference compound is added at constant concentration levels to each sample. The relative intensity of the analyte line is then ratioed to the intensity of the corresponding line emitted by the internal reference compound and the intensity ratio is related to the concentration of the analyte. To serve as an ideal internal reference compound, the latter should exhibit the following properties.

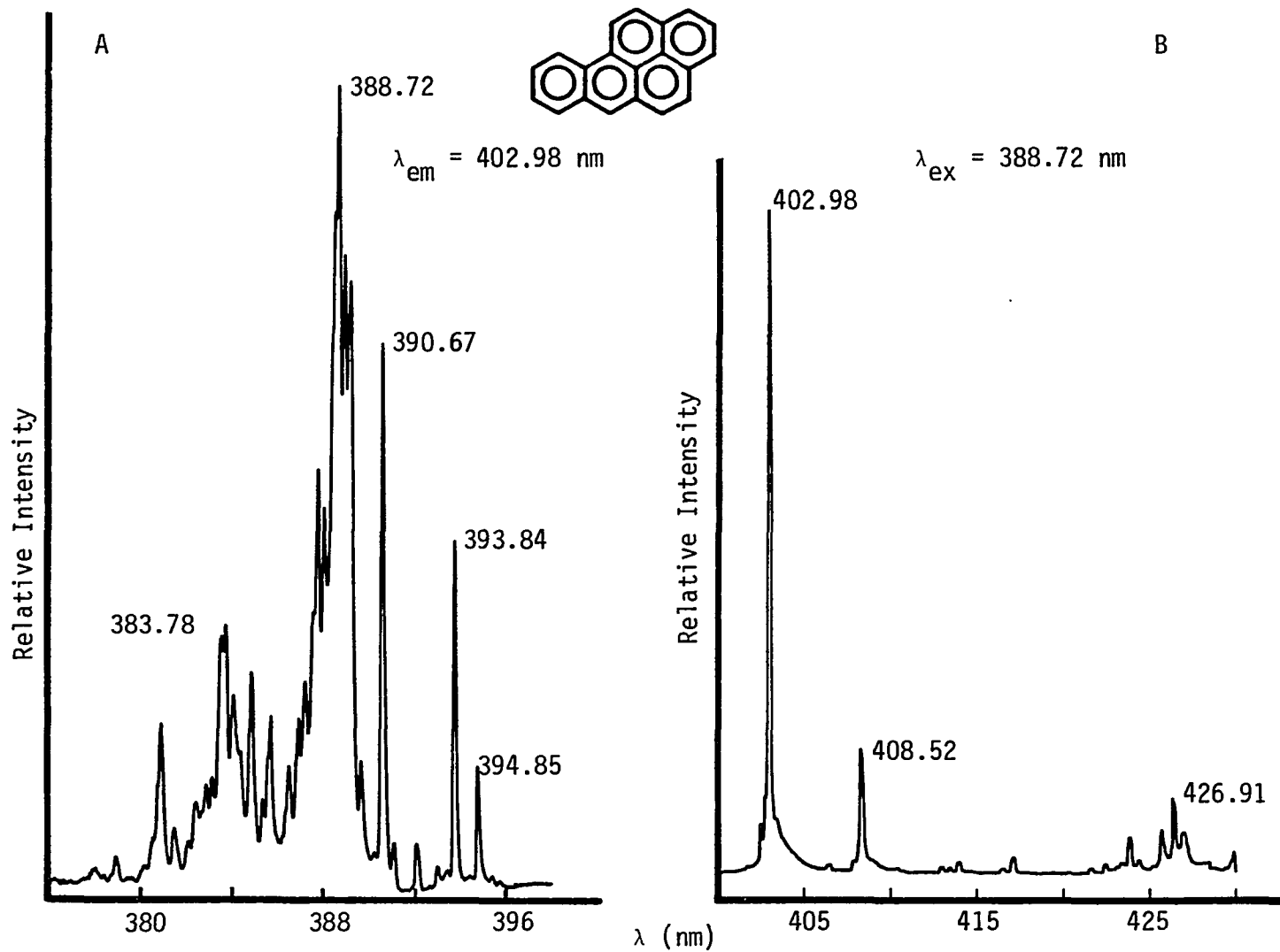


Figure 12. Excitation (A) and fluorescence emission (B) spectra of benzo(a)pyrene in n-octane

1. Its spectroscopic properties should be as similar as possible to those of the analyte being determined so that the internal reference compound will provide adequate compensation for the emission variation associated with intermolecular interactions and inner filter and enhancement effects.
2. It should be absent in the sample.
3. It should be in a high state of purity with respect to the analyte being determined.
4. The spectral lines of the internal reference and analyte compound of interest should be free of spectral interferences arising from emissions of other sample constituents.
5. The spectral lines selected should be free of self-absorption.
6. It is preferable to employ the same excitation wavelength for the reference and analyte, whenever possible.

A comparison of Figs. 12 and 13 shows the high degree to which deuterated benzo(a)pyrene ($B(a)P-d_{12}$) serves as an internal reference for $B(a)P$. In fact, $B(a)P-d_{12}$ satisfies the stated criteria to an unusually high degree.

Phosphorescence spectra

In molecules where the singlet S_1 and triplet T_1 energy levels are closely spaced, there is a significant probability that the excited molecules can drop into the lower energy T_1 state through an intersystem crossing process (see Fig. 4). The molecule can then return to the ground state by emitting its characteristic phosphorescence. As with fluorescence emission, the spectra of phosphorescence emissions are

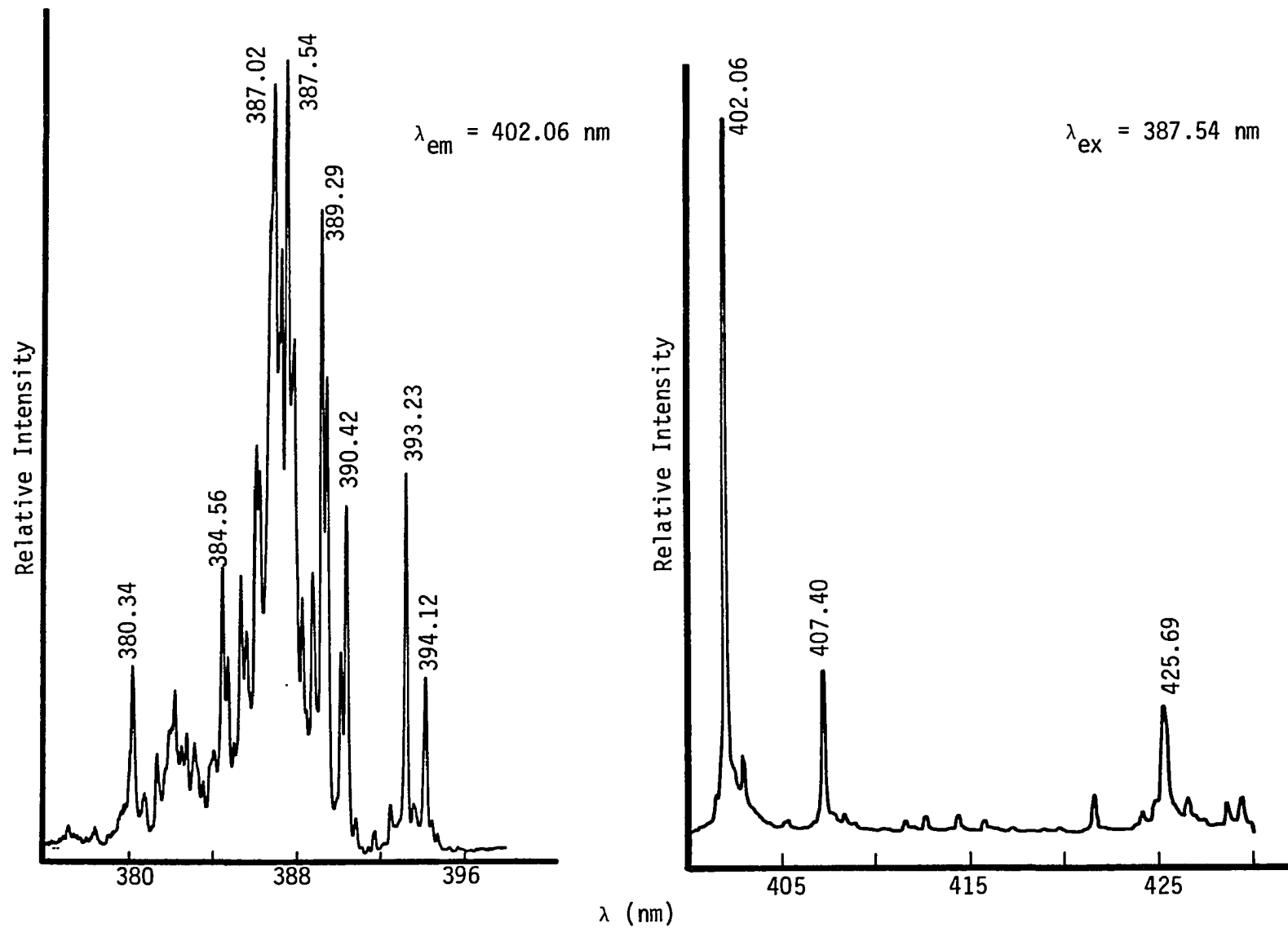


Figure 13. Fluorescence excitation (left) and emission (right) spectra of benzo(a)pyrene-d₁₂ in n-octane

unique in regard to its frequency, lifetime, quantum yield, and vibrational pattern and such properties are useful for qualitative identification. The correlation of intensity with concentration can also serve as a basis for quantitative measurement. Although the phosphorescence emissions of PAH compounds are normally very weak compared to the fluorescence emission, the former are occasionally of analytical value. As shown in Fig. 14, the concentration required to produce useful spectra for the compounds are in the 100 to 200 ppm range. These phosphorescence spectra show that at least two sites are occupied for each compound. This observation was in conflict with fluorescence emission observation (see Figs. 12 and 13), which showed that only one site was substantially occupied. These contradictory observation may be explained as follows. At low concentration ($\sim 10^{-6}$ M), only one site appears to be substantially occupied; the other sites evidently were not sufficiently populated to show detectable fluorescence. At higher concentration, two sites appear to be populated, as reflected in the phosphorescence emission. This interpretation was confirmed in the fluorescence spectra of B(a)P and B(a)P-d₁₂ when higher concentration samples were examined.

Detrimental effects of frost film formation

The precautions that were taken to avoid the deposition of frost films on the interface of the quartz sample holder plate on the sample cell and the high vacuum space were described earlier (Chapter 3). When these precautions failed and films were formed, the quality of the spectra deteriorated. In addition to causing a reduction of S/N ratio

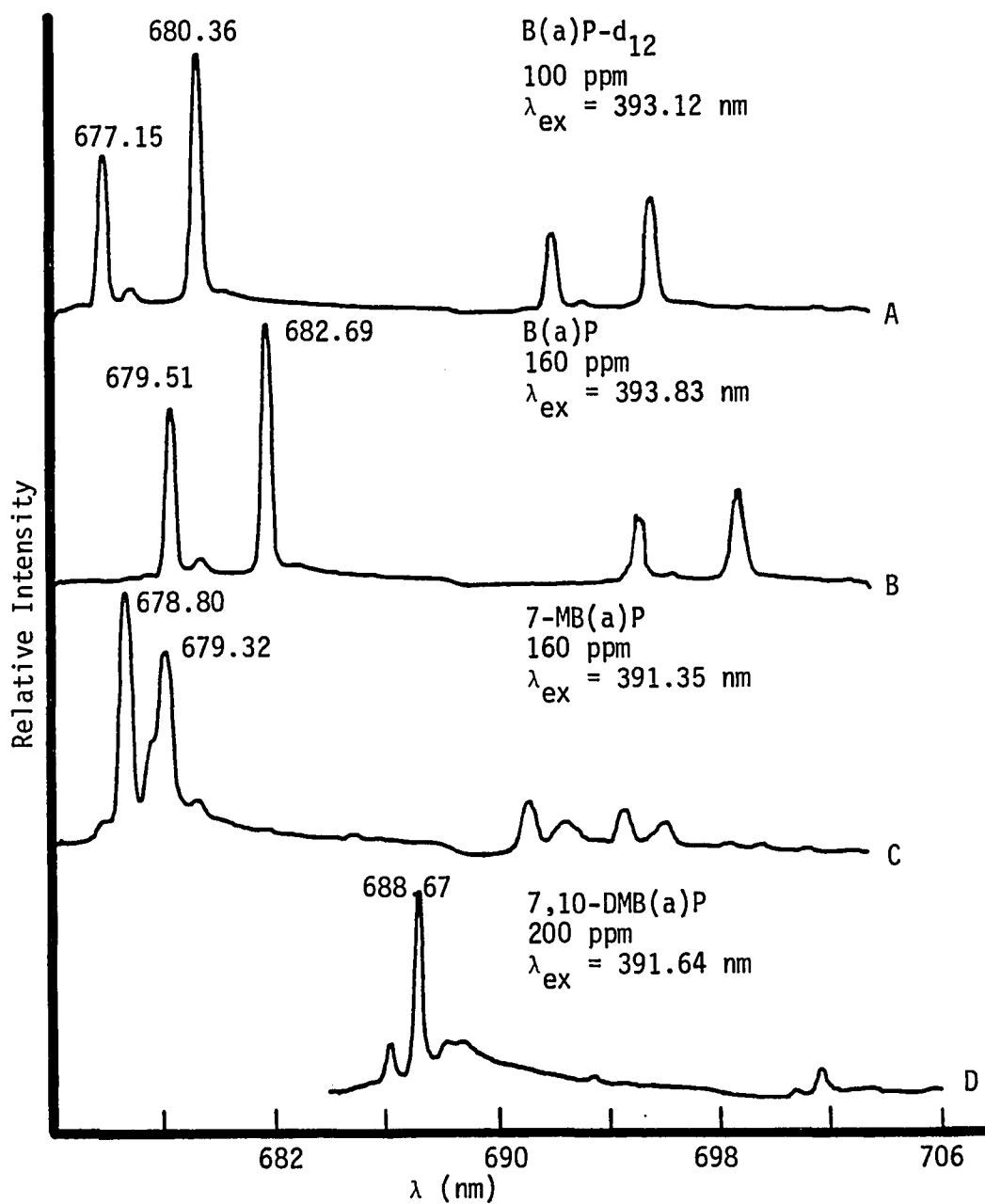


Figure 14. Comparison between phosphorescence emission spectra of B(a)P-d₁₂, B(a)P, 7-MB(a)P, and 7,10-DMB(a)P in n-octane at $\lambda_{ex} = 339$ nm

through scattering of the excitation radiation and blockage of the emitted fluorescence, the presence of the frost film usually also led to severe broadening of the emitted spectra, especially when samples in n-pentane hosts were irradiated. The degree of line broadening caused by the presence of the frost film was indicative of a temperature of $\sim 100^\circ\text{K}$ at the surface of the sample, i.e., the interface between the frozen sample and the quartz plate. These observations strongly suggest the presence of or formation of intolerable temperature gradients through the sample, perhaps through preferential warming of the frost film by the incident laser beam. Clearly, the formation of frost film cannot be tolerated.

Inhomogeneous solid solution formation

The formation of inhomogeneous solid solutions can be detected by irradiating different areas of the sample surface and observing the reproducibility of the intensity distributions in the spectra. With some of the sample holder designs evaluated during this study, especially those with larger, more massive cells, nonreproducible spectra were consistently observed, whereas these difficulties were rarely encountered in the small cell described in this thesis. In view of the different thermal conductivities of various components of the cell in contact with the sample, their rate of cooling would be expected to be quite different, leading in all likelihood, to different rates of cooling for different areas of the solid host. Empirically, it was found that reproducible Shpol'skii effect spectra could be consistently observed if the following four conditions were met: (a) a very fast,

first stage solidification (quenching) by immersing the sample holder in liquid N₂; (b) miniaturized sample holder, as described in this thesis; (c) solute concentration in the 10⁻⁶ mole region (to prevent aggregate formation during the cooling cycle); and (d) avoidance of low melting point solvents such as n-pentane, whose rate of solidification is so slow that solute migration and aggregation may occur, even during the fast liquid N₂ immersion stage.

Spectrum of 7-methylbenzo(a)pyrene; an example of line overlap

Nonselectively excited fluorescence emission spectrum as well as site-specific spectra for this compound in n-octane are shown in Fig. 15. The excitation wavelength indicated in Figs. 15B to E for each one of the four sites was selected to be as free as possible from spectral overlap with excitation wavelengths of other site molecules.

It is of interest to note that the multiplet site spectra of both B(a)P and 7-MB(a)P exhibit an intense line at 402.98 nm (see Figs. 11 and 15C'). This overlap may have been caused by the following factors: (a) the individual compounds each emit coincident lines; or (b) the 7-MB(a)P sample contained B(a)P impurity or vice versa; or (c) both factors (a) and (b) may have contributed to the overlap.

To unequivocally identify the nature of this overlap, detailed comparison of the site-specific excitation and emission spectra in other hosts beside n-octane were undertaken. These spectra as well as those of B(a)P-d₁₂ are shown in Figs. 16 to 23.

A comparison of the six excitation spectra at $\lambda_{em} = 402.98$ nm in Fig. 16 clearly show that the two compounds possess different excitation

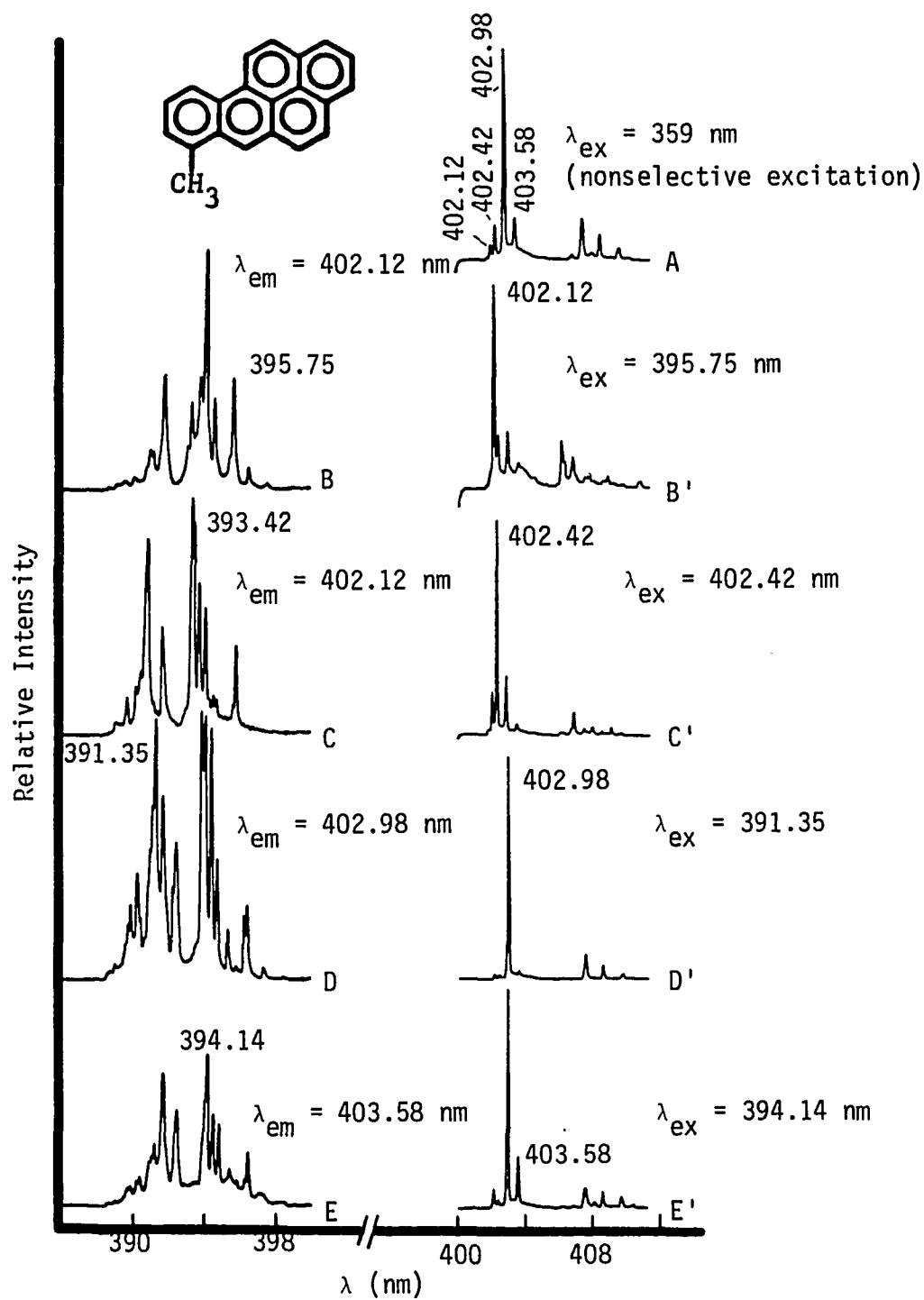


Figure 15. Fluorescence excitation and emission spectra of 7-methylbenzo(a)pyrene at a concentration of 0.5 ppm in n-octane

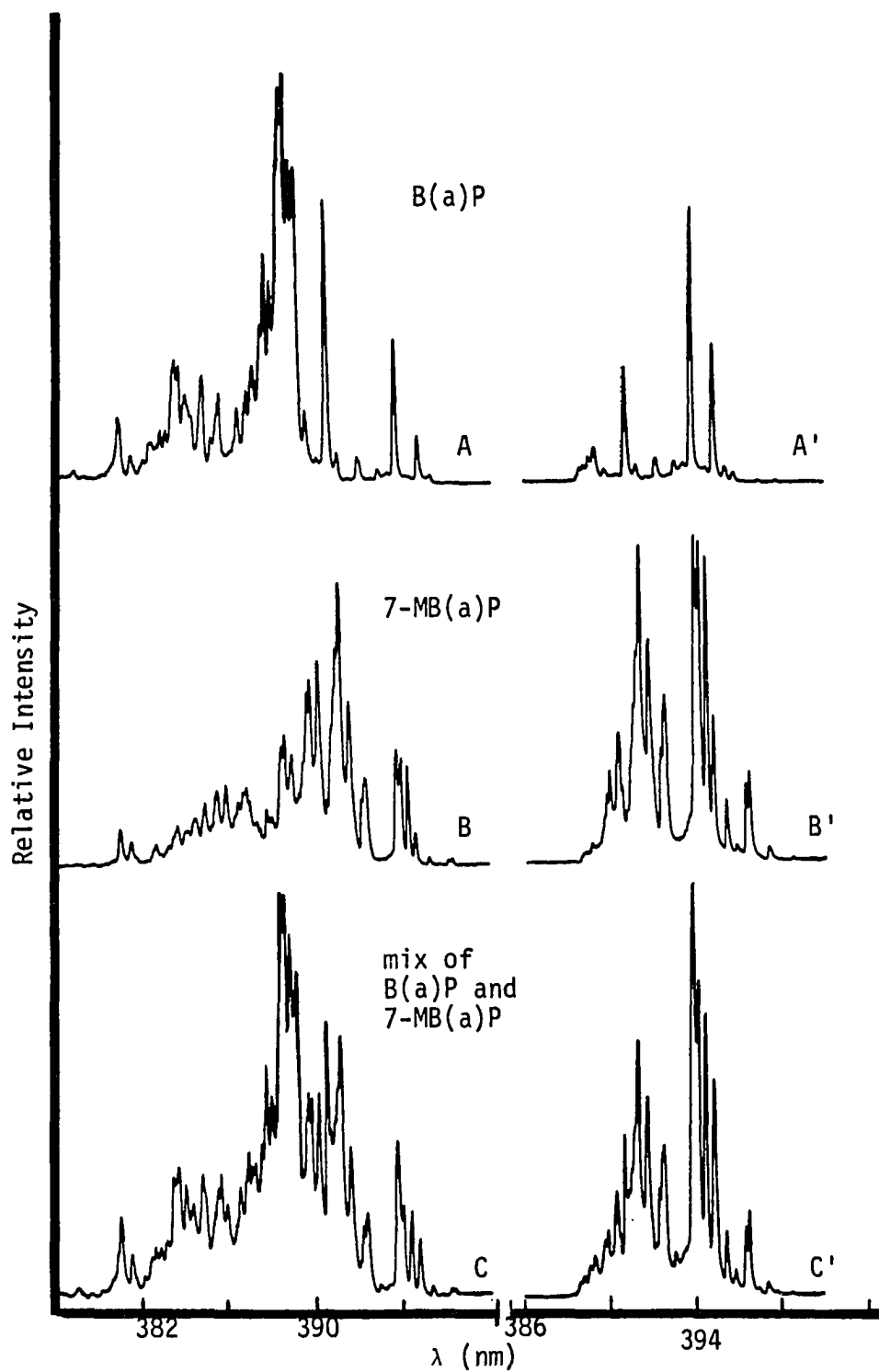


Figure 16. Comparison of the excitation spectra of B(a)P, 7-MB(a)P, and mix of B(a)P and 7-MB(a)P in n-octane at $\lambda_{em} = 402.98$ nm

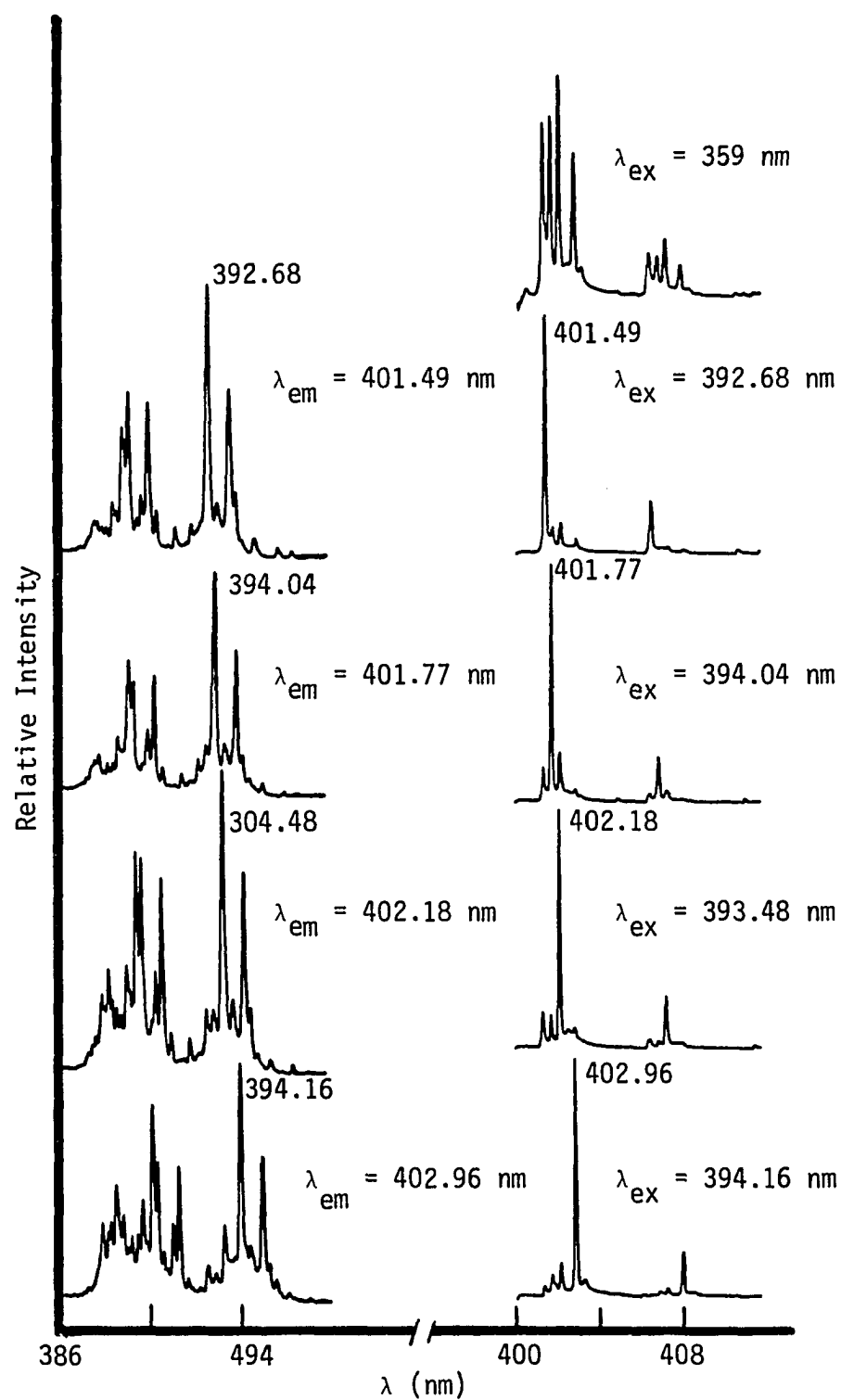


Figure 17. Fluorescence excitation and emission spectra of benzo(a)-pyrene-d₁₂ at a 1 ppm in n-heptane

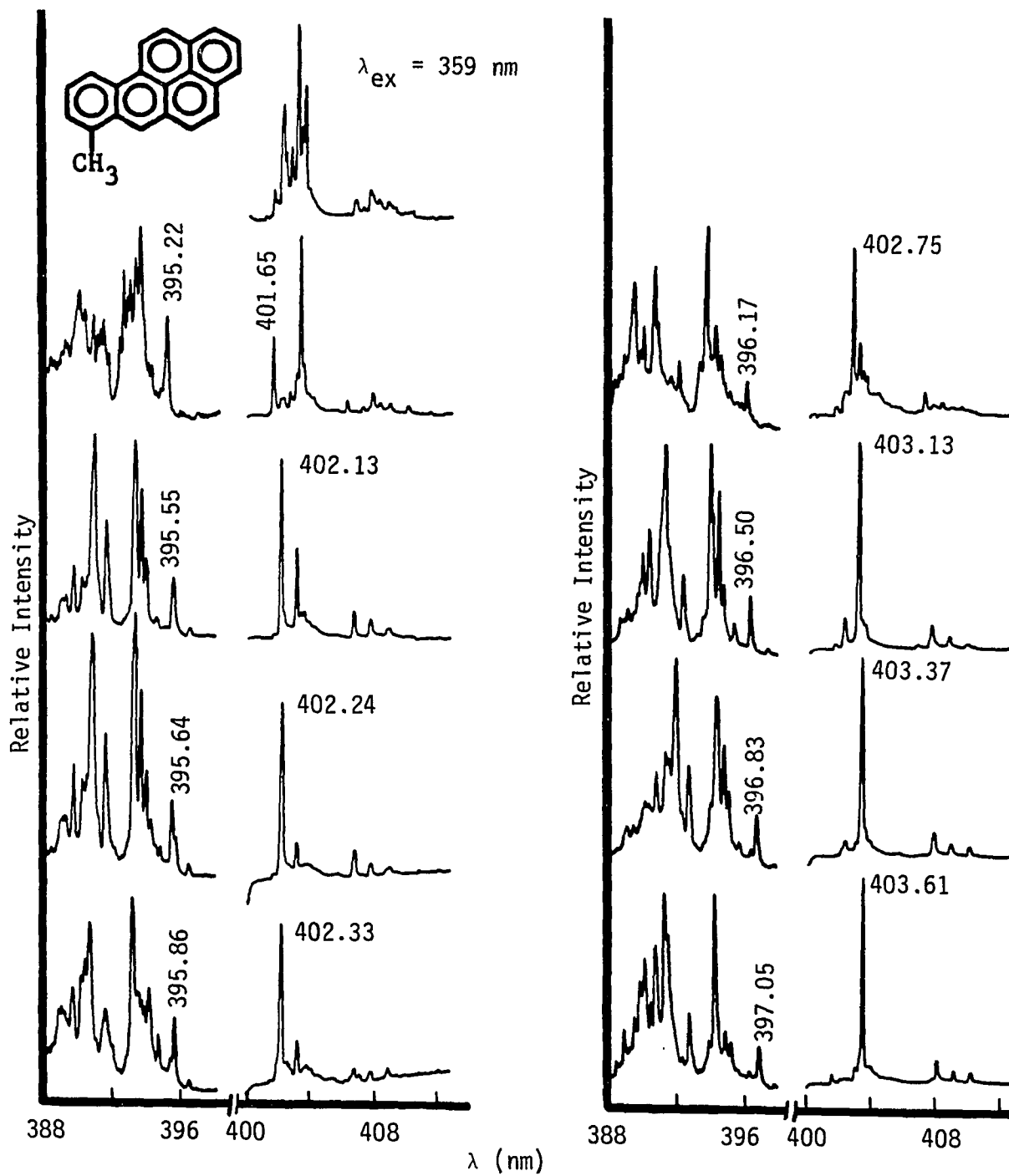


Figure 18. Fluorescence excitation and emission spectra of 0.5 ppm 7-methylbenzo(a)pyrene in n-heptane. Wavelengths used to obtain the excitation and emission spectra are indicated above for each site

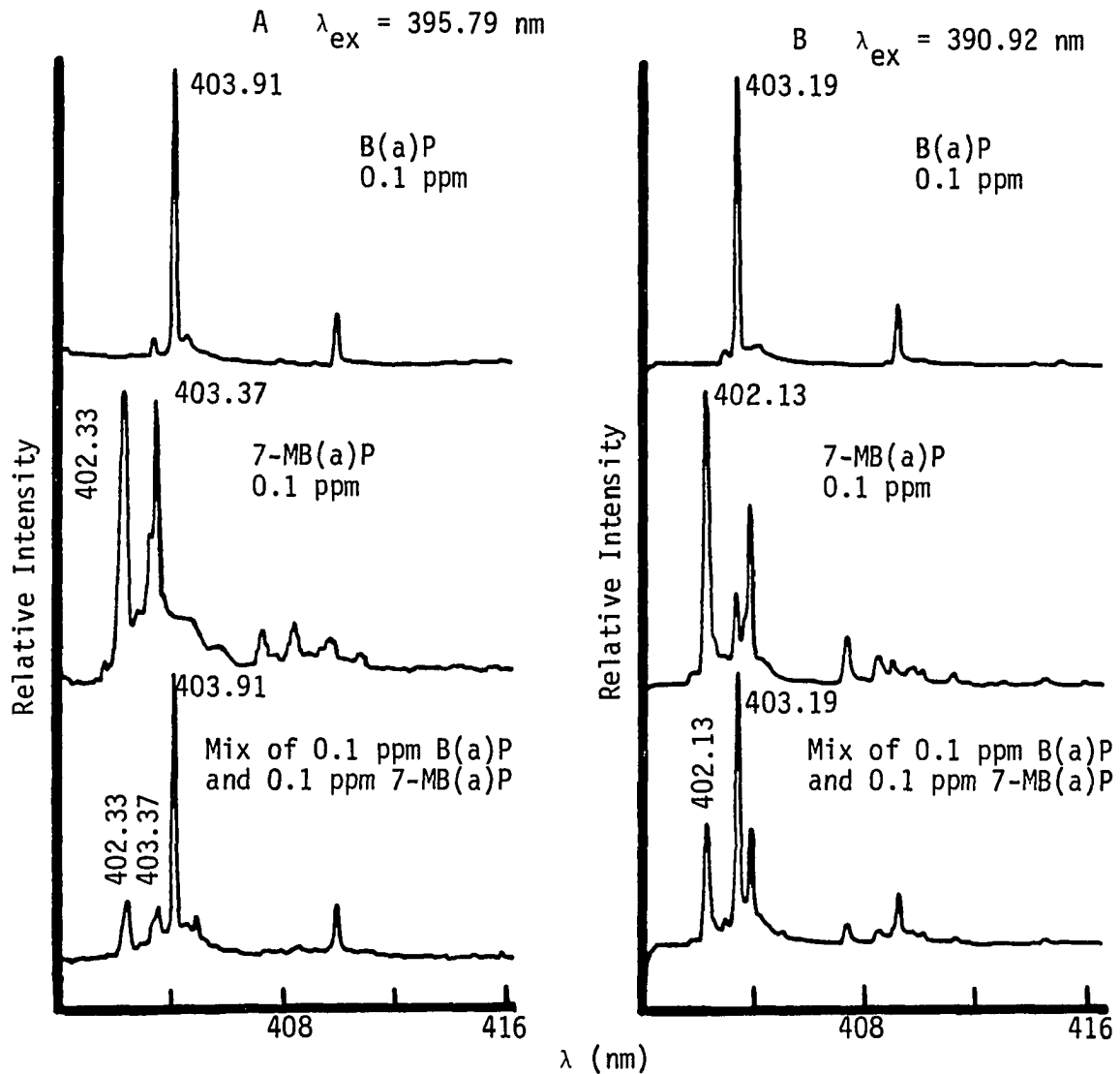


Figure 19. Comparison between fluorescence emission of benzo(a)pyrene and 7-methylbenzo(a)pyrene in n-heptane at excitation wavelength 395.79 nm (A) and 390.92 nm (B)

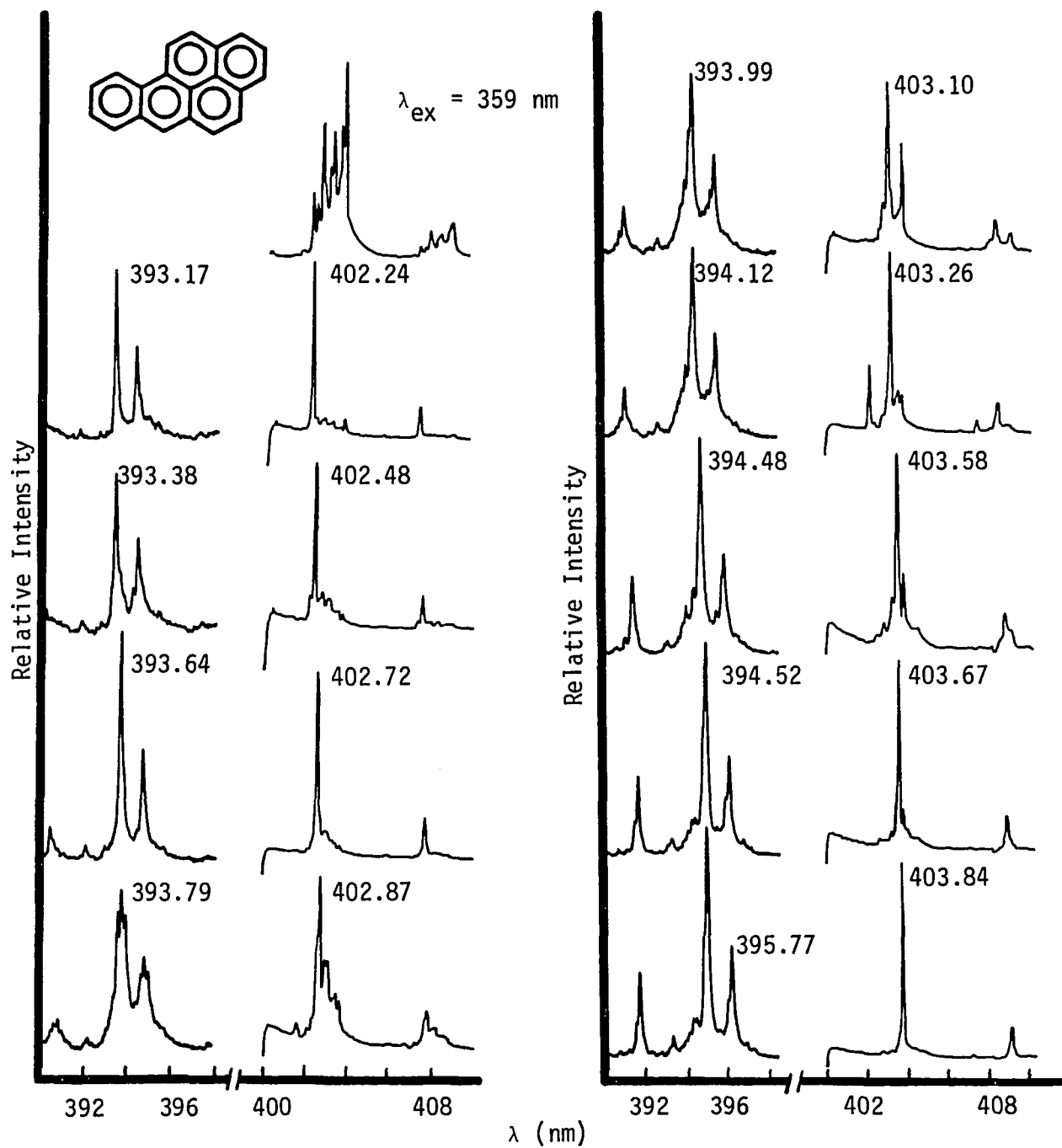


Figure 20. Fluorescence excitation and emission spectra of 0.5 ppm benzo(a)pyrene in n-nonane. Wavelengths used to obtain the excitation and emission spectra are indicated above for each site

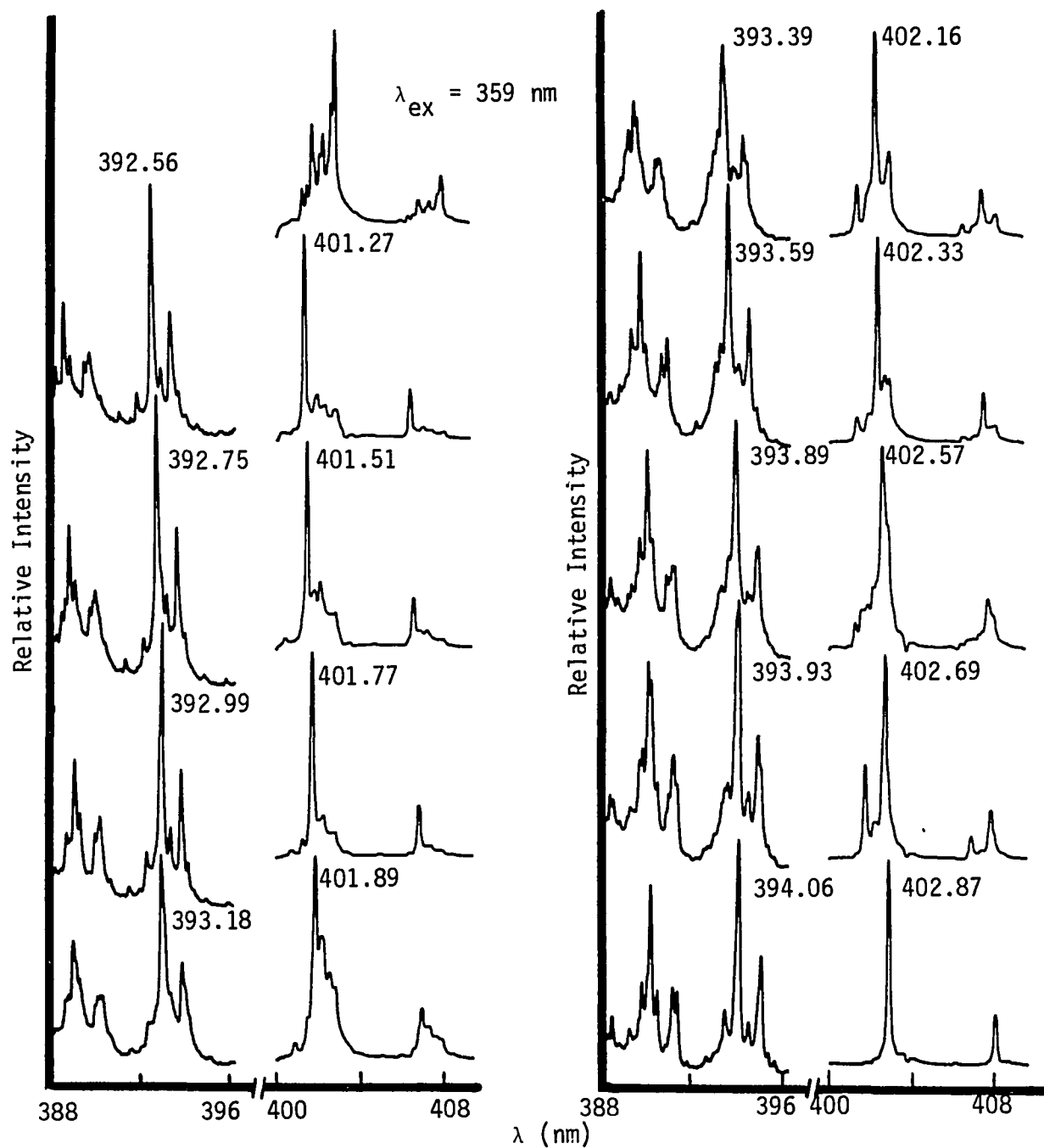


Figure 21. Fluorescence excitation and emission spectra of 1 ppm benzo(a)pyrene- d_{12} in n-nonane. Wavelengths used to obtain the excitation and emission spectra are indicated above for each site

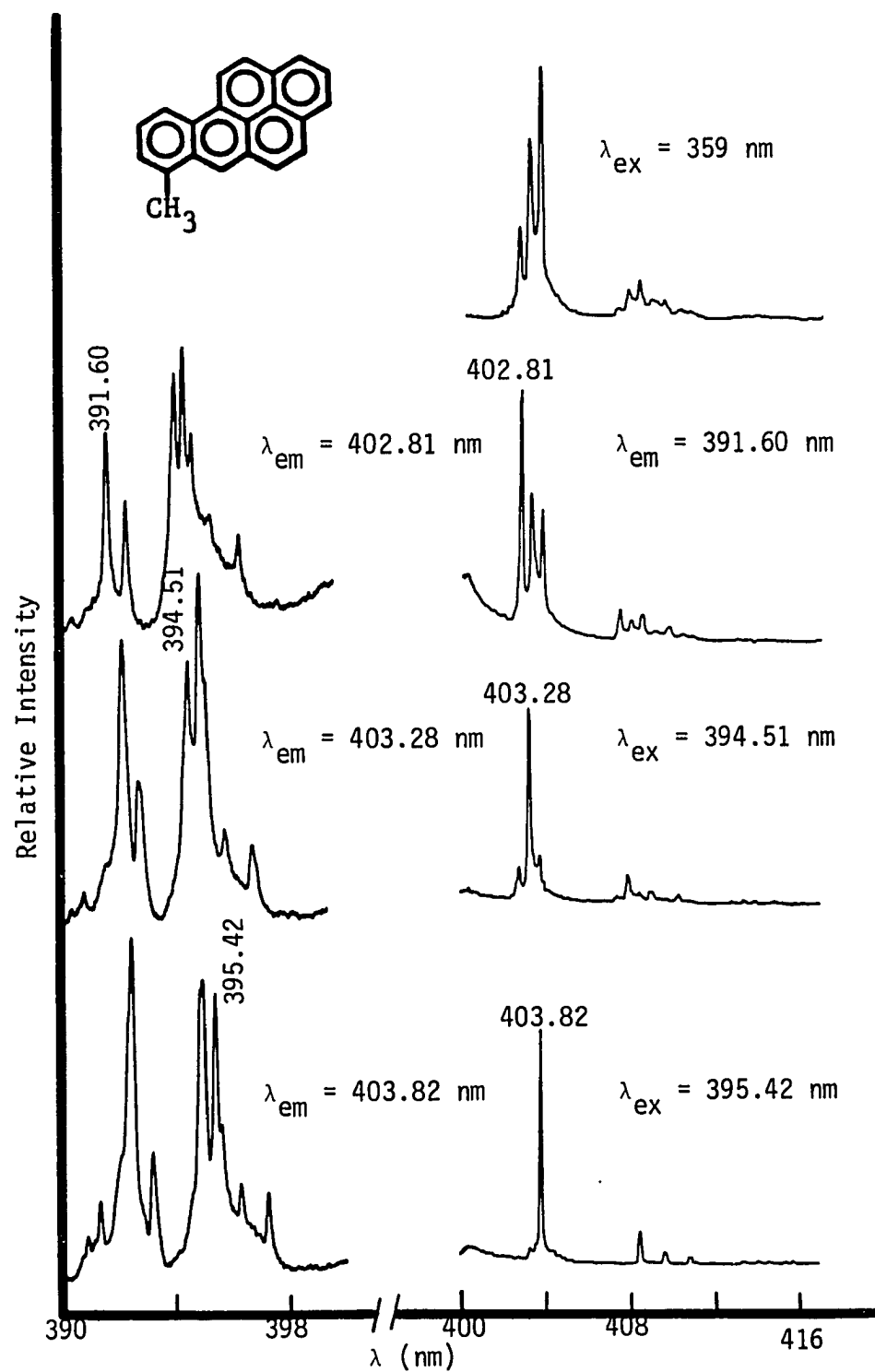


Figure 22. Fluorescence excitation and emission spectra of 0.5 ppm 7-methylbenzo(a)pyrene in n-nonane

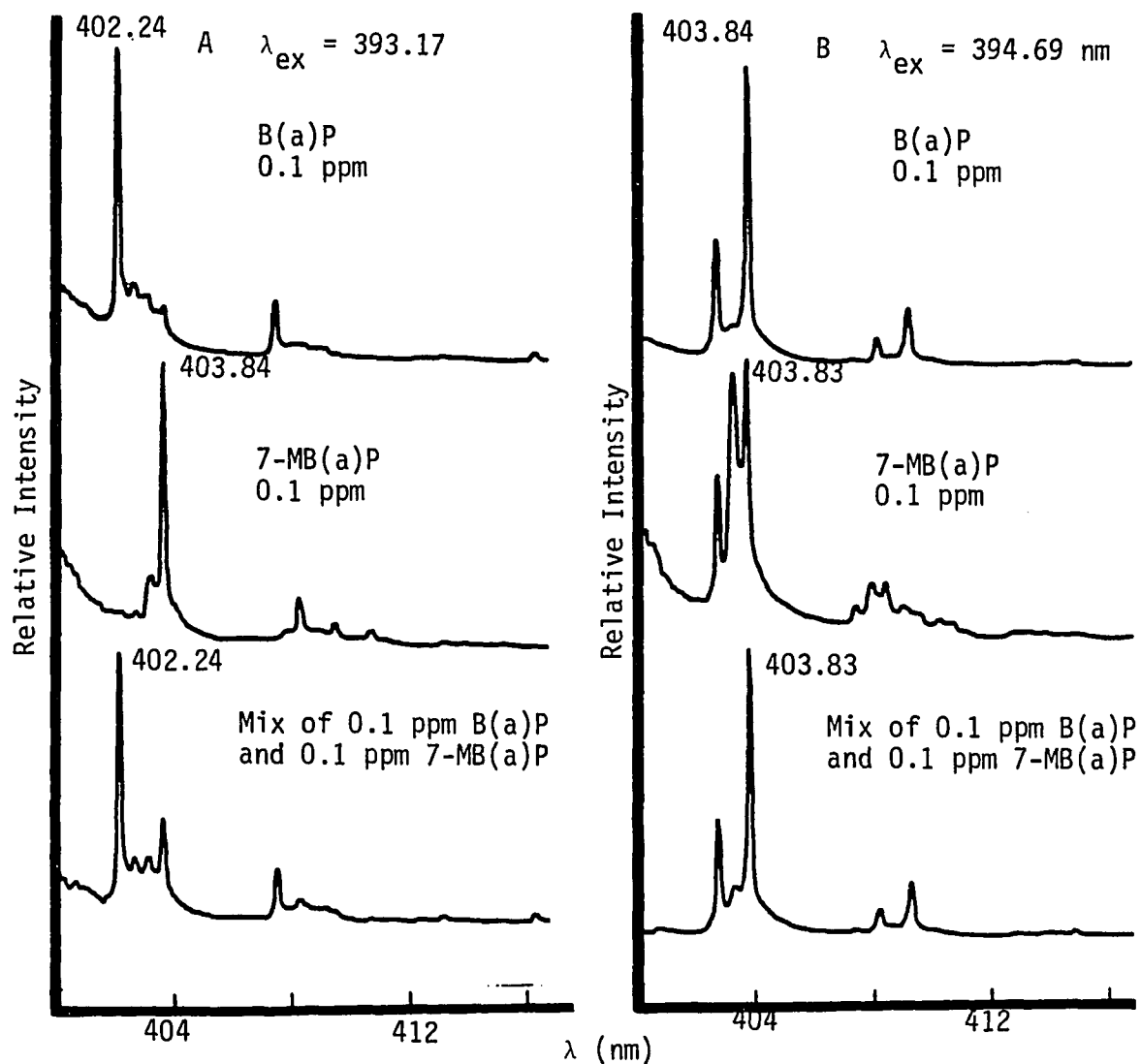


Figure 23. Comparison between fluorescence emission of benzo(a)pyrene and 7-methylbenzo(a)pyrene in n-nonane at excitation wavelengths 393.17 nm (A) and 394.38 nm (B)

spectra and that the two compounds are quite pure. The above conclusion was further confirmed when the phosphorescence spectrum of 7-MB(a)P was compared with that of B(a)P (see Fig. 14) and when other solvent hosts were used. In *n*-octane solvent, the prominent fluorescence line at 402.98 nm appears in the emission spectra of both compounds at all excitation wavelengths shorter than 402.98 nm. However, its intensity depends on λ_{ex} . Therefore, even selective excitation will not tell whether only one compound or both compounds are present in real samples.

In *n*-heptane solvent, site-selective spectra for B(a)P were given previously in Fig. 11. As expected, B(a)P-d₁₂ molecules in *n*-heptane are also distributed in four sites and their 0-0 transitions are blue-shifted with respect to those of B(a)P in the same solvent, as shown in Fig. 17. The site-selective spectra of 7-MB(a)P in *n*-heptane shown in Fig. 18 suggest that 7-MB(a)P is distributed in at least 8 sites. A critical examination of the various 0-0 transitions of both B(a)P and 7-MB(a)P indicated that for this solvent the two compounds could be determined in the presence of each other. This conclusion was tested on a synthetic mixture of the two compounds (see Fig. 19). The examination showed that the 0-0 line at 403.91 nm (Fig. 11) can be used to determine B(a)P at $\lambda_{\text{ex}} = 395.79$ nm. At the same λ_{ex} , 7-MB(a)P can be determined via its line at 402.33 nm. Furthermore, 7-MB(a)P can be determined via its line at 402.13 nm at $\lambda_{\text{ex}} = 390.92$ nm without interference from B(a)P. For quantitative analysis, B(a)P-d₁₂ can be used as an internal reference. The emission line of shortest wavelength at 401.49 nm of B(a)P-d₁₂ is well situated to be an appropriate internal reference

line because it will not suffer interference from any of the lines of B(a)P and 7-MB(a)P. Further, no interference from B(a)P-d₁₂ will occur to B(a)P at 403.91 nm or to 7-MB(a)P at 402.33 nm.

Site-selective spectra for B(a)P, B(a)P-d₁₂, and 7-MB(a)P are given in Figs. 20 to 22, respectively. While B(a)P and B(a)P-d₁₂ are distributed in at least 9 sites in n-nonane, the molecules of 7-MB(a)P are present mainly in only 3 sites. Examination of these three figures shows that B(a)P can be determined in the presence of 7-MB(a)P, as shown in Fig. 23, i.e., B(a)P can be determined via its fluorescence line at 402.26 nm, using $\lambda_{\text{ex}} = 393.17$ nm, and 7-MB(a)P will not interfere. However, if B(a)P-d₁₂ is used as the internal reference, interference at 402.24 nm of B(a)P by B(a)P-d₁₂ will occur. In this case, another internal reference should be used. For 7-MB(a)P, the three site-specific 0-0 transition wavelengths of 7-MB(a)P overlap those of B(a)P (see Figs. 20 and 22) to such a degree that they are not useful. The observations on 7-methylbenzo(a)pyrene summarized above provide an excellent example of: (a) how the capability to generate site-specific spectra can circumvent some serious line overlap; (b) how the sample introduction of a methyl group to a PNA can alter the orientation of a solute in the Shpol'skii host and impact the site population patterns; and (c) how the proper choice of Shpol'skii solvent can solve spectral coincidence problems.

7,10-Dimethylbenzo(a)pyrene

The nonselectively excited fluorescence of this compound is shown in Fig. 24A and the site-specific spectra in n-octane are shown in Fig.

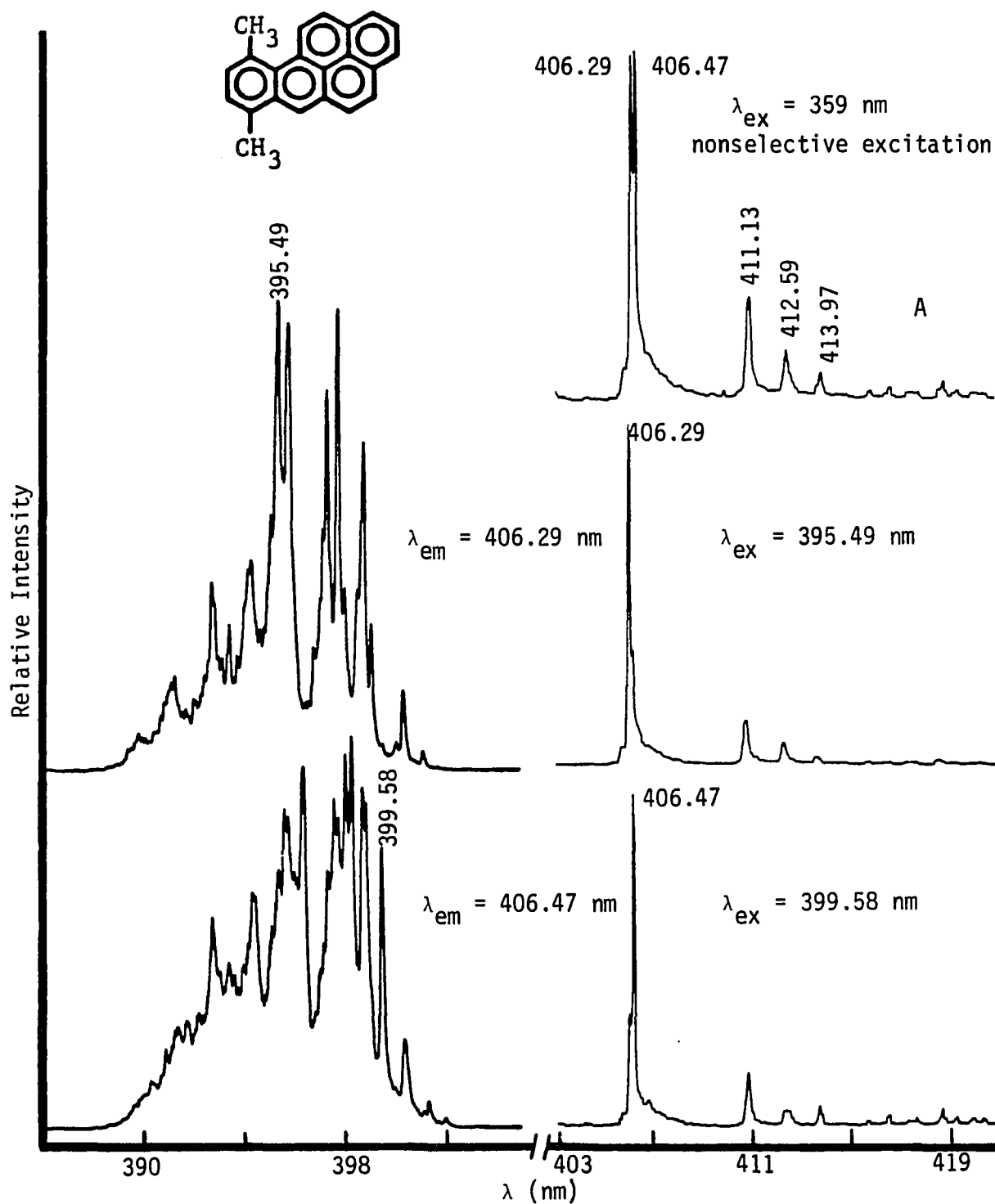


Figure 24. Fluorescence excitation and emission spectra of 1 ppm 7,10-dimethylbenzo(a)pyrene in n-octane

24. This figure shows that the 0-0 transitions of 7,10-DMB(a)P are red-shifted with respect to those of B(a)P and 7-MB(a)P and are not subject to interference from them. The phosphorescence spectrum of 7,10-DMB(a)P is given in Fig. 14D.

Benzo(e)pyrene; an example of the analytical utility of phosphorescence emission

The fluorescence emission of benzo(e)pyrene (B(e)P) in n-octane excited at a nonselective wavelength of 339 nm is shown in Fig. 25A. Under identical experimental conditions, the phosphorescence spectrum shown in Fig. 25B was recorded. The intensity ratio of the strongest fluorescence and phosphorescence lines is $\sim 9:5$ which is considerably lower than is typically observed. This fact makes the phosphorescence of B(e)P of considerable analytical importance.

The emission maximum at 388.27 nm for B(e)P was selected to record the fluorescence excitation spectrum shown in Fig. 26A. From that figure, the most promising wavelength for exciting the fluorescent emission at 388.27 nm is at 366.58 nm. With the laser tuned to this wavelength, the selectively excited fluorescence emission shown in Fig. 26B was recorded. The sloping baseline, more so on the shorter wavelength side, arises from scatter of the laser radiation. In a similar way, the phosphorescence excitation and emission spectra were obtained. These spectra are shown in Fig. 27. Figures 26A and 27A show that the two excitation spectra obtained through monitoring the fluorescence and phosphorescence emissions are identical. A general advantage of phosphorescence excitation spectrum is that the high background from light scat-

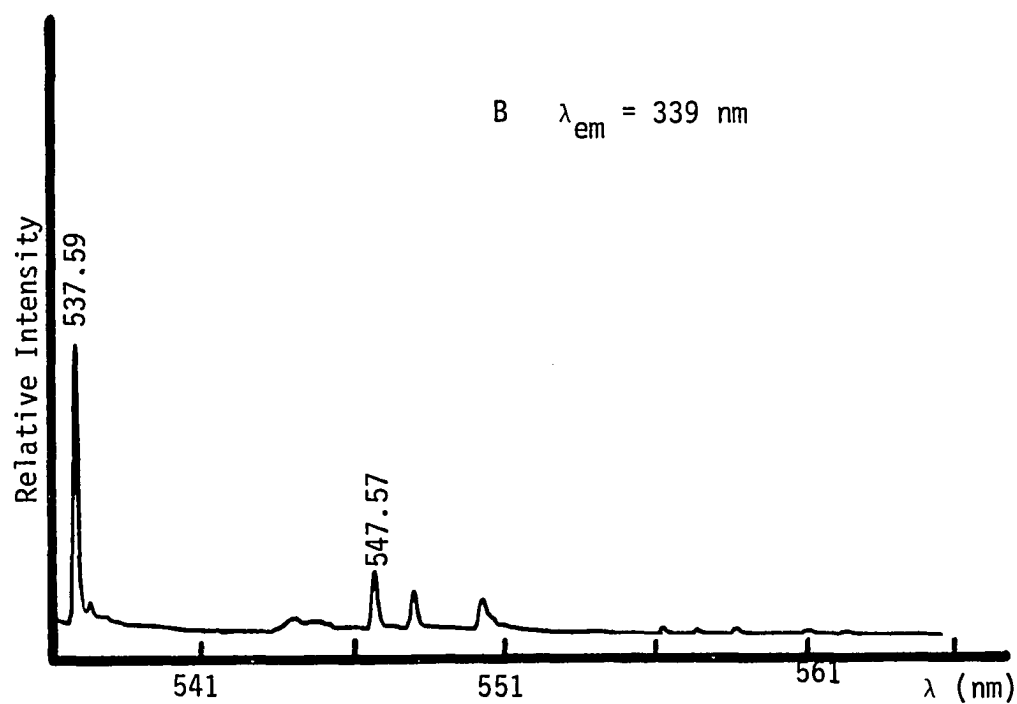
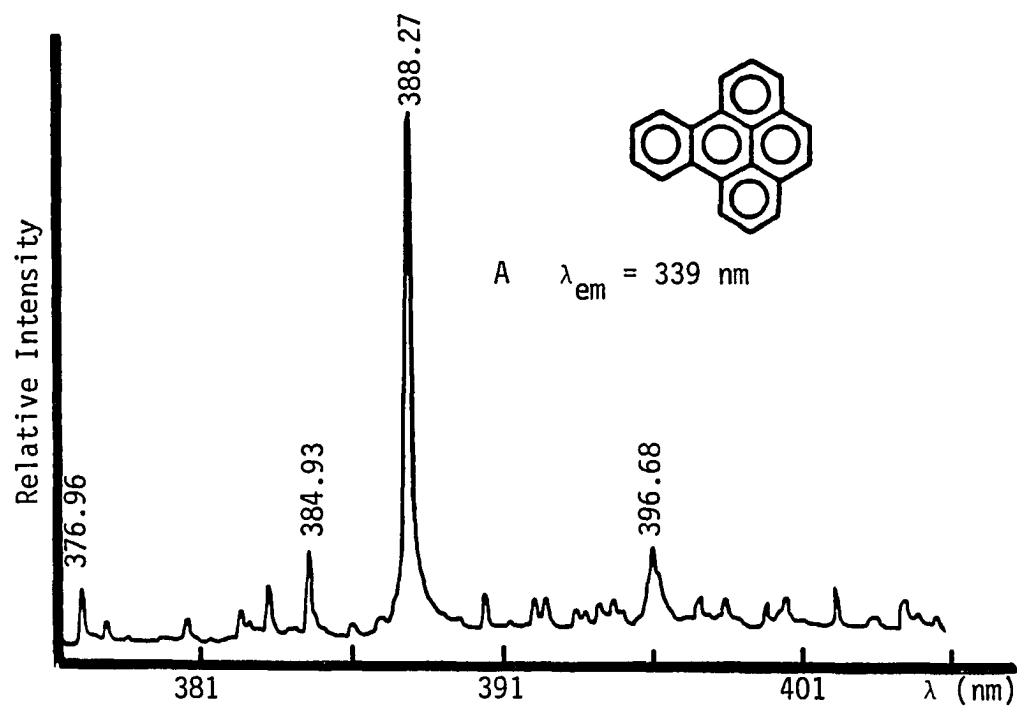
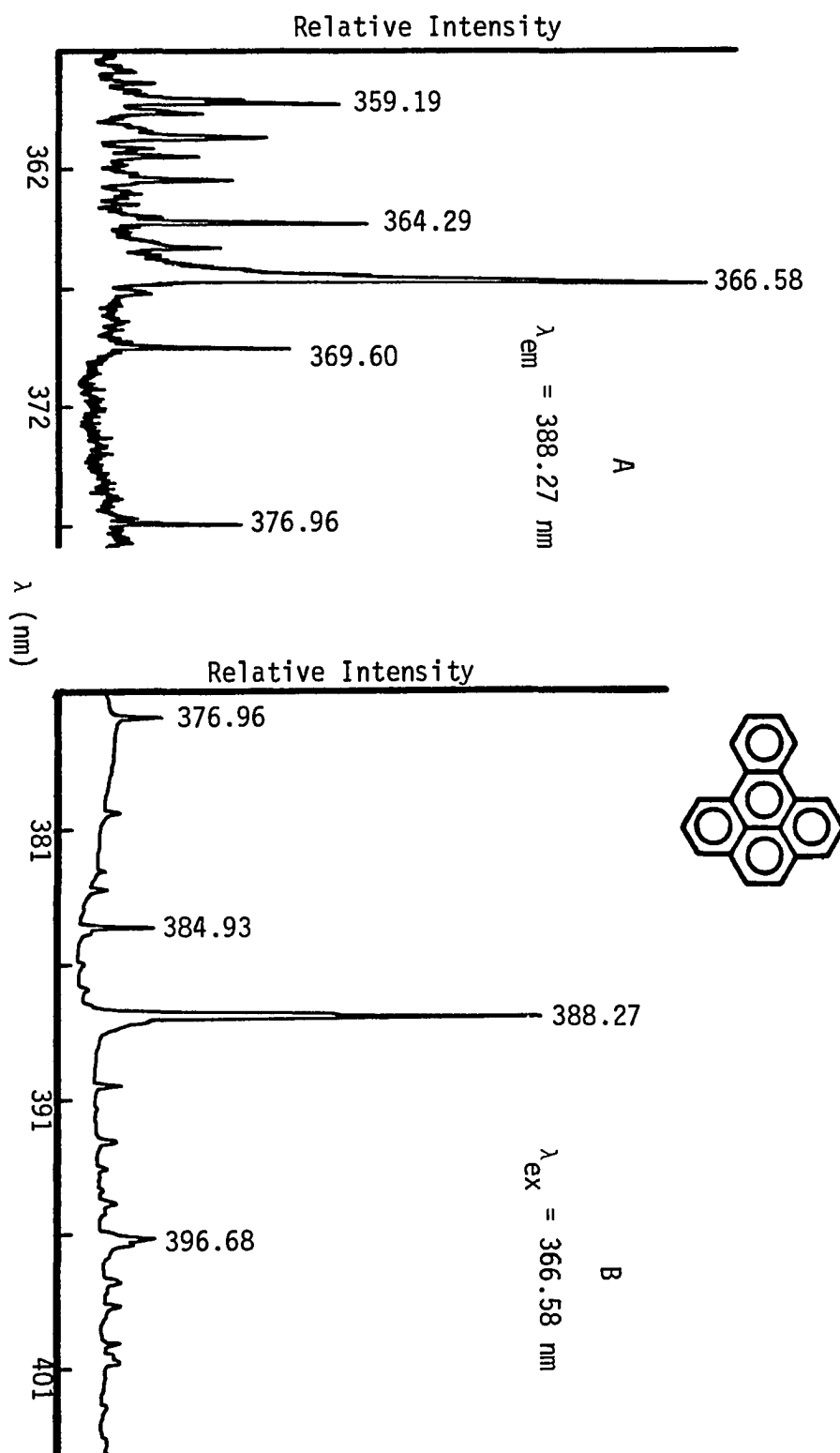


Figure 25. Nonselectively excited fluorescence (A) and phosphorescence (B) of benzo(e)pyrene at 10 ppm in n-octane

Figure 26. Fluorescence excitation (A) and emission (B) spectra of benzo(e)pyrene at 1 ppm in n-octane



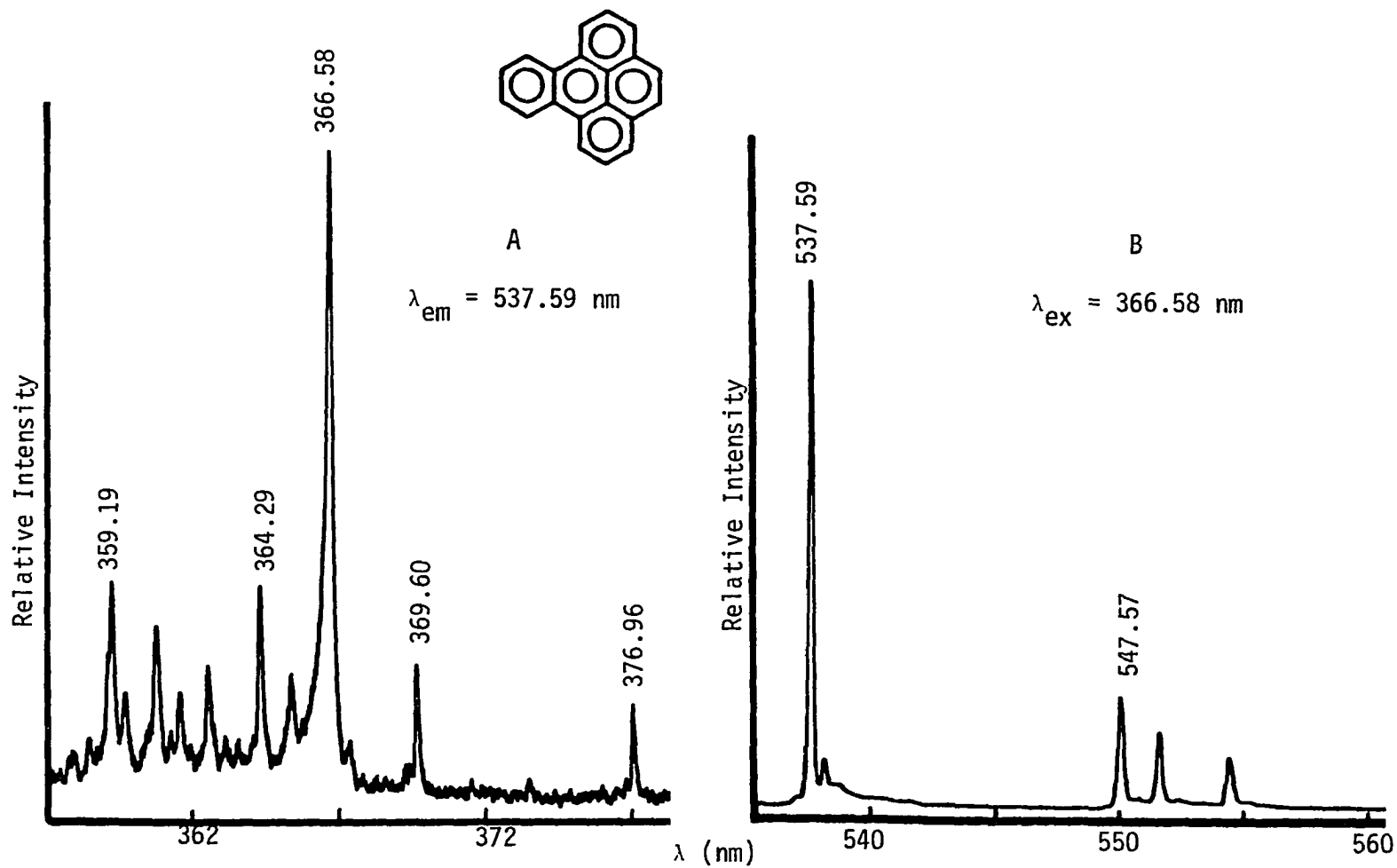


Figure 27. Phosphorescence excitation (A) and emission (B) spectra of benzo(e)pyrene at 1 ppm in n-octane

tering (which sometimes distorts the fluorescence excitation spectrum) is avoided. Figures 26A and 27A also show that the 0-0 transition of B(e)P occurs at 376.96 nm, which is the minimum energy required to excite a molecule of B(e)P.

Perylene and Perylene-d₁₂; an example of strong self-absorption

The nonselectively-excited, fluorescence emission spectrum of perylene in n-octane is shown in Fig. 28A. The selectively excited ($\lambda_{\text{ex}} = 420.52$ nm) spectra at decreasing concentrations from 10 to 0.1 ppm are shown in Figs. 28B, C and D. In recording the spectra shown in Figs. 28B to D, the signals were attenuated by adjusting the slit width so that the most intense lines in the individual spectra remained on scale, i.e., less than 16,800 counts for an integration time of 30 sec. on the OMA. It is readily apparent that as the concentration decreases the intensity ratio of $I_{451.64}/I_{444.57}$ also decreases. In other words, the intensity of the line at 444.57 nm decreases relative to that at 451.64 nm as the concentration increases. These observations strongly suggest that as the perylene concentration increases from 0.1 to 10 ppm, strong self-absorption (inner filter effect) occurs at 444.57 nm. The self-absorption of the 0-0 transition at 444.57 nm and the enhancement of the transition at 451.64 nm at high concentrations may be interpreted by Fig. 28E.

The observed self-absorption indicates clearly that the emission not only originates from the surface of the frozen matrix, but also from the bulk of the matrix. This reflects the importance of using constant sample volumes in the cell for a given analysis and of avoiding any

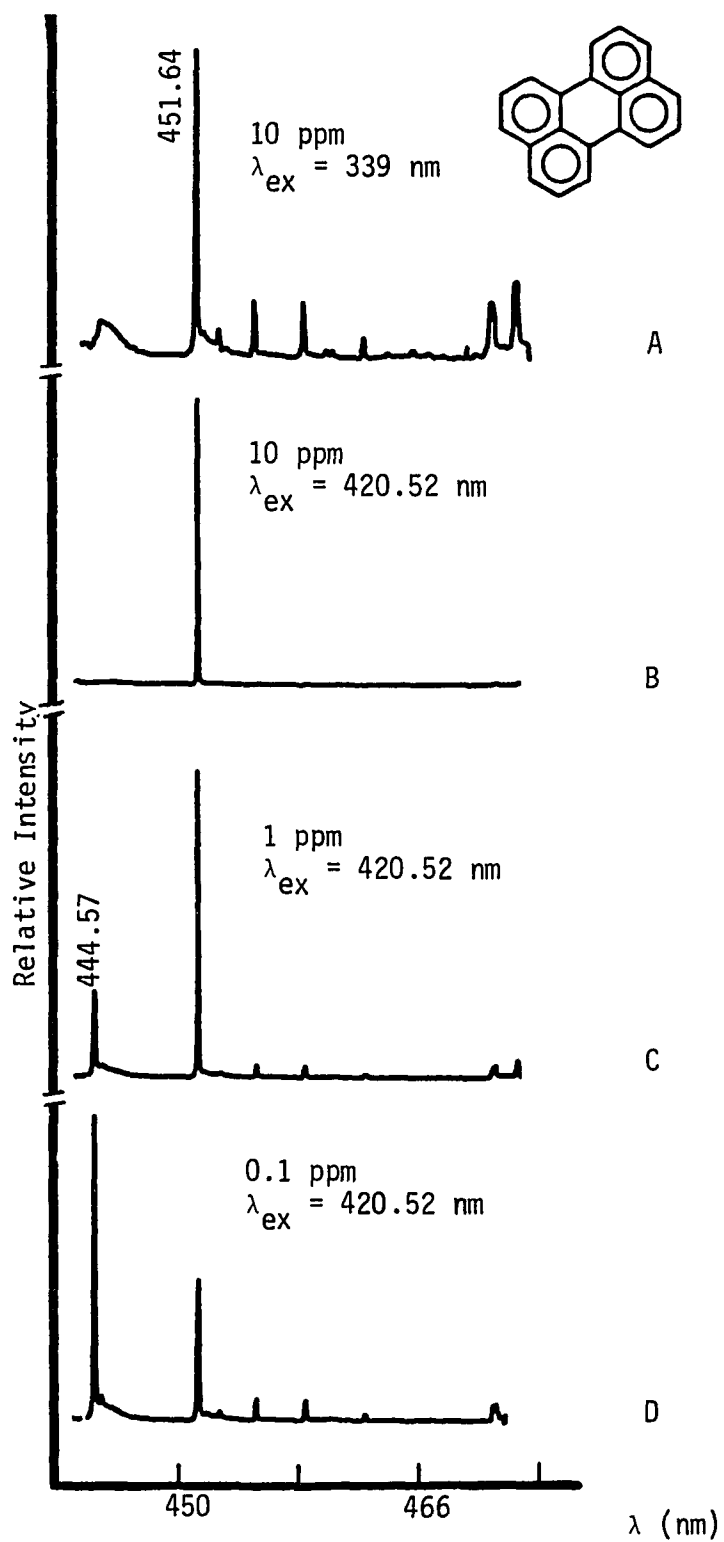


Figure 28. Fluorescence emission spectra of perylene in n-octane

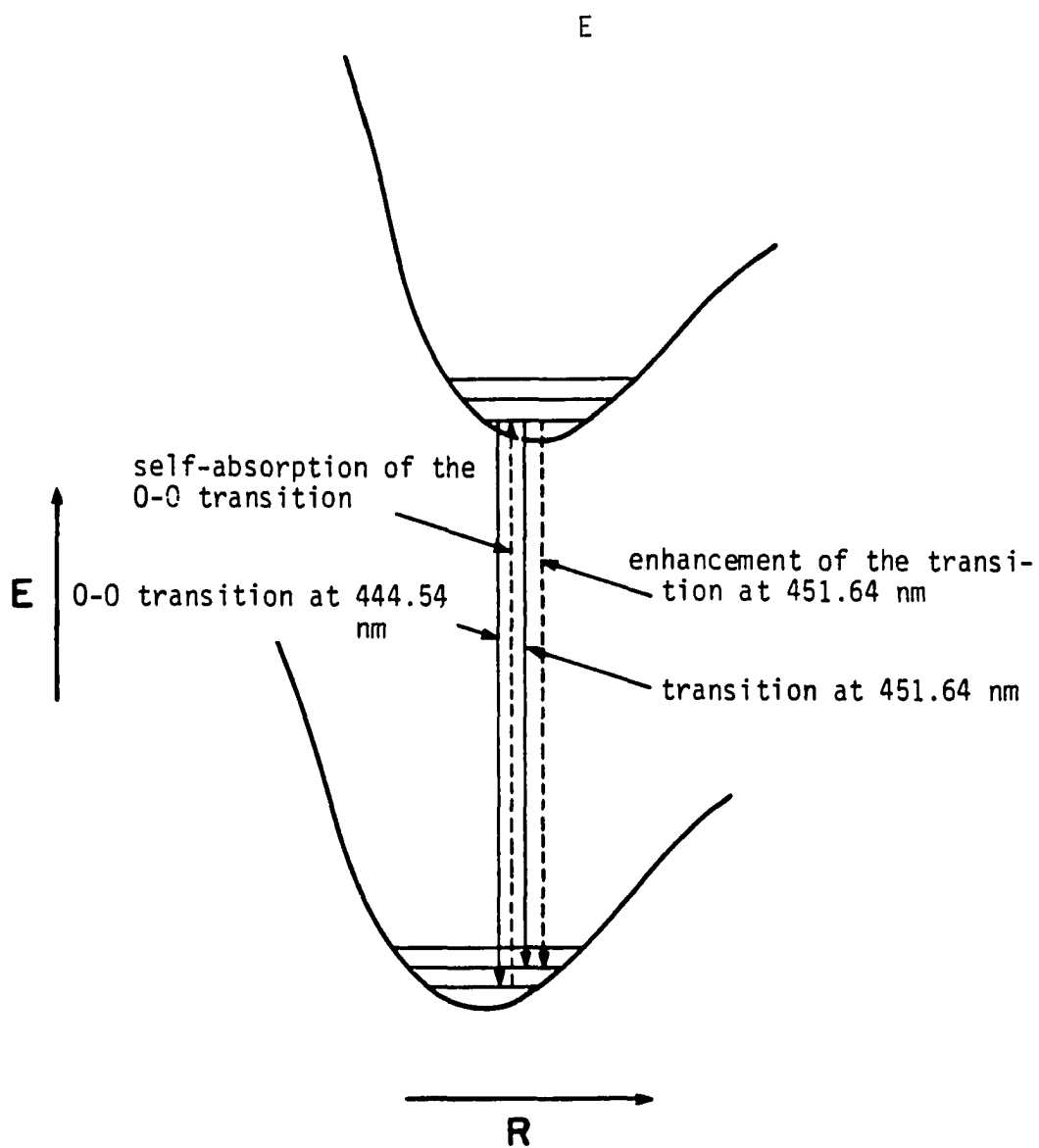
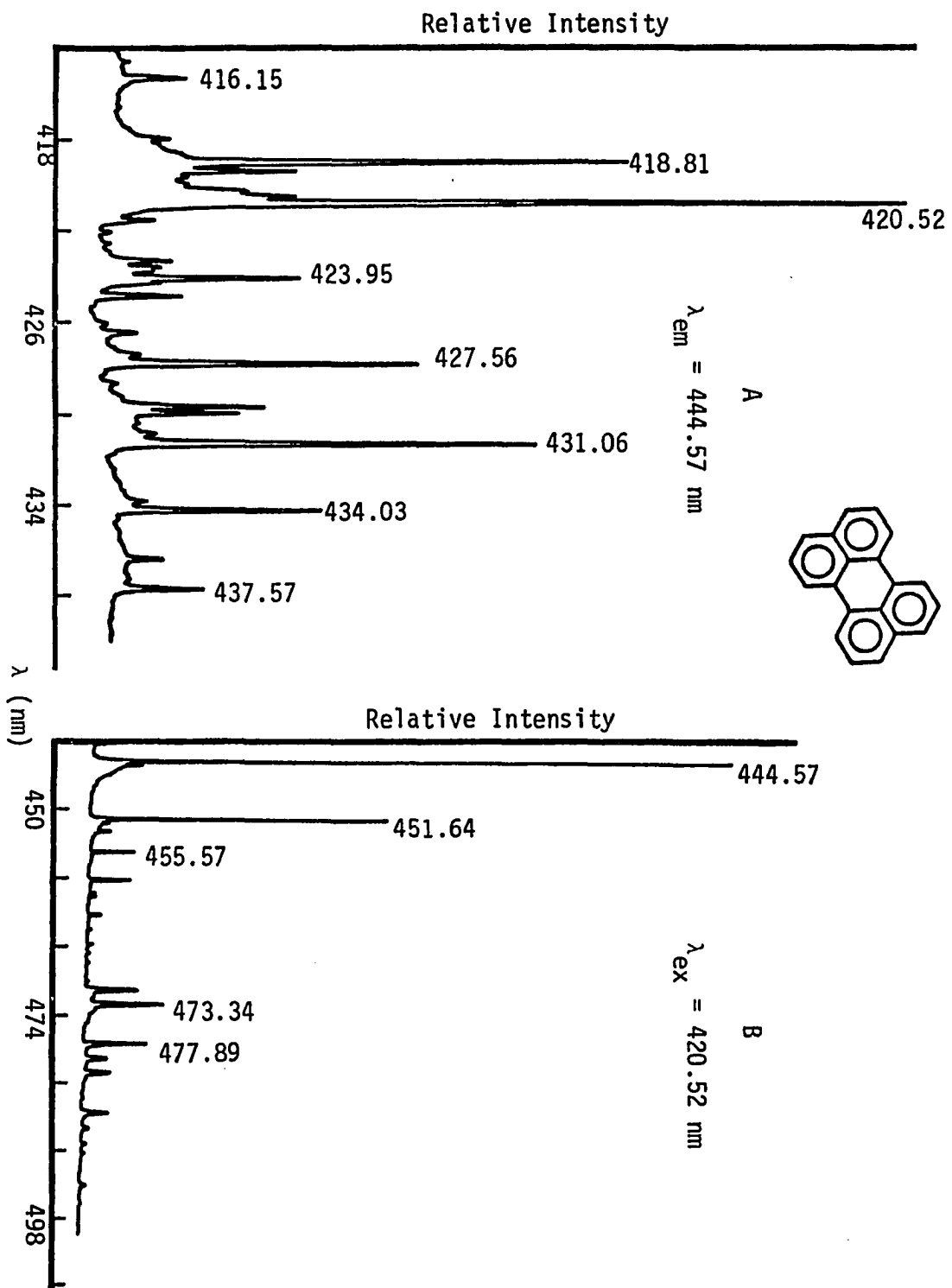


Figure 28.(continued) Simplified energy level diagram for a perylene molecule

Figure 29. Excitation (A) and fluorescence emission (B) spectra of 0.1 ppm perylene at a concentration of 0.1 ppm in n-octane



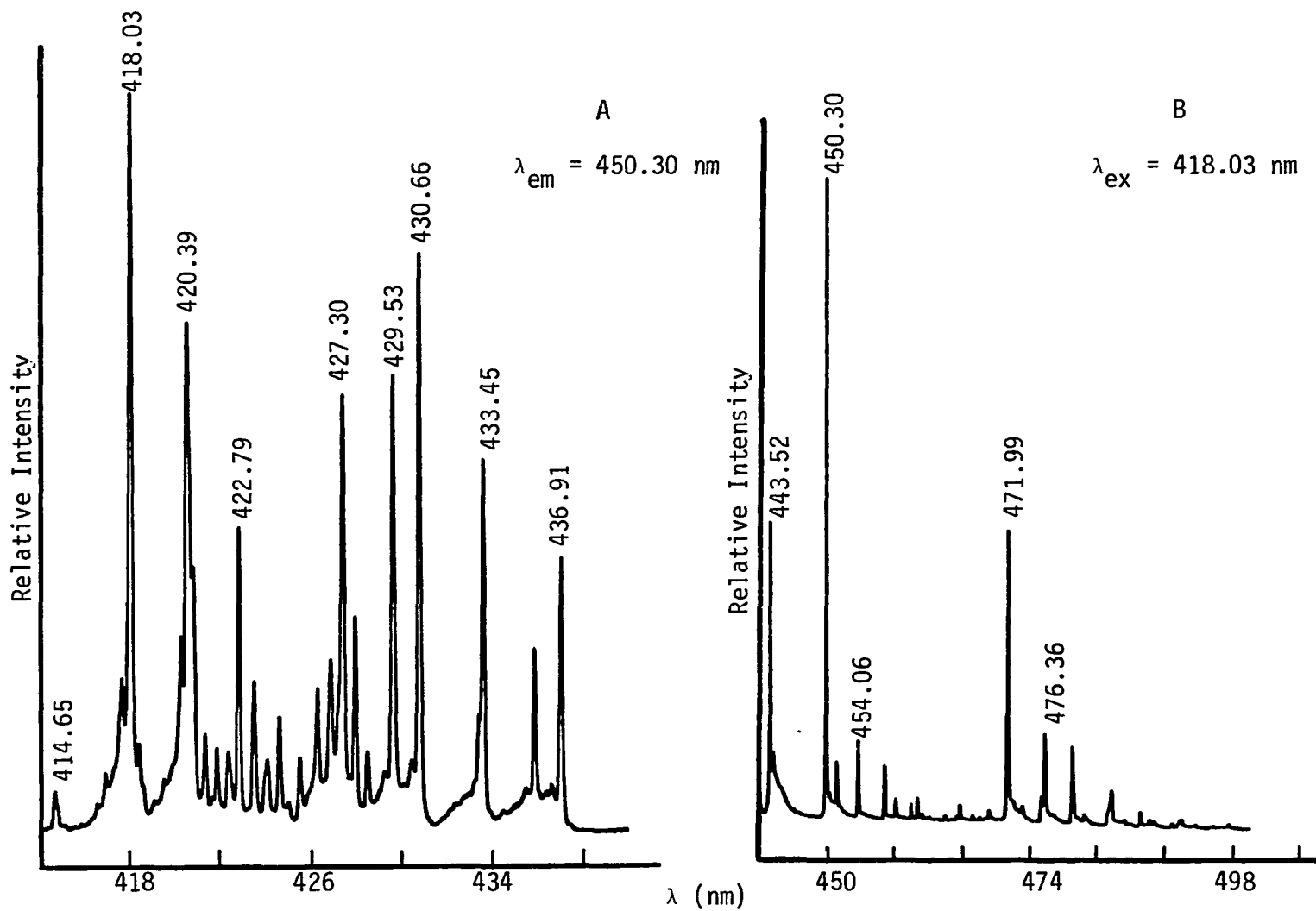


Figure 30. Excitation (A) and fluorescence emission (B) spectra of perylene-d₁₂ at a concentration of 1 ppm in n-octane

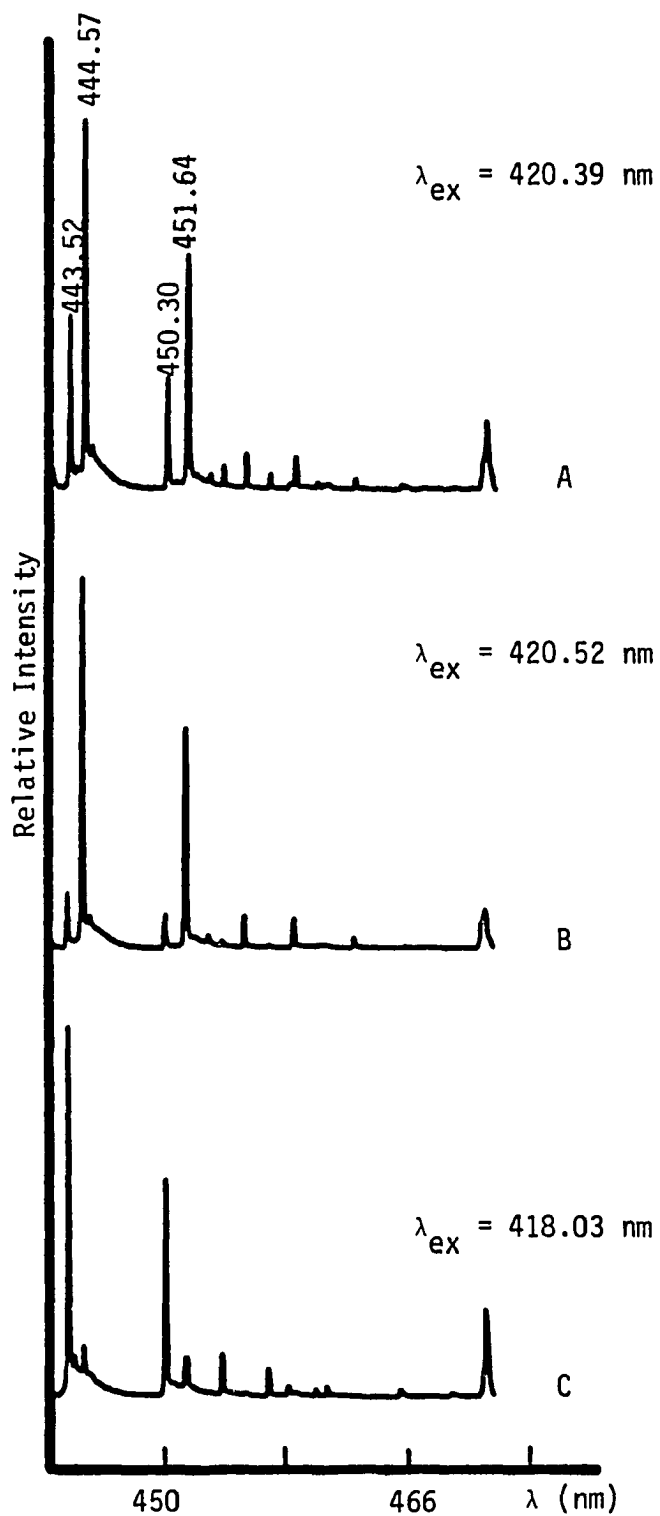


Figure 31. Fluorescence spectra of a mixture of perylene and perylene- d_{12} in n-octane at different excitation wavelengths

trapped gas bubbles in the matrix. Furthermore, these observations reemphasize the importance of using some sort of an internal reference compound if quantitative analysis is desired. As indicated earlier, perylene- d_{12} should serve this purpose. Site-selective spectra for perylene and perylene- d_{12} are shown in Figs. 29 and 30, respectively. The ideality of perylene- d_{12} as an internal reference compound for perylene is shown in Fig. 31 for a mixture of the two compounds. This ideality arises from the following considerations: (a) the behavior of perylene- d_{12} , especially with respect to self-absorption, were found to be similar to that of perylene; (b) perylene- d_{12} is unlikely to be present in real samples; (c) perylene- d_{12} is available commercially with high purity; (d) the lines of perylene- d_{12} are well resolved from those of perylene and in close proximity to them; and (e) it is possible to excite the fluorescence emission of both compounds at one λ_{ex} , which is at 420.39 nm.

Indeno(1,2,3-cd)pyrene, anthanthrene, benzo(k)fluoranthene, and benzo(b)fluoranthene; examples of relatively large shifts in the multi-site spectra

The characteristic LESS spectra of these compounds are shown in Figs. 32 to 39. For all of the emission spectra, the recorded signals were adjusted by varying the slit width, so that the most intense line in the individual spectra remained on scale.

Typically, the difference in wavelengths between two adjacent 0-0 lines in multiplet site structures is a few tenths of a nanometer, as can be seen, e.g., in Fig. 11 for B(a)P in n-heptane. The above four

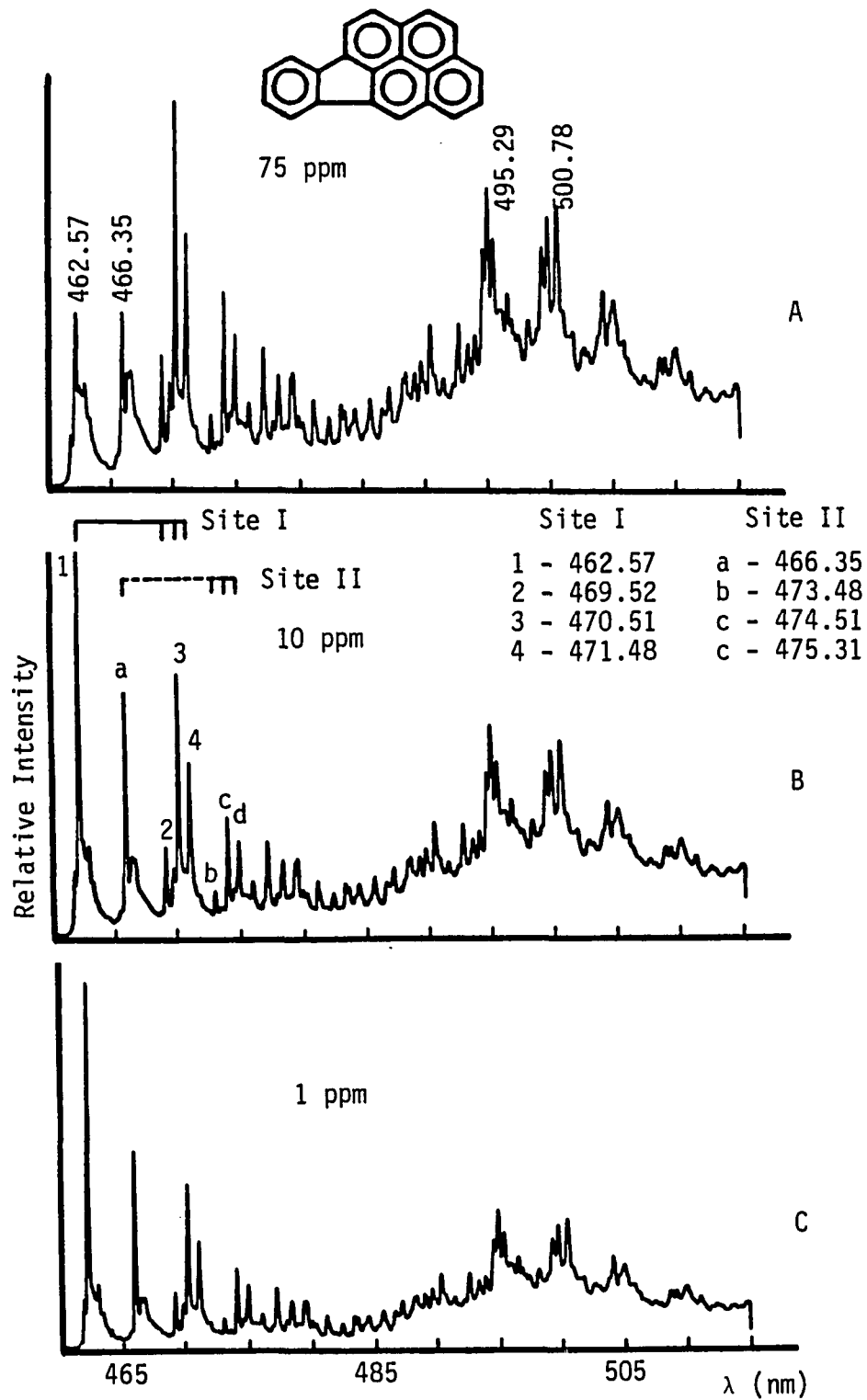


Figure 32. Nonspecifically excited fluorescence spectra of indeno-(1,2,3-cd)pyrene in n-octane at $\lambda_{ex} = 339$ nm

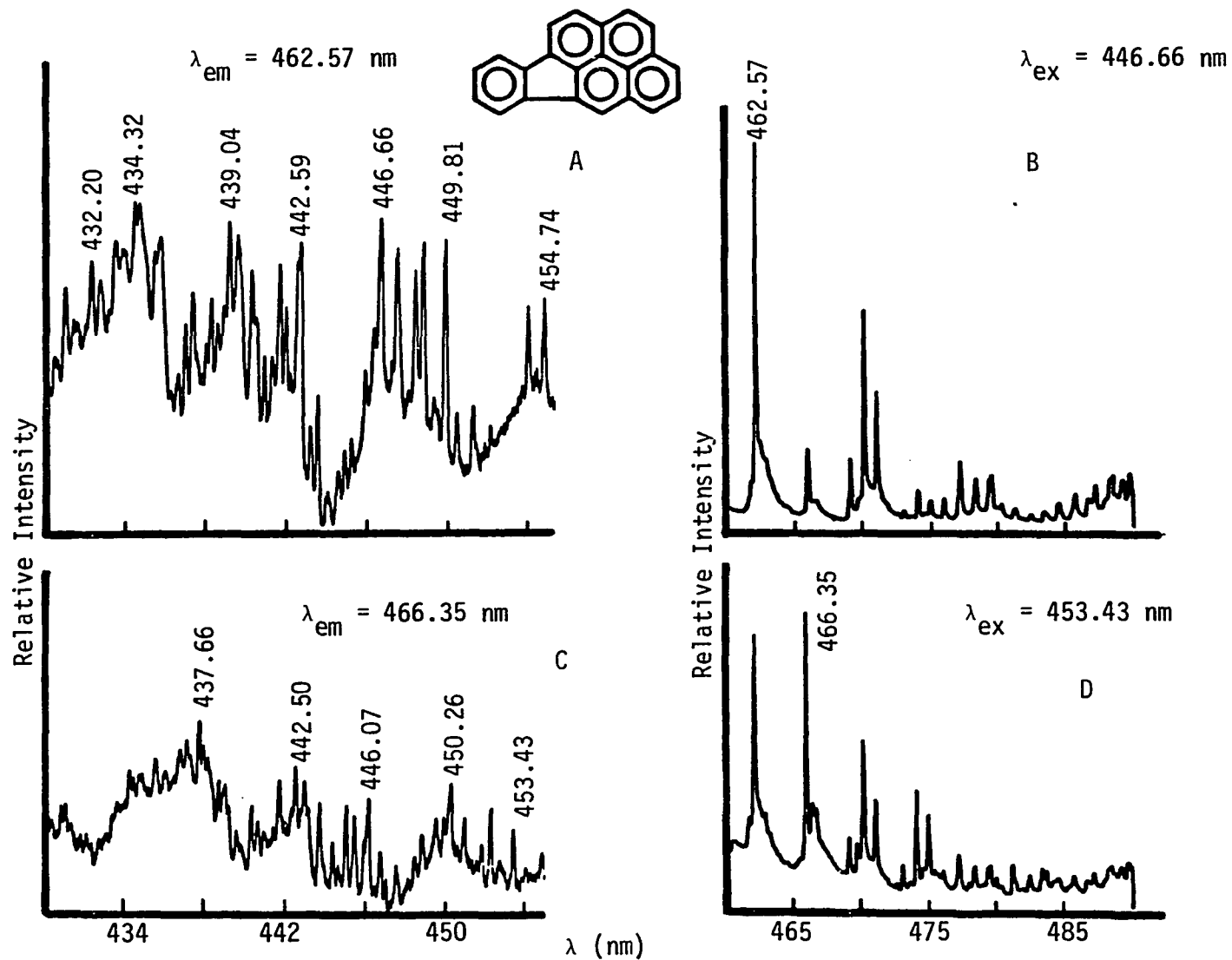


Figure 33. Excitation and selectively excited fluorescence emission spectra of indeno(1,2,3-cd)-pyrene at 10 ppm in n-octane

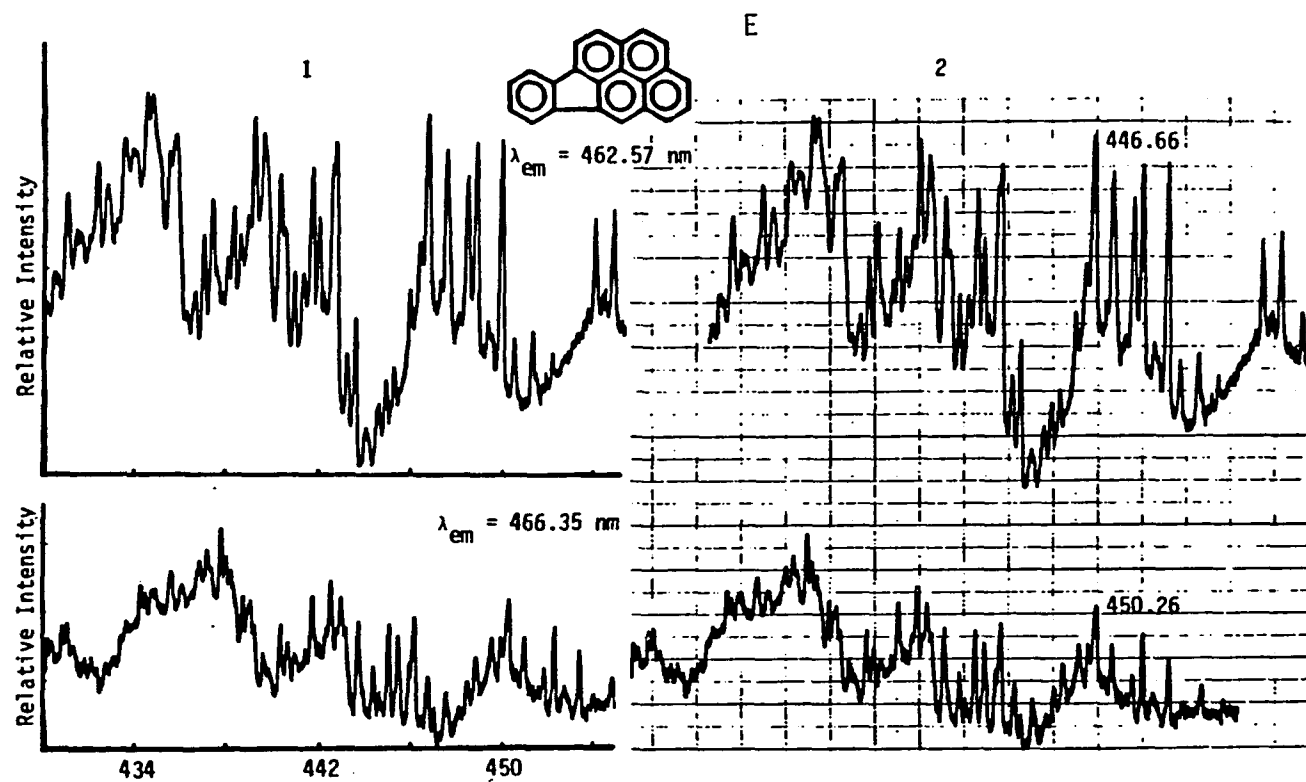


Figure 33.(continued) Comparison between excitation spectra of indeno(1,2,3-cd)pyrene at emission wavelengths 462.57 and 466.35 nm: (1) excitation spectra in their regular positions and (2) excitation spectra positioned in order to indicate the similarity

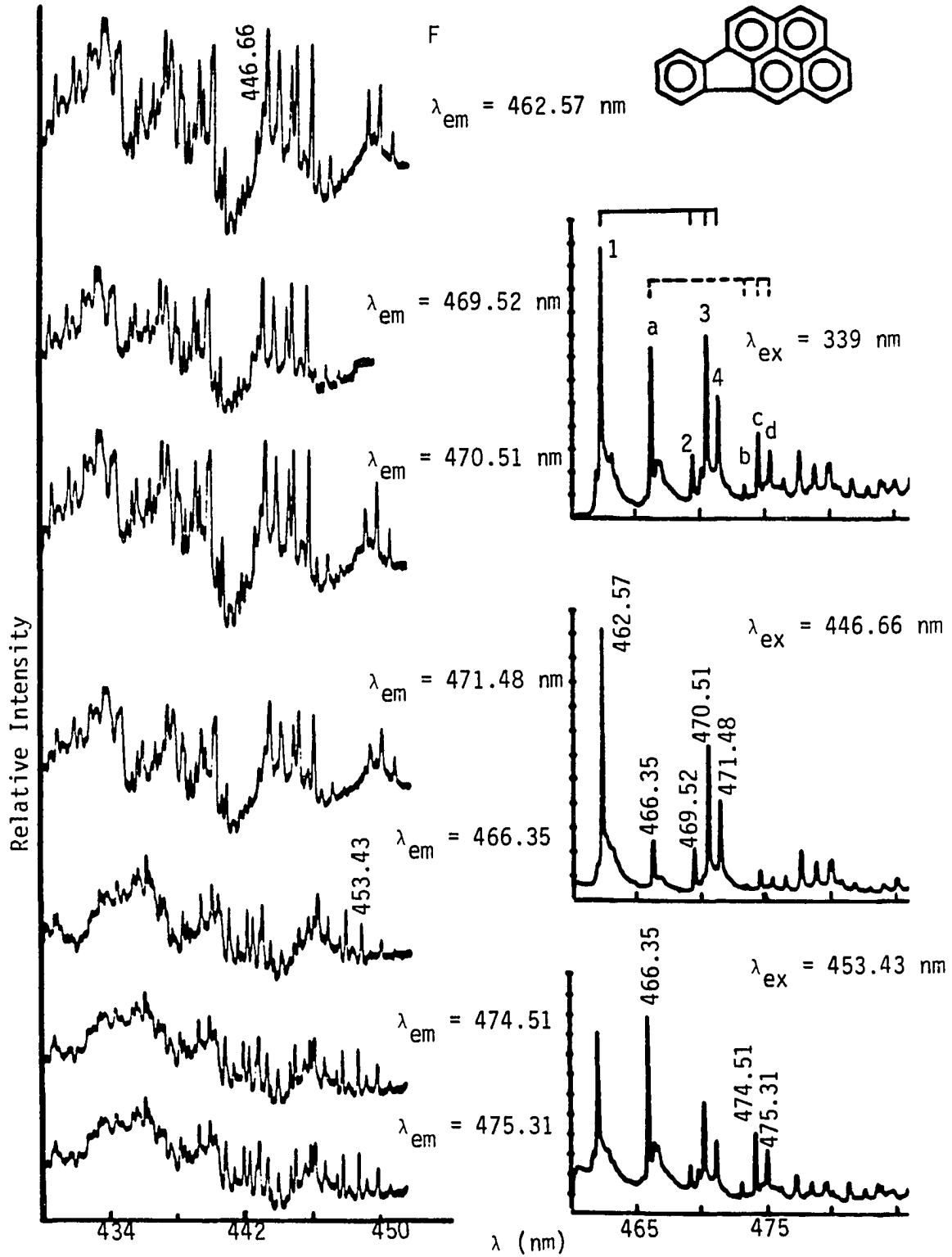


Figure 33.(continued) Site-selective spectra of indeno(1,2,3-cd)pyrene in n-octane

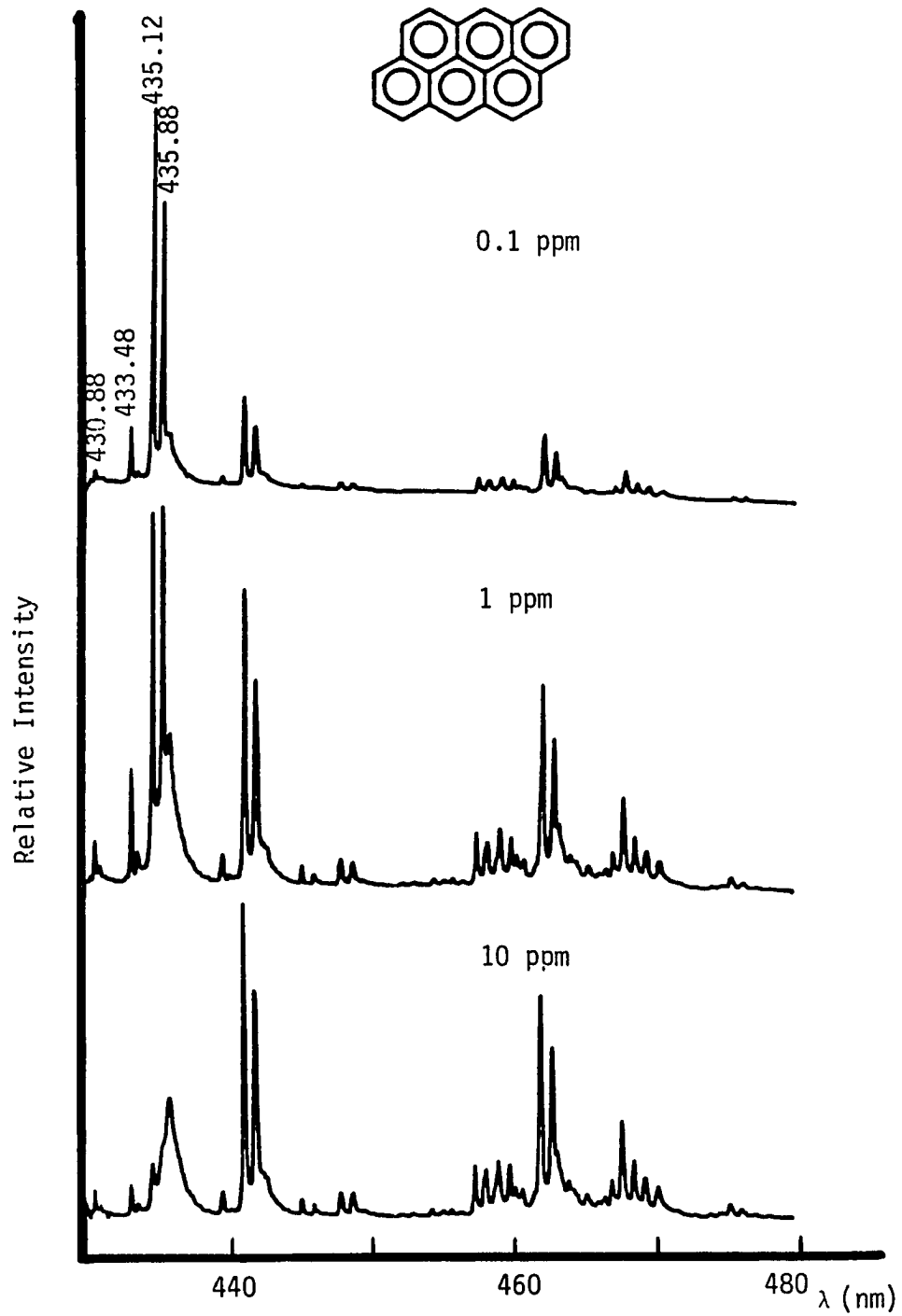


Figure 34. Nonselectively excited fluorescence spectra of anthanthrene in n-octate at $\lambda_{\text{ex}} = 359$ nm (different y axis scale)

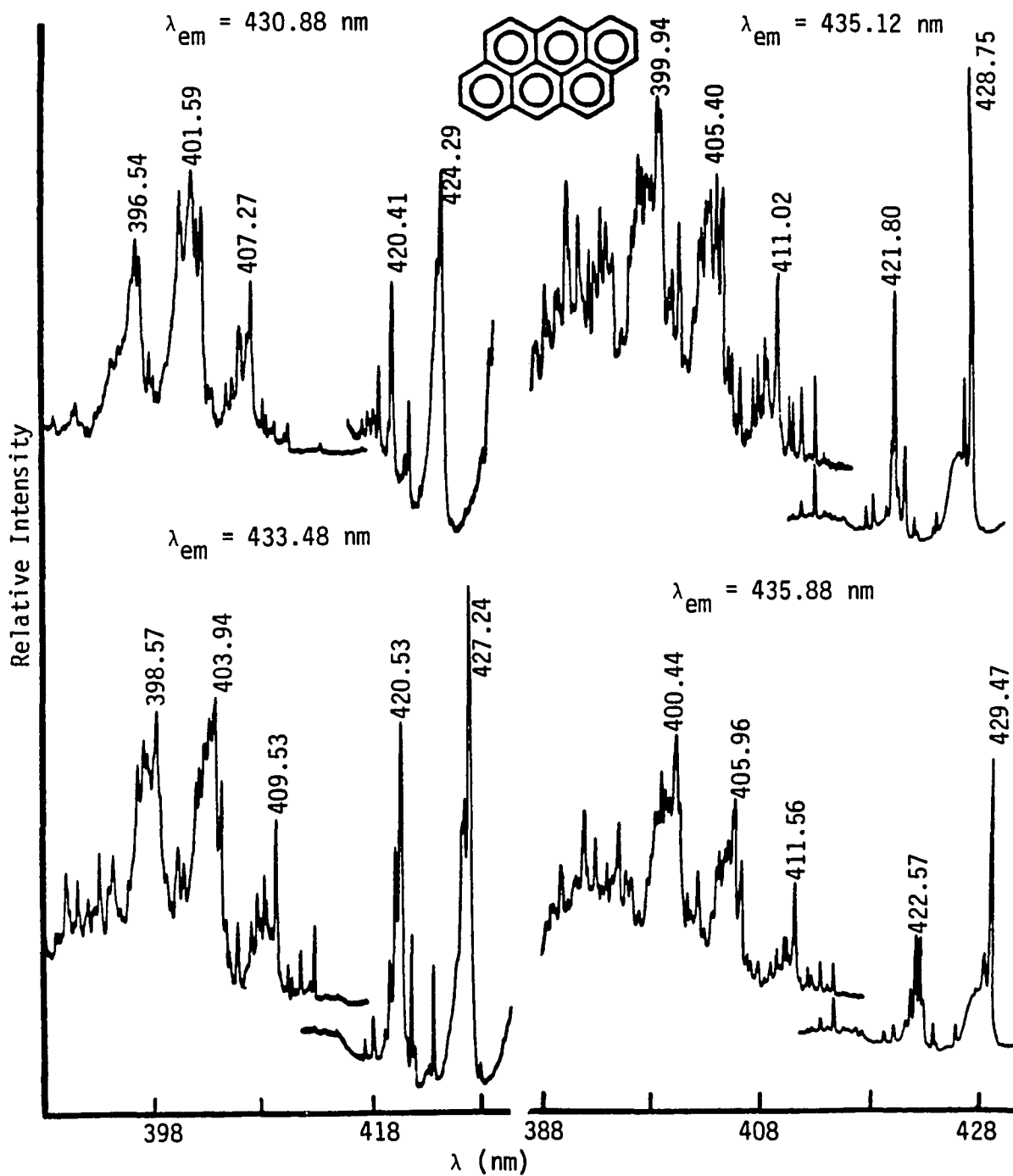


Figure 35. Excitation spectra of anthanthrene at 1 ppm in n-octane

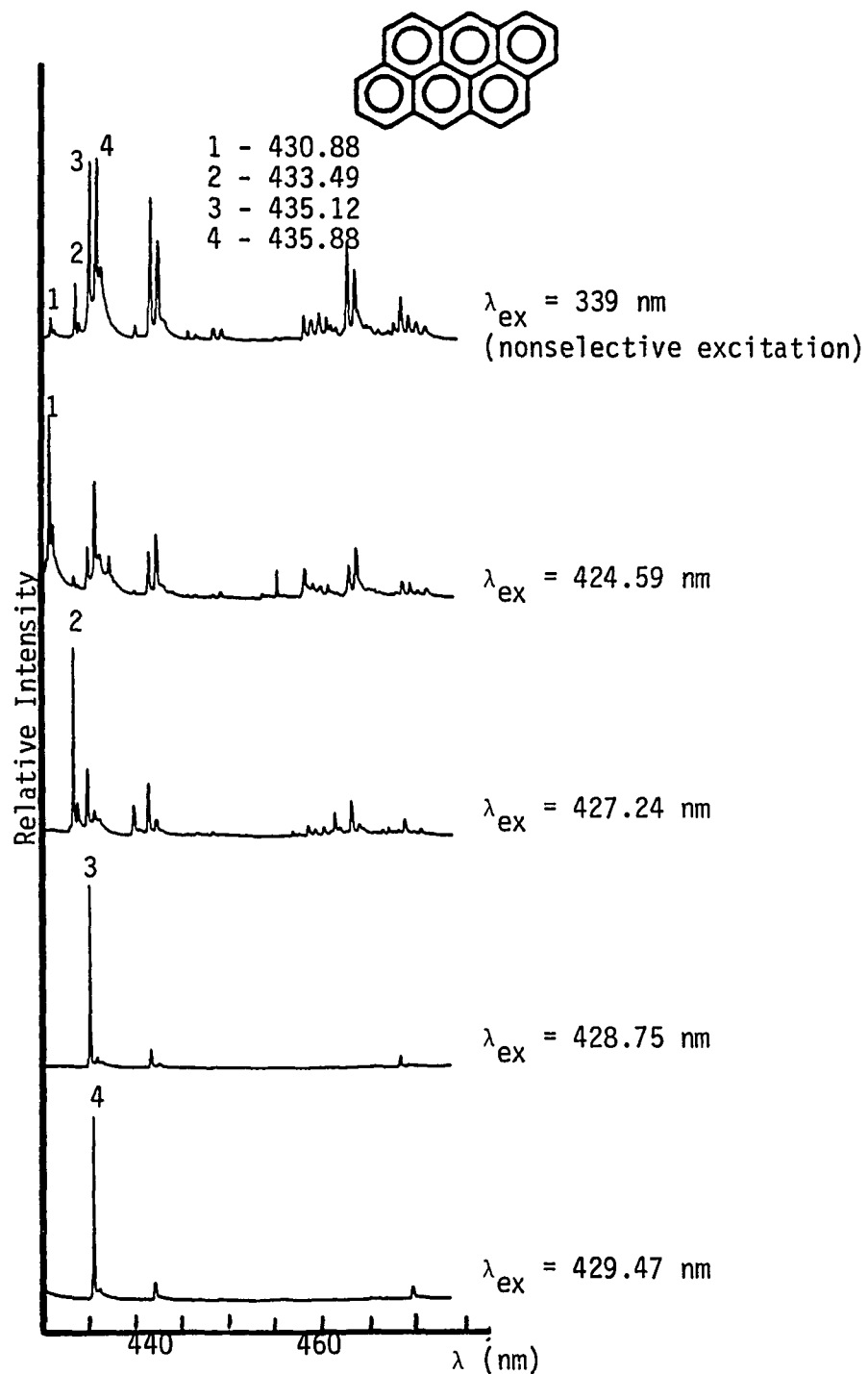


Figure 36. Nonselectively and selectively excited fluorescence spectra of anthanthrene at 1 ppm in n-octane

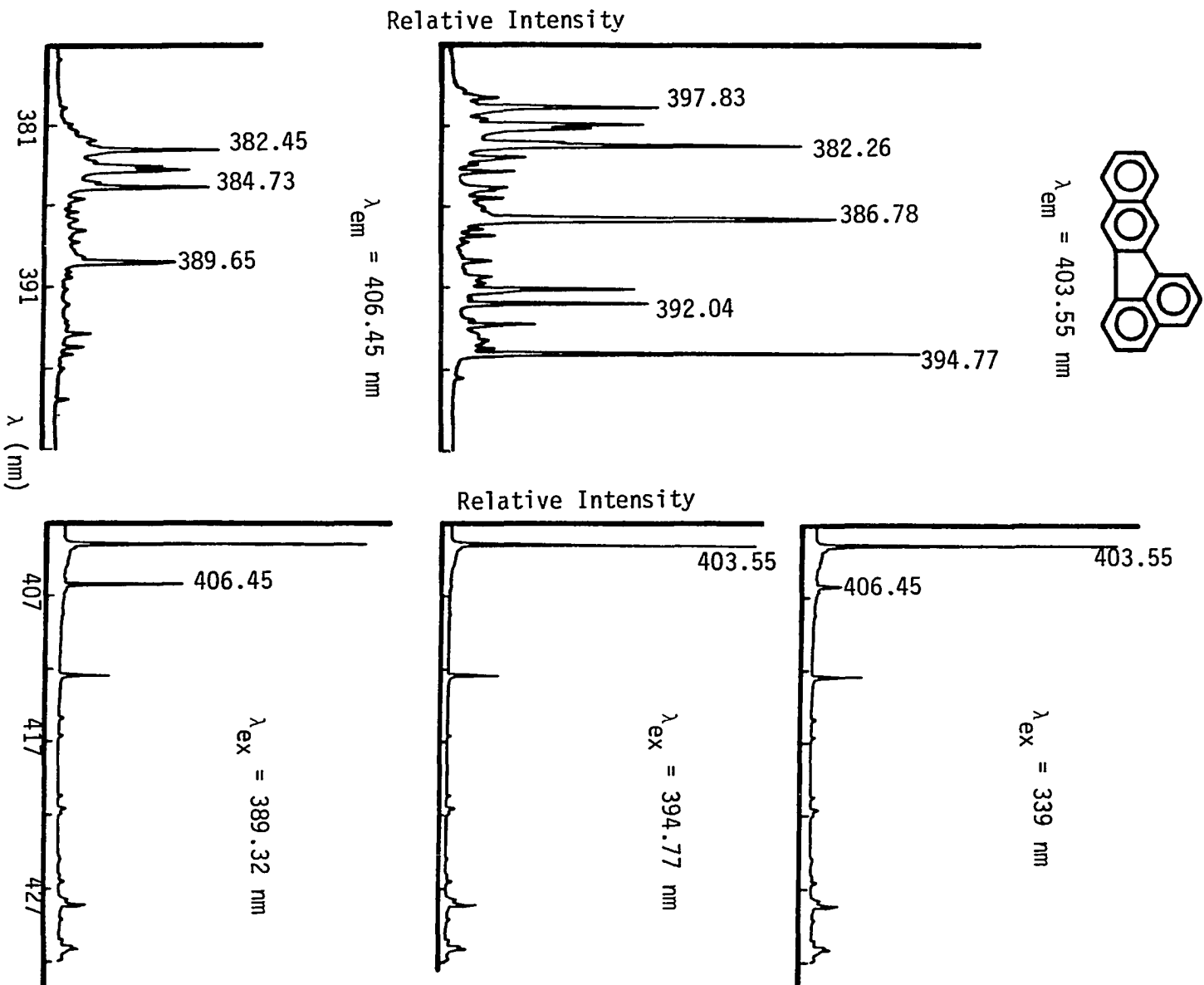


Figure 37. Site-selective fluorescence spectra of benzo(b)fluoranthene at 0.1 ppm in n-octane

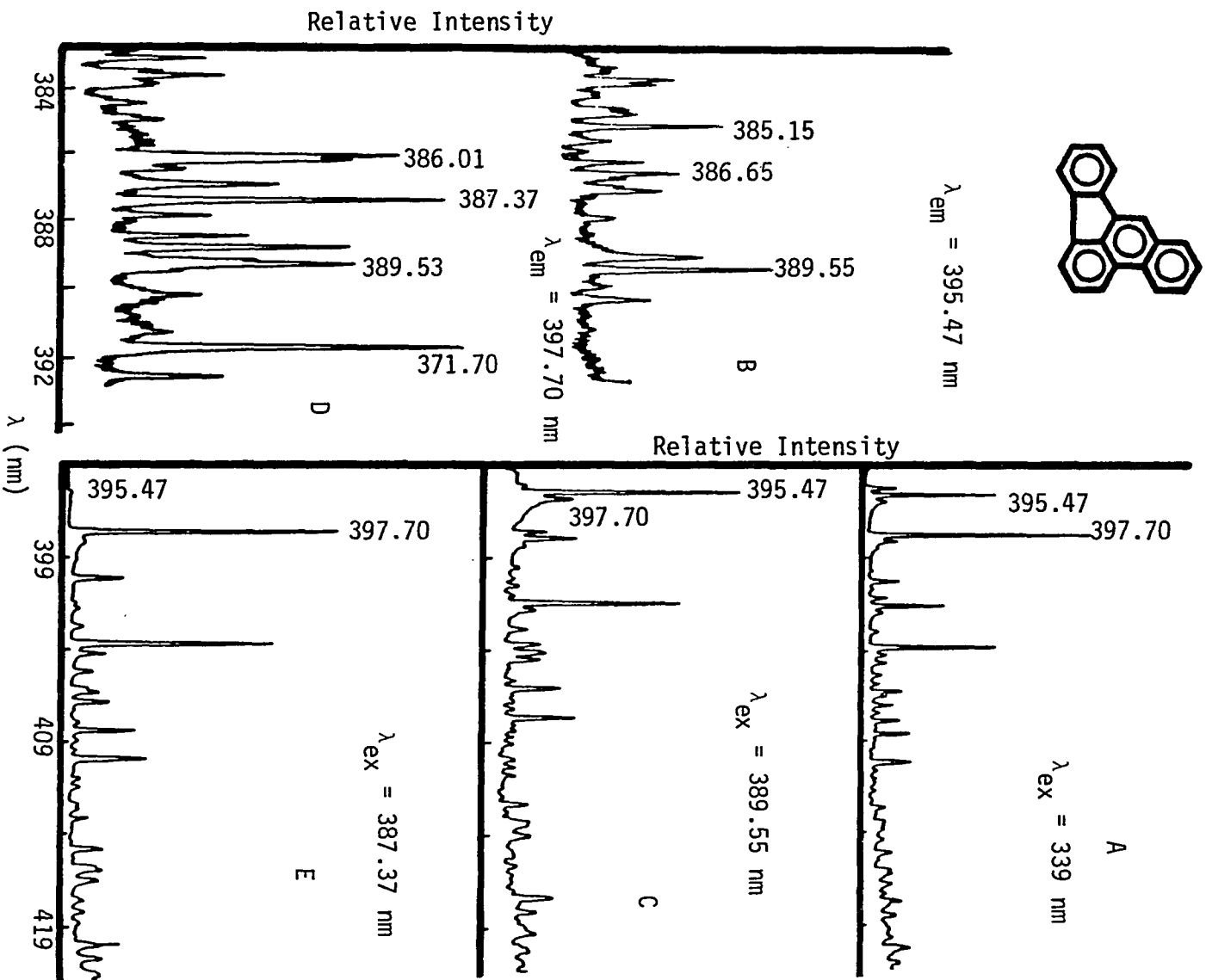


Figure 38. Site-selective fluorescence spectra of benzo(b)fluoranthene at 10 ppm in n-octane

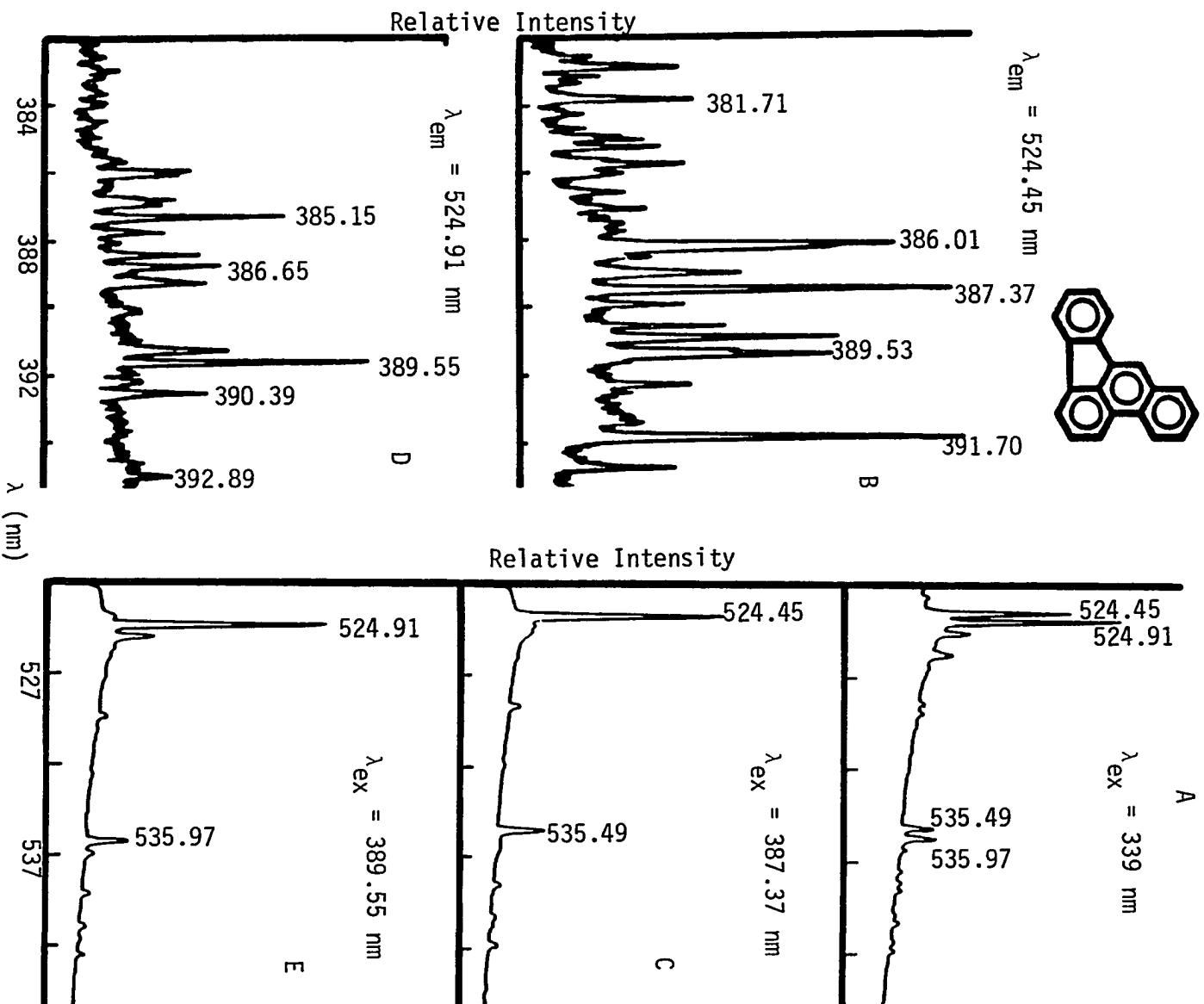
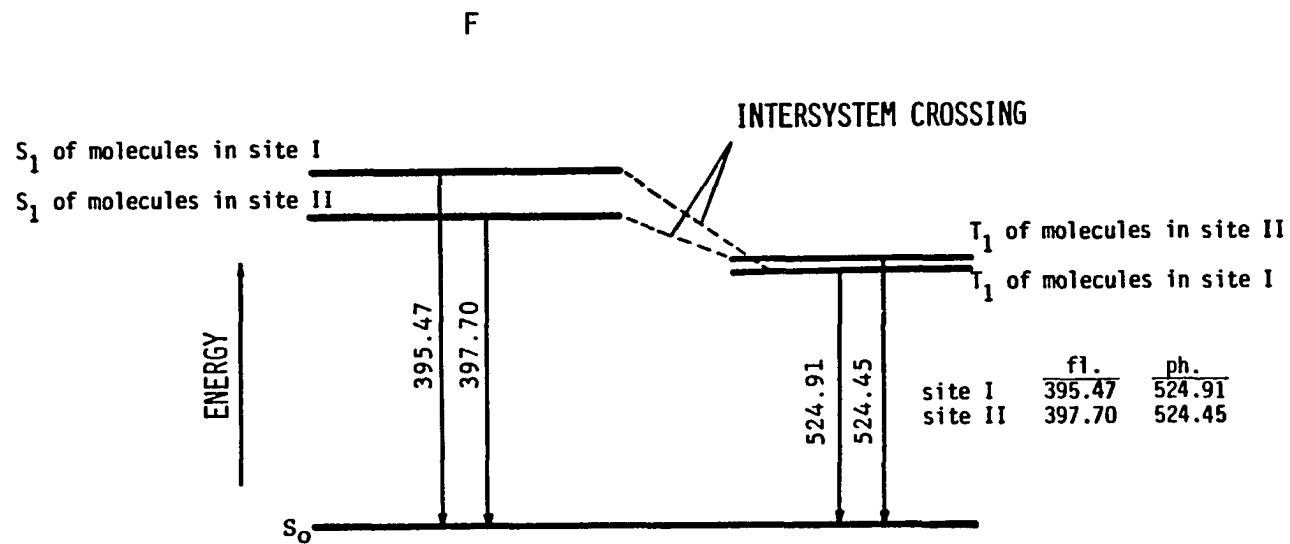


Figure 39. Site-selective phosphorescence spectra of benzo(b)fluoranthene at 10 ppm in n-octane



106

106

Figure 39.(continued) Simple Jablonski diagram for benzo(b)fluoranthene

compounds show considerable deviation from this typical difference. For example, the nonselectively excited spectra for indeno(1,2,3-cd)pyrene shown in Fig. 32, at decreasing concentrations from 75 to 1 ppm, reveal a separation of 3.78 nm between the prominent site lines at 462.52 and 466.35 nm. These same lines appear to suffer from strong self-absorption, i.e., their relative intensities relative to other lines in the spectra decreased with concentrations. The evident self-absorption of these lines indicates that both of them are 0-0 lines. This last conclusion was further confirmed by the work described below.

Excitation spectra observed at λ_{em} of 462.57 and 466.35 nm for indeno(1,2,3-cd)pyrene are shown in Fig. 33A and C, respectively. The two excitation spectra are complicated and at first glance, they seem different. However, when the two spectra are placed as shown in Fig. 33E, the structural similarity becomes clear. A comparison of line intensities in Figs. 32B and 33B and D for nonselective and selective excitation fluorescence, respectively (collected in Fig. 35F for easy comparison), suggests that there are two groups of lines; each group belonging to a different site. These sites are marked in Fig. 32B as site I and site II. Similarities in the excitation spectra (see Fig. 33F) indicated that lines marked in Fig. 32B as 1,2,3,4 and a,b,c,d originate from molecules residing in site I and II, respectively. From these observations, it can be concluded that the fluorescence spectrum of indeno(1,2,3-cd)pyrene is the sum of two subspectra, which have similar structure, with the group originating from site II being shifted by

about 4 nm to a longer wavelength relative to the group originating from site I.

The excitation-emission profiles of the compounds anthanthrene, benzo(k)fluoranthene and benzo(b)fluoranthene were obtained by utilizing experimental procedures similar to those used for obtaining the spectra of indeno(1,2,3-cd)pyrene and are shown in Figs. 34 to 39. Of the four compounds, only benzo(b)fluoranthene exhibited relatively intense phosphorescence. It is apparent that there are similarities in the excitation spectra shown in Figs. 38B and 39D, and Figs. 38D and 39B, which leads to the conclusion that the phosphorescence lines 524.91 nm and 524.45 nm originate from site I and II, respectively. A Jablonski diagram based on the above conclusions is shown in Fig. 40. From the figure, it is apparent that there is an inversion in the energy levels of T_1 states relative to the S_1 states for the molecules originating from the two sites. Apparently, the crystal field effects induce more substantial shifts in the energy of the T_1 state at site I than at site II. A more critical theoretical investigation will probably reveal the reasons for the above observations.

Coronene; an example of impurity effect on the spectrum of a given compound

Nonselectively-excited, luminescence spectra of coronene in n-octane for two different commercial products are shown in Fig. 40. The two spectra were approximately the same, but they were not in agreement with previously published spectra of coronene (206). The obtained spectra, however, and the published spectra showed a strong well-resolved

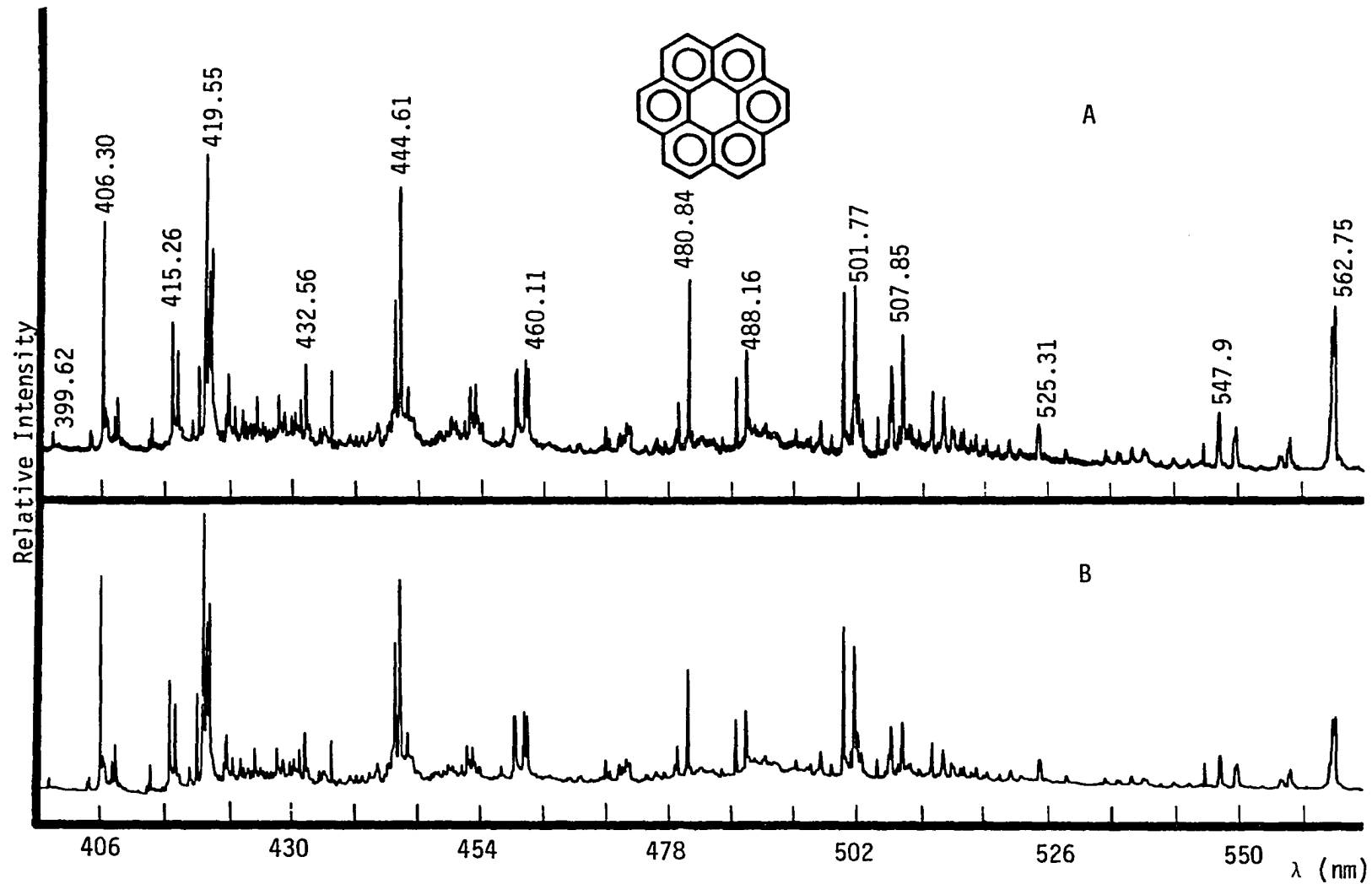


Figure 40. Nonselective excitation luminescence spectrum of two commercial brands of 2 ppm coronene in n-octane at $\lambda_{ex} = 359$ nm

phosphorescence line at 562.75 nm. Because this line could be conveniently measured, it was used as the λ_{em} for determining the λ_{ex} for coronene and for identifying the 0-0 excitation line. The obtained excitation spectrum, which is shown in Fig. 41, reveals that the longest wavelength line in this spectrum is at 425.60 nm (there were no peaks observed at higher wavelengths). When the excitation wavelength at 400.73 nm (see Fig. 41) was used to excite the fluorescence emission, the spectrum shown in Fig. 42 was obtained. This spectrum is now in a good agreement with previously published (206) spectrum of coronene. When the two emission wavelengths at 443.93 and 444.54 nm (see Fig. 42) were used to record the excitation spectra, the spectra shown in Fig. 43 were obtained. From these two spectra, the excitation wavelength at 408.17 and 408.57 nm were selected to obtain the site-selective spectra, which are given in Fig. 44.

The present study of coronene shows clearly how the presence of certain impurities can effect the spectrum of a given compound and how by applying LESS, one can discriminate against these impurities. The study also shows that LESS technique can be used to study the purity of PAH commercial products.

Observed Luminescence Spectra of PNAs

Beside the PAH compounds previously discussed, a number of other PNAs were also studied. The obtained luminescence spectra are shown in Figs. 45 to 76. As can be seen from these figures, the compounds studied included normal PAHs, 4 amino derivatives, 3 nitrogen-, 5 sulfur-, and 2 oxygen-heterocyclic compounds. Comments on a few of the unusual

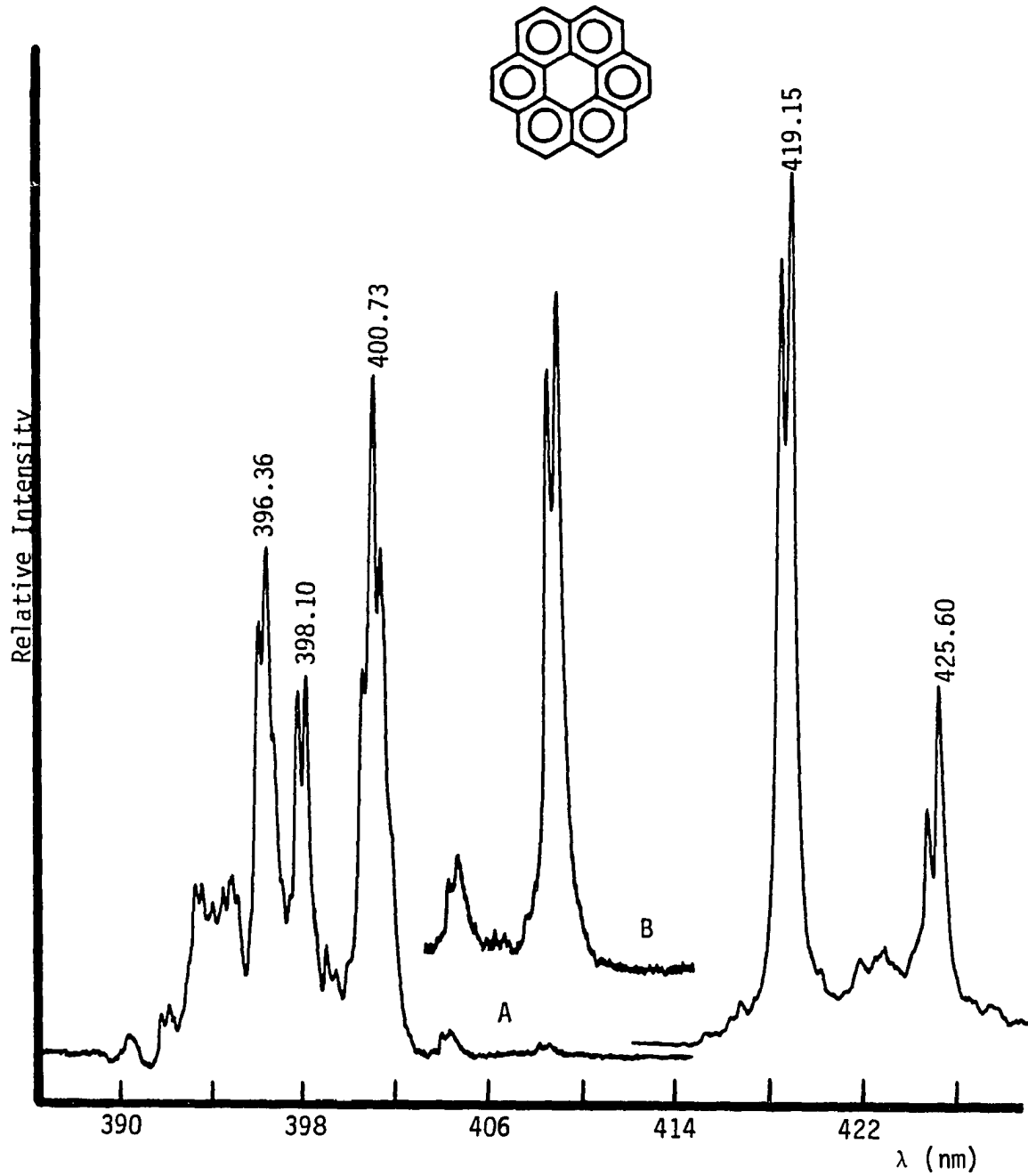


Figure 41. Phosphorescence excitation spectra of impure coronene at 2 ppm in n-octane at $\lambda_{em} = 562.75$ nm

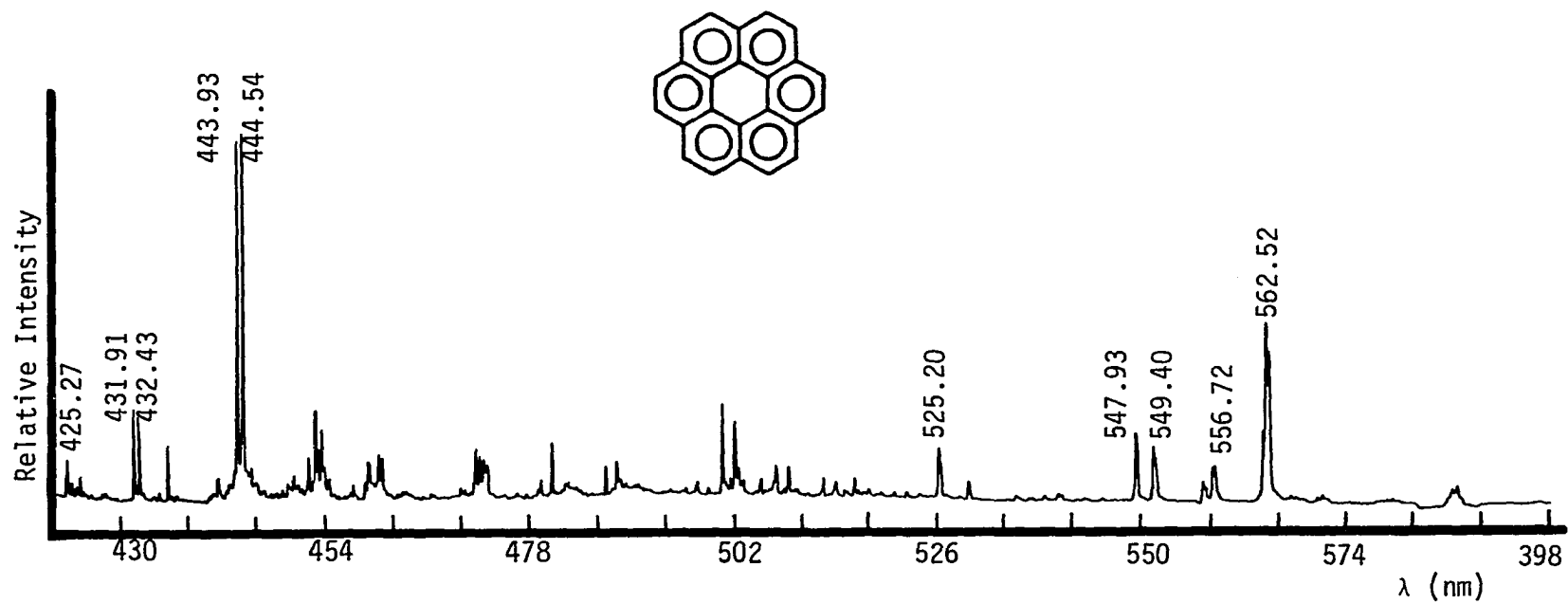
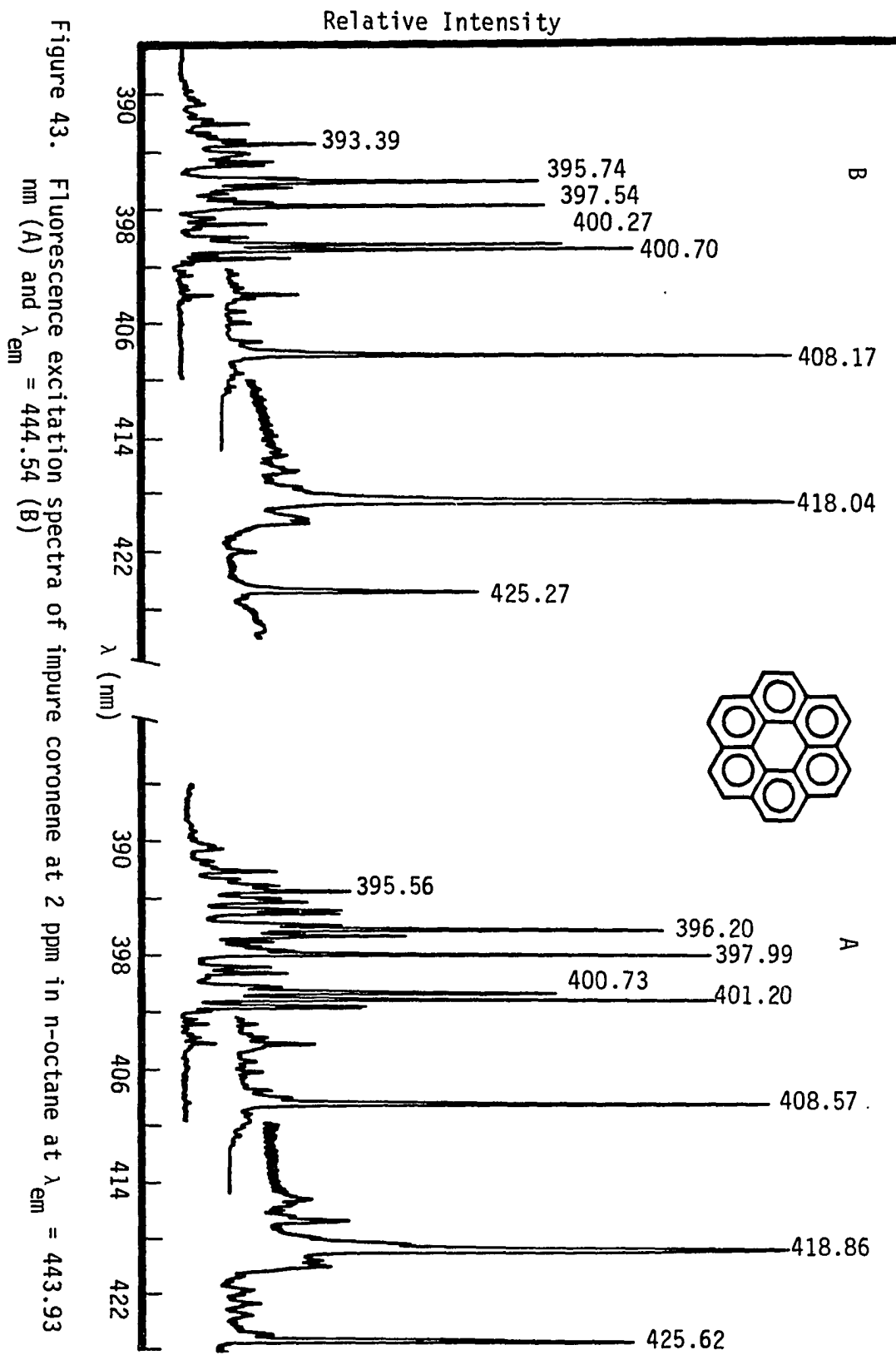


Figure 42. Luminescence emission spectrum of impure coronene at 2 ppm in n-octane at $\lambda_{\text{ex}} = 400.73 \text{ nm}$



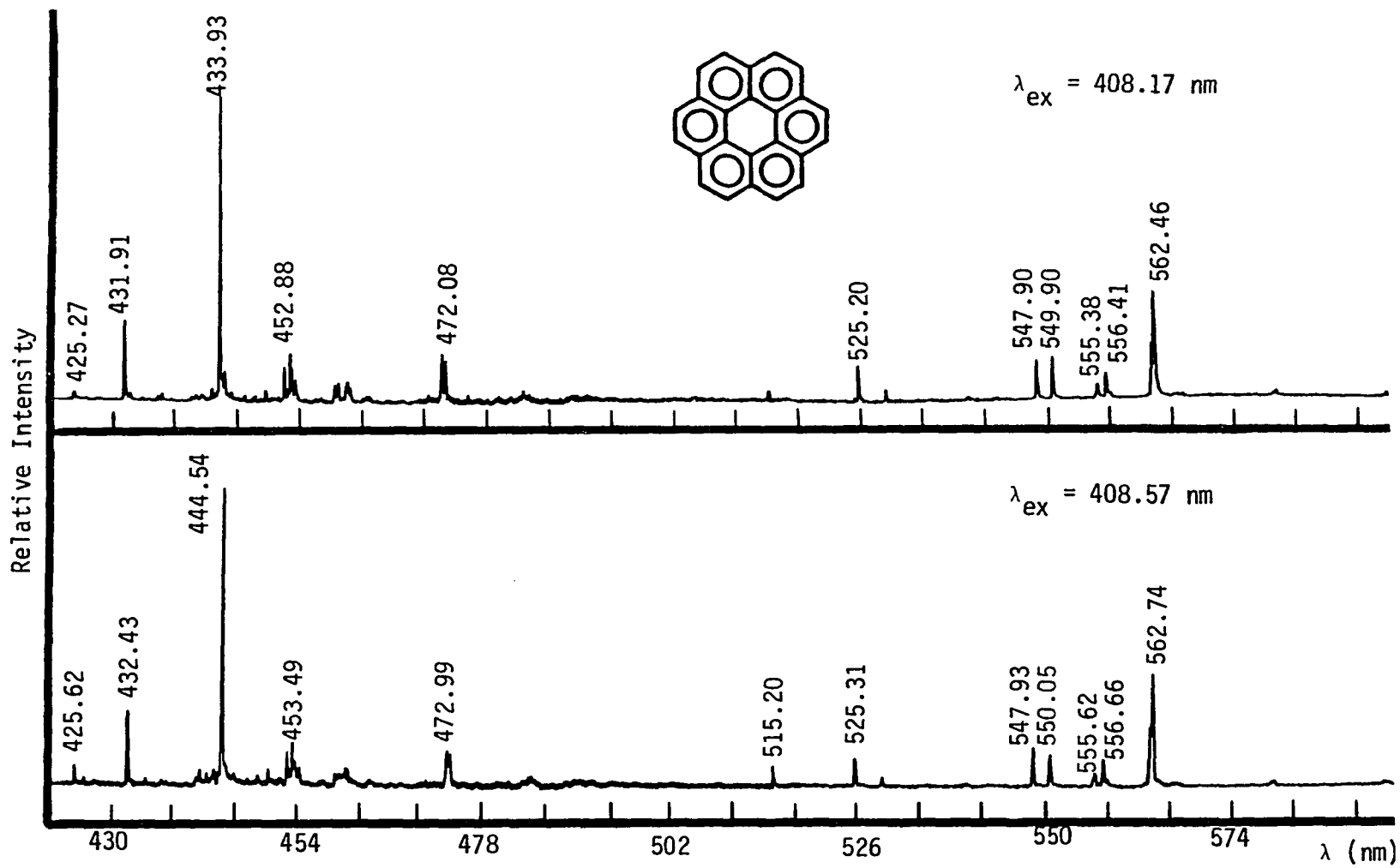


Figure 44. Selective excitation luminescence spectra of impure coronene at 2 ppm in n-octane

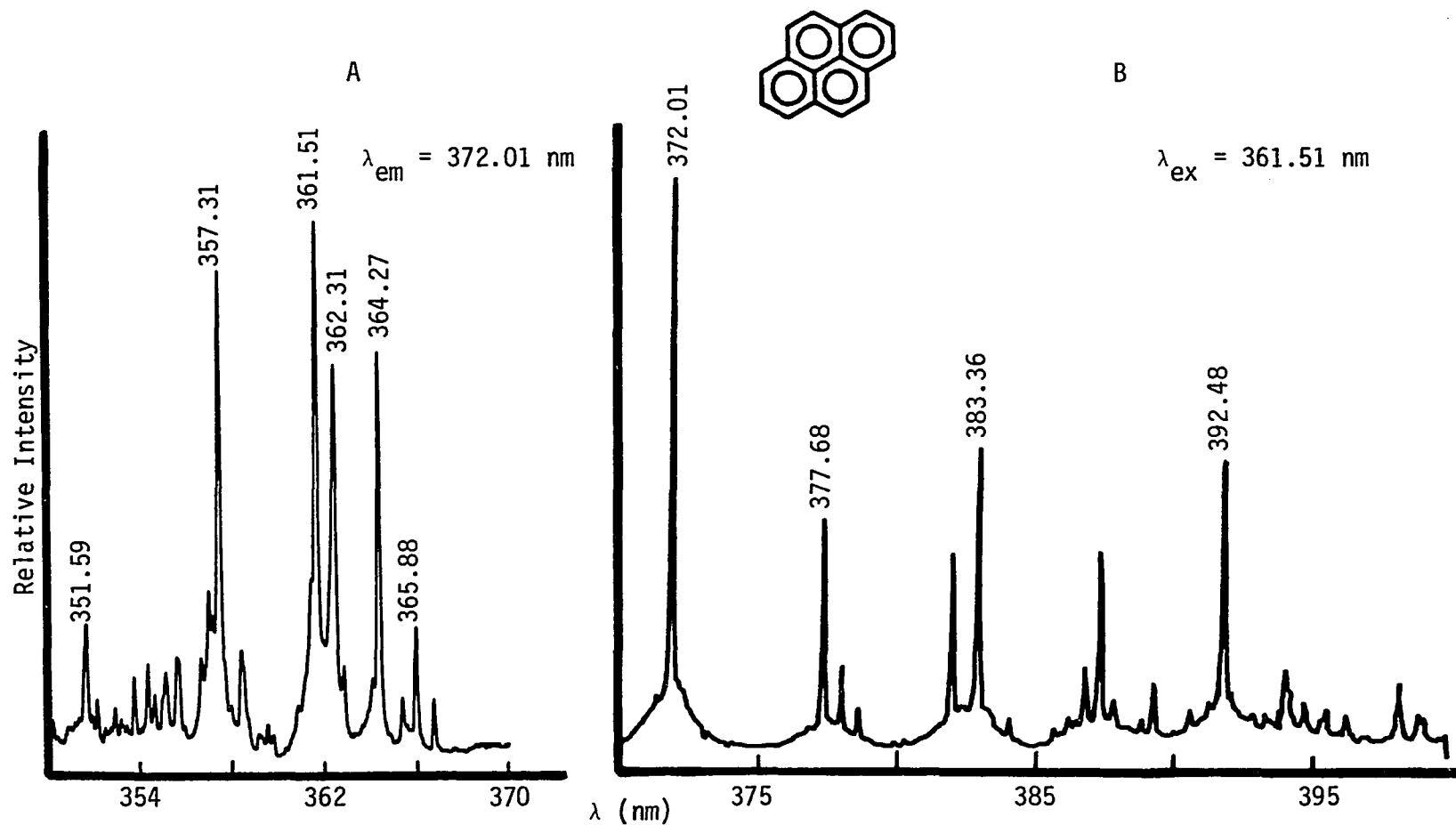


Figure 45. Excitation (A) and fluorescence emission (B) spectra of pyrene at 1 ppm in n-octane

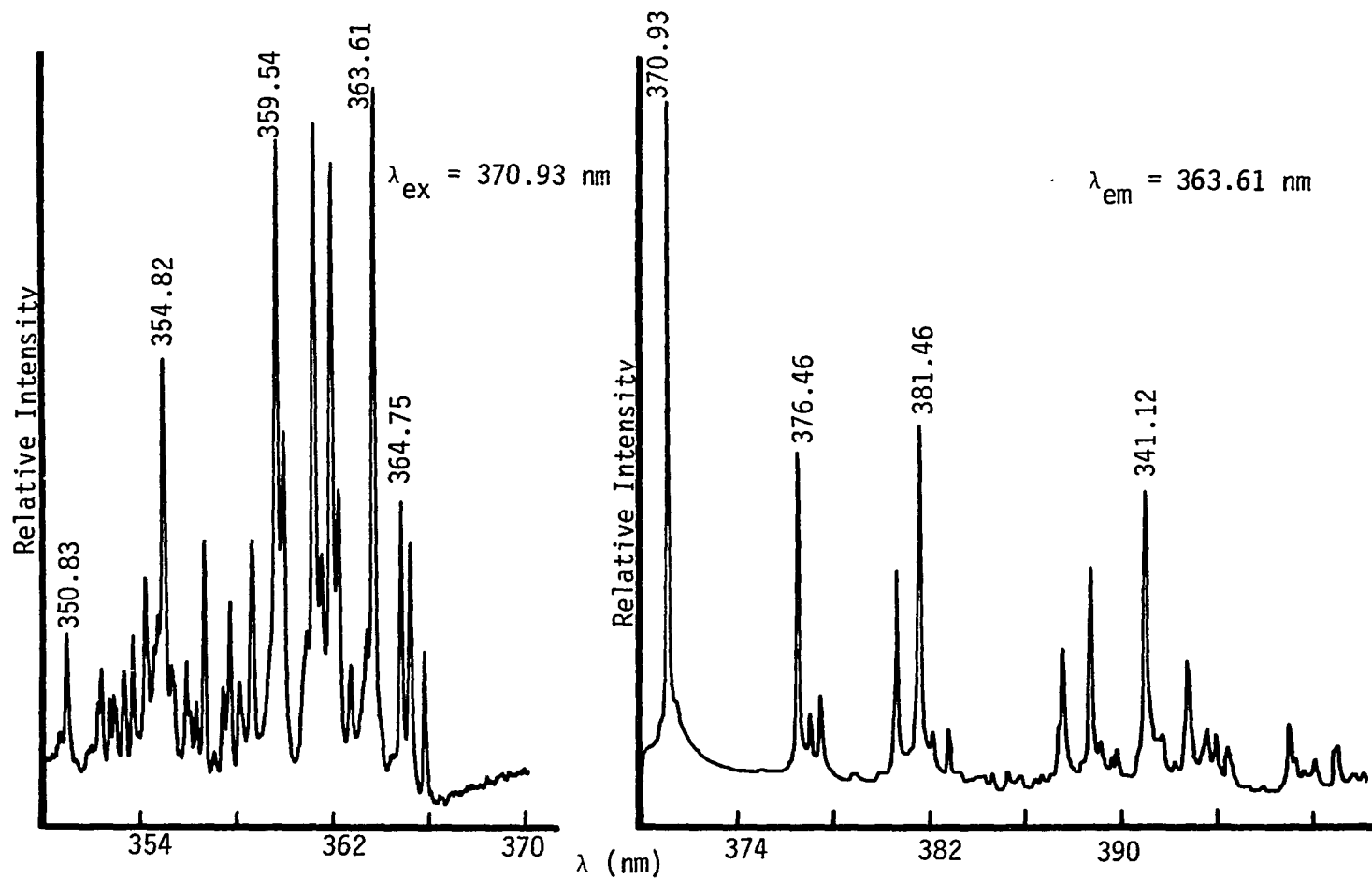


Figure 46. Excitation and selectively excited fluorescence spectra of pyrene-d₁₀ at 1 ppm in n-octane

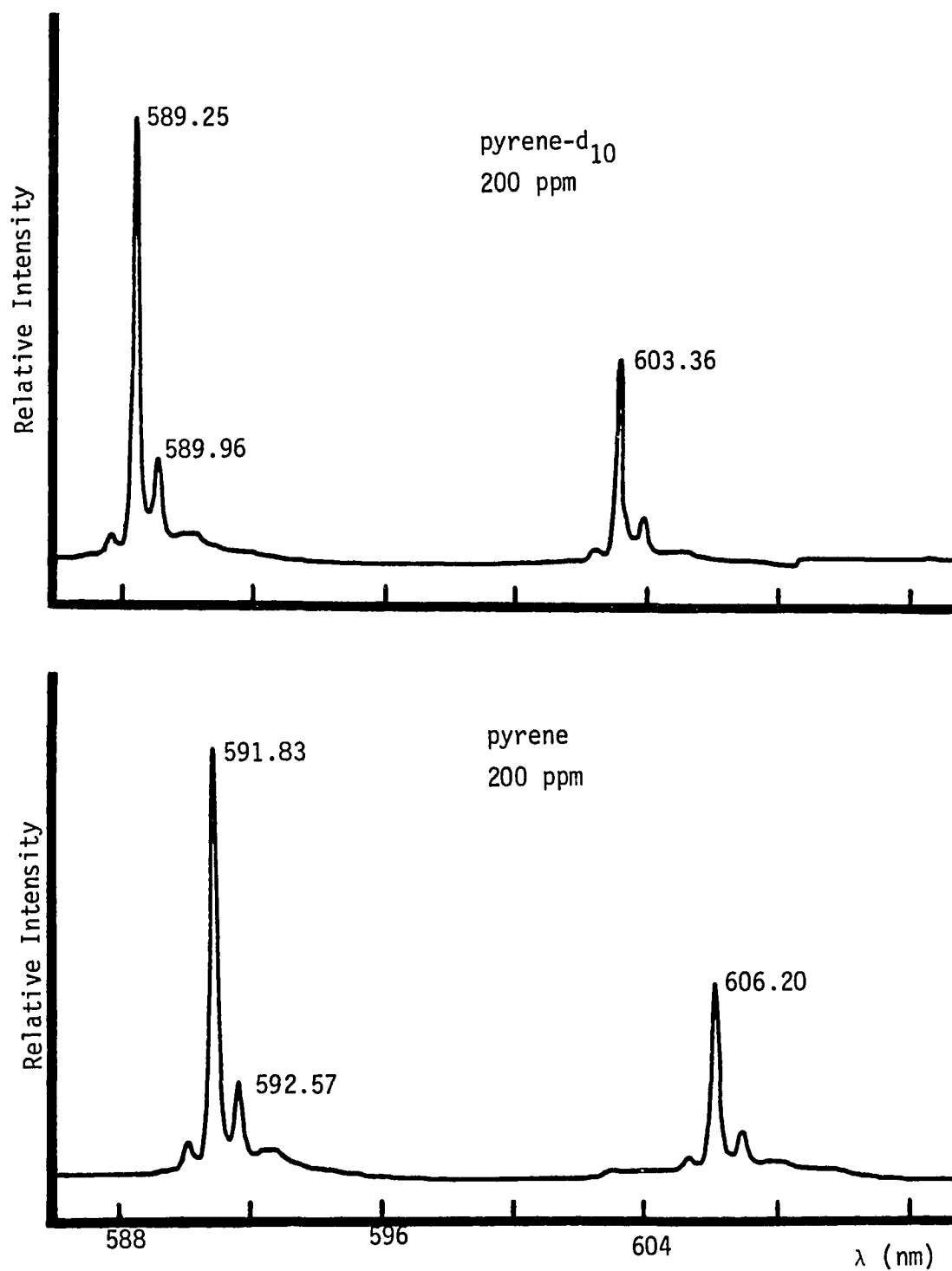


Figure 47. Nonselectively phosphorescence emission spectra of pyrene-d₁₀ and pyrene in n-octane at $\lambda_{\text{ex}} = 339$ nm

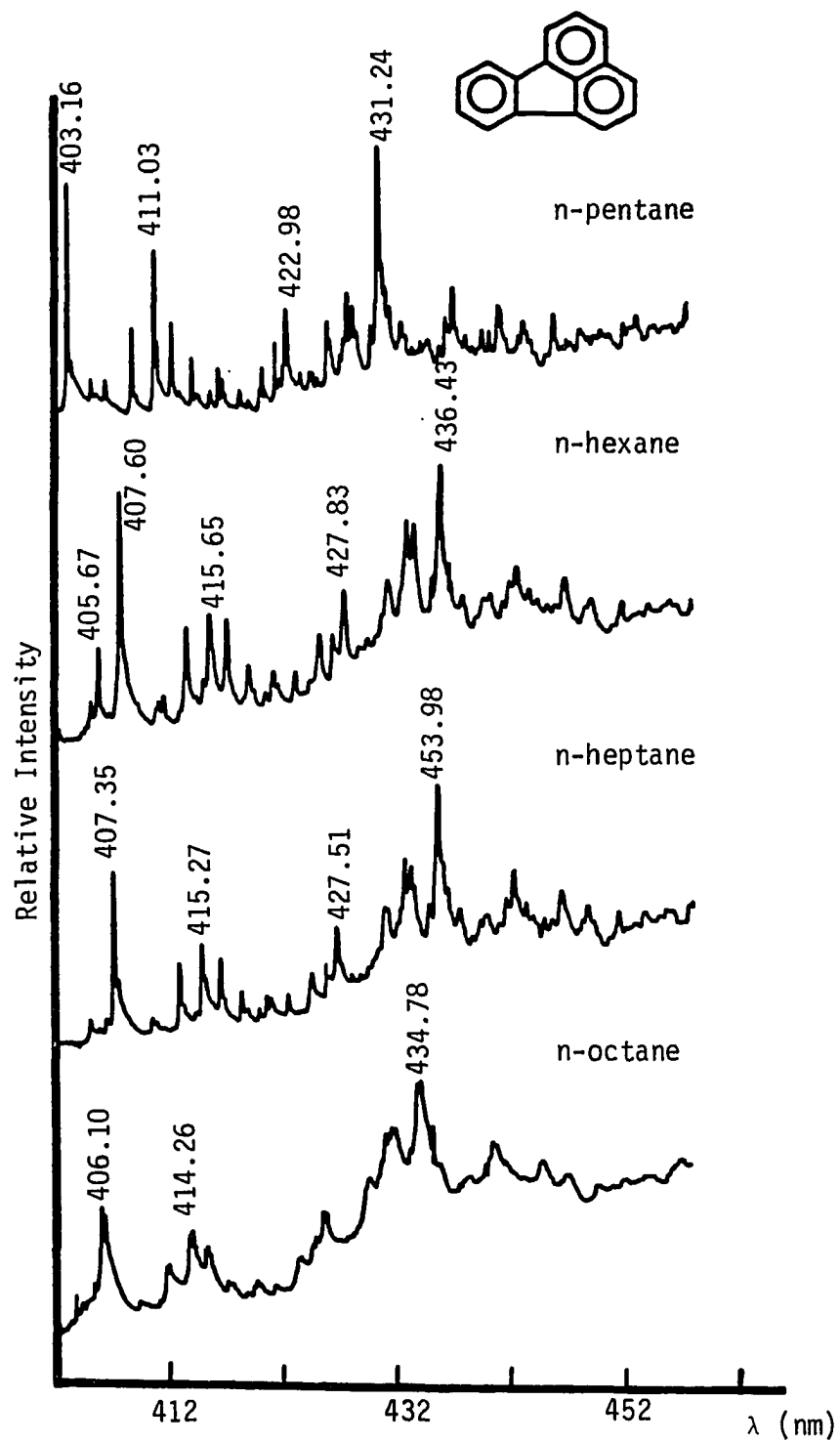


Figure 48. Fluorescence emission spectra of fluoranthene at 10 ppm in different n-alkane solvents at $\lambda_{\text{ex}} = 339$ nm

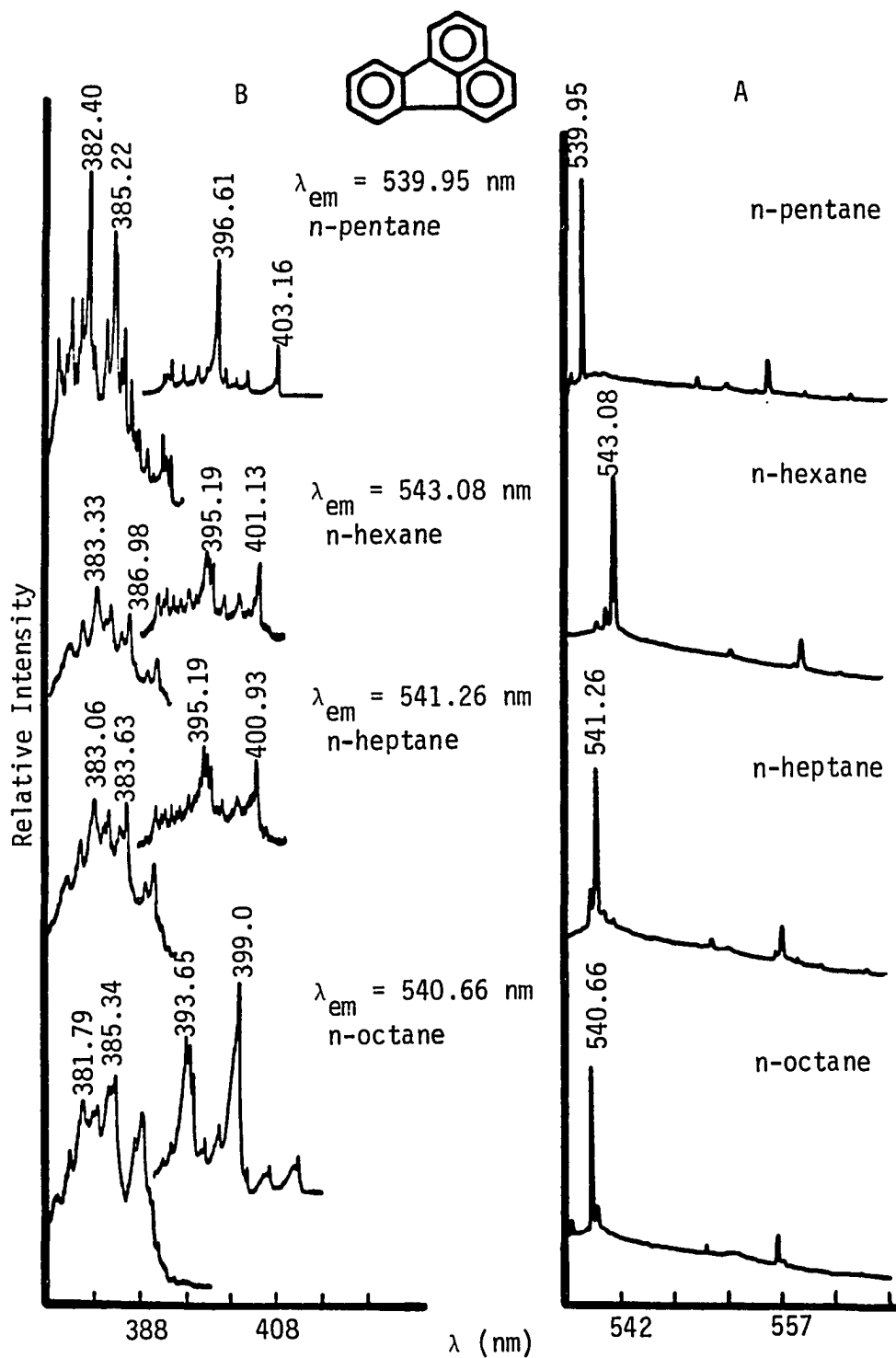


Figure 49. Nonselectively excited phosphorescence emission at $\lambda_{ex} = 339$ nm (A) and excitation (B) spectra of fluoranthene at 10 ppm in different n-alkane solvents

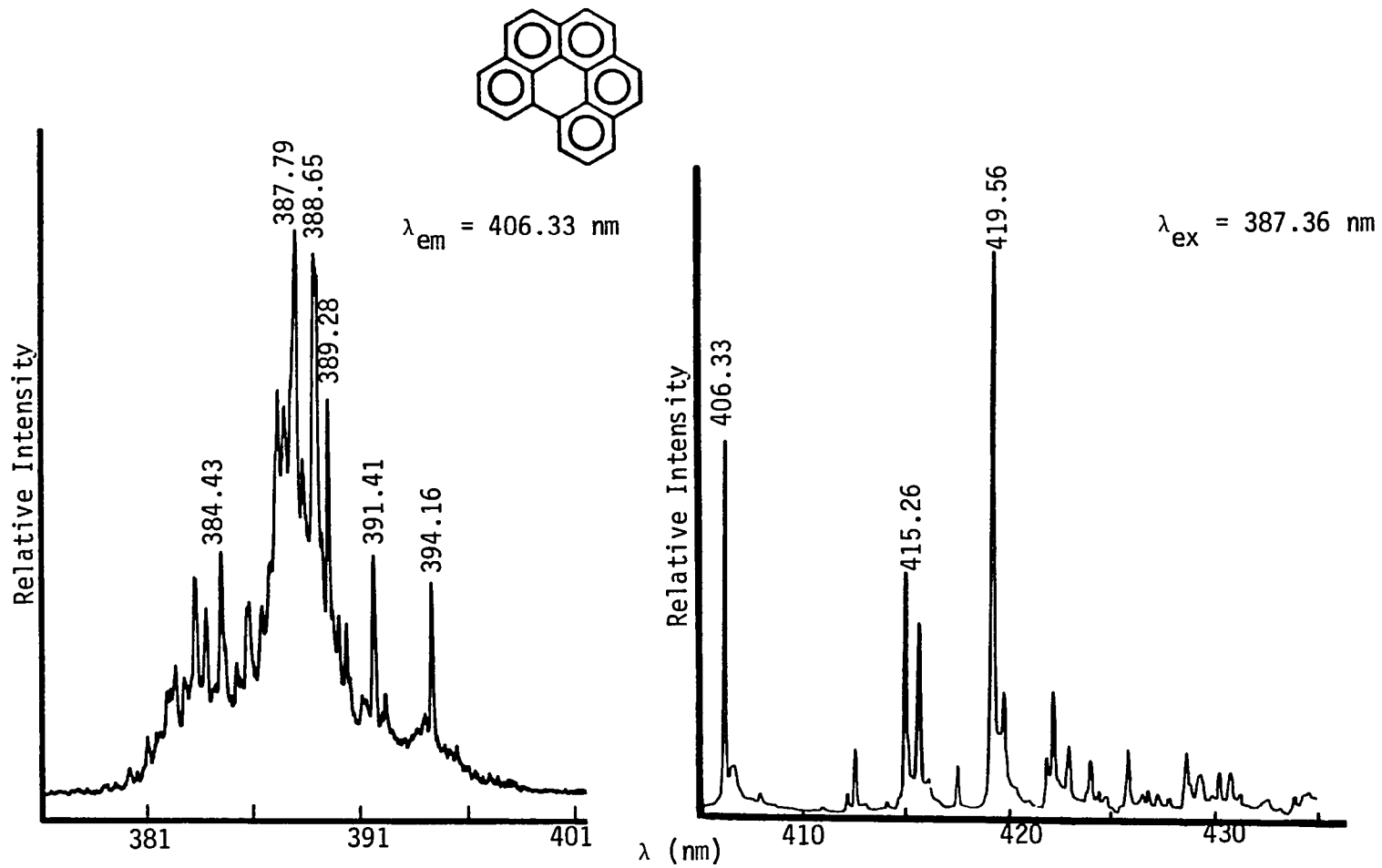


Figure 50. Excitation and selectively excited fluorescence emission spectra of benzo(ghi)perylene at 1 ppm in n-octane

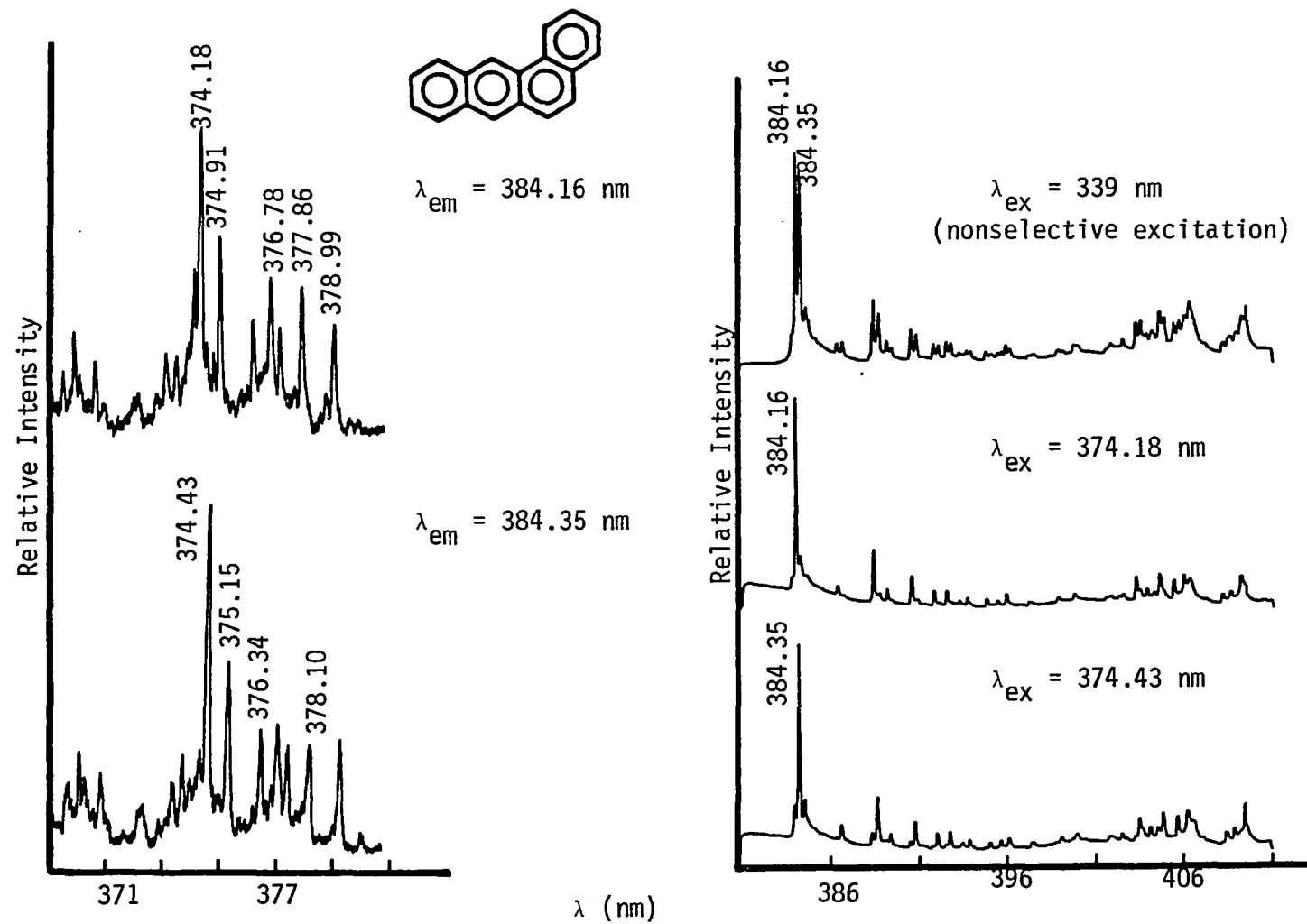


Figure 51. Site-selective excitation of fluorescence of benzo(a)anthracene at 1 ppm in n-octane

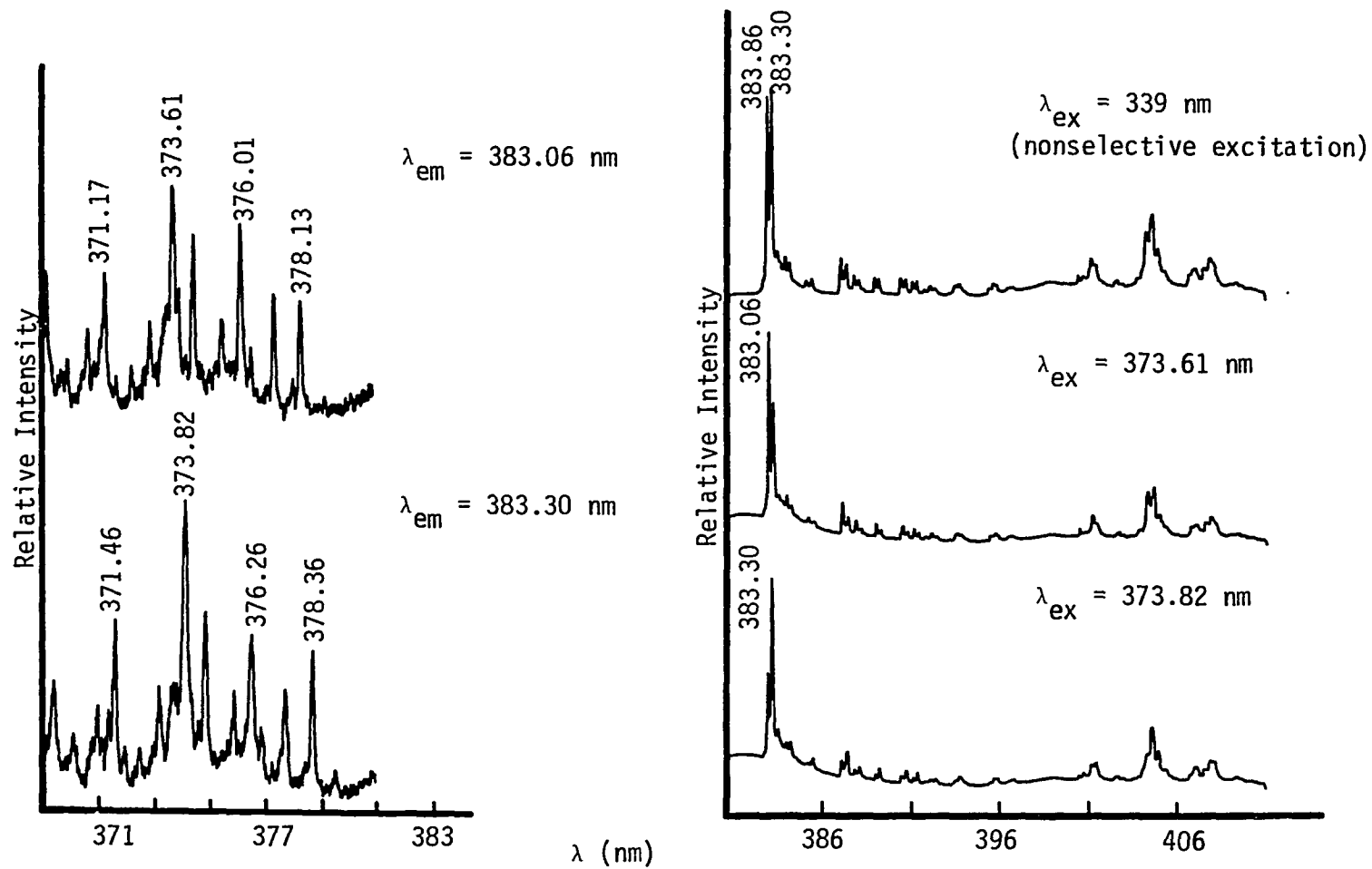


Figure 52. Site-selective excitation of the fluorescence of benzo(a)anthracene-d₁₂ at 1 ppm in n-octane

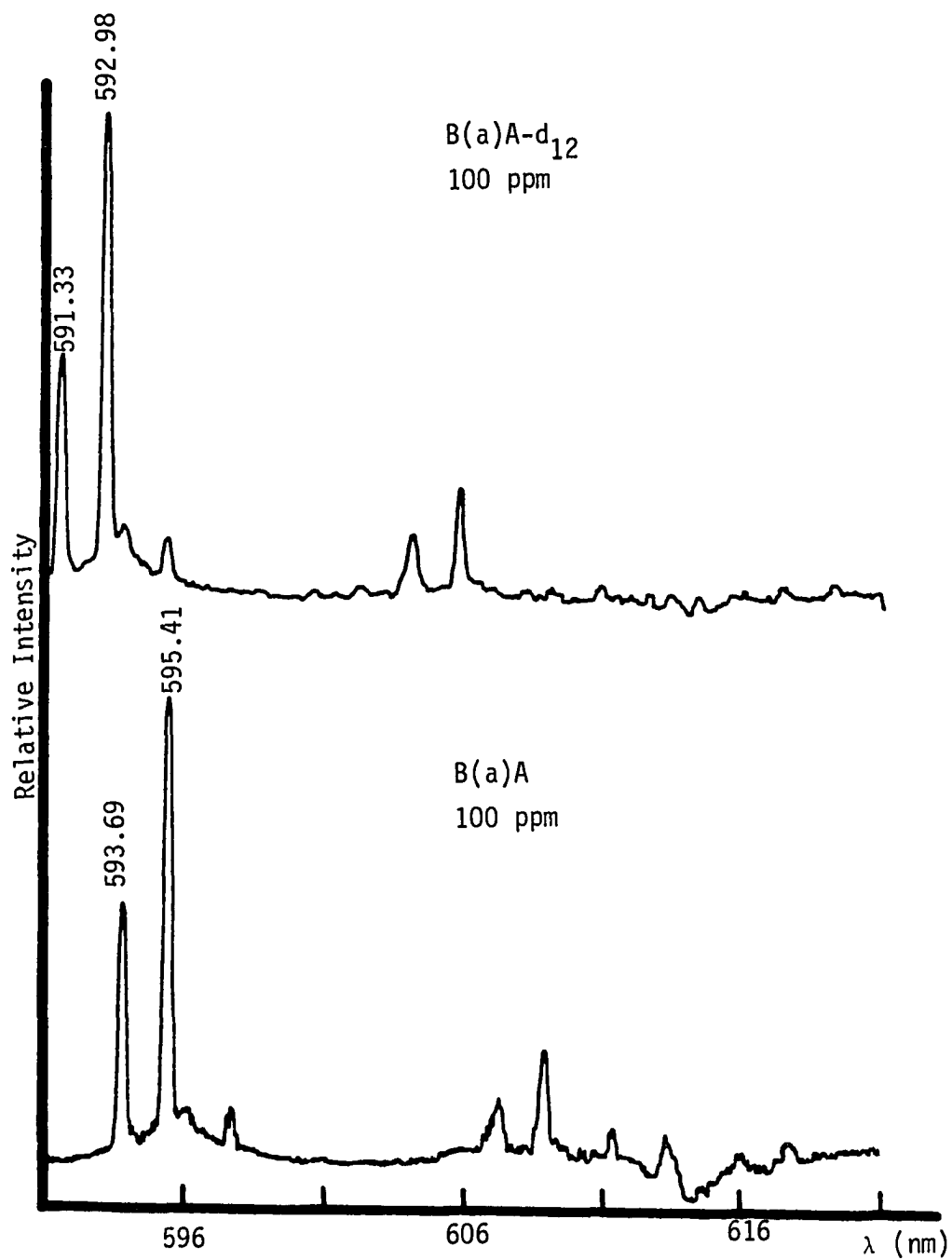


Figure 53A. Nonselectively excited phosphorescence emission spectra of benzo(a)anthracene-d₁₂ and benzo(a)anthracene in n-octane at $\lambda_{\text{ex}} = 339$ nm

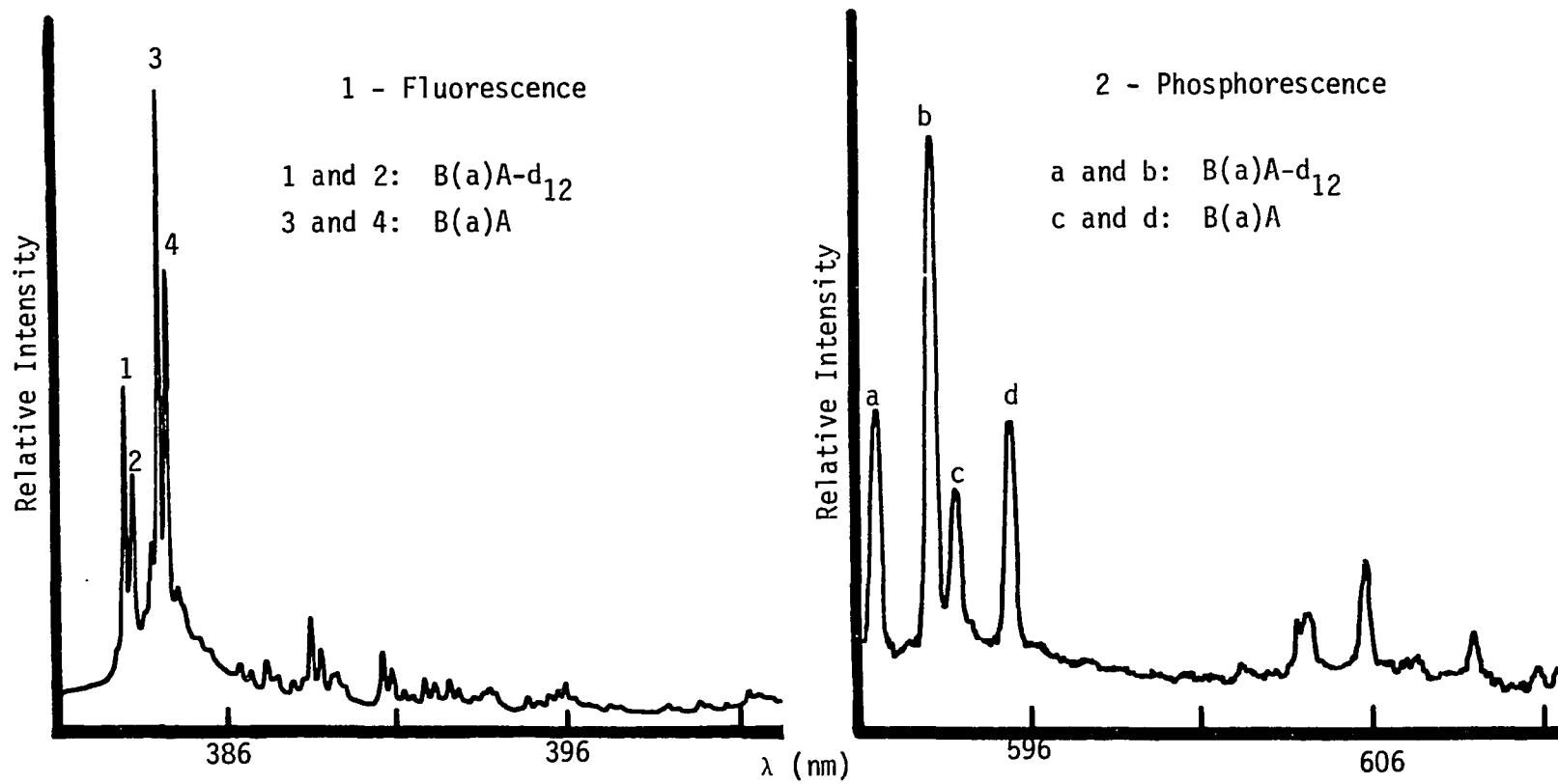


Figure 53B. Nonselective excitation luminescence spectra of a mixture of benzo(a)anthracene and benzo(a)anthracene-d₁₀; each at a concentration of 10 ppm in n-octane at $\lambda_{\text{ex}} = 365 \text{ nm}$
 1 - Fluorescence intensity of B(a)A is larger than that of B(a)A-d₁₂
 2 - Phosphorescence intensity of B(a)A is smaller than that of B(a)A-d₁₂

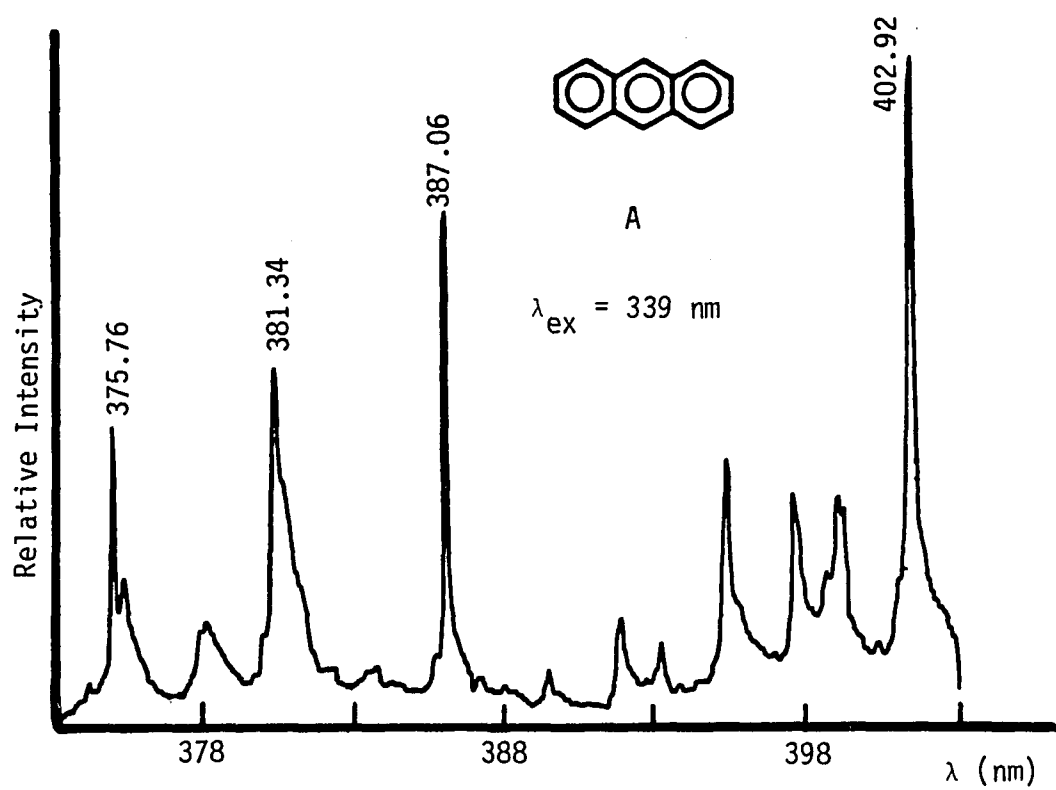


Figure 54. Nonselectively excited fluorescence emission spectrum of anthracene at 10 ppm in n-heptane

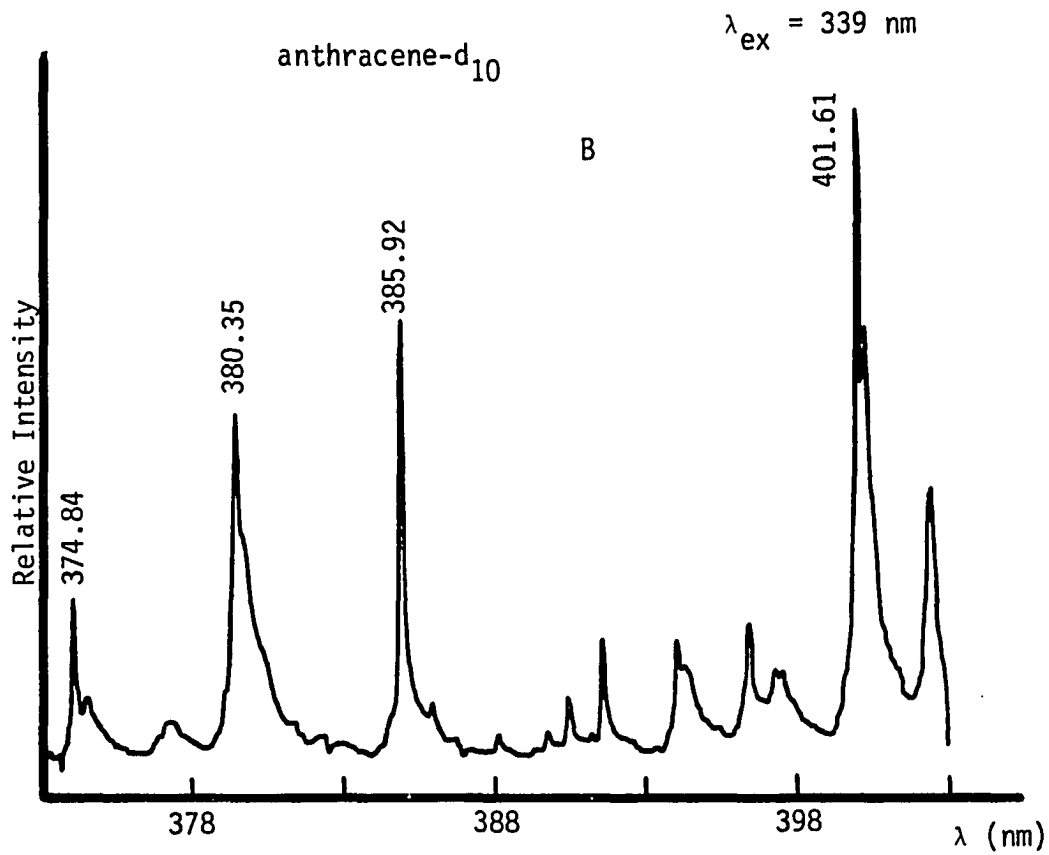
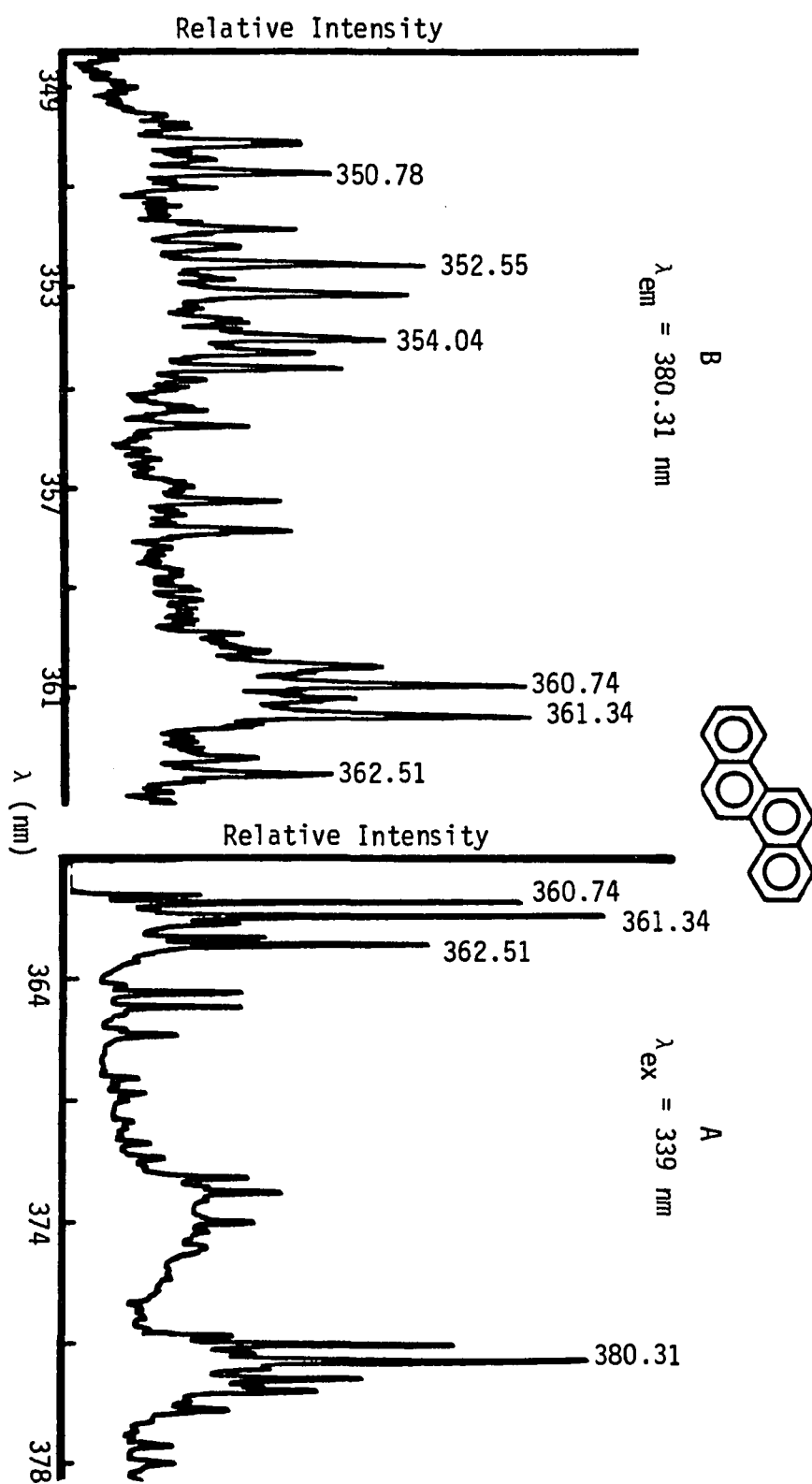


Figure 55. Nonselectively excited fluorescence emission spectrum of anthracene-d₁₀ at 10 ppm in n-heptane

Figure 56. Nonselectivity fluorescence emission (A) and excitation (B) spectra of chrysene at 10 ppm in octane



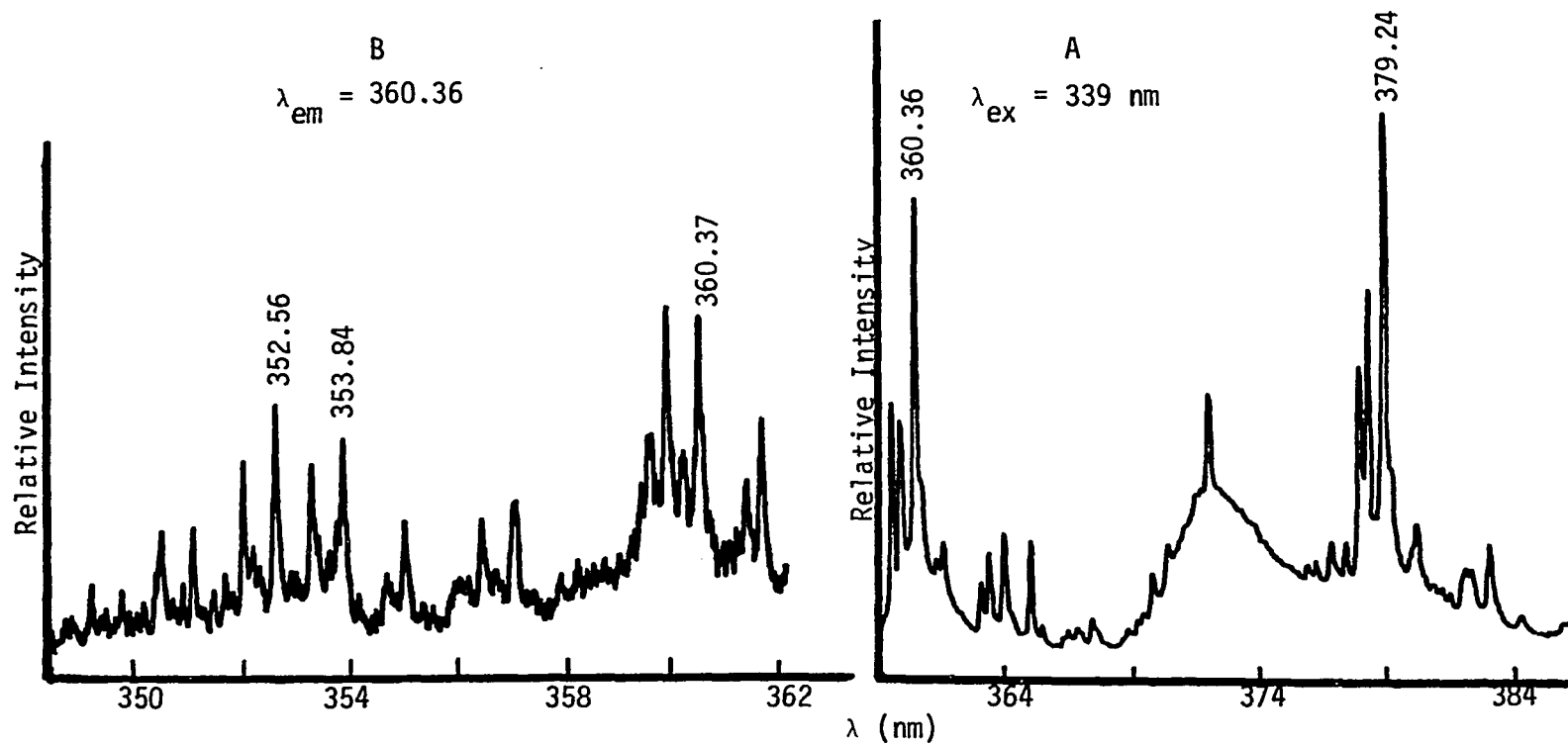


Figure 57. Nonselectively fluorescence emission (A) and excitation (B) spectra of chrysene-d₁₂ at 50 ppm in n-octane

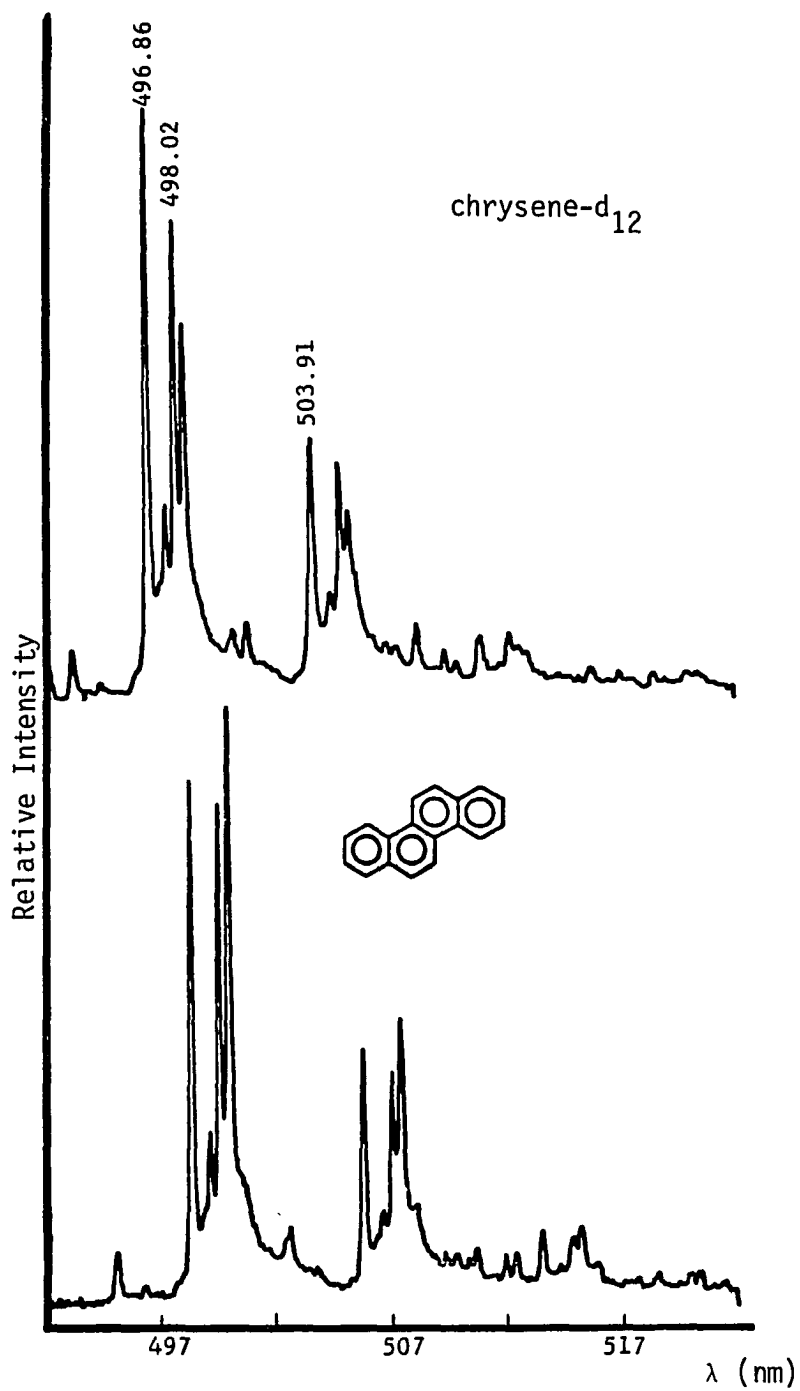


Figure 58. Nonselectively phosphorescence emission of chrysene-d₁₂

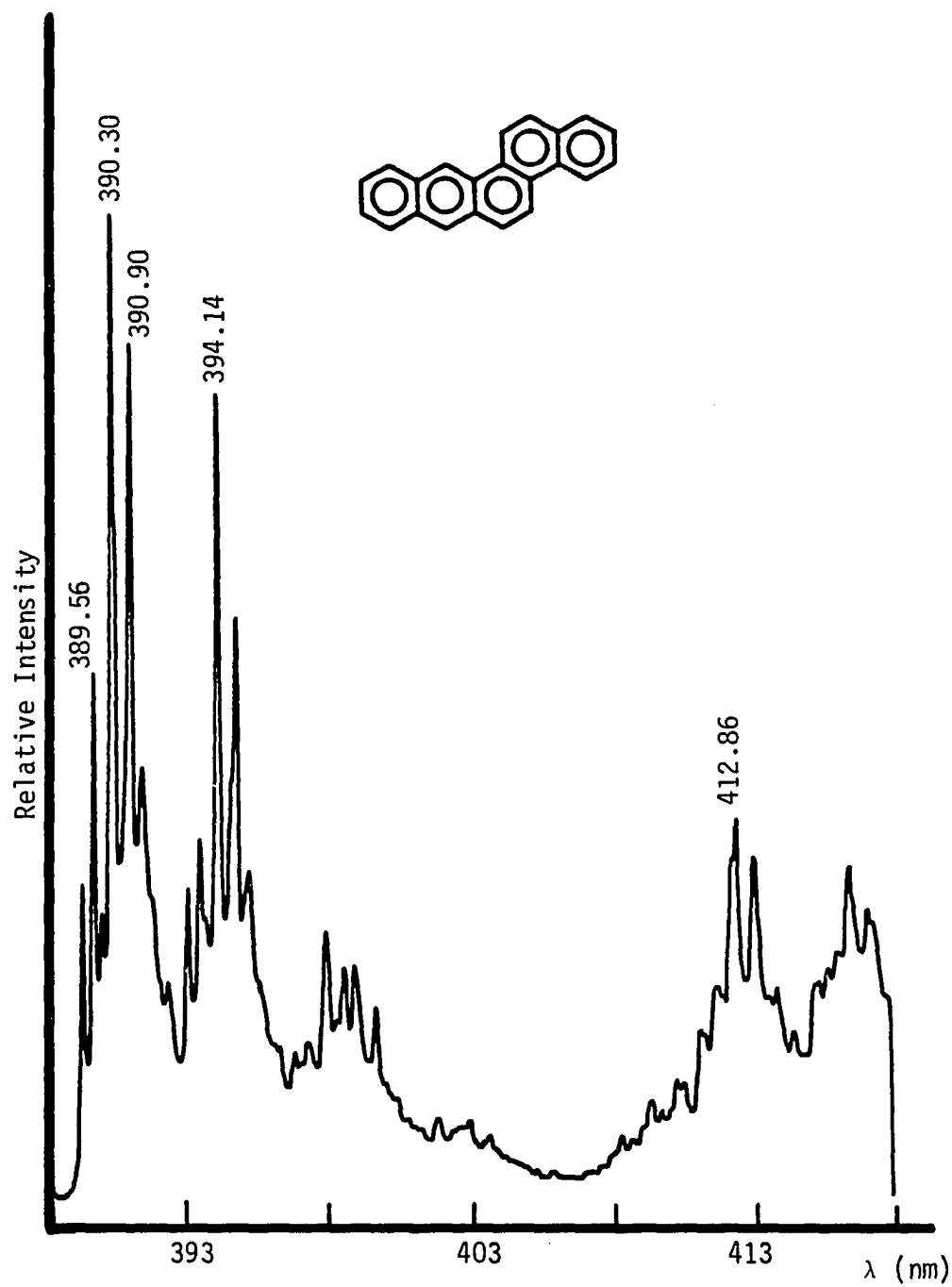


Figure 59. Nonselectively excited fluorescence spectrum of benzo(b)-chrysene in n-octane

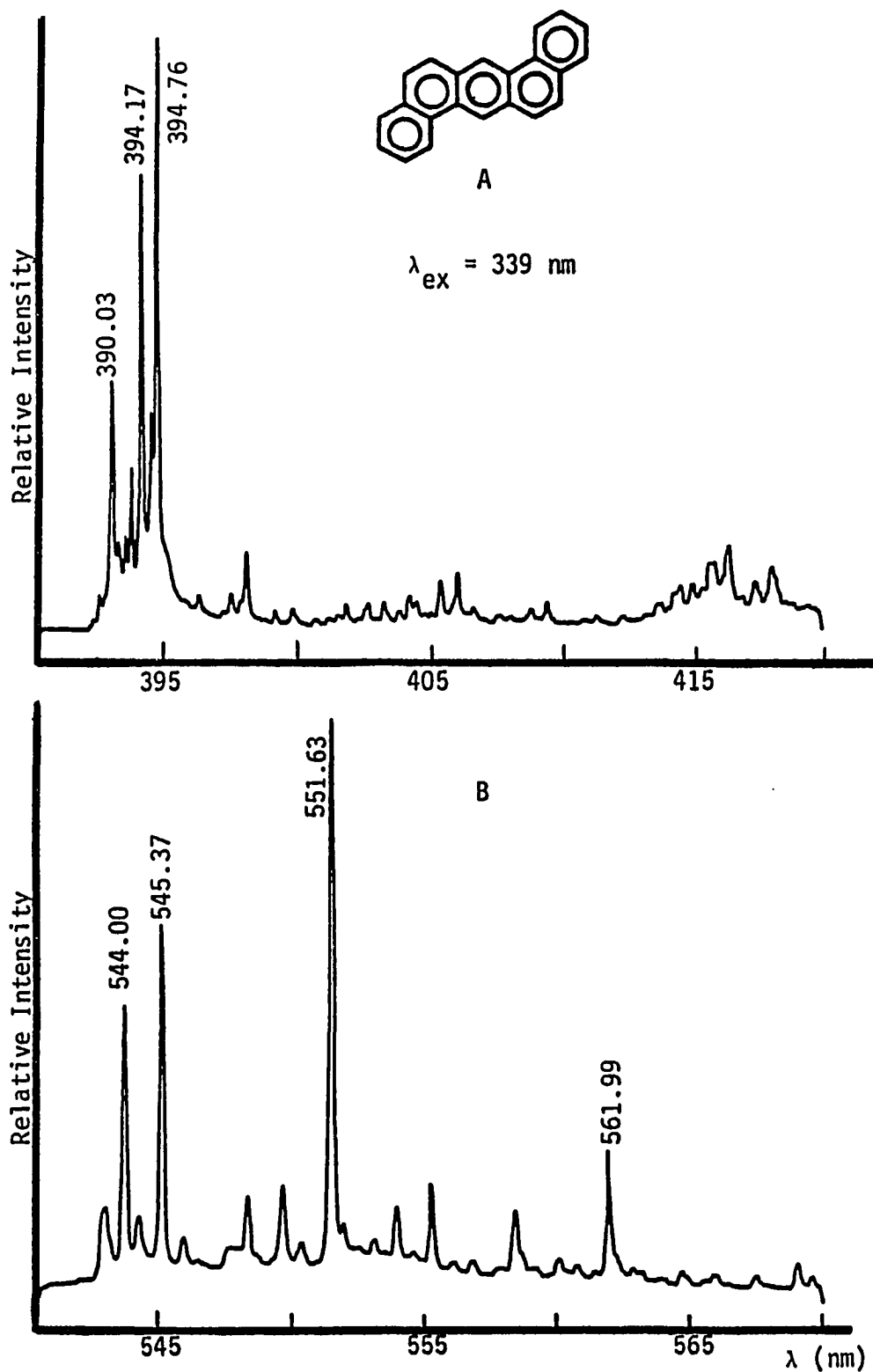


Figure 60. Nonselectively excited fluorescence (A) and phosphorescence (B) emissions of 1,2,5,6-dibenzoanthracene in n-octane

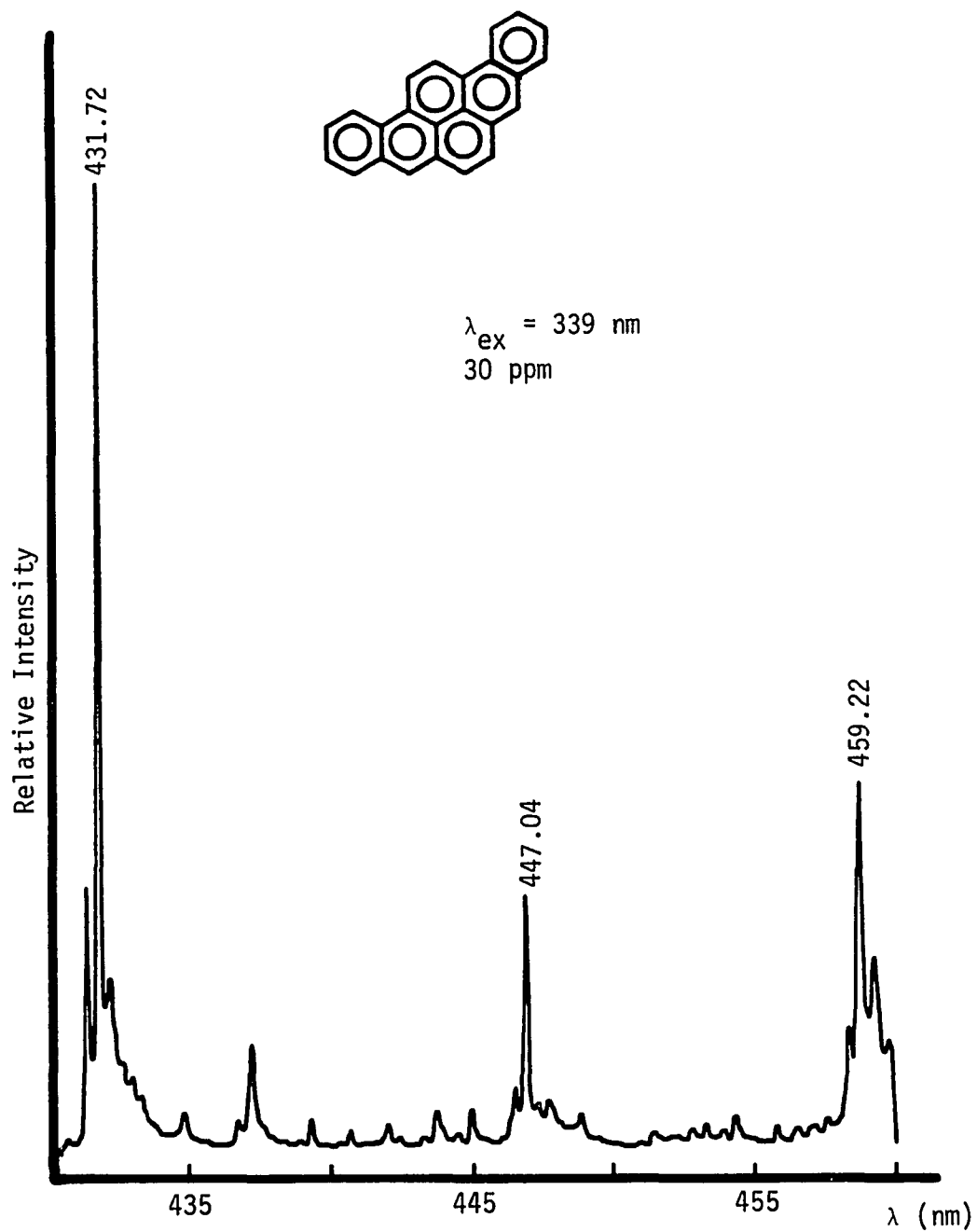


Figure 61. Nonselectively excited fluorescence spectrum of dibenzo-(a,i)pyrene in n-octane

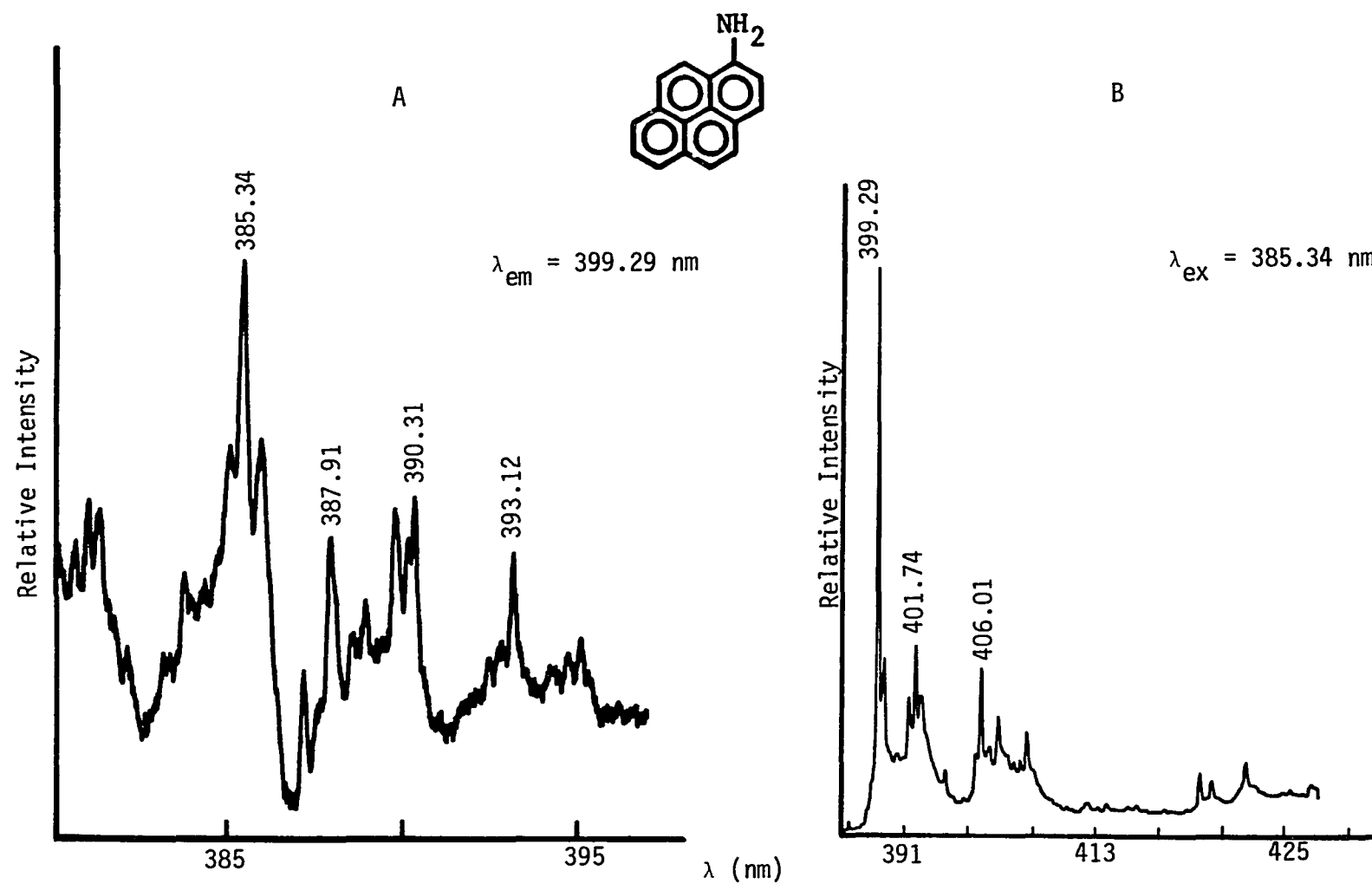


Figure 62. Excitation (A) and fluorescence emission (B) of 1-aminopyrene at 1 ppm in n-octane

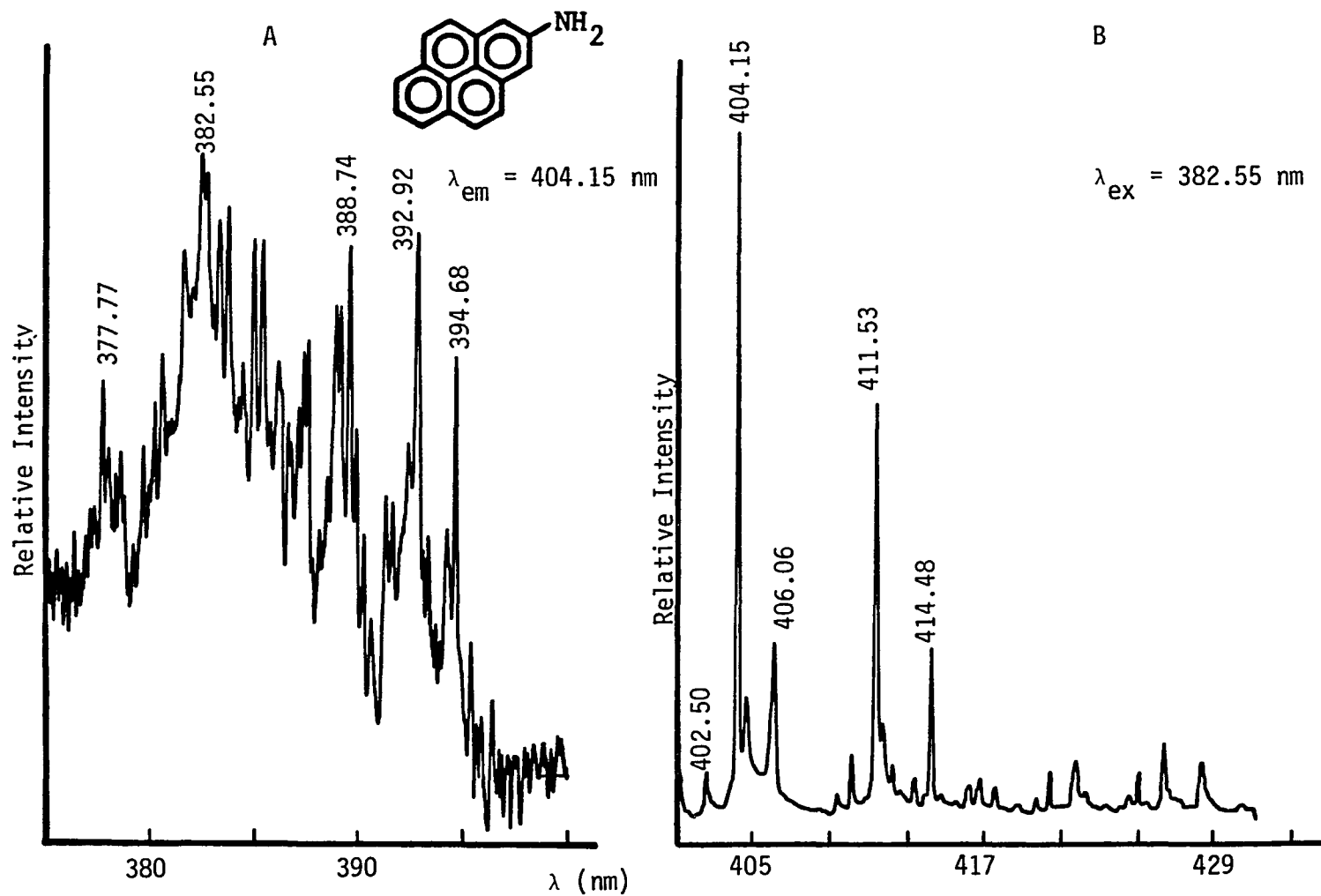


Figure 63. Excitation (A) and fluorescence emission (B) of 2-aminopyrene at 1 ppm at 10 ppm in *n*-octane

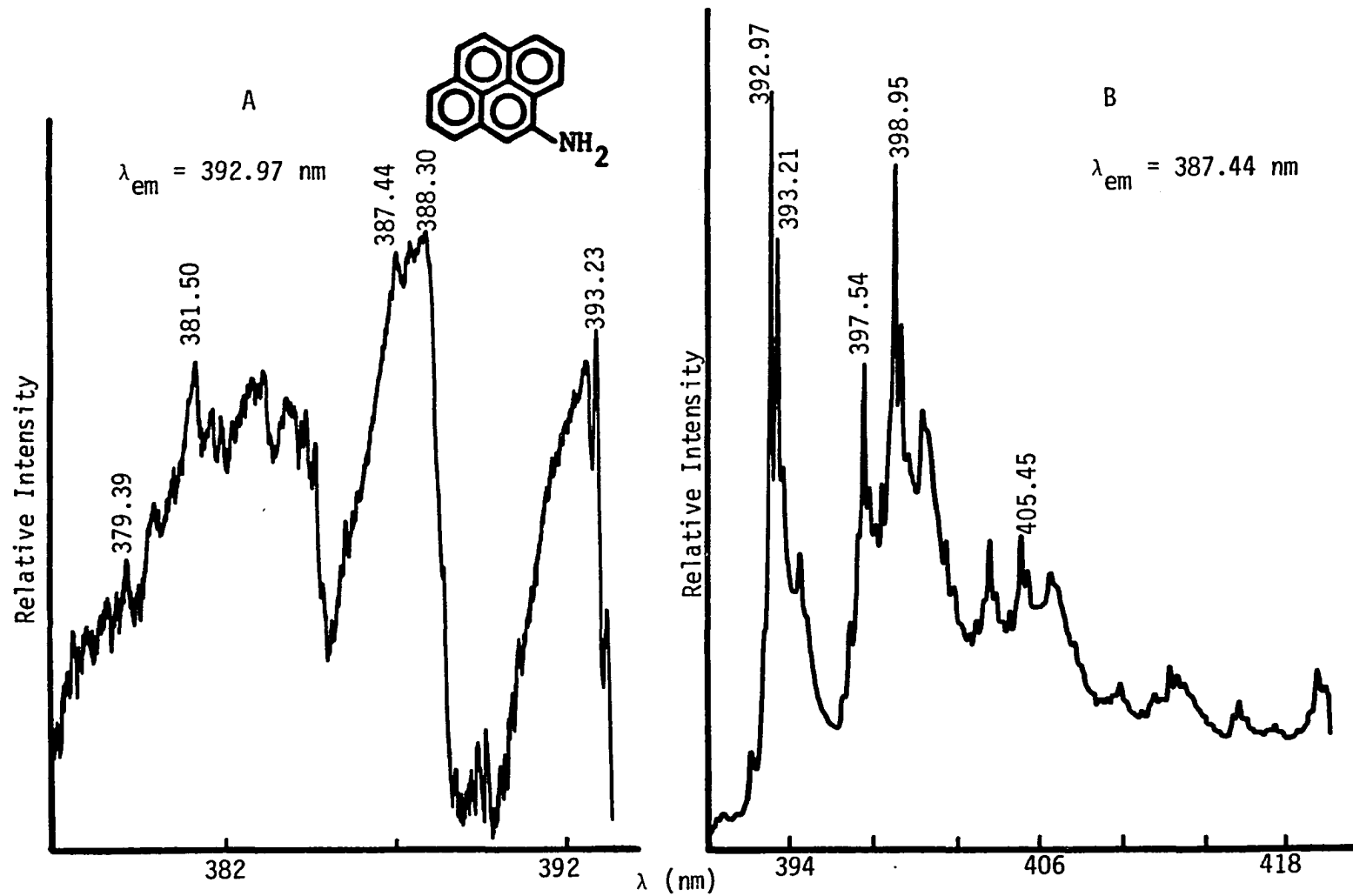


Figure 64. Excitation (A) and fluorescence emission (B) of 10 ppm 4-aminopyrene at 10 ppm in n-octane

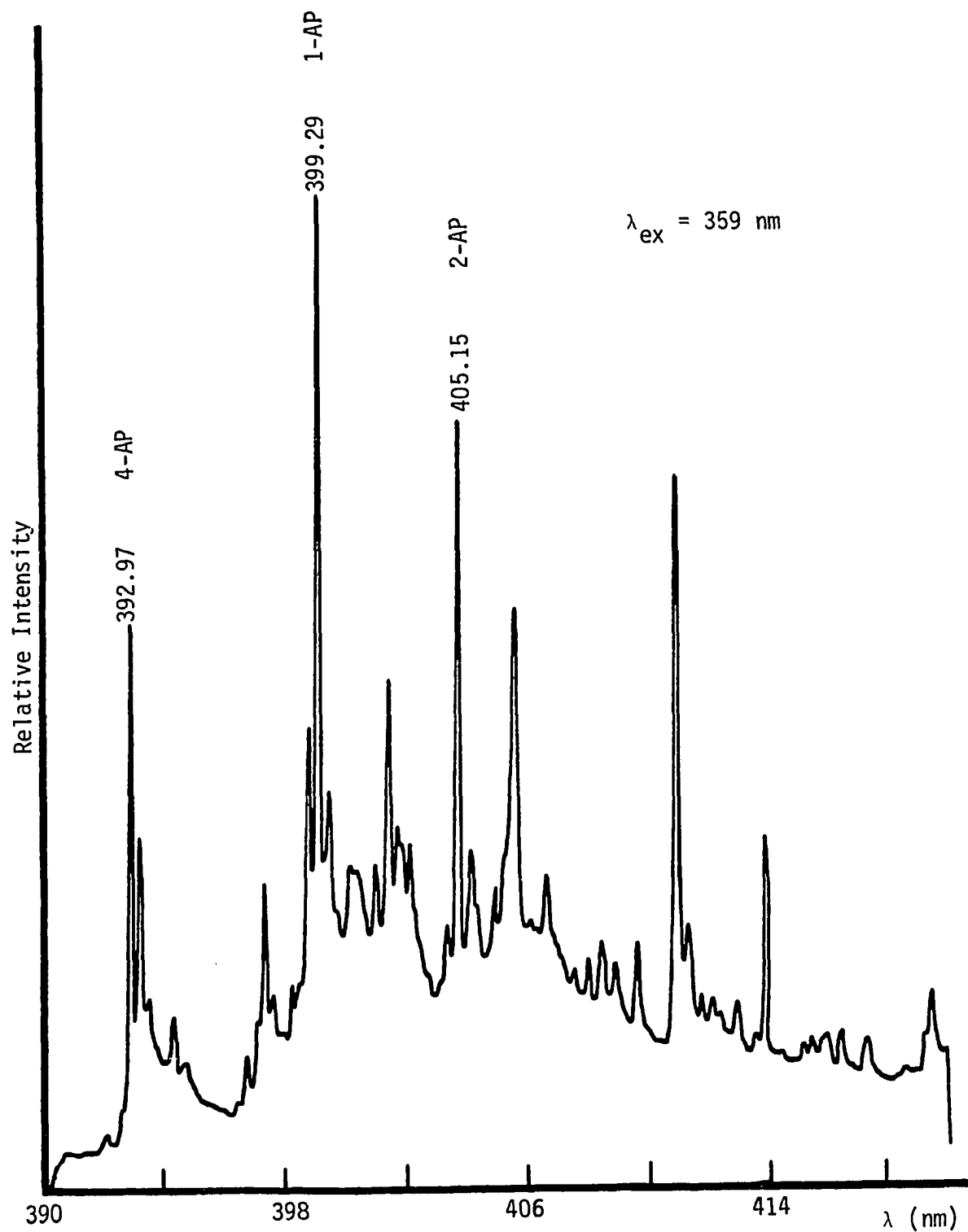


Figure 65. The Shpol'skii effect spectra of a mixture of 1-, 2- and 4-aminopyrenes (AP) in n-octane at 15 K

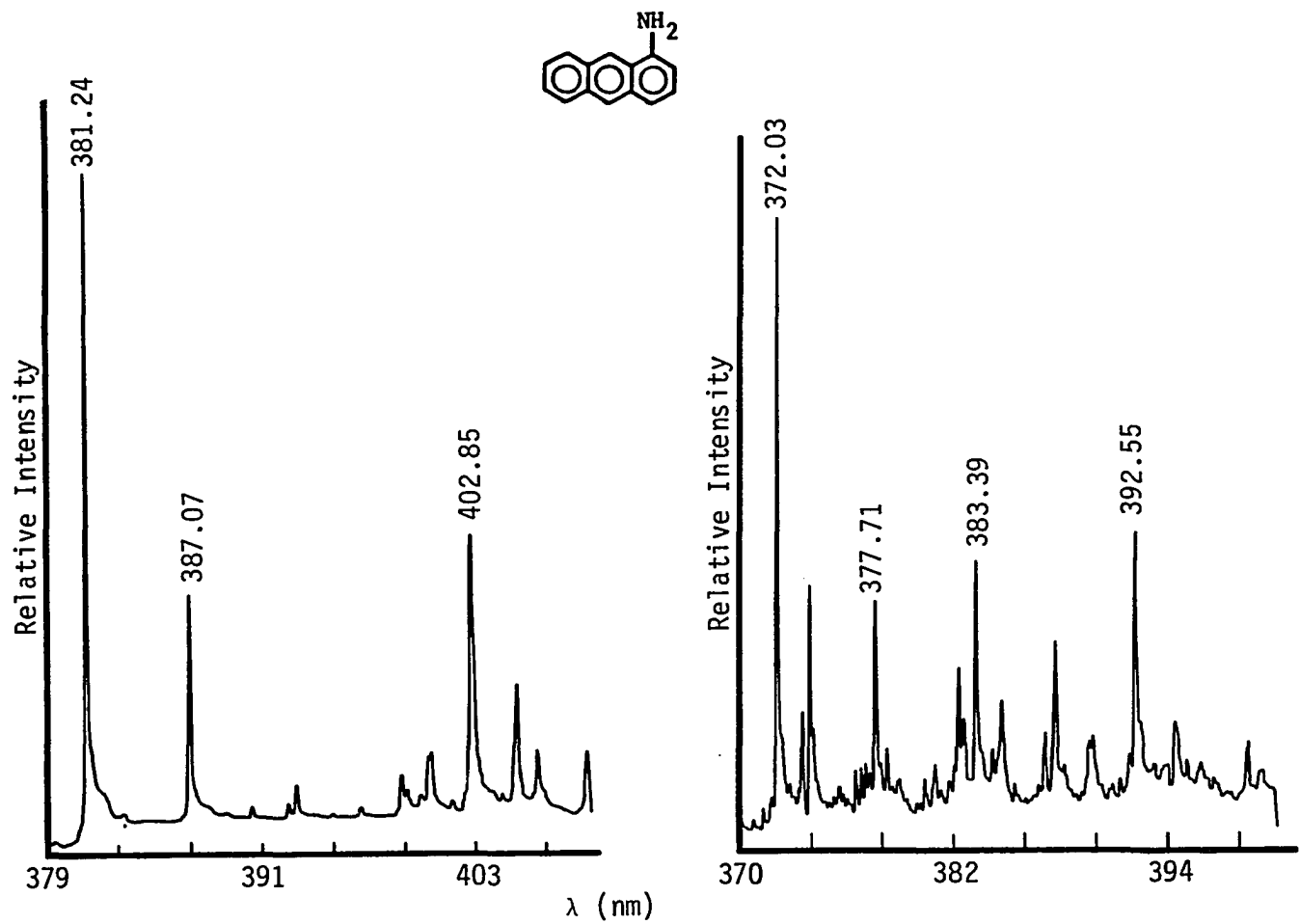


Figure 66. Nonselectively excited fluorescence spectra of two commercial products of 1-aminanthracene at 10 ppm in n-heptane

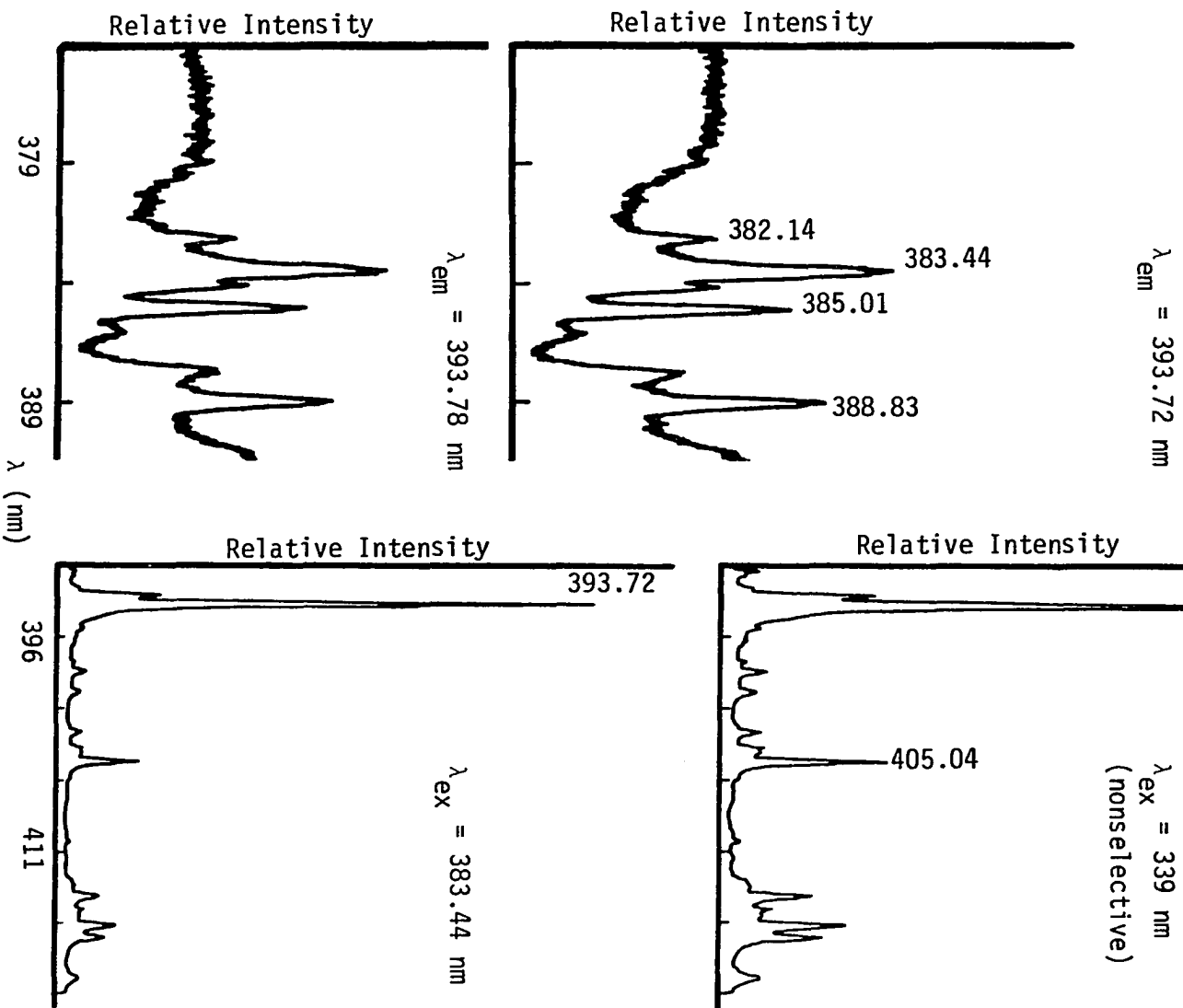
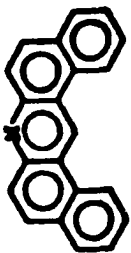


Figure 67. Fluorescence emission and excitation spectra of 13H-dibenzo-(a,j)acridine at 10 ppm in n-octane

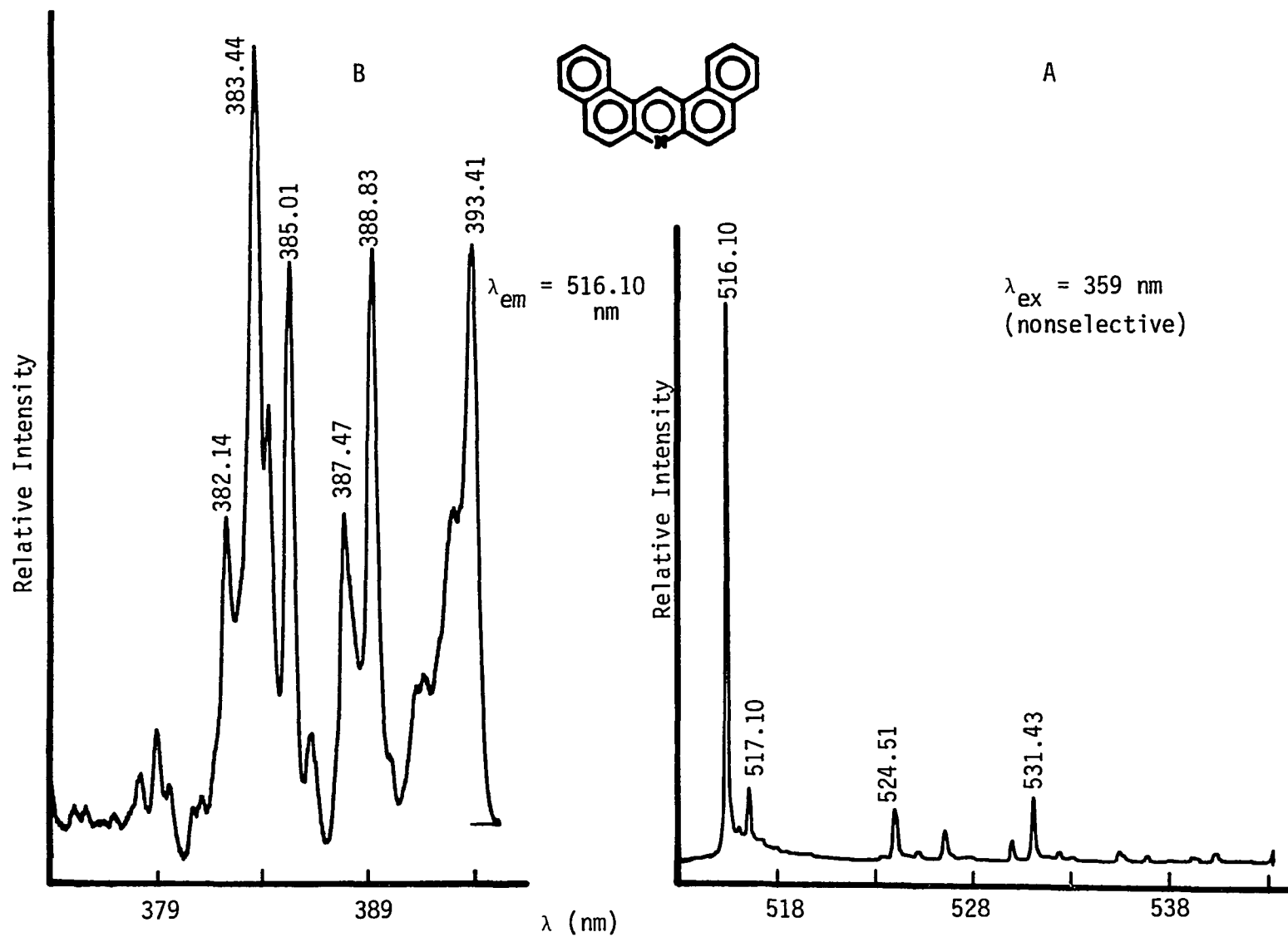


Figure 68. Phosphorescence emission (A) and phosphorescence excitation (B) of 13H-dibenzo(a,j)-acridine at 50 ppm in n-octane

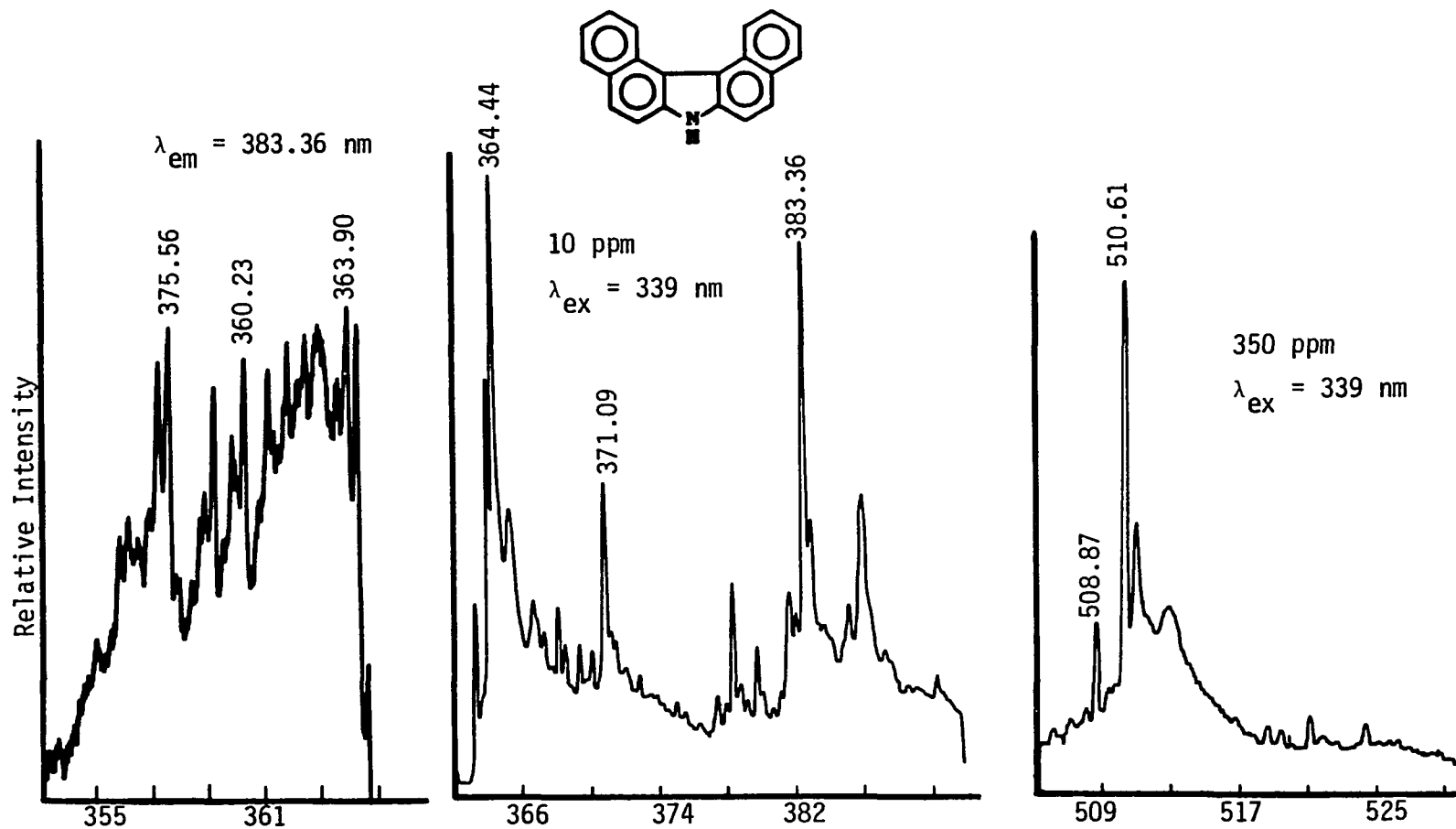


Figure 69. Luminescence spectra of 7H-dibenzo(a,j)carbazole in n-octane

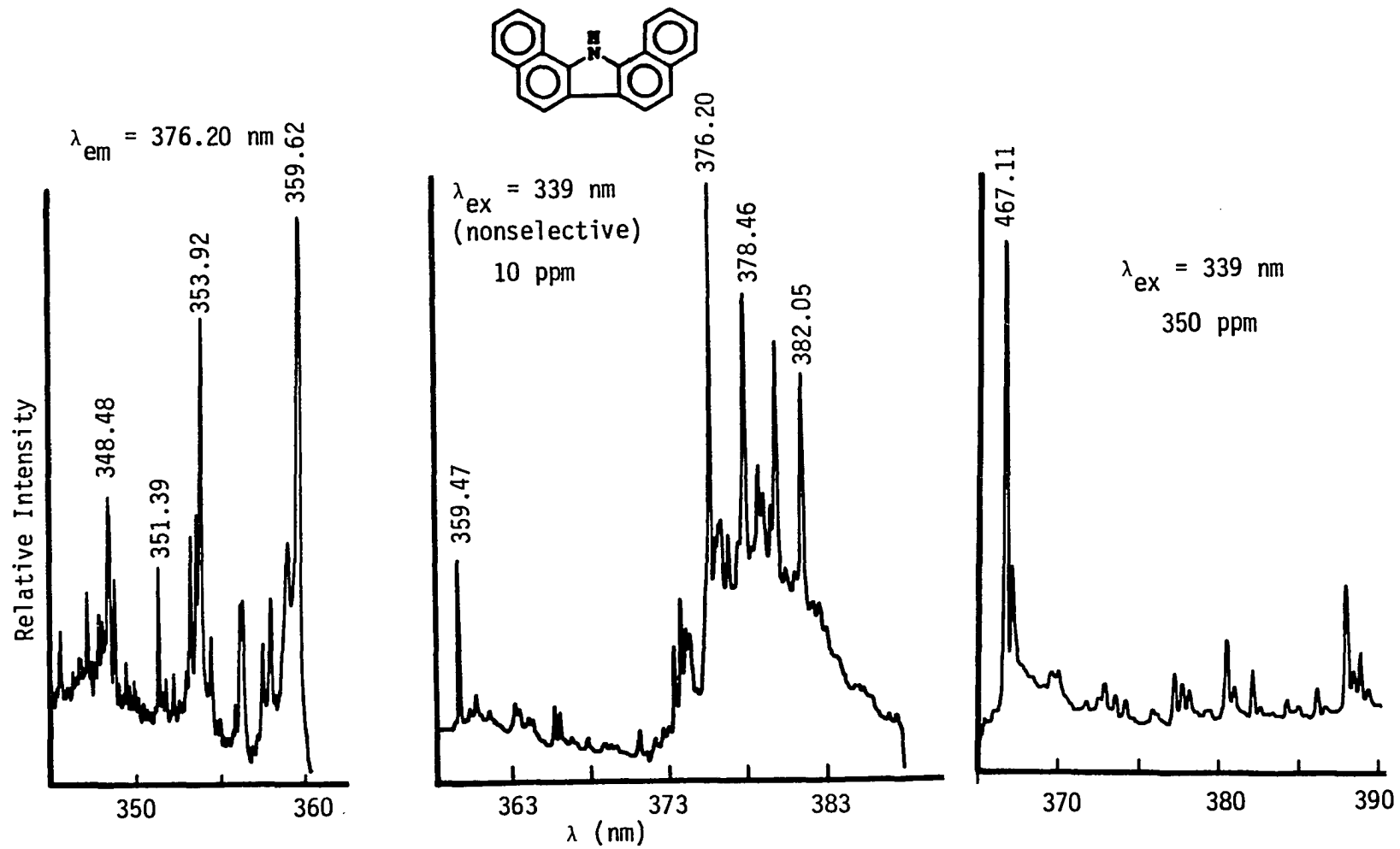


Figure 70. Luminescence spectra of 13H-dibenzo(a,i)carbazole in n-octane

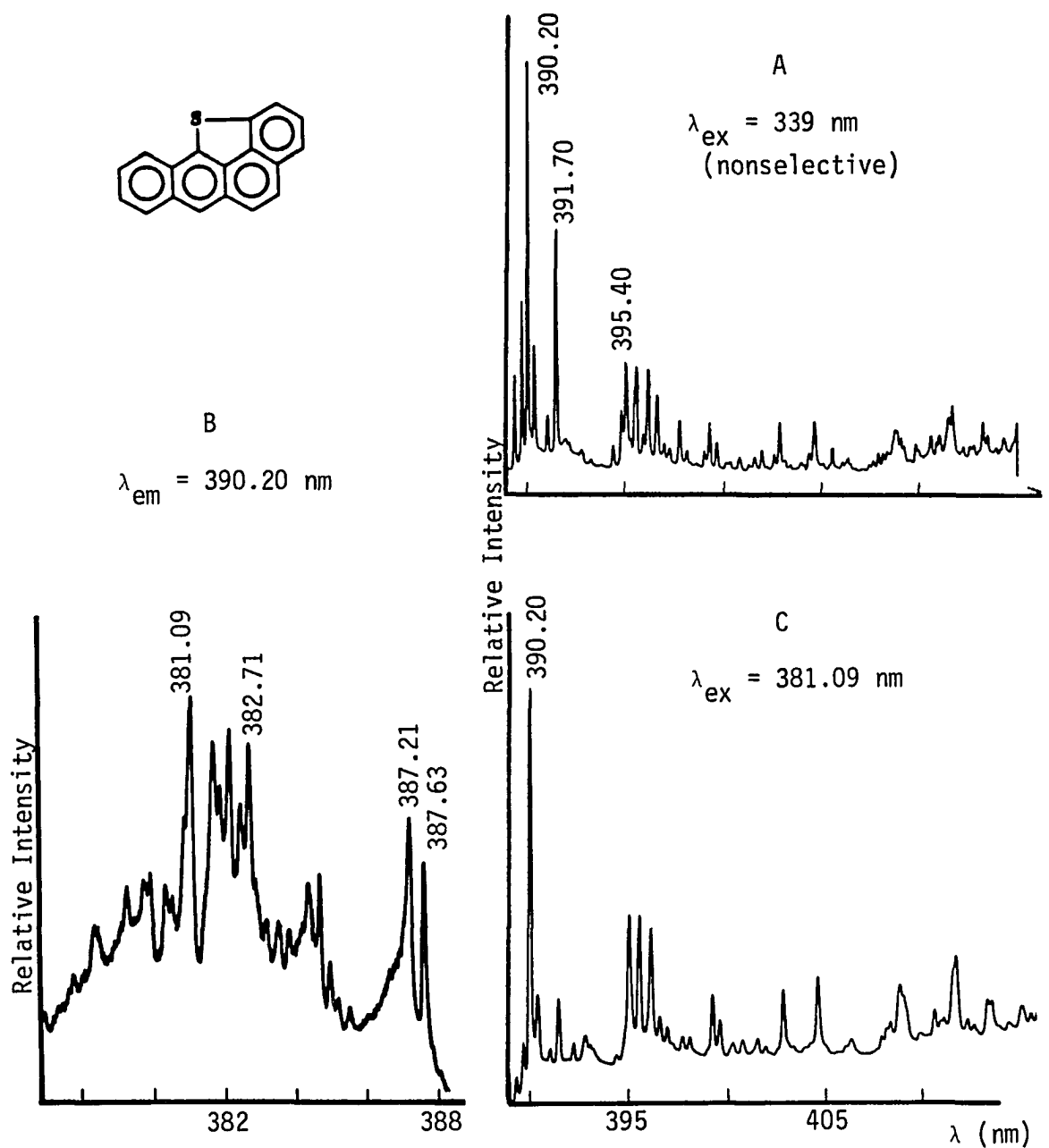


Figure 71. Nonselectively excited fluorescence emission (A), excitation (B), and selectively excited fluorescence (C) of benzo(2,3)-phenanthro(4,5-bcd)thiophene at 1 ppm in n-hexane

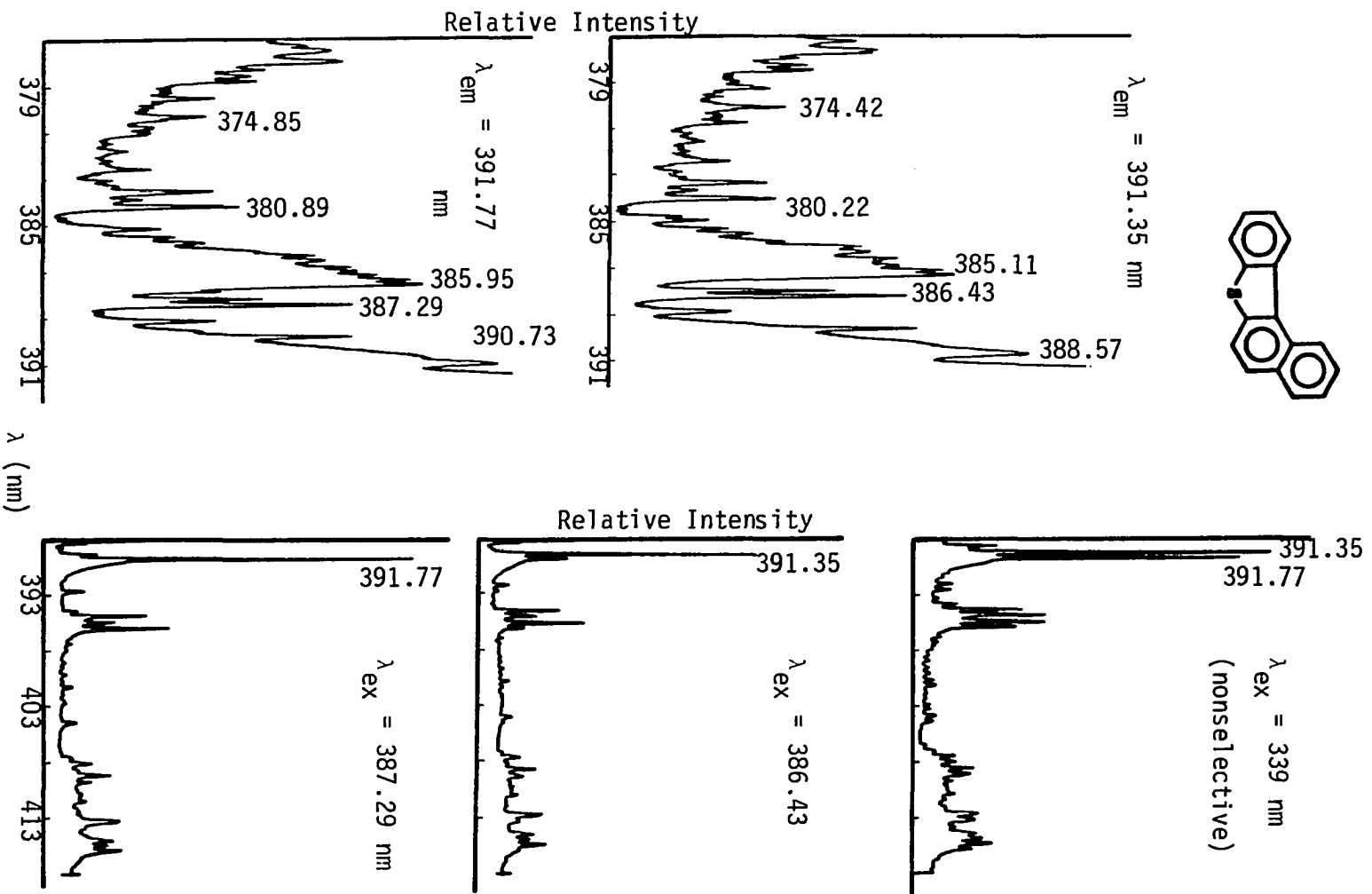
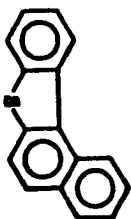


Figure 72A. Site selective spectra of benzo(b)naphtho(1,2-d)thiophene at 10 ppm in n-heptane

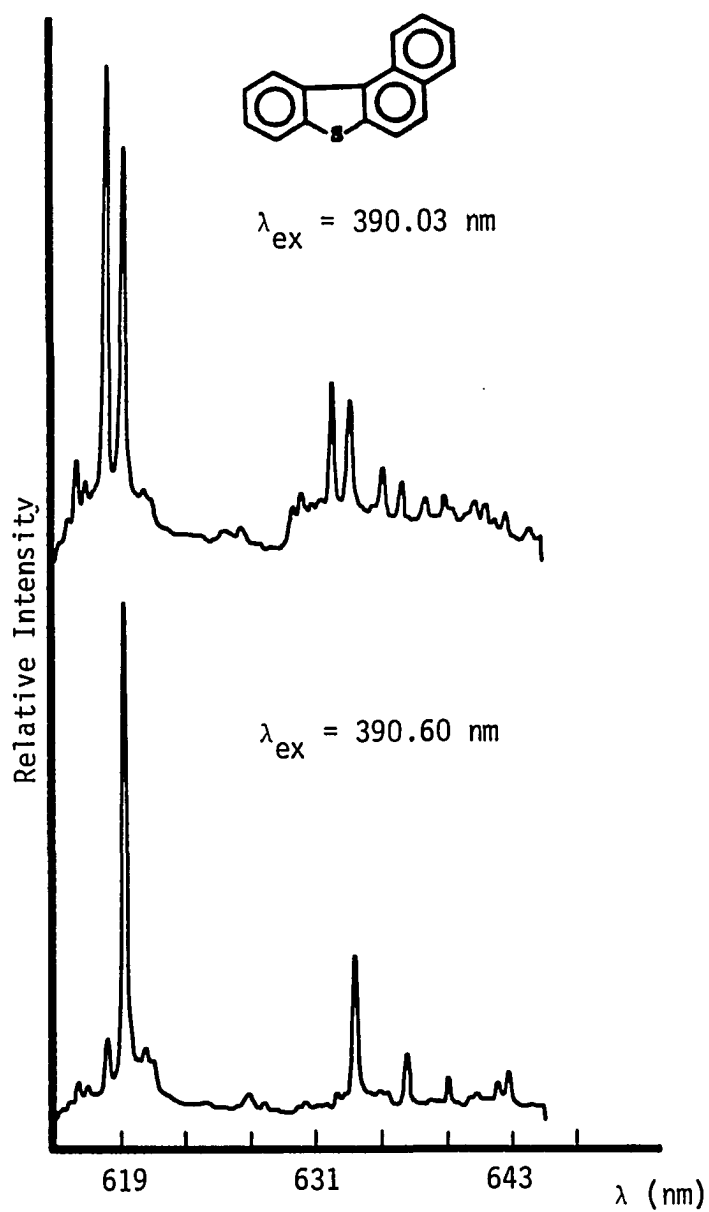


Figure 72B. Selectively excited phosphorescence emission of benzo(b)-naphtho(1,2-d)thiophene at 10 ppm in n-heptane

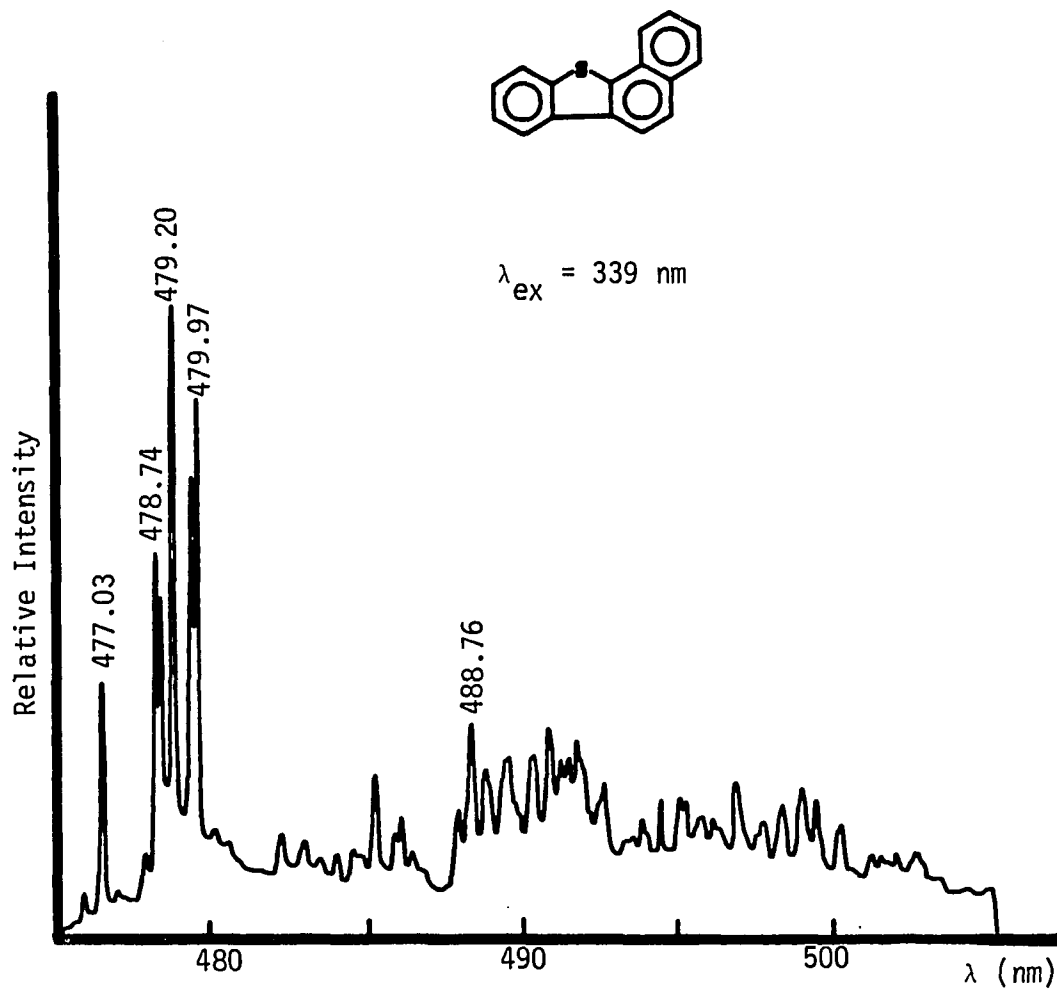


Figure 72C. Nonselectively excited phosphorescence emission spectra of benzo(b)naphtho(2,1-d)thiophene at 100 ppm in n-heptane

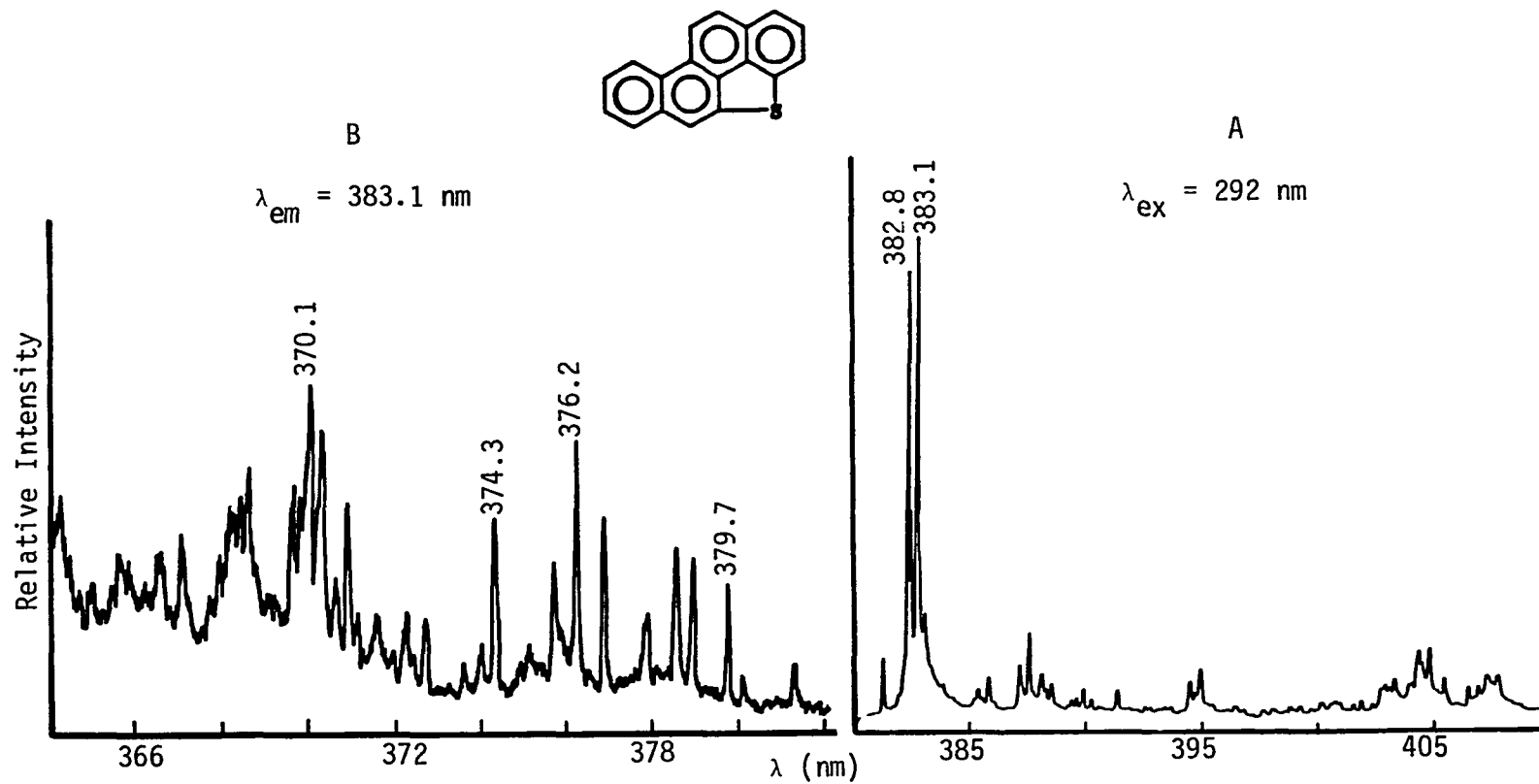


Figure 73. Nonselectively excited fluorescence emission (A) and excitation (B) of chryseno(4,5-bcd)-thiophene at 1 ppm in n-hexane

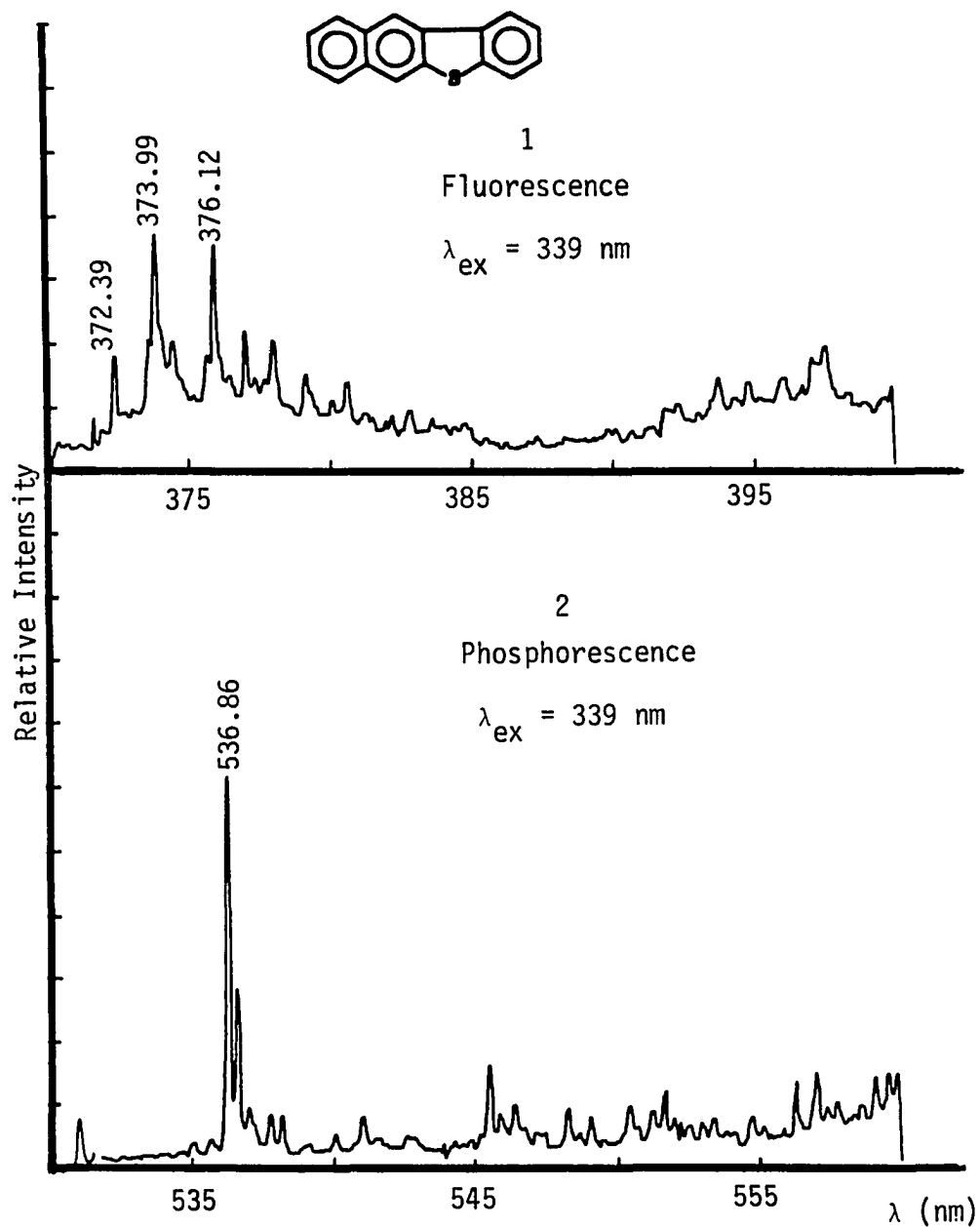


Figure 74A. Comparison between nonselectively excited fluorescence (1) and phosphorescence (2) of benzo(b)naphtho(2,3-d)thiophene at 10 ppm in n-heptane. Both spectra were recorded under identical conditions

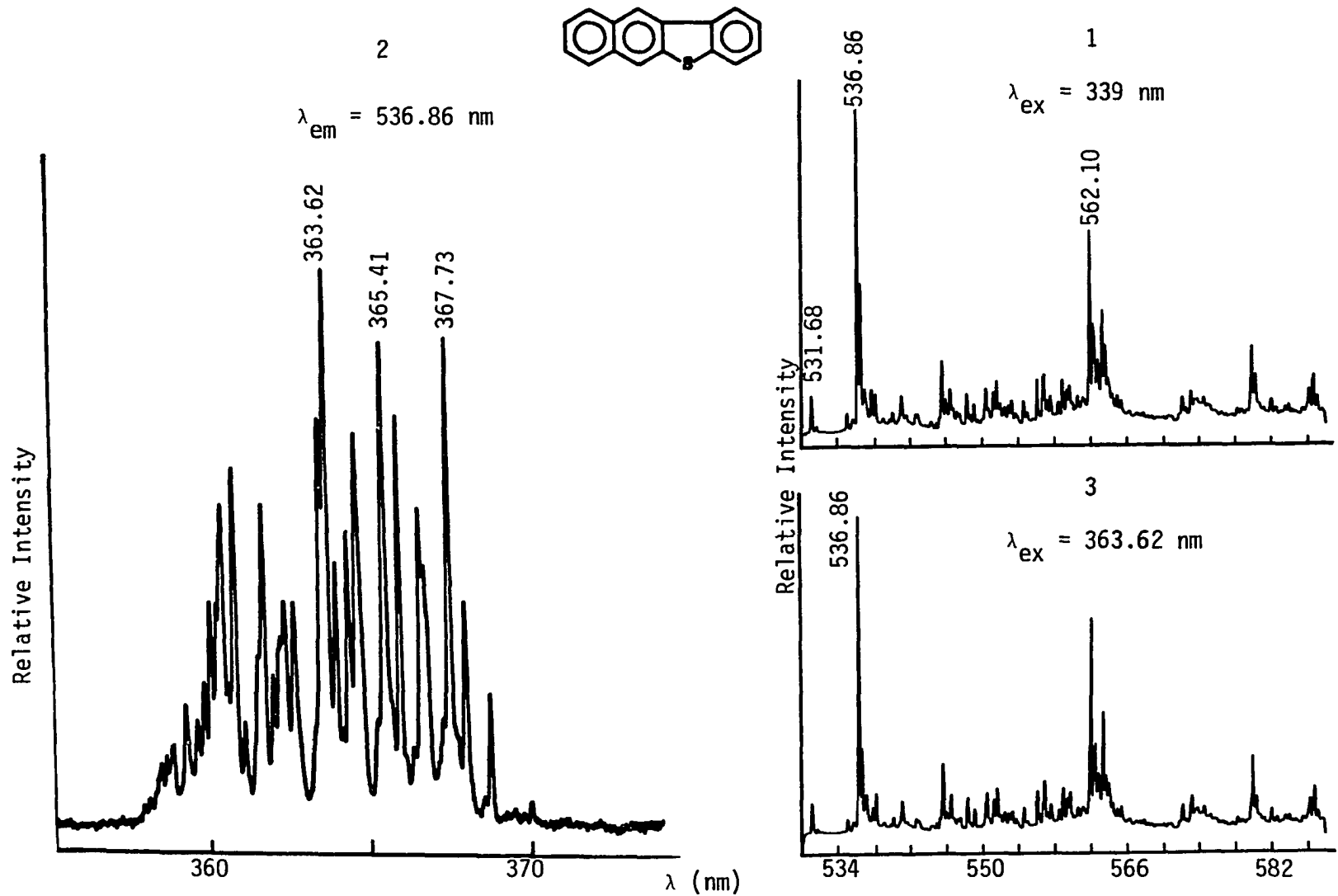


Figure 74B. Nonselective phosphorescence emission (1), phosphorescence excitation (2) and selectively excited phosphorescence emission (3) of benzo(b)naphtho(2,3-d)thiophene at 10 ppm in n-heptane

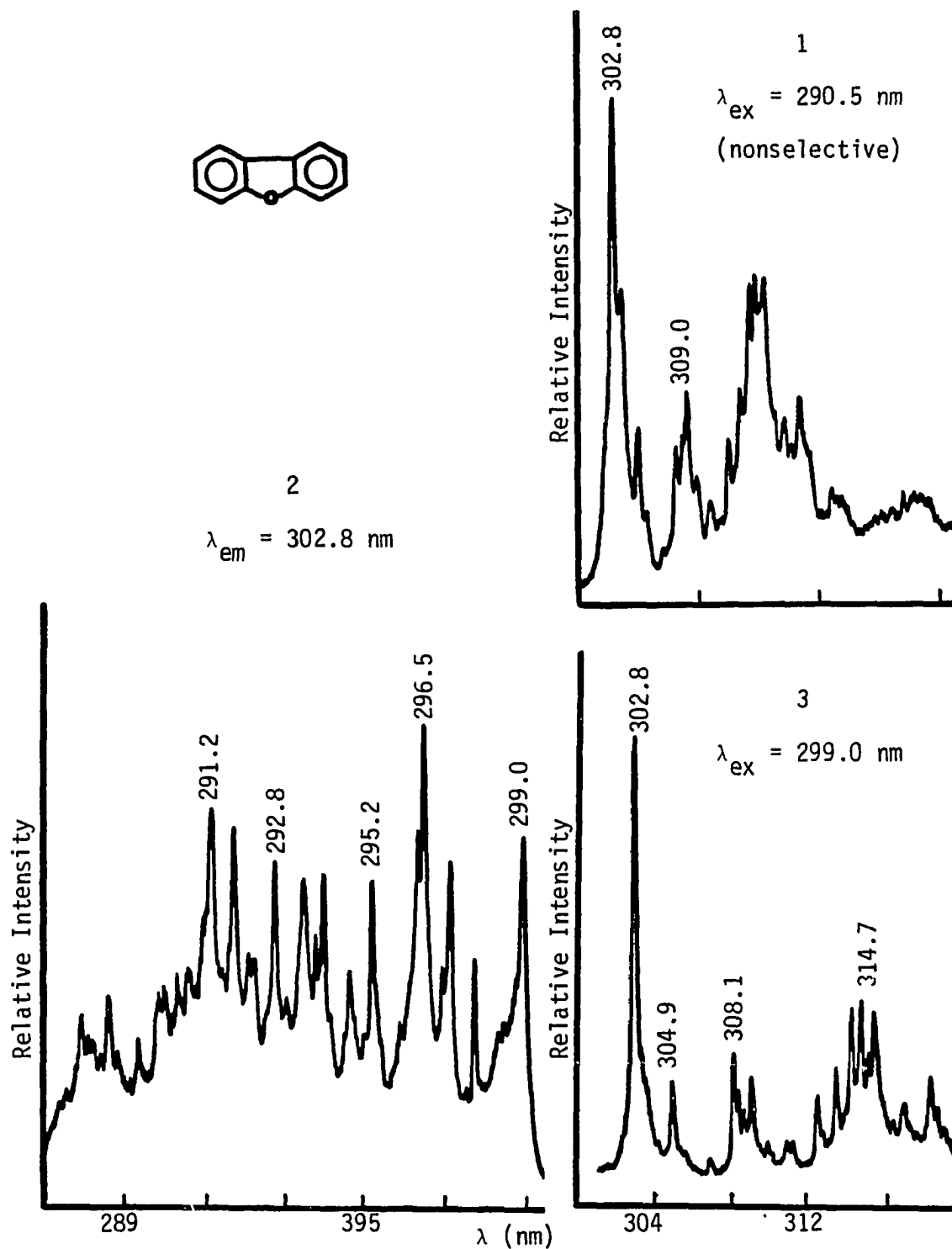


Figure 75A. Nonselectively excited fluorescence emission (1), excitation (2), and selectively excited fluorescence emission (3) of dibenzofuran at 1 ppm in n-hexane

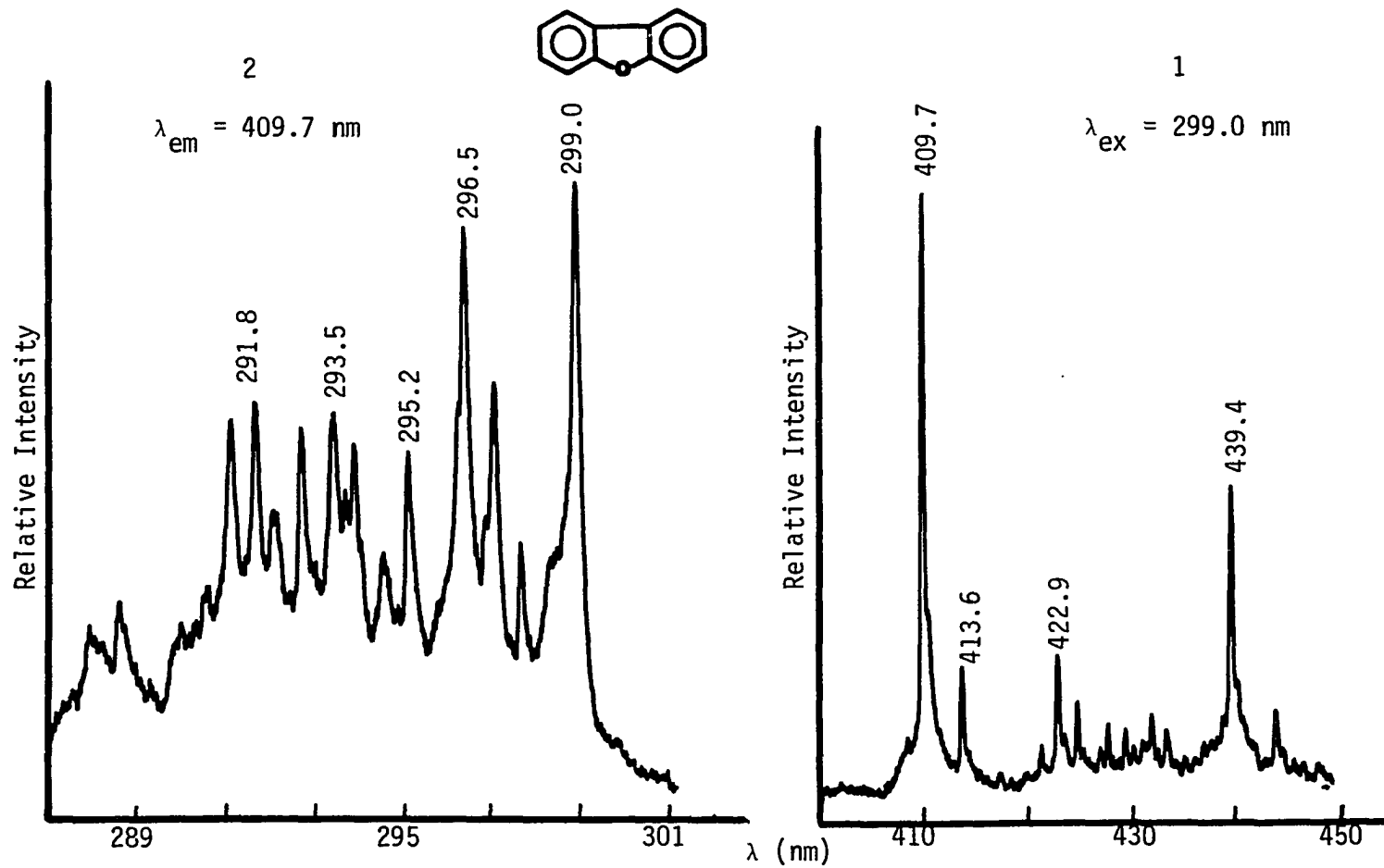
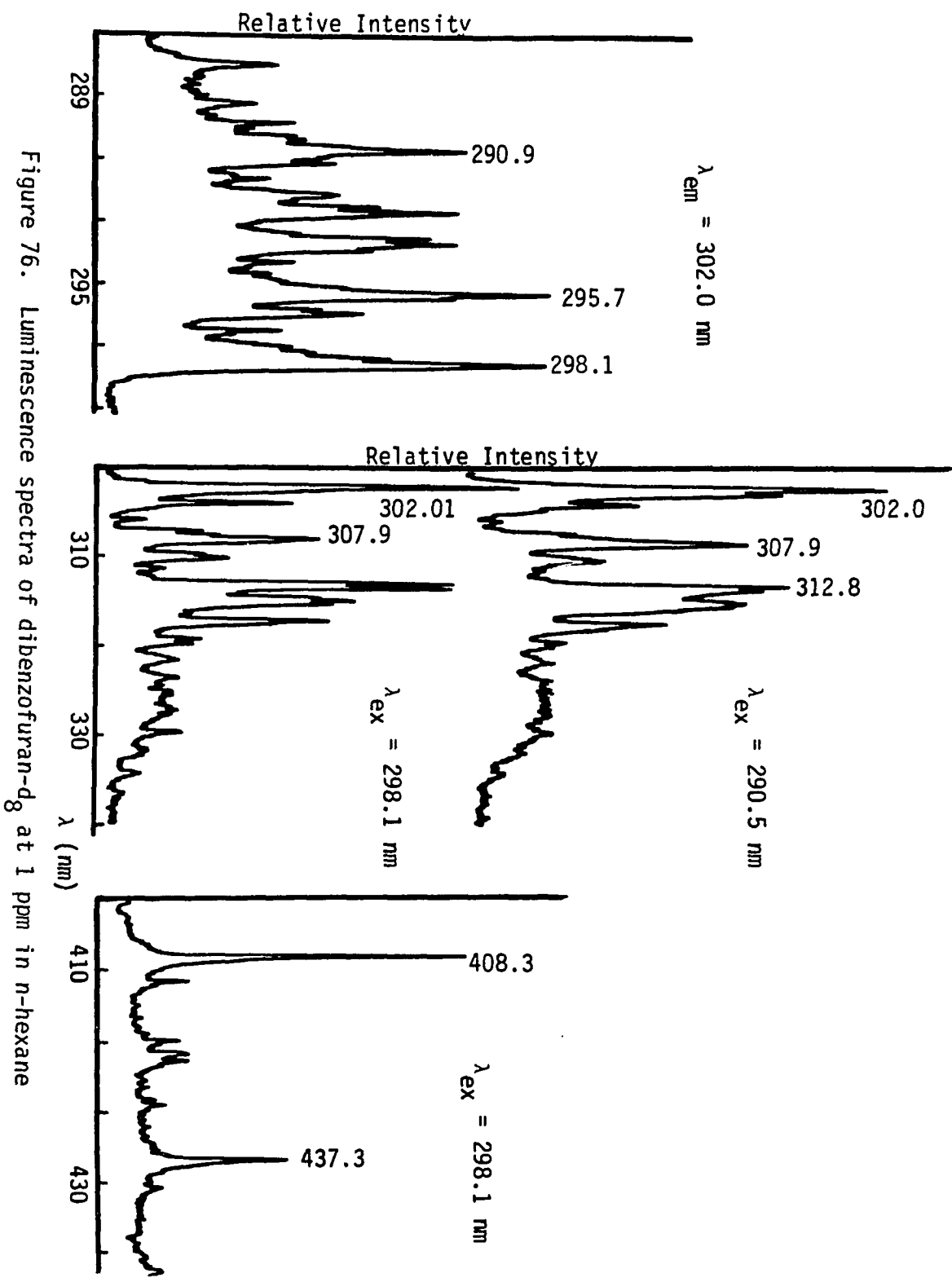


Figure 75B. Selectively excited phosphorescence emission (1) and phosphorescence excitation (2) of dibenzofuran at 1 ppm in n-hexane



observations are made below. When no unusual observations were made, their luminescence spectra are simply given as a nucleus of the LESS atlas to be completed in the near future.

Fluoranthene is a four ring compound exhibiting unusual solvent effects. As is seen in Figs. 48 and 49, the sharpest excitation and emission (fluorescence and phosphorescence) spectra are observed in a n-pentane solvent in contrast to n-heptane, which is an ideal solvent for pyrene, another four ring compound. However, n-pentane is not a suitable solvent for analytical work for reasons discussed earlier. Thus, the choice of an adequate solvent is limited to either n-hexane or n-heptane with the possibility of detecting either fluorescence or phosphorescence. For the analysis of complex mixtures, the latter is to be preferred as it provides a simple spectrum. The excitation-emission spectra for 1-aminopyrene, 2-aminopyrene and 4-aminopyrene are shown in Figs. 62 to 64. The sharp line excitation spectra observed for the first two compounds is an indication that they are appropriately incorporated in n-octane microcrystals to facilitate the observation of the Shpol'skii effect. In contrast, 4-aminopyrene does not appear to be incorporated in the host in a suitable manner resulting in broad band excitation spectra. This will preclude the selective excitation of the compound in complex mixtures. However, in a simple mixture, the three compounds can be readily identified as is seen in Fig. 65. Because of the sharp-line excitation spectra, it is feasible to selectively excite the fluorescence of 1- or 2-aminopyrene in the mixture but emission from 4-aminopyrene will also be observed as the broad band excitation spectra

of 4-aminopyrene will always overlap the excitation spectra of the other two compounds.

The nonselectively excited fluorescence spectra for two commercial products of 1-aminoanthracene are shown in Fig. 66. Clearly, the two spectra are different and at least one of the two commercial products is not 1-aminoanthracene. This reemphasizes what was previously mentioned, that is, LESS can be used to determine the identity of a given PAH if the LESS reference spectra for that compound are available.

The use of LESS to study heterocyclic aromatic compounds (to our knowledge) has hitherto not been reported. This is due partially to the lack of standard substances and partially to the fact that many heterocyclic compounds have low quantum efficiency. The heterocyclic compounds studied in the present work showed typical Shpol'skii spectra. A general observation for these compounds is that photodecomposition occurs, especially under prolonged exposure to the laser radiation. This was concluded from the gradual decrease in the peak intensities with time of exposure.

CHAPTER 5. ANALYTICAL APPLICATIONS

The Shpol'skii effect has opened up new possibilities for research on luminescence spectra for purposes of qualitative and quantitative analysis of polynuclear aromatic hydrocarbons. As a result of their high selectivity, individuality and sensitivity, the quasilinear luminescence spectra of frozen n-alkane solutions of these compounds have found wide use for analytical ends. In the present study, the analytical investigation was not meant to determine as many PNAs as possible in one sample, but to examine the feasibility of utilizing LESS to identify and quantitate selected PNA compounds in a number of samples of various complexity.

Samples Analyzed

Urban air particulate sample (SRM 1649)

The sample was prepared from atmospheric particulate matter collected in the Washington, DC area. The material was collected over a period in excess of one year and, therefore, represents a time-integrated sample (207).

Diesel particulate (SRM 1650)

These are exhaust particulates emitted by diesel engines (208).

SRC-II

SRC is defined as the pyridine-soluble coal-derived product boiling generally above about 800°F (209).

The above three samples were provided by NBS as part of the round-robin analysis for the NBS surrogate reference materials program. The

objective of this program is to evaluate, with provided material, the effectiveness of the various techniques utilized by different laboratories for the determination of trace organic constituents in these samples.

Carbon blacks

Carbon blacks are used in the reinforcing of rubber for tires and other articles and as a pigment in inks and paints. Carbon blacks are produced by the "furnace combustion" method. By this method, raw material (mineral oils, natural gas, or other hydrocarbons) are submitted to "cracking" and the cracked products are burned in refractory lined furnaces with a deficiency of air (210). A carbon black sample was provided by Prof. Milton L. Lee, Department of Chemistry, Brigham Young University, Provo, UT.

Sample Extraction Procedures

Particulate samples

These procedures should meet the following criteria: (a) high extraction efficiencies for a wide range of organic and organometallic compounds without limitation on molecular weight; (b) feasibility of extraction from small sized samples, preferably less than 100 mg; (c) shorter extraction times to facilitate the analysis of a large number of samples; (d) small solvent volumes (<1 to 2 ml) to facilitate direct analysis of the extract and to minimize losses that may occur on evaporation of large solvent volumes; and (e) the use of solvents that are compatible with the LESS analytical approach.

An overall procedure that satisfies these criteria to a high degree is based on moderately high temperature extractions (240°C) with high boiling solvents (>250°C) that are directly compatible for the direct determination of the PAHs with LESS (170).

The high temperature extractions were accomplished as follows. To particulate samples weighing between 50 mg and 200 mg contained in a 10 ml test tube, diphenylmethane (B.p. 265°C) was added and the mixture was heated for five minutes in a molten salt bath maintained at 240°C. The salt bath consisted of an equimolar mixture of NaNO_3 and KNO_3 . The hot extract was immediately filtered through a glass microfiber filter (Whatman 934-AH) fitted to a small Buchner funnel set in a test tube with a side arm attached to a vacuum filtration system. The extract was separated from the particulate matter in less than one minute after extraction to prevent reabsorption of organics on cooling. The extracts were immediately frozen and kept frozen until analyzed to preserve the compositional integrity. Solvent blanks were also obtained under the above conditions.

SRC-II sample

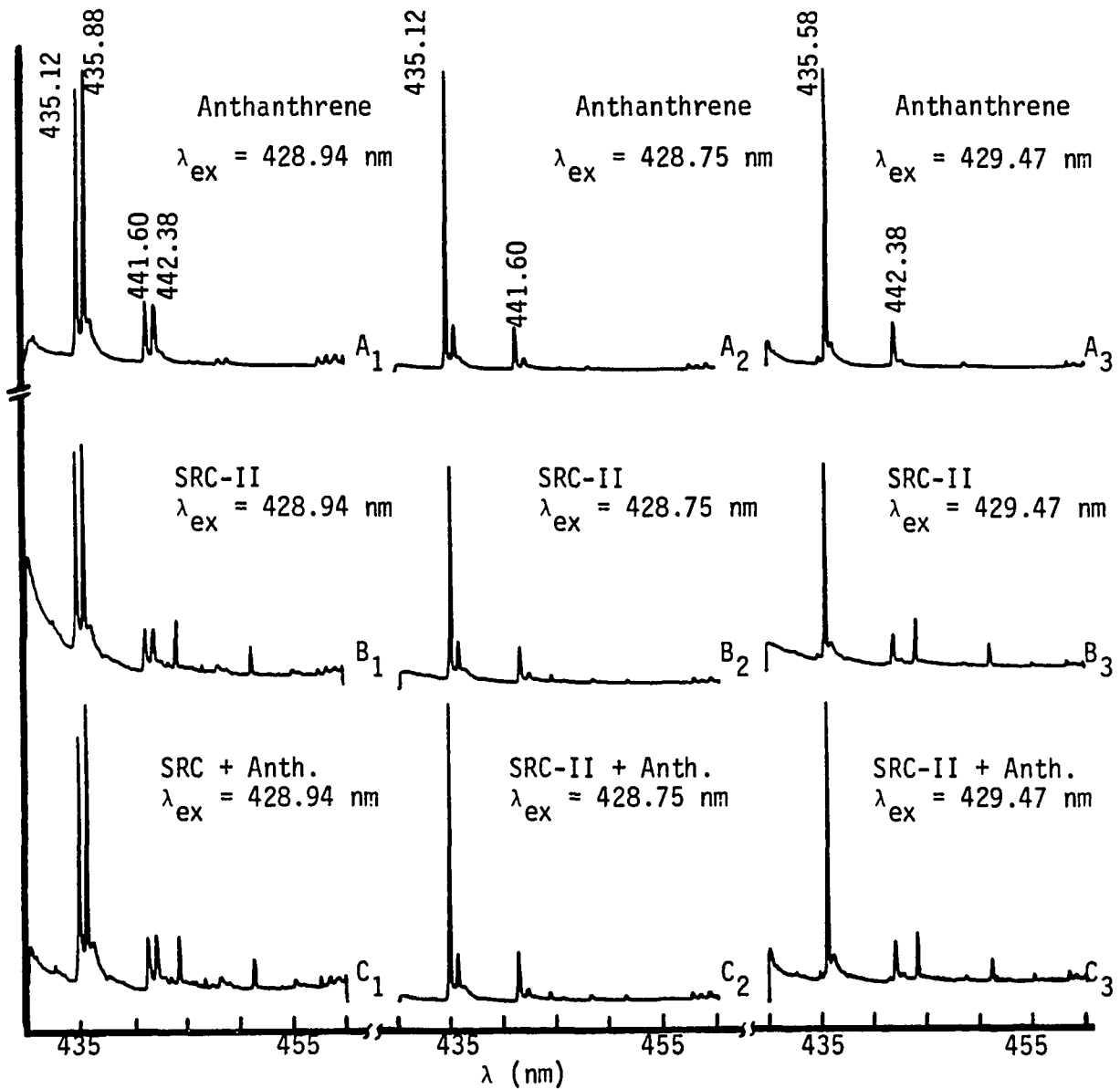
A 0.1 ml portion of SRC-II sample was pipetted into a 10 ml volumetric flask and diluted with n-octane solvent to the mark. The resulting solution was agitated using a mechanical shaker at room temperature for at least 10 minutes, and then left unagitated for 2 hours, agitated again for 10 minutes, and then left unagitated for several hours, usually overnight, to allow the insoluble residue to settle to the bottom of the solution flask. For qualitative analysis, the solu-

tion portion of the dilute solution was pipetted into a volumetric flask for further dilution prior to spectroscopic investigations.

Identification of PNAs in SRC-II and Carbon Black

The most direct LESS method of qualitative analysis is to compare the LESS emission spectrum of the substance being analyzed with that of the compound of interest. The procedure is simple and can often be very efficient. However, for many complex samples, spectral identification is not always straightforward because the component of interest is buried inside a composite spectrum with overlapping bands. In such cases, the standard addition technique can be used to confirm the spectral identification. The compound of interest is added to the sample at increasing concentration levels and the spectra of the mixture (sample plus added compound) is recorded. If the suspected compound was already present in the original sample, then only the characteristic peaks will increase in intensity. A practical example illustrating these two methods (spectral identification and standard addition) is shown in Fig. 77 for the identification of anthantherene in SRC-II sample. In this figure, site-specific spectra unambiguously identify anthantherene. The figure shows the specificity achieved with the use of the LESS emission spectra for identification, especially when the compound of interest is a major component in the sample and has a high quantum yield.

In the same manner for the heterocyclic compound studied in the present work, SRC-II was examined for nitrogen compounds and dibenzofuran, and carbon black was examined for sulfur compounds. The data



- A_1 , A_2 and A_3 : pure anthanthrene at 50 ppb in octane
- B_1 , B_2 and B_3 : SRC-II at dilution ratio of (200:1) in n-octane
- C_1 , C_2 and C_3 : SRC-II (100:1) spiked with 5 ppb anthanthrene
- spectra of B_1 to C_3 were recorded under identical conditions at wavelengths indicated above

Figure 77. Selectively excited fluorescence emission of anthanthrene

Table 4. Analysis of SRC-II and carbon black for PNAs

Compound	SRC-II	Compound	Carbon Black
dibenzo(a,j)acridine	X	benzo(b)naphtho(1,2-d)thiophene	X
13-H dibenzo(a,i)carbazole	ND	benzo(2,3)phenanthro(4,5-bcd)thiophene	X
7-H dibenzo(c,j)carbazole	ND	chryseno(4,5-bcd)thiophene	X
dibenzofuran	X	benzo(b)naphtho(2,3-d)thiophene	ND

obtained are summarized in Table 4. The PNA that was searched for is indicated either by a check mark (identified), or by ND (not detected).

Quantitative Determination of PAHs in Urban Air and Diesel Particulate Samples

Seven PAHs were identified and quantitated in both urban air particulate (SRM 1649) and diesel particulate (SRM 1650) samples. For a given PAH, one of the following methods was used for quantitation.

Internal reference method

For quantitative determinations, the internal reference principle was adopted to compensate for: (a) any variations of the sample cell position in the optical path; (b) drift in the single beam laser output; (c) possible variations in the inhomogeneity of the front surface of the sample, which may give rise to variable reflectivity; and (d) intermolecular interactions that may occur in samples of widely varying composition (170). The selection criteria of an internal reference compound was discussed on page 65.

In the internal reference method, a number of reference solutions with increasing concentrations for the target PAH are prepared to cover the concentration range of interest. During the preparation of these standard as well as sample solutions, the internal reference is added in constant concentration to all of them. An analytical calibration curve is plotted as the ratio of the luminescence line intensities of the analyte to that of the internal reference line. The ratio of line intensities of the internal reference and the sample is then used to calculate the unknown concentration of the PAH in the sample.

Standard addition method

Because of the complex nature of many samples, the "inner filter effect" may result in quenching or enhancement of the observed luminescence (75). In the absence of a suitable internal reference, the analytical bias that may be occasioned by this effect can usually be eliminated through the standard additions approach (182). In this approach, the procedure for quantifying a given analyte in a sample consists of first preparing a series of solutions containing the same amount of the original sample but increasing amounts of added analyte. All the mixtures are then analyzed under identical experimental conditions. The analyte emission readings for these mixtures are then corrected for background and plotted against the concentrations of the added reference compound present in the solution. The resulting extrapolated line intersecting the concentration axis indicates the concentration of the analyte in the sample.

Internal reference-standard addition combination

In making up the series of solutions for analysis by the standard addition method, an internal reference substance can be introduced in the same concentration into the solution.

The PAHs quantitated and the method of quantitation for each compound are given in Table 5. The two particulate samples were extracted by the high temperature extraction procedure described before using diphenylmethane. It was found that a dilution ratio of 200 using, e.g., n-octane for the obtained extract was appropriate. At lower dilution ratios, e.g., 100, the diphenylmethane concentration disturbed the crys-

Table 5. Quantitated PAHs and the method of quantitation for each compound

Compound			Method Used	Internal Reference ^a		Urban Air Part. (SRM 1649)		Diesel Particulate (SRM 1650)	
Name	λ_{ex} (nm)	λ_{em} (nm)		Name	λ_{em}	LESS ppm	NBS ppm	LESS ppm	NBS ppm
benzo(a)pyrene	388.72	402.98	internal ref.	B(a)P-d ₁₂	402.06	3.2±0.2 ^b	2.9±0.3 ^c	1.7±0.2 ^b	1.9±1.7 ^c
benzo(k)- fluoranthene	386.78	403.55	internal ref.	B(a)P-d ₁₂	402.06	2.5±0.3	2.0±0.2	0.5±0.1	2.0±0.4
benzo(ghi)- perylene	387.79	419.56	internal ref.	B(a)P-d ₁₂	402.06	6.3±0.4	4.7±0.2	2.4±0.2	3.9±2.4
benzo(a)- anthracene	374.18	384.16	internal ref.	B(a)A-d ₁₂	383.66	2.8±0.2	2.5±0.3	5.8±0.3	7.7±3.8
pyrene	357.31	372.01	internal ref.	pyrene-d ₁₀	370.93	6.6±0.3	6.3±0.4	50.7±1.5	42.9±6.9
benzo(e)pyrene	366.58	537.59	standard add.	-	-	3.2±0.2	3.3±0.2	9.7±0.3	9.3±2.7
perylene	420.52	444.57	standard add. and internal ref.	perylene-d ₁₂	443.52	0.73±0.04	-	0.15±0.01	0.13±0.01

^a λ_{ex} for the internal reference was the same as that of the target compound.

^bDeviation from the mean of replicate values.

^cHalf of the range of the values reported by different laboratories.

talline matrix and effected the quasilinear spectrum of the analyte of interest. At higher dilution ratios, e.g., 400, the analyte concentration became too diluted to a given measurable signal. Background correction was performed for all the peaks utilized for the calculation. The background was measured at both sides of the base of the peak of interest. The average of the two measurements was then subtracted from the total signal. The results of the determination are given in Table 4 as well as the data from NBS for comparison. Examples of actual spectra of PAHs in the real samples are shown in Fig. 78. Analytical calibration curves for the seven compounds determined are shown in Figs. 79 to 83. In case of perylene, the internal standard-standard additions method was used to obtain the best straight line fit of the data points and to avoid possible error in the slope of that line. This was performed when the qualitative examinations showed that the concentration of perylene was low, as can be seen in Table 5. When the diesel particulate sample was analyzed by different laboratories, benzo(k)fluoranthene was reported only by the NBS and by the LESS. The NBS value for B(k)F was 4 times that obtained by the LESS technique. Repetition of LESS analysis for B(k)F confirmed the value of 0.5 ± 0.1 ppm.

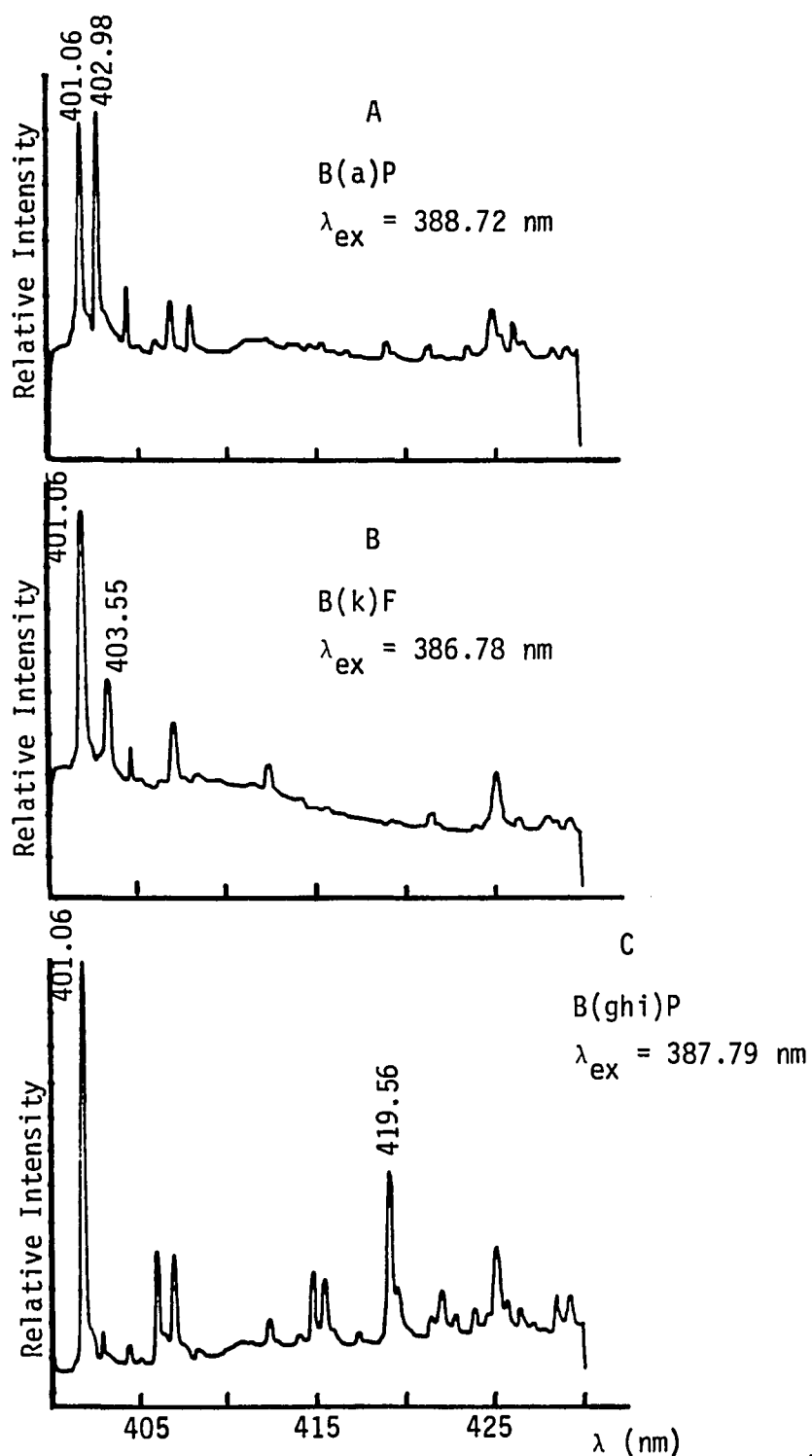


Figure 78. Selectively excited fluorescence spectra of benzo(a)-pyrene (A), benzo(k)fluoranthene (B), and benzo(ghi)-perylene (C) in diesel particulate sample

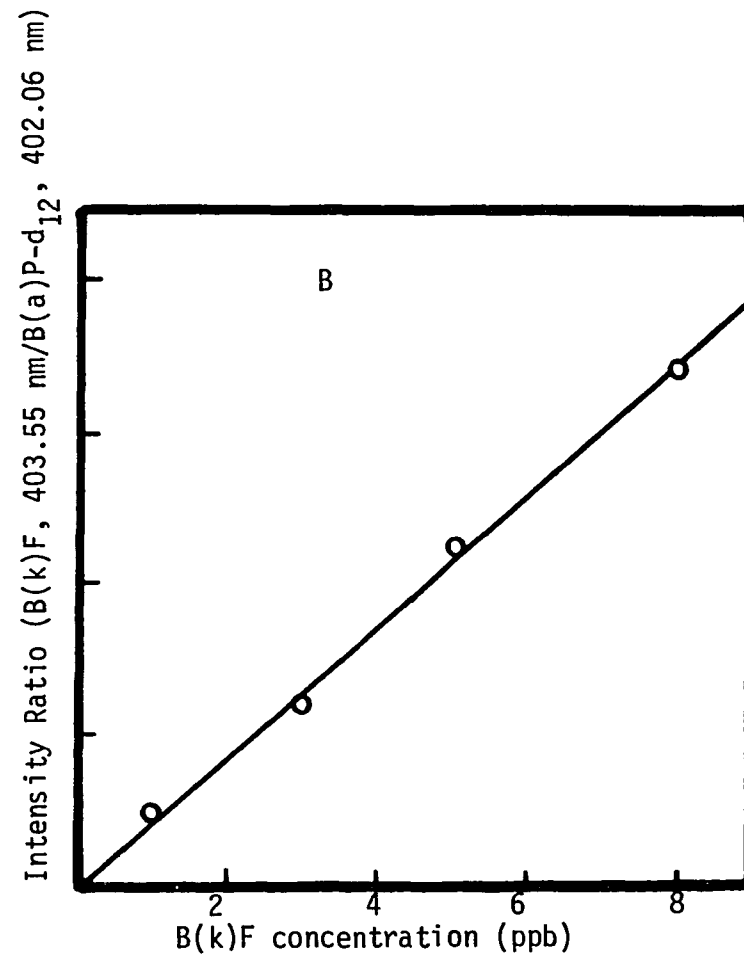
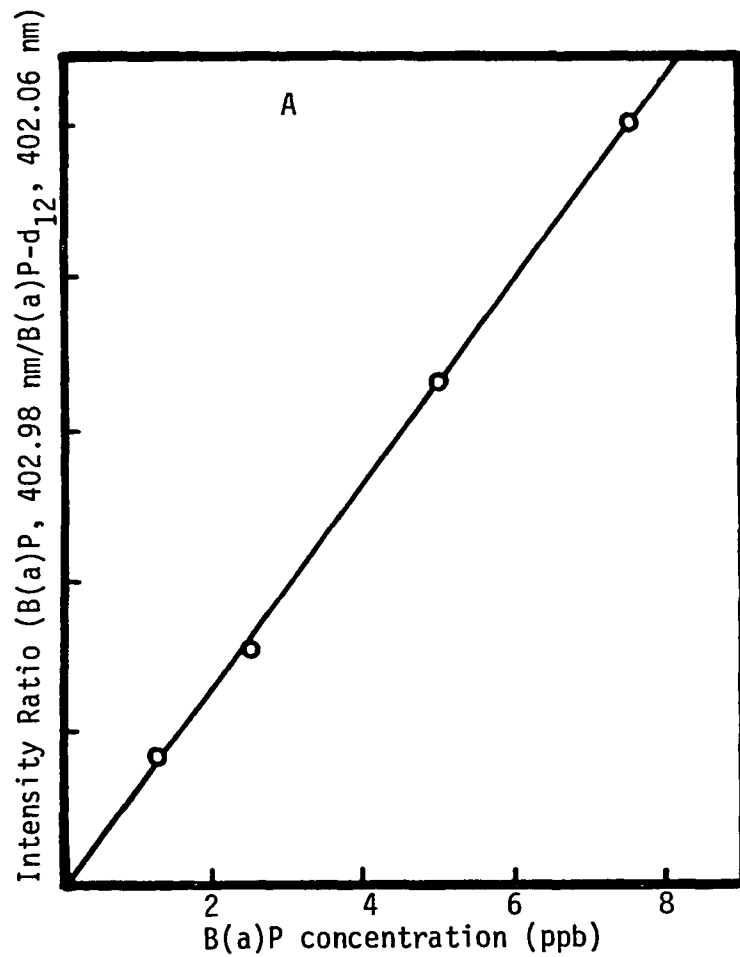
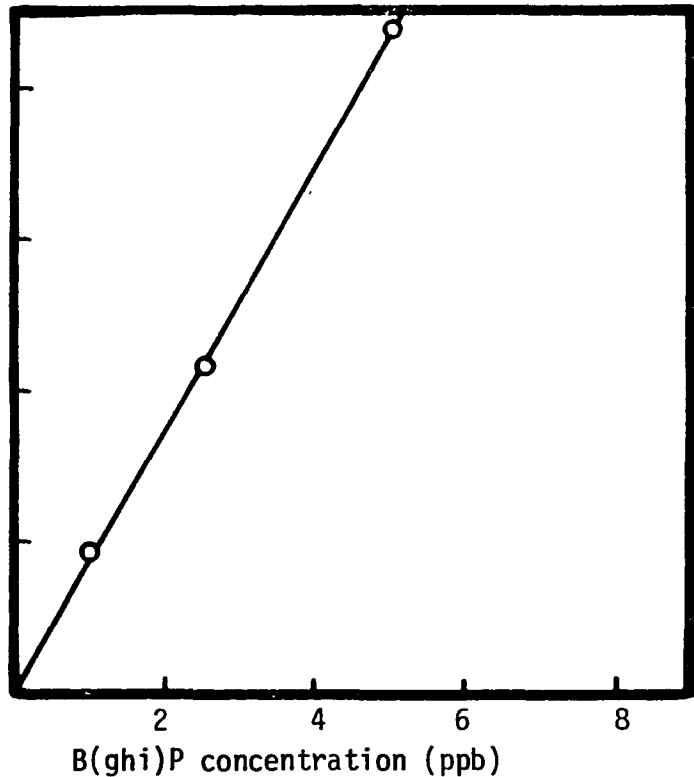


Figure 79. Analytical calibration curves for benzo(a)pyrene (A) and benzo(k)fluoranthene (B) utilizing benzo(a)pyrene-d₁₂ as internal reference. Excitation and emission wavelengths are given in Table 5

Intensity Ratio (B(ghi)P, 419.56 nm/B(a)P-d₁₂, 402.06 nm)



Intensity Ratio (B(a)A, 384.16 nm/B(a)A-d₁₂, 383.66 nm)

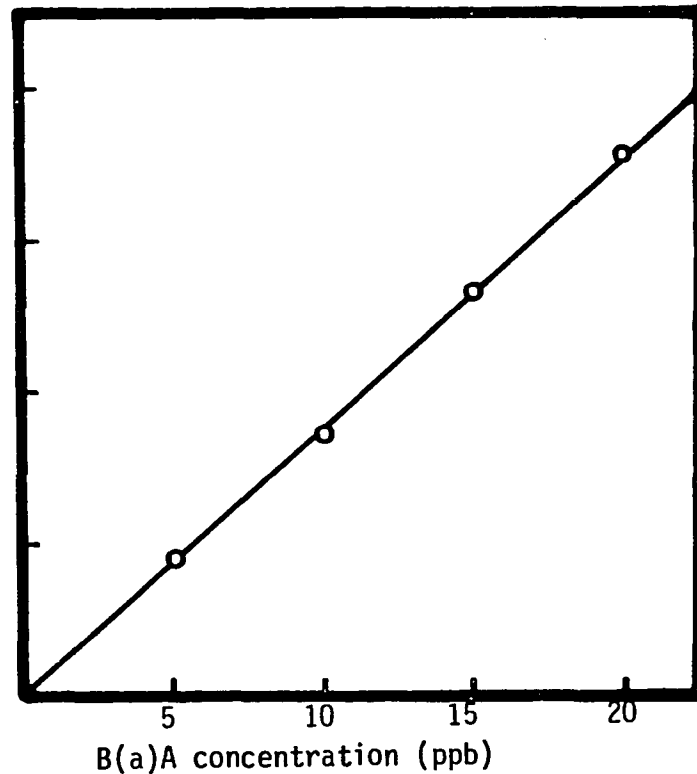


Figure 80. Analytical calibration curves for benzo(ghi)perylene utilizing benzo(a)pyrene-d₁₂ (10 ppb) as internal reference (A) and benzo(a)anthracene utilizing benzo(a)-anthracene-d₁₂ (15 ppb) as internal reference (B). Excitation and emission wavelengths are given in Table 5

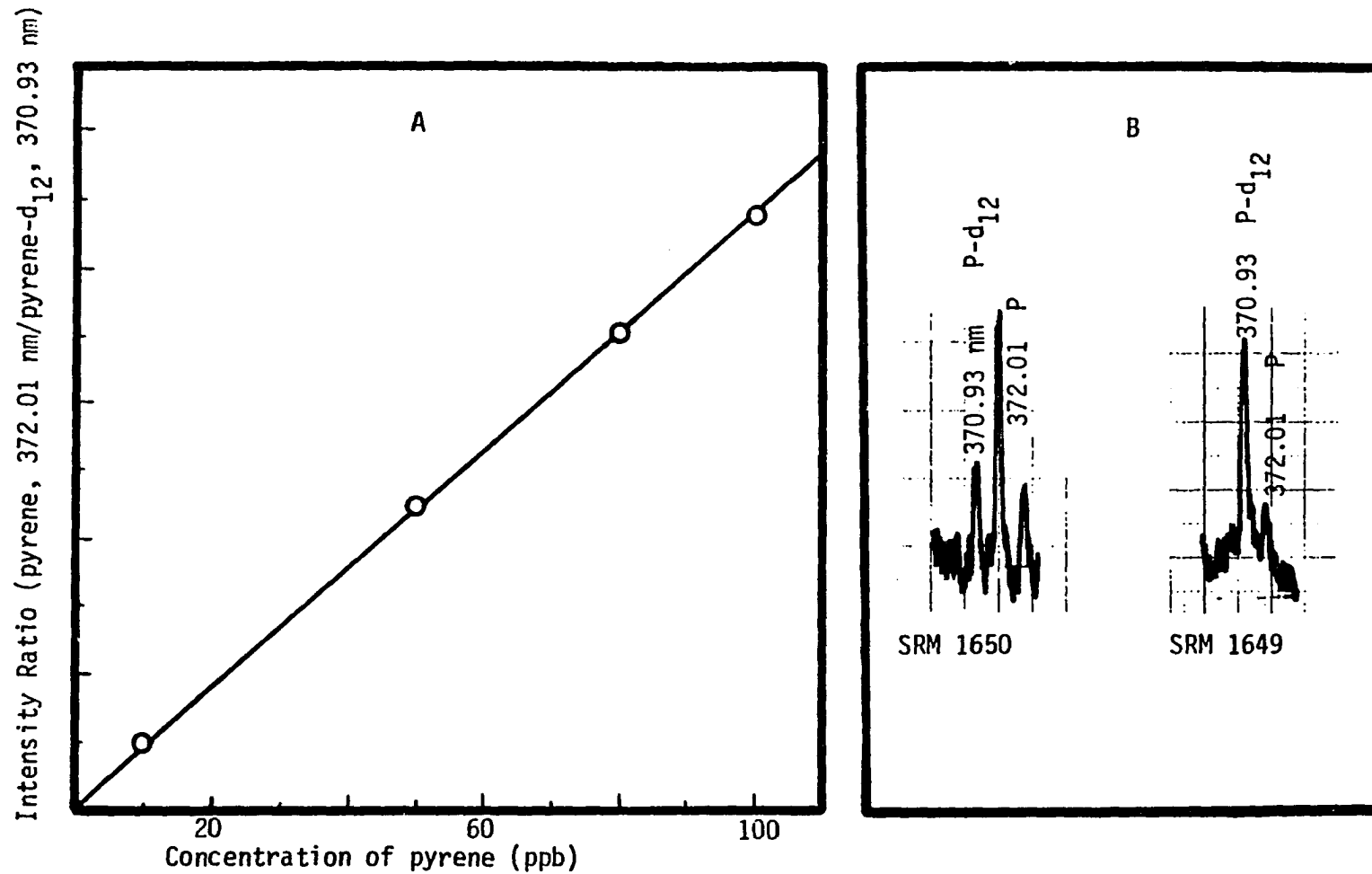


Figure 81. Analytical calibration curve for pyrene utilizing pyrene-d₁₀ (10 ppb) as internal reference (A) and selectively excited fluorescence emission of pyrene in particulate sample spiked with pyrene-d₁₀ (B). Excitation and emission wavelengths are given in Table 5

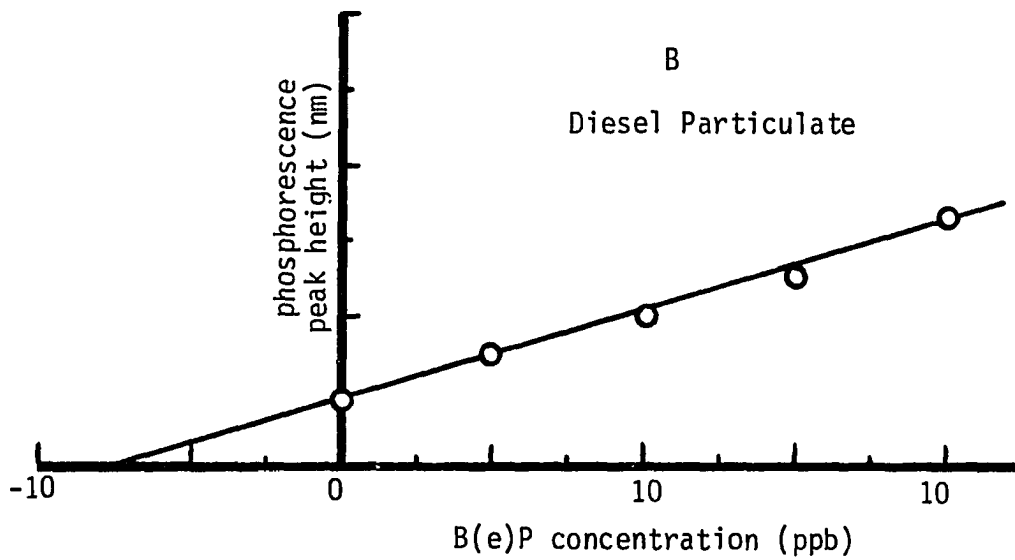
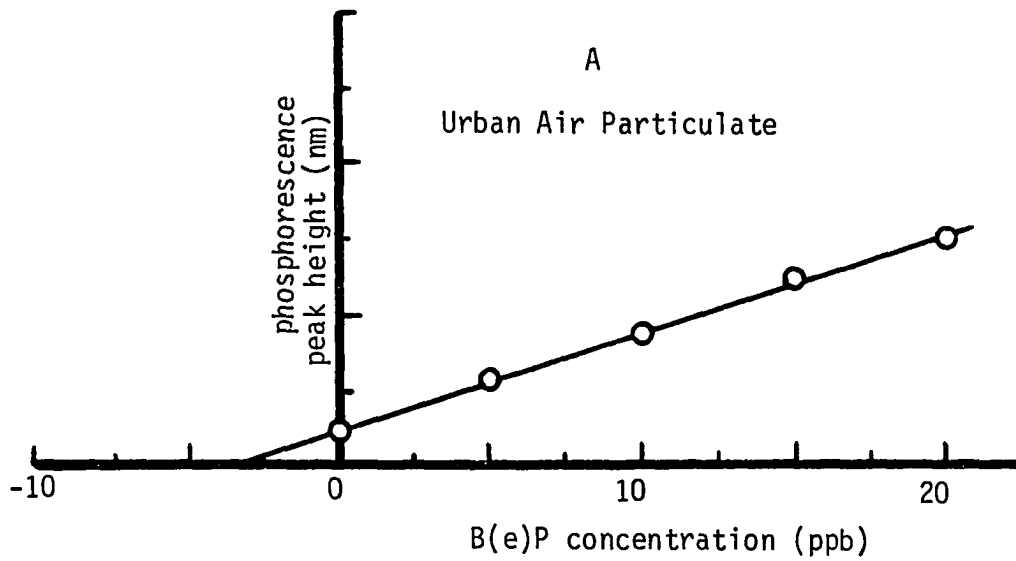


Figure 82. Calibration curves for benzo(e)pyrene by the method of standard additions. Excitation and emission wavelengths are given in Table 5

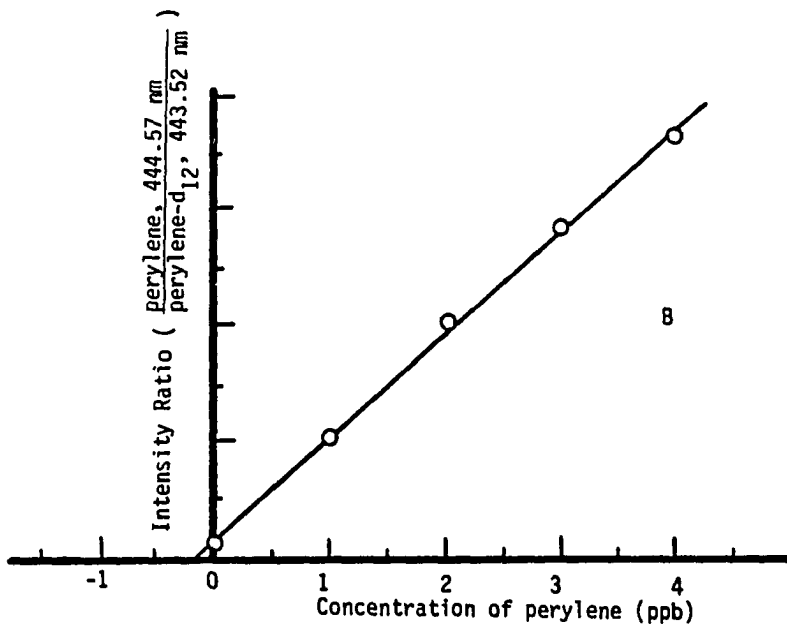
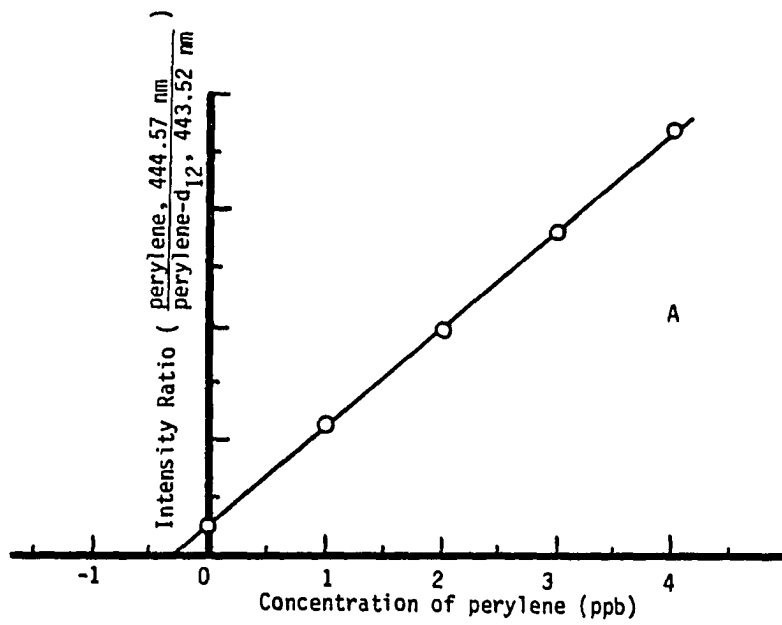


Figure 83. Calibration curves for perylene in SRM 1649 (A) and in SRM 1650 (B) by the method of internal reference standard additions. Excitation and emission wavelengths are given in Table 5

REFERENCES

1. Clar, E. "Polycyclic Hydrocarbons"; Academic Press: New York, 1964; Vol. 1.
2. Committee on the Biological Effects of Atmospheric Pollutants: Particulate Polycyclic Organic Matter; National Academy of Science: Washington, DC, 1972.
3. Boulos, B. M. In "Polynuclear Aromatic Hydrocarbons: Mechanisms, Methods and Metabolism", Eighth International Symposium; Cooke, M.; Dennis, A. J., Eds.; Battelle Press: Columbus, OH, 1985.
4. Wynder, E. L.; Mabuchi, K. Prev. Med. 1972, 1, 300.
5. Emmelot, P.; Kriek, E. "Environmental Carcinogenesis"; Elsevier: North-Holland, 1979; p. 9.
6. Shubik, P. Proc. Natl. Acad. Sci., USA 1972, 69, 1052.
7. Dipple, A. In "Chemical Carcinogens"; Searle, C. E., Ed.; American Chemical Society: Washington, DC, 1976.
8. Bridbord, K.; French, J. G. In "Polynuclear Aromatic Hydrocarbons: Carcinogenesis - A comprehensive survey"; Jones, P. W.; Freudenthal, R. I., Eds.; Raven Press: New York, 1978; Vol. 3.
9. Thornton, S. C.; Diamond, L.; Hite, M.; Baird, W. M. In "Polynuclear Aromatic Hydrocarbons: Chemical Analysis and Biological Fate", Fifth International Symposium; Cooke, M.; Dennis, A. J.; Eds.; Battelle Press: Columbus, OH, 1981.
10. Hoffman, D.; Wynder, E. L. Cancer 1971, 27, 848.
11. Singer, B.; Kusmierek, J. T. Ann. Rev. Biochem. 1982, 52, 655.
12. C. E. Searle, Ed. "Chemical Carcinogens", ACS Monograph 173; American Chemical Society: Washington, DC, 1976.
13. Rhim, J. S.; Vass, W.; Cho, H. Y.; Huebner, R. J. Int. J. Cancer 1971, 7, 65.
14. Gelboin, H. V. Rev. Can. Biol. 1972, 31, 39.
15. Selkirk, J. K.; Croy, R. G.; Whitlock, J. P.; Gelboin, H. V. Cancer Res. 1975, 35, 3651.
16. Harvey, R. G. Am. Scientist 1982, 70, 386.

17. Pullman, A.; Pullman, B. Adv. Cancer Res. 1955, 3, 117.
18. Acros, J. C.; Argus, M. F. Adv. Cancer Res. 1968, 11, 305.
19. Pataki, J.; Malick, R. J. J. Med. Chem. 1972, 15, 905.
20. Hueper, W. C.; Conway, W. D. In "Chemical Carcinogenesis and Cancers", Thomas, C. C., Ed.; Springfield, IL, 1964.
21. Schoental, R. In "Polycyclic Hydrocarbons"; Clar, E., Ed.; Academic Press: New York, 1964; Vol. 2.
22. Dunning, W. F.; Curtis, M. R. J. Natl. Cancer Inst. 1960, 25, 387.
23. Phillips, D. H. Nature 1983, 303, 468.
24. Pataki, J.; Huggins, C. Cancer Res. 1969, 29, 506.
25. Huggis, C. B.; Pataki, J.; Harvey, R. G. PNAS 1967, 58, 2253.
26. Lacassagne, A.; Buu-Hoi, N. P.; Danel, R.; Zajdela, F. Adv. Cancer Res. 1965, 9, 316.
27. Guerin, M. R.; Ho, C.-H.; Rao, T. K.; Clark, B. R.; Epler, J. L. Environ. Res. 1980, 23, 42.
28. Ho, C.-H.; Ma, C. Y.; Clark, B. R.; Guerin, M. R.; Rao, T. K.; Epler, J. L. Environ. Res. 1980, 22, 412.
29. Wilson, B. W.; M. R. Petersen; Pelroy, R. A.; Cresto, J. T. Fuel 1981, 60, 289.
30. Lao, R. C.; Thomas, R. S.; Oja, H.; Dubois, L. Anal. Chem. 1973, 45, 908.
31. Lee, M. L.; Novetny, M.; Bartle, K. D. Anal. Chem. 1976, 48, 1566.
32. Youngblood, W. W.; Blumer, M. Geochim. Cosmochim. Acta 1975, 39, 1303.
33. Harrison, R. M.; Perry, R.; Wellings, R. A. Water Res. 1975, 9, 331.
34. Laflamme, R. E.; Hites, R. A. Geochim. Cosmochim. Acta 1978, 42, 289.
35. Hoffmann, D.; Wynder, F. L. In "Chemical Carcinogens", ACS Mongraph 173; Searle, C. E., Ed.; American Chemical Society: Washington, DC, 1976.

36. Guerin, M. R. In "Polycyclic Hydrocarbons and Cancer", Gelboin, H. V.; Ts'o, P. O. P., Eds.; Academic Press: New York, 1978; Vol. 1.
37. Snyder, L. R. Acc. Chem. Res. 1970, 3, 290.
38. Lee, M. L.; Novotny, M. V.; Bartle, K. D. "Analytical Chemistry of Polynuclear Aromatic Compounds"; Academic Press: New York, 1981.
39. Bartle, K. D.; Lee, M. L.; Wise, S. A. Chem. Soc. Rev. 1981, 10, 113.
40. Seifert, B. J. Chromatogr. 1977, 417, 131.
41. Sawicki, E. Crit. Rev. Environ. Control 1970, 1, 280.
42. Schaad, R. E. Chromatogr. Rev. 1970, 13, 61.
43. Beernaert, H. J. Chromatogr. 1979, 173, 109.
44. Borwitzky, H.; Schmburg, G. J. Chromatogr. 1979, 170, 99.
45. Lankmayr, E. P.; Muller, K. J. Chromatogr. 1979, 170, 139.
46. Nielsen, T. J. Chromatogr. 1979, 170, 147.
47. Hirate, Y.; Novotny, M. J. Chromatogr. 1980, 186, 521.
48. Janini, G. M.; Johnson, K.; Zielinski, W. L. Anal. Chem. 1975, 47, 670.
49. Gouw, T. H.; Jentoft, R. E. Adv. Chromatogr. 1975, 13, 2.
50. Gouw, T. H.; Jentoft, R. E. J. Chromatogr. 1972, 68, 303.
51. Scharbon, J. F.; Hurtubise, R. J.; Silver, H. F. Anal. Chem. 1979, 51, 1426.
52. Voigtman, E.; Jurgensen, A.; Winefordner, J. D. Anal. Chem. 1981, 53, 1921.
53. Katz, M.; Chan, C. Environ. Sci. Technol. 1980, 14, 838.
54. Jurgensen, A.; Inman, E. L.; Winefordner, J. D. Anal. Chim. Acta 1981, 131, 187.
55. Aaron, J. J.; Winefordner, J. D. Talanta 1975, 22, 707.
56. Vo-Dinh, T.; Martinez, P. R. Anal. Chim. Acta 1981, 125, 13.

57. Vo-Dinh, T.; Gammage, R. B.; Martinez, P. R. Anal. Chem. 1981, 53, 253.
58. Vo-Dinh, T.; Gammage, R. B.; Martinez, P. R. Anal. Chim. Acta 1980, 118, 313.
59. O'Haver, T. C.; Parks, W. M. Anal. Chem. 1974, 46, 1886.
60. Dickinson, R. B.; Wehry, E. L. Anal. Chem. 1979, 51, 778.
61. Sepaniak, M. J.; Yeung, E. S. Anal. Chem. 1977, 49, 1554.
62. Johnson, D. W.; Callis, J. B.; Christian, G. D. Anal. Chem. 1974, 49, 575.
63. Schwager, I.; Yen, T. F. Anal. Chem. 1979, 51, 569.
64. Hembree, D. M.; Garrison, A. A.; Crocombe, R. A.; Tokley, R. A.; Whery, E. L.; Mamantov, G. Anal. Chem. 1981, 53, 1783.
65. Johnson, C. R.; Asher, S. A. Anal. Chem. 1984, 56, 2258.
66. Bartle, K. D.; Jones, D. W. Adv. Org. Chem. 1972, 8, 317.
67. Sawicki, E. Talanta 1969, 16, 1231.
68. Richardson, J. H.; Ando, M. E. Anal. Chem. 1977, 49, 955.
69. Borneff, J. In "Fate of Pollutants in the Air and Water Environment"; Suffet, I. H., Ed.; Wiley: New York, 1977; Part 2; p. 393.
70. Vo-Dinh, T.; Hooyman, J. R. Anal. Chem. 1979, 51, 1915.
71. Katz, M.; Sakuma, T.; Ho, A. Environ. Sci. Technol. 1978, 12, 909.
72. Bentz, A. P. Anal. Chem. 1976, 48, 454A.
73. Wehry, E. L.; Hamantov, G. In "Modern Fluorescence Spectroscopy"; Wehry, E. L., Ed.; Plenum Press: New York, 1981; Vol. V.
74. Lamola, A. A. In "Energy Transfer and Organic Photochemistry"; Lamola, A. A.; Turro, N. J., Eds.; Interscience: New York, 1969.
75. Parker, C. A. "Photoluminescence of Solutions"; American Elsevier: New York, 1968; p. 220.
76. Birke, I. B.; Munro, I. H. Progr. Reaction Kinetics 1967, 4, 239.

77. Shpol'skii, E. V. Sov. Phys. Usp. (Engl. Transl.) 1962, 5, 522.
78. D'Silva, A. P.; Fassel, V. A. Anal. Chem. 1984, 56, 985A.
79. Maple, J. R.; Wehry, E. L. Anal. Chem. 1981, 53, 266.
80. Wehry, E. L.; Gore, R. R.; Dickinson, R. B. In "Lasers in Chemical Analysis"; Hieftje, G. M.; Travis, J. C.; Lytle, F. E., Eds.; Humana Press: New York, 1981.
81. Maple, J. R.; Wehry, E. L.; Mamantov, G. Anal. Chem. 1980, 52, 920.
82. Heisig, V.; Jeffery, A. M.; McGlade, M. J.; Small, G. J. In "Polynuclear Aromatic Hydrocarbons: Mechanisms, Methods and Metabolism", Eighth International Symposium; Cooke, M.; Dennis, A. J., Eds.; Battelle Press: Columbus, OH, 1985.
83. Chiang, I.; Hayes, J. M.; Small, G. J. Anal. Chem. 1982, 53, 315.
84. Brown, J. C.; Edelson, M. C.; Small, G. J. Anal. Chem. 1978, 50, 1399.
85. Amirav, A.; Even, U.; Jortner, J. Anal. Chem. 1982, 54, 1666.
86. Levy, D. H.; Snelly, R. E. In "Chemical and Biochemical Applications of Lasers"; Moore, C. B., Ed.; Academic Press: New York, 1977; p. 1.
87. Warren, J. A.; Hayes, J. M.; Small, G. J. Anal. Chem. 1982, 54, 138.
88. Bolotnikova, T. N. Opt. Spectrosc. USSR (Engl. Transl.) 1959, 7, 138.
89. McClure, D. S. J. Chem. Phys. 1954, 22, 1968.
90. Sidman, J. W. J. Chem. Phys. 1956, 25, 122.
91. Osterag, R.; Wolf, H. C. Phys. Status Solidi 1969, 31, 139.
92. McClure, D. S. J. Chem. Phys. 1956, 24, 1.
93. Shpol'skii, E. V.; Il'ina, A. A.; Klimova, L. A. Dokl. Akad. Nauk. SSSR 1952, 87, 935.
94. Colmsjo, A. "The Practice and Utility of the Shpol'skii Effect in Chemical Analysis"; University of Stockholm: Stockholm, 1981.
95. Shpol'skii, E. V. Sov. Phys. Usp. (Engl. Transl.) 1960, 3, 372.

96. Shpol'skii, E. V.; Bolotnikova, T. N. Pure Anal. Chem. 1974, 37, 183.
97. Bolotnikova, T. N.; Zhukov, V. A.; Utkina, L. F. J. Appl. Spectrosc. 1982, 37, 1286.
98. Shpol'skii, E. V.; Il'ina, A. A.; Klimova, L. A. Dokl. Akad. Nauk SSSR, 1952, 87, 935.
99. Shpol'skii, E. V.; Klimova, L. A.; Nersesova, G. N.; Gladkovskii, V. I. Opt. Spectrosc. USSR (Engl. Transl.) 1968, 24, 52.
100. Grebenshchikov, D. M. Opt. Spectrosc. USSR (Engl. Transl.) 1968, 25, 368.
101. Lamotte, M.; Merle, A. M.; Dupuy, F. Chem. Phys. Lett. 1975, 35, 410.
102. Merele, A. M.; Pitts, W. M.; El-Sayed, M. A. Chem. Phys. Lett. 1978, 54, 211.
103. Kohler, B. E. In "Chemical and Biochemical Applications of Lasers", Moore, C. B., Ed.; Academic Press: New York, 1979; Vol. 4, p. 31.
104. Meyer, B. "Low Temperature Spectroscopy"; American Elsevier: New York, 1971.
105. Lemaistre, J. P.; Zewail, A. H. Chem. Phys. Lett. 1979, 68, 296.
106. Mikhailenko, V. I.; Redkin, Y. R.; Grosul, V. P. Opt. Spectrosc. 1975, 39, 50.
107. Grebenshchikov, D. M.; Kovrijnikh, N. A.; Kozlov, S. A. Opt. Spectrosc. 1971, 31, 214.
108. Vo-Dinh, T.; Wild, U. P. J. Lumin. 1973, 6, 296.
109. Pitts, W. M.; Merle, A. M.; El-Sayed, M. A. Chem. Phys. 1979, 36, 437.
110. Saari, P. M.; Tamm, T. B. Opt. Spectrosc. 1976, 40, 395.
111. Vo-Dinh, T.; Kreibich, U. T.; Wild, U. P. Chem. Phys. Lett. 1974, 24, 352.
112. Merle, A. M.; Nicol, M. F.; El-Sayed, M. A. Chem. Phys. Lett. 1978, 59, 386.

113. Lamotte, M.; Jousset-Dubien, J. Chem. Phys. 1973, 2, 245.
114. Svischev, G. M. Opt. Spectrosc. 1965, 18, 350.
115. Personov, R. I. Zh. Anal. Khim. 1962, 17, 506.
116. Colmsjo, A. L.; Stenberg, U. Chem. Scripta 1976, 9, 227.
117. Pfister, C. Chem. Phys. 1973, 2, 171.
118. Dokunikhin, N. S.; Kizel, V. A.; Sapozhnikov, M. V.; Solodar, S. L. Opt. Spectrosc. 1968, 25, 42.
119. Colmsjo, A. L.; Stenberg, U. Chem. Scripta 1977, 11, 220.
120. Dinse, K. P.; Winscom, C. J. J. Lumin. 1979, 18/19, 500.
121. Mishina, L. A.; Nakhimovskaya, L. A. Izv. Akad. Nauk SSSR, Ser. Fiz. 1975, 39, 2387.
122. Rebane, K. K.; Khizhnyakov, V. V. Opt. Spectrosc. 1963, 14, 193.
123. Dibartolo, B.; Powell, R. C. "Phonons and Resonance in Solids"; Wiley: New York, 1976; p. 348.
124. Rebane, K. K. "Impurity Spectra of Solids"; Plenum Press: New York, 1970; p. 35.
125. Sapozhnikov, M. N. Phys. Stat. Sol. 1976, 75, 11.
126. Richards, J. L.; Rice, S. A. J. Chem. Phys. 1971, 54, 2014.
127. Sapozhnikov, M. N. J. Chem. Phys. 1978, 68, 2352.
128. Personov, R. I.; Al'shits, E. I.; Bykovskaya, L. A. Opt. Commun. 1973, 7, 417.
129. Klimova, L. A. Opt. Spectrosc. 1963, 15, 185.
130. Grebenshchikov, D. M.; Koyrizhnykh, N. A.; Kozlov, S. A. Opt. Spectrosc. 1971, 31, 392.
131. Kirkbright, G. F.; de Lima, C. G. Chem. Phys. Lett. 1976, 37, 165.
132. Canters, G. W.; Noort, M.; Vander Waals, J. H. Chem. Phys. Lett. 1975, 30, 1.

133. Litvin, F. F.; Personov, R. I.; Korotaev, O. N. Dokl. Akad. Nauk. SSSR 1969, 188, 1169.
134. Nikitina, A. N.; Ponomareva, N. A.; Yanovskaya, L. A.; Dombrovskii, V. A.; Kucherov, V. F. Xith European Congress on Molecular Spectroscopy, Abstract No. 192; Tallinn, 1973.
135. Bolotnikova, T. N.; Artemova, L. K. Opt. Spectrosc. 1972, 33, 371.
136. Shpol'skii, E. V. Sov. Phys. Usp. 1963, 6, 411.
137. Dekkers, J. J.; Hoornweg, G. Ph.; Visser, G.; Maclean, C.; Velthorst, N. H. Chem. Phys. Lett. 1977, 47, 357.
138. Merle, A. M.; Lamotte, M.; Risemberg, S.; Harew, C; Galtier, J.; Grivet, A. J. Chem. Phys. 1977, 22, 207.
139. Tuan, V. D.; Wild, U. P.; Lamotte, M.; Merle, A. M. Chem. Phys. Lett 1976, 39, 118.
140. Lamotte, M.; Jousot-Dubien, J. J. Chem. Phys. 1974, 61, 1892.
141. Dekkers, J. J.; Hoornweg, G. Ph.; MacLean, C.; Velthorst, N. H. J. Mol. Spectrosc. 1977, 68, 56.
142. Bolotnikova, T. N.; Naumova, T. N. Opt. Spectrosc. 1968, 25, 253.
143. Nakhimovskaya, L. A. Opt. Spectrosc. 1968, 24, 105.
144. Causey, B. S.; Kirkbright, G. F.; de Lima, C. G. Analyst 1976, 101, 367.
145. Dokunikhin, N. S.; Kizel, V. A.; Sapozhnikov, M. N.; Soloda, S. L. Optics Spectrosc. 1968, 25, 42.
146. RiMa, J.; Nakhimovsky, L. A.; Lamotte, A.; Jousot-Dubien, J. J. Phys. Chem. 1984, 88, 19.
147. Gorbachev, S. M.; Zaleskii, I. E.; Nizhnikov, V. V. Opt. Spectrosc. USSR 1980, 49, 37.
148. Canters, G. W.; Van Egmond, J.; Schaafsma, T. J.; Van der Waals, J. H. Mol. Phys. 1972, 24, 1203.
149. Pfister, C. Chem. Phys. 1973, 2, 181.
150. Klimova, L. A.; O'Globlina, A. I.; Shpol'skii, E. V. Bull. Acad. Sciences USSR Phys. Ser. 1970, 34, 1210.

151. Nakhimovsky, L. A. Opt. Spectrosc. USSR 1968, 24, 105.
152. Rima, J.; Lamotte, M.; Merle, A. M. Nouv. J. Chimie 1981, 5, 605.
153. Ustugova, L. N.; Nakhimovskya, L. A. J. Appl. Spectrosc. USSR (Engl. Transl.) 1968, 9, 1396.
154. Kitaigorodskii, A. I. Sov. Phys. (Engl. Transl.) 1957, 2, 456.
155. Moysya, E. G. Opt. Spectrosc. 1966, 21, 107.
156. Shpol'skii, E. V.; Klimova, L. A. Sov. Phys. Dokl. (Engl. Transl.) 1956, 111, 1227.
157. Shpol'skii, E. V.; Klimova, L. A. Opt. Spectrosc. 1962, 13, 174.
158. Klimova, L. A. Opt. Spectrosc. 1963, 15, 344.
159. Nurmukhametov, R. N. Russ. Chem. Rev. (Engl. Transl.) 1969, 38, 180.
160. Wittenberg, M.; Jarosz, J.; Paturel, L.; Vial, M.; Martin-Bouyer, M. Analisis 1985, 13, 249.
161. Colmsjo, A. L.; Ostman, C. E.; Zebuhr, Y. U. In "Polynuclear Aromatic Hydrocarbons: Mechanisms, Methods and Metabolism", Eighth International Symposium; Cooke, M.; Dennis, A. J., Eds.; Battelle Press: Columbus, OH, 1985.
162. Colmsjo, A.; Zebuhr, Y.; Ostman, C. Chem. Scripta 1984, 24, 95.
163. Wittenberg, M.; Jarosz, J.; Paturel, L. Anal. Chim. Acta 1984, 160, 185.
164. Garrigues, P.; De Vazelhes, R.; Ewald, M.; Jousot-Dubien, J. Anal. Chem. 1983, 55, 138.
165. Lai, E. P.; Inman, E. L., Jr.; Winefordner, J. D. Talanta 1982, 29, 601.
166. Garrigues, P.; Ewald, M.; Lamotte, M.; Rima, J.; Veyres, A.; Lapouyade, R.; Jousot-Dubien, J. Intern. Environ. Anal. Chem. 1982, 11, 305.
167. Colin, J. M.; Vion, G. J. Chromatogr. 1981, 204, 135.
168. Ewald, M.; Lamotte, M.; Redero, F.; Tissier, M. J.; Albrecht, P. Phys. Chem. Earth 1980, 12, 275.

169. Jozefov, E. M. M.S. Thesis, Iowa State University, Ames, IA, 1984.
170. Renkes, G. D.; Walters, S. N.; Woo, C. S.; Iles, M. K.; D'Silva, A. P.; Fassel, V. A. Anal. Chem. 1983, 55, 2229.
171. Yang, Y.; D'Silva, A. P.; Fassel, V. A. Anal. Chem. 1981, 53, 894.
172. Yang, Y.; D'Silva, A. P.; Fassel, V. A. Anal. Chem. 1981, 53, 2107.
173. Yang, Y. Ph.D. Dissertation, Iowa State University, Ames, IA, 1981.
174. Yang, Y.; D'Silva, A. P.; Fassel, V. A.; Iles, M. Anal. Chem. 1980, 52, 1350.
175. Brown, J. C.; Duncanson, J. A., Jr.; Small, G. J. Anal. Chem. 1980, 52, 1711.
176. Lukasiewicz, R. J.; Winefordner, J. D. Talanta 1972, 19, 381.
177. Grebenschikov, D. M.; Kovizhnykh, N. A.; Kozolov, S. A. Opt. Spectrosc. 1974, 37, 155.
178. LeBel, G. L.; Laposa, J. D. J. Mol. Spectrosc. 1972, 41, 249.
179. McDonald, R. J.; Selinger, B. K. Aust. J. Chem. 1971, 24, 249.
180. Al'Shits, E. I.; Bykovskaya, L. A.; Personov, R. I.; Romanovskii, Ya. V.; Kharlamov, B. M. J. Molec. Stru. 1980, 60, 219.
181. Stroupe, R. C.; Tokousbalides, P.; Dickinson, R. B., Jr.; Wehry, E. L.; Mamantov, G. Anal. Chem. 1977, 49, 701.
182. Kirkbright, G. F.; de Lima, C. G. Analyst 1974, 99, 338.
183. Filseth, S. V.; Morgan, F. J. In "Polynuclear Aromatic Hydrocarbons: Mechanisms, Methods and Metabolism", Eighth International Symposium; Cooke, M.; Dennis, A. J., Eds.; Battelle Press: Columbus, OH, 1985.
184. Farooq, R.; Kirkbright, G. F. Analyst 1976, 101, 566.
185. Hieftje, G. M.; Travis, J. C.; Lytle, F. E., Eds. "Laser in Chemical Analysis"; Humana Press: New York, 1981.
186. Wright, J. C.; Wirth, M. J. Anal. Chem. 1980, 52, 989A, 1087A.

187. Allkins, J. R. Anal. Chem. 1975, 47, 752A.
188. Hutchinson, M. H. Appl. Phys. 1980, 21, 95.
189. Webb, C. E. In "Lasers: Physics, Systems and Techniques"; Firth, W. J.; Harrison, R. G., Eds.; Scottish Universities Summer Schol in Physics: Great Britain, 1983.
190. Rhodes, Ch. K.; Egger, H.; Pummer, H., Eds. "Excimer Laser - 1983"; American Institute of Physics: New York, 1983.
191. Krauss, M.; Mies, F. H. In "Excimer Lasers, Topics in Applied Physics"; Rhodes, Ch. K., Ed.; Springer: Berlin, 1984; Vol. 30.
192. Telle, H.; Huffer, W.; Basting, D. Opt. Commun., 1981, 38(5,6), 402.
193. Schafer, F. P., Ed. "Dye Lasers, Topics in Applied Physics", 2nd Ed.; Springer: Berlin, 1977; Vol. 1.
194. Latz, H. W. In "Modern Fluorescence Spectroscopy", Wehry, E. L., Ed.; Plenum Press: New York, 1976; Vol. 1.
195. Sacchi, C. A.; Svelto, O. In "Analytical Laser Spectroscopy"; Elving, P. J.; Winefordner, J. D., Eds.; Wiley: New York, 1979.
196. Myer, J. A.; Johnson, C. L.; Kierstead, E.; Sharma, R. D.; Itzkan, I. Appl. Phys. Lett. 1970, 16, 3.
197. Hansch, T. W.; Schawlow, A. L. Bull. Am. Phys. Soc. 1970, 15, 1638.
198. Hansch, T. W. Appl. Opt. 1972, 11, 895.
199. Wright, J. C. In "Laser in Chemical Analysis"; Heiftje, G. M.; Travis, J. C.; Lytle, F. E., Eds.; Humana Press: New York, 1981.
200. Baldwin, G. D. "An Introduction to Nonlinear Optics"; Plenum Press: New York, 1969.
201. Stitch, M. L., Ed. "Laser Handbook"; North-Holland: New York, 1979; Vol. 3.
202. Maeda, M. "Laser Dyes: Properties of organic compounds for dye lasers"; Academic Press: New York, 1984.
203. Annual Book of ASTM Standards, Part 42 Standard E 388-72; American Chemical Society for Testing and Materials: 1972.

204. Guilbault, G. G. "Practical Fluorescence"; Marcel Dekker: New York, 1973.
205. Chen, R. F. Anal. Biochem. 1967, 20, 339.
206. Colmsjo, A.; Ostman, C. E. "Atlas of Shpol'skii spectra and other low temperature fluorescence spectra"; University of Stockholm: Stockholm, 1981.
207. Wise, S. A.; Bowie, S. L.; Chesler, S. N.; Cuthrell, W. F.; May, W. E.; Rebert, R. E. In "Polynuclear Aromatic Hydrocarbons: Physical and Biological Chemistry", Sixth Inter. Symposium; Cooke, M.; Dennis, A. J.; Fisher, G. L., Eds.; Battelle Press: Columbus, OH, 1982.
208. Schuetzle, D.; Lee, F.; Prater, T. Int. J. Environ. Anal. Chem. 1981, 9, 93.
209. Boduszynski, M. M.; Hurtubise, R. J. Anal. Chem. 1982, 54, 375.
210. Locati, G.; Fantuzzi, A.; Consonni, G.; Ligotti, I.; Bonomi, G. Am. Ind. Hyg. Assoc. J. 1979, 40, 644.

ACKNOWLEDGEMENTS

I am very grateful to Professor Velmer A. Fassel for counsel, guidance and critical review of the work presented in this dissertation.

I would like to thank Mr. Arthur P. D'Silva for the helpful and stimulating discussion during the development of this work. I wish to express my appreciation to Dr. Stephan Weeks and Roy Dobson for their help in solving the instrumental problems. It is a pleasure to thank all members of our group for the friendly atmosphere that have made the many hard hours of the work as pleasant as it could be. I also thank Mrs. Lesley Hawkins for her fast, neat and excellent typing. The financial support of Ames Laboratory for the present work is greatly appreciated.

I am deeply indebted to my wife, Ebtessam, for her love, patience and encouragement, and the sacrifices she made over the past several years. To my children Hosam, Gehan and Moataz, I must apologize for the many hours, rightfully theirs, that were consumed by this work.

Above all, I thank my mother and my late father for their endless love and unlimited support given to me over the years. I would like to dedicate this dissertation to them.